Title

AN ANALYSIS OF SELENIUM AND CHLORIDE MOVEMENT THROUGH A POND SEDIMENT AT KESTERSON RESERVOIR

Authors

R.H
Long

Publication Date

1988-12-21

Lawrence Berkeley Laboratory
UNIVERSITY OF CALIFORNIA

EARTH SCIENCES DIVISION

An Analysis of Selenium and Chloride Movement through a Pond Sediment at Kesterson Reservoir

R.H. Long
(M.S. Thesis)

September 1988

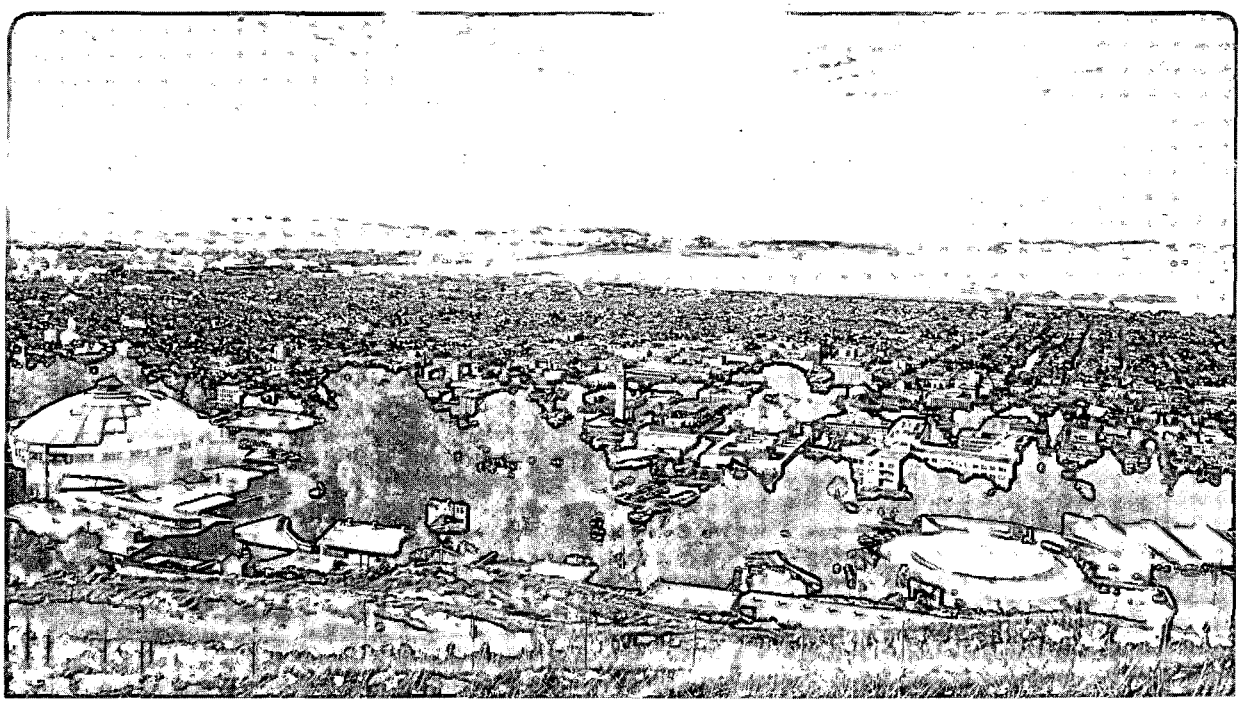

Prepared for the U.S. Department of Energy under Contract Number DE-AC03-76SF00098.

DISCLAIMER

LBL-25874

An Analysis of Selenium and Chloride Movement through a Pond Sediment at Kesterson Reservoir

Robert Helms Long
(M.S. Thesis)

Earth Sciences Division
Lawrence Berkeley Laboratory
1 Cyclotron Road
Berkeley, California 94720

September 1988

AN ANALYSIS OF SELENIUM AND CHLORIDE MOVEMENT THROUGH A POND SEDIMENT AT KESTERSON RESERVOIR

Robert Helms Long

ABSTRACT

Kesterson Reservoir, Merced County, CA, a disposal facility for agricultural drain water, became the object of intense scientific investigation after the discovery in 1983 that the disposal of Se-laden agricultural drain waters was having serious effects on the reproductive success of waterfowl. A remedial measure involving permanent flooding with low-Se water, aimed at taking advantage of low Se solubility under reducing conditions, was proposed as a means of limiting Se movement into groundwater and biota. A field experiment was undertaken to evaluate the feasibility of the proposed remedial measure, its impact on the quality of shallow groundwater and for quantifying Se immobilization and transport through a newly-flooded pond bottom soil. Extensive soil water and groundwater sampling demonstrated that although the soluble Se concentrations in the top 1.22 m of soil were initially as high as 1000s of $\mu g\ L^{-1}$, Se concentrations declined dramatically after flooding and elevated concentrations below 1.22 m were observed at only one of five sampling sites. Analysis of the temporal and spatial changes in the distribution of dissolved Se and Cl^- indicated that 66 to 108% of the initial soluble Se present in the top 1.22 m was immobilized shortly after flooding. These estimates were consistent with the low Se concentrations observed in shallow monitoring wells. The extent to which Se immobilization occurred was found to correlate inversely with average pore water velocity. Redox measurements indicated that Eh conditions following flooding shifted sufficiently in magnitude and rate to conceivably account for the observed immobilization of selenium. Data presented suggest that reducing conditions in the newly flooded soils lead to the microbially mediated transformation of selenate to less soluble forms.

The primary focus of the experiment was to gain insight into the mechanism of selenium

migration and immobilization. As a means of confirming the fluid velocity estimates made in the mass balance calculations, history-matching of breakthrough curves of a conservative solute, chloride, was performed at 40 sampling locations within 5 sites throughout the pond following pond-flooding. A deterministic one-dimensional fluid flow and transport mathematical model utilizing the integrated finite difference method (IFDM) was employed in the effort. Reasonable matches were obtained between the observed and calculated concentrations with the advective-dispersive code. Fluid velocity estimates, in general, confirmed the earlier predictions and resulted in negligibly different immobilization estimates. Extreme lateral variability of soil hydraulic properties was demonstrated between and within field plots with values of permeability and apparent dispersion coefficient varying by one to two orders of magnitude. The flow and transport properties determined throughout the field were found to conform to a log-normal distribution. The apparent dispersion coefficient was shown to be velocity dependent and exhibited a linear relationship with average pore water velocity. Estimates of dispersivity at the 40 locations are high in relation to values measured typically in the laboratory. A general trend was observed of greater dispersivity values with increasing travel distance.

Table of Contents

LIST OF FIGURES

LIST OF TABLES

NOMENCLATURE

A	area, L^2
C	solute concentration, M solute·(M water)$^{-1}$
$C_{Cl,in}$	chloride concentration of waters entering the study block, M Cl·(M water)$^{-1}$
$C_{Cl,out}$	chloride concentration of waters exiting the study block, M Cl·(M water)$^{-1}$
C_i	initial solute concentration, M solute·(M water)$^{-1}$
C_o	input solute concentration, M solute·(M water)$^{-1}$
$C_{Se,in}$	selenium concentration of waters entering the study block, M Se·(M water)$^{-1}$
$C_{Se,out}$	selenium concentration of waters exiting the study block, M Se·(M water)$^{-1}$
D_e	effective coefficient of molecular diffusion, $L^2 \cdot T$
D_h	apparent dispersion coefficient, $L^2 \cdot T$
$D_{h,l}$	longitudinal component of the apparent dispersion coefficient, $L^2 \cdot T$
$D_{h,t}$	transverse component of the apparent dispersion coefficient, $L^2 \cdot T$
D_m	coefficient of mechanical dispersion, $L^2 \cdot T$
D_o	coefficient of molecular diffusion, $L^2 \cdot T$
$d_{l,m}$	distance between nodal points l and m, L
$F_{l,m}$	advectance from the upstream node l to the node m, $L^3 \cdot T$
g	gravitational constant, $L \cdot T^2$
h	hydraulic head, L
J_a	mass of solute flowing through a unit cross-sectional area per unit time due to advection, $M \cdot L^{-2} \cdot T^{-1}$
J_d	mass of solute flowing through a unit cross-sectional area per unit time due to molecular diffusion, $M \cdot L^{-2} \cdot T^{-1}$
J_h	mass of solute flowing through a unit cross-sectional area per unit time due to apparent dispersion, $M \cdot L^{-2} \cdot T^{-1}$
J_m	mass of solute flowing through a unit cross-sectional area per unit time due to mechanical dispersion, $M \cdot L^{-2} \cdot T^{-1}$
K	hydraulic conductivity, $L \cdot T^{-1}$
K_s	saturated hydraulic conductivity, $L \cdot T^{-1}$
k	permeability, L^2
k_d	first-order reaction constant, T^{-1}
k_h	macropore permeability, L^2
k_m	matrix permeability, L^2
$M_{c,l}$	fluid mass capacity of the element l, $M \cdot L^{-1}$
M_{Cl}	mass of chloride in the study block, M
$M_{Cl,in}$	mass of chloride entering the study block, M
$M_{Cl,o}$	initial mass of chloride in the study block, M
$M_{Cl,out}$	mass of chloride exiting the study block, M

$M_{Cl,t}$	mass of chloride in the study block at time t, M
$M_{f,l}$	mass of fluid in the element l, M
M_{Imm}	mass of selenium immobilized the study block, M
M_{Se}	mass of selenium, M
$M_{Se,in}$	mass of selenium entering the study block, M
$M_{Se,o}$	initial mass of selenium in the study block, M
$M_{Se,out}$	mass of selenium exiting the study block, M
$M_{Se,t}$	mass of selenium in the study block at time t, M
$\vec{n}_l$	outward unit normal, 1
Pe_l	peclet number for the element l, 1
q	soil water flux, $L \cdot T^{-1}$
R	retardation factor, 1
S_s	specific storage, L^{-1}
T_o	intial day from which history-matching begins
t	time, T
V	volume, L^3
$V_{b,l}$	bulk soil volume in the element l, L^3
V_w	volume of water in the element l, L^3
v	average pore water velocity, $L \cdot T^{-1}$
$\tilde{v}$	effective average pore water velocity, $L \cdot T^{-1}$
$Y_{l,m}$	chemical conductance between nodes l and m, $L^3 \cdot T$
z	uni-dimensional axis coordinate, L
α_l	longitudinal dispersivity, L
$\Gamma_{l,m}$	interface between elements l and m, L^2
Γ_V	boundary surface of a closed surface V, L^2
μ	fluid viscosity, $M \cdot L^{-1} \cdot T^{-1}$
ϕ	porosity, 1
Ψ	pressure head, L
ρ_f	fluid density, $M \cdot L^{-3}$
τ	tortuosity, 1
θ	volumetric water content, 1

ACKNOWLEDGEMENT

First and most importantly, I would like to express my sincere thanks and appreciation to Sally Benson for the patient help and constant support that she provided to me throughout the course of this work. This thesis is as much a product of her own enthusiasm and encouragement as it is of any efforts of mine, and I feel truly indebted to her for the assistance that she provided. Her sincere interest, technical excellence, and humour all contributed to significantly enhance the quality and enjoyment of my educational experience at Berkeley. I would like to thank my advisor, Dr. Paul Witherspoon, for his encouragement and guidance and for providing me the initial opportunity to come and study at Berkeley.

I also would like to express my appreciation to Dr. Tetsu Tokunaga for his patient readiness to spend time in helpful discussion and his generous and unselfish willingness in helping me with many practical details of the field. His superior level of dedication and technical competence have been a true learning experience, and I feel fortunate, both on a technical and personal level, to have had his assistance.

I would like to recognize and thank Robin Lisa Branstetter for her friendship, perseverance, and patient support. The maintenance of my sanity and hopeful outlook owes much to her gentle influence.

I am grateful to Ray Solbau for the time he provided in the collection of much of the data and for the field technical expertise he brought in the fabrication of field equipment. His talents were invaluable and his humour always welcome. I would also like to thank John Daggett for the many hours he spent with me collecting data and for the positive attitude that he always brought. And to Mohsen Alavi I would like to express gratitude for the many hours he provided in assisting me in the successful operation of the computer codes used in this study.

Finally, I would like to thank the taxpayers of the United States and the Bureau of Reclamation for providing the research funds that allowed me the opportunity to take part in this work and assisted me in meeting my educational expenses. This work was also partly

supported through US DOE contract No. DE-AC03-76SF00098.

PART I. ANALYSIS OF SELENIUM MOBILITY THROUGH A POND SEDIMENT AT KESTERSON RESERVOIR

1. INTRODUCTION

1.1. Background

Kesterson Reservoir, a 520-ha (1283-acre) agricultural drain water disposal facility located along the western side of the San Joaquin Valley in Merced County, California (Figure 1.1), is operated by the US Bureau of Reclamation (USBR) as part of the Central Valley Project, and is fed by the San Luis Drain, a 137 km (85 mile) long concrete-lined canal that extends from the Five Points area in Fresno County. Agricultural drain water originates in subsurface tile drains installed in irrigated fields of the Westlands Water District, a major user of federally supplied irrigation water in the Valley. Construction of the two facilities was authorized by Congress in 1960 and took place from 1968 to 1975. Originally, the Reservoir was intended to function as a holding facility midway to the San Francisco Bay Delta, the ultimate disposal destination for the drain water. Budgetary constraints and controversy surrounding potential adverse environmental impacts on wildlife of the Delta, lead to a halting of San Luis Drain construction at Kesterson. The Reservoir has since functioned as a series of shallow evaporation and seepage ponds for the disposal of 5000 to 8000 acre-ft per year of mineral-laden drain water (total dissolved solids $\approx$ 10000 ppm).

The Reservoir is also a part of the 2387-ha (5900-acre) Kesterson National Wildlife Refuge, administered by the US Fish and Wildlife Service, and it sits along a major flyway of migratory waterfowl. From 1971, when water first began flowing to the Reservoir, until 1981, the majority of the water flowing into the Reservoir consisted of surface runoff. However, eventually as a large number of tile drain connections were made with the San Luis Drain, inflowing waters were comprised primarily of subsurface drain water. In 1982 a problem was first observed when several species of fish died-off in the Reservoir. In 1983 impaired

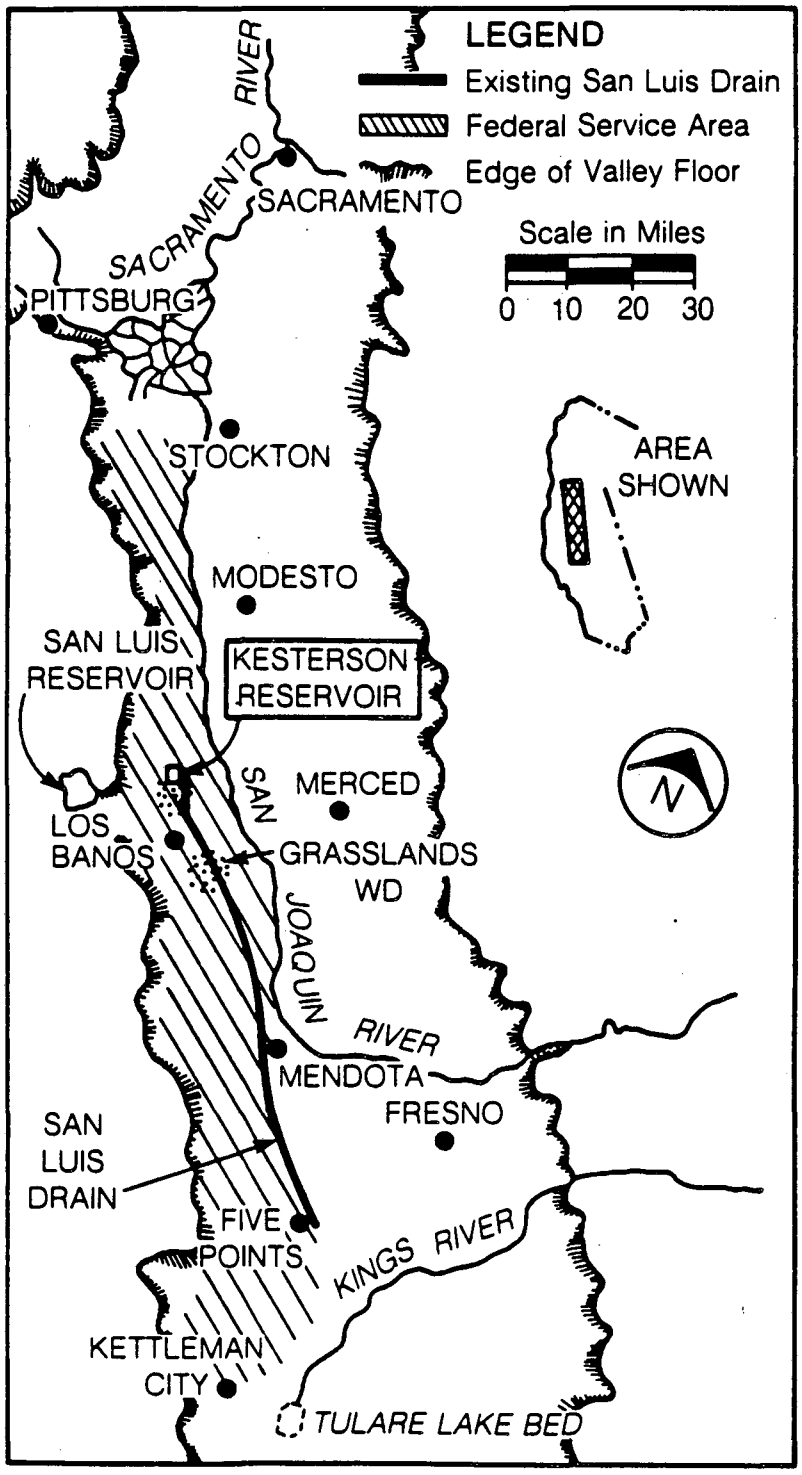

XBL 859-10731

Figure 1.1 Location of Kesterson Reservoir within California.

reproductive success and birth deformities were observed in waterfowl living at the Reservoir. It was later determined that high concentrations of selenium (Se ≈ 300 ppb) in agricultural drain water had entered into the food chain and lead to the observed mortality rates in waterfowl *(Ohlendorf et al.,* 1986). In 1984 studies indicated that selenium was entering into local groundwaters in limited areas and that soil and vegetation at the Reservoir were contaminated with selenium. During the period 1981 to 1986, it has been estimated that approximately 9000 kg of selenium were delivered to the Reservoir.

Selenium is a naturally-occurring element in soils of this region derived from Cretaceous shales of the Coast Ranges including irrigated farmlands of the Panoche fan. Leaching of valley farm soils by percolating irrigation water is the source of selenium in drain water which is then carried to the Reservoir via the San Luis Drain. Tile drains, installed and designed to prevent already shallow groundwaters from rising closer than approximately 1.5 m from the surface, have as their primary purpose the prevention of soil root-zone buildup of salts that could potentially lead to reduced crop yields. Agricultural difficulties associated with shallow water table conditions affect nearly 100,000 ha (247,000 acres) in the San Joaquin Valley *(USBR,* 1984).

The State Water Resources Control Board (SWRCB), in response to a petition filed by an adjacent landowner, ordered the Bureau of Reclamation in February 1985, in Water Quality Order 85-1, to either close Kesterson Reservoir to further discharges of drainwater or to upgrade Kesterson to meet requirements for a hazardous waste surface impoundment. In March 1985 the Secretary of the Interior ordered Kesterson closed, and in April the Department entered into an agreement with Westlands Water District to gradually curtail agricultural drain water inflows into the San Luis Drain. By August of 1986 subsurface agricultural drain water flow into the Reservoir had essentially ceased. In July of 1985, the Bureau submitted to the SWRCB a framework plan for closure and cleanup of Kesterson Reservoir. In October of 1986 the final Environmental Impact Statement was filed. The Kesterson Program, designed to meet the requirements set forth in WQ 85-1, identified alternative plans for

Reservoir cleanup and land use, San Luis Drain cleanup, and wetland mitigation, which protect public health and the environment, and are cost effective *(USBR,* 1986). In December of 1986 the Bureau's closure and post-closure plan was submitted to the SWRCB for review and approval. It included the controversial "Wet-Flex" plan for permanently flooding the Kesterson ponds as a means of immobilizing the selenium inventory in the near surface sediments of the pond bottoms. In March of 1987, the SWRCB issued an order rejecting the Wet-Flex alternative and requiring the Bureau to implement the Onsite Disposal Plan (ODP) for Kesterson Reservoir clean-up, a more costly alternative involving excavating the most contaminated soils and putting them in an engineered landfill.

1.2. The Setting of Kesterson

1.2.1. Geologic Setting

Kesterson Reservoir is located along the western side of the San Joaquin valley, or Great Valley, a northwest-trending geomorphic province and structural trough bounded on the east by the granitic rocks of the Sierra Nevada and on the west by the folded sedimentary rocks of the Coast Range, and extending from the Tehachapi Mountains in the south to the Klamath mountains in the north. The valley floor is comprised of an approximately 4570 m (15000 ft) thick sequence of loosely consolidated sands, gravels and clays arranged in a synclinal structure of Jurassic to recent age. Sediments rest on a basement floor of igneous and metamorphic rocks *(Prokopovich,* 1967).

Kesterson Reservoir rests within a Quaternary flood plain terrace west of the San Joaquin River, bordered on the west by piedmont alluviam and on the east by lower flood plain deposits *(Rowell et al.,* 1983). Underlying the Reservoir, basin fill deposits extend to depths of 61.0 to 91.4 m (200 to 300 ft) and consists of alternating layers of sands, clays, and silts. Silty to clean sand predominates with lesser amounts of clay and silt arranged in lenses. The near surface material is an alluvial sediment, again consisting of a complex arrangement of interfingering and intergrading, discontinuous layers of sand, clay and silt. In most portions

of the Reservoir, the upper 3.0 to 6.1 m (10 to 20 ft) of alluvium is classified as a sandy loam and covers silty sands and silts that extend to a depth of 24.4 m (80 ft), where an approximately 3.0 m (10 ft) thick finer grained layer of relatively low permeability is located. A sandy unit extends below this layer to a depth of approximately 61.0 m (200 ft) where a relatively thick, continuous and impermeable layer is located. The Corcoran Clay, member of the Tulare Formation, is the principal confining layer for the deep aquifer underlying the western portion of the San Joaquin valley. Its thickness varies from 12.2 to 24.4 m (40 to 80 ft) in the San Luis Drain area, and its depth varies from 70.1 m (230 ft) at Kesterson to approximately 182.9 m (600 ft) near the south end of the drain *(USBR,* 1965). In isolated areas at the surface, the fine-grained veneer of clayey soil is not present and the silty sands and silts extend to the surface. During ponded conditions, a layer of mud several centimeters to as much as ½ m thick and rich in organic matter covers the bottoms of the ponds.

1.2.2. Hydrologic Setting

Two distinct hydrologic regimes can be distinguished under Kesterson Reservoir. A confined aquifer below the Corcoran Clay has been designated the lower water-bearing zone, and the units above the Corcoran Clay to the ground surface comprise the shallow aquifer *(Hotchkiss and Balding,* 1971). Water from the shallow aquifer is used locally for livestock watering and irrigation. The lower water-bearing zone contains water fit for human consumption, however, because of its depth and isolation beneath the Corcoran Clay, and because drainage water has not been found to have migrated near it or to pose a threat of contamination, the lower water-bearing zone has received little attention in investigations aimed at subsurface geologic characterization.

Regional groundwater flow within the shallow aquifer is toward the northeast with an average gradient of approximately 5×10^{-4} to 9×10^{-4} meters of water/meter of linear distance *(State of California,* 1967) and a pre-Kesterson groundwater pore water velocity that is believed to have averaged from 6.1 to 9.1 m/year (20 to 30 ft/year). The existence of the Reservoir has led to the development of a groundwater mound which varies in height from

0.9 m (3 ft) in the winter months to up to 3.0 m (10 ft) in the summer and to the creation of a saline plume which has moved away laterally from the site at an estimated average rate of 45.7 m/year (150 ft/year) and vertically at an estimated rate of 4.6 m/year (15 ft/year) *(Lawrence Berkeley Laboratory,* 1987c, p. xvii). The average depth to the water table varies over the local area from 0.5 m (1.5 ft) in the east to 3.0 m (10 ft) in the western portion of the Reservoir. Seasonal flooding and increased winter precipitation cause fluctuations of roughly 1.5 m (5 ft) in the water table elevation, causing it to rise above the ground surface in places *(Lawrence Berkeley Laboratory,* 1987c, p. 16).

The major surface water drainage feature in this portion of the valley is the San Joaquin River (Figure 1.2). Mud Slough is located immediately adjacent to much of the western border of the Reservoir. Salt Slough is located approximately 2.5 km to the east. Both channels drain the marshland and empty into the San Joaquin River.

Kesterson Reservoir is situated within a seasonal wetland region that attracts large numbers of migratory waterfowl and that supports a diversity and abundance of life within the confines of a distinct ecosystem. Within a 124-square-mile area centered on Kesterson, the 520-ha (1283-acre) facility accounts for 8% of the total wetland acreage. Numerous duck clubs are located in the vicinity of the Reservoir and their seasonally flooded wetlands account for 18% of the total acreage *(Mandle and Kontis,* 1986).

1.2.3. Hydrologic Properties of the Pond Bottom Soils

An early survey of the Reservoir area classified the soils as belonging to the Waukena soil series *(Soil Conservation Service,* 1952). These soils contain high-soluble salt levels and have been characterized as moderately to strongly salt-affected. Salt contents in the general vicinity of Kesterson, based on information provided in the SCS survey, range from 0.1 to 1.95%, with 0.1 to 0.7% representing fairly typical values. These percentages represent the mass of soluble salts per unit mass of air-dried soil averaged over the upper 0.30 m (1 ft) of soil. Varying amounts of carbonates are present. Some soils in the area have been mapped as

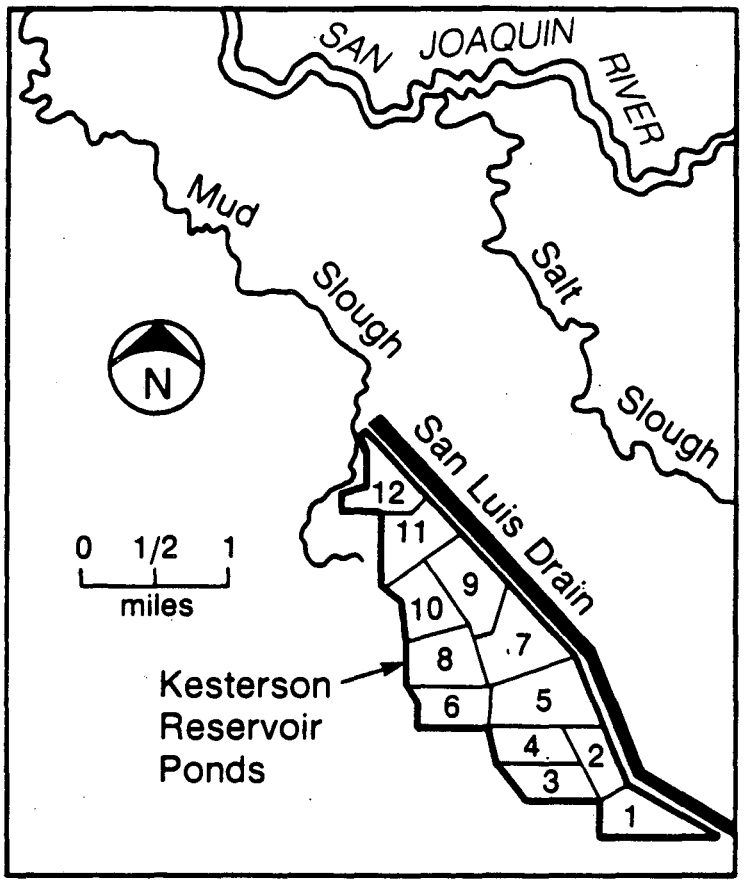

XBL 859-10732

Figure 1.2 Map of Kesterson Reservoir.

sodic. X-Ray analysis of Kesterson evaporite samples has identified thenardite (Na_2SO_4), gypsum ($CaSO_4 \cdot 2H_2O$), and calcite ($CaCO_3$) as the major evaporite minerals. These minerals, as well as bloedite ($Na_2Mg(SO_4)_2 \cdot 2H_2O$) and halite (NaCl) also comprised minor portions of some of the samples *(Lawrence Berkeley Laboratory,* 1988). Halite was the only chloride-bearing mineral identified.

The surface 1 to 2 m of the pond soils are generally of finer texture than than deeper materials. Clay and silt sized material each make up approximately 20-30% by weight of the surface mineral soils. Individual surface samples can be classified in a range of textures from sandy loams to clay loams. Samples collected below 2 m tend to be dominated by the sand fraction. The primary physical barrier to seepage into the shallow aquifer and contamination of shallow groundwater is the presence of this surficial fine-textured layer. X-Ray diffraction analysis of samples collected within the upper 3.0 m (10 ft) of Reservoir soils has identified smectite as the major clay mineral. Lesser amounts of kaolinite and illite are present.

The US Bureau of Reclamation performed a series of infiltration tests, prior to Reservoir construction, in ponded and unponded soils located in the vicinity of the present Kesterson Reservoir site. Based on data presented in *USBR* (1967), arithmetic mean and geometric mean saturated hydraulic conductivities (K_s) in non-ponded soils were calculated as 4.6 m/year (15 ft/year) and 2.6 m/year (8.6 ft/year) respectively *(Lawrence Berkeley Laboratory,* 1985, p. 5-5). At the previously ponded sites, arithmetic mean and geometric mean saturated hydraulic conductivities were determined to be 3.4 m/year (11 ft/year) and 0.9 m/year (3 ft/year) respectively. *Luthin* (1966), in another early study of the Reservoir site, also measured the saturated hydraulic conductivity of the surficial clay layer with an infiltrometer. *CH2M Hill* and *Jones and Stokes Associates,* (1985), based on data obtained from the work of *Luthin,* reported a somewhat higher average value, than the above mentioned reports, of 11 m/year (37 ft/year).

Because of the limited vertical penetration of the infiltrating wetting-front over the course of

an infiltrometer test, K_s values determined in this manner cannot necessarily be considered representative of the full-thickness of the surficial layer. In fact, in most of the tests reported in *USBR* (1967), the wetting front did not even penetrate past 0.15 m (0.5 ft) *(Lawrence Berkeley Laboratory,* 1985, p. 5-5). In a soil that possesses layered heterogeneity, the effective hydraulic conductivity, K_z, is a harmonic mean of the values of K_s measured in each individual layer, i,

$$K_z = \frac{d}{\sum_{1}^{n} \frac{d_i}{K_i}} \tag{1}$$

where K_i represents the saturated hydraulic conductivity in each individual layer of thickness d_i. This harmonic mean value is strongly weighted towards layers of low K_s, and therefore it is likely that effective K_s is considerably smaller than the values reported above.

A survey employing a constant head, auger hole method with a Guelph permeameter was made of K_s throughout the Reservoir by personnel from Lawrence Berkeley Laboratory during 1986 and 1987. These measurements resulted in profiles of K_s to depths as deep as 0.84 m (2.75 ft) within Pond 1, allowing for the calculation of K_z at a number of locations. A high degree of spatial variability was observed in the measurements, with values ranging by 2 orders of magnitude in some cases within individual profiles. In general, due to the presence of surficial macropores (cracking), the material to a depth of approximately 0.3 m displays quite high values of K_s, as high as 100 m/year. At a depth of 0.3 to 2 m, a low permeability barrier is encountered with values on the order of 1 to 10 m/year commonly observed. Harmonic mean values at 4 sites within Pond 1 were determined to be 1 m/year, 3.7 m/year, 4.3 m/year and 20 m/year.

2. THE CHEMISTRY OF SELENIUM AT KESTERSON

As mentioned in Section 1.1, the annual inflow to Kesterson Reservoir ranged from approximately 5000 to 8000 acre-ft/year over the period 1978 to 1984. After measuring inflows and calculating evaporation losses, the Bureau estimated that approximately 50% of the water that had been delivered to the Reservoir had percolated down through the bottom sediments into the shallow aquifer *(USBR,* 1986). The remaining portion was either lost through evaporation or transpired by plants. Even though selenium concentrations in SLD water typically were 200 to 300 ppb, selenium concentrations in groundwater samples collected through extensive sampling of monitoring wells were low and generally remained below 5 ppb. (The current federal Drinking Water Standard is 10 ppb, however, a 50 ppb level has been proposed by EPA as a new selenium standard.) A groundwater plume with selenium levels greater than 10 ppb was identified in the southern portion of the Reservoir, however, the extent of the subsurface contamination was found to be rather limited. In their chemical composition with respect to major element chemistry and the presence of trace elements such as boron, groundwaters underlying the Reservoir and SLD water exhibited similar characteristics, suggesting that the surface, interstitial and groundwaters have been in direct communication with one another. *(Lawrence Berkeley Laboratory,* 1985 p. 4-10). The vertical penetration of selenium, however, does not correspond to the maximum vertical penetration of pond water *(Lawrence Berkeley Laboratory,* 1986a p. 50). The low selenium levels in groundwater relative to surface water suggest a selenium removal mechanism in the near-surface soil profile. It was this observation and the observation that a large fraction of the selenium inventory is confined in the first few inches of soil that guided much of the early work performed by Lawrence Berkeley Laboratory and others at Kesterson and which motivated the performance of the Pond 1 Resaturation Monitoring, the subject of this thesis.

2.1. Summary and Review of Relevant Literature

2.1.1. Selenium Toxicity and Relative Abundance

Selenium is both beneficial and harmful to animal life and man. Selenium is an essential trace nutrient which is toxic at high concentrations. Deficiency diseases in animals appear in areas having selenium levels in plants < 0.1 ppm while toxicity is observed when plant selenium concentrations exceed 5 ppm *(Frost,* 1967). The symptoms of selenium toxicity have been known in this country since the 1850's, and the first reported incidence is found in a statistical report on health issues in the US Army *(Madison,* 1860). The report referred to a "very fatal disease" among horses at a post near what is now central South Dakota. The author very correctly referred to the source of the illness, later called "alkali disease" as pasturage. An awareness of the disease occurred some 200 years earlier in Mexico when people who ate produce grown on outwash from mining activities suffered health-related problems. And there is evidence that as early as 1275 A.D. in western China, Marco Polo observed similar troubles in the health of animals that ate certain "poisonous plants" growing there *(Komroff,* 1926).

Nutritional problems in grazing livestock, that we now know to have resulted from selenium toxicity, have been widely recognized, and economic losses have been reported for centuries. In this country, however, until the 1930's, nutrient deficiencies in forage were largely felt to be the cause. In the 30's, through work sponsored by various federal and state agencies, including the US Department of Agriculture and the South Dakota and Wyoming Agricultural Experiment Stations, the role of selenium in agriculture came into view *(Anderson et al.,* 1961). Extensive surveys were performed of its occurrence in soils, rocks, plants and animals and numerous publications and articles resulted.

Selenium occurs in minute quantities throughout the earth and rarely exceeds 100 ppm concentration in any material *(Lakin,* 1961). The geochemistry of selenium is closely tied with the geochemistry of sulfur, and in nature selenium frequently occurs as a trace substituent, substituting for a small fraction of sulfur in minerals such as pyrite or native sulfur. Estimates of the average concentration in the earth's crust range from .03 to .8 ppm *(Fleischer,*

1953). In sea water, the selenium concentration is very low. *Byers* (1938) concluded that selenium does not exceed .25 ppb in waters of the ocean except near the mouths of rivers and streams. In igneous rocks average selenium concentration has been estimated at .09 ppm *(Goldschmidt,* 1937). The selenium concentration of sedimentary rocks in the western US generally ranges from less than .02 to 2 ppm. Shales commonly contain more selenium than do other sedimentary rocks. The distribution of selenium, however, in various rock types and soils varies greatly, both vertically and areally. Certain geologic materials in the western US posses anomalously high concentrations, as high as 1500 ppm, and include tuffs, shales, sandstones, and soils. From Devonian to Miocene time, some 260 to 10 million years ago, intermittent volcanic activity occurring along the present approximate boundary of the Western United States *(Eardley,* 1951) may have injected selenium, one of the volatile components in magma, into the atmosphere. These emanations, combined with the prevailing eastward winds and subsequent introduction into sediments, are assumed by many geologists to account for the primary source of selenium in the Western Plains *(Lakin,* 1961). Cretaceous formations have received considerable attention because of the large areas of farm soils extending eastward from the Rocky Mountains and the many acres of range and irrigated land in northwestern New Mexico, western Colorado and Utah that are derived from these materials.

2.1.2. Criteria for Selenium Solubility

The various forms of selenium that can exist in soils include selenide(-II), elemental Se(O), selenite(IV), selenate(VI), and various ill-defined organic selenium compounds *(Rosenfeld and Beath,* 1964). Selenium is most mobile in the Se(IV) and Se(VI) forms *(Adriano,* 1986). The speciation and concentration of selenium in soils are controlled by various physical-chemical factors expressed in terms of pH, dissociation constants, solubility products, and oxidation-reduction potential. Our understanding of the effects of these factors is incomplete. *Lakin* (1961) pointed to the importance of selenite precipitation with ferric hydroxide in acid or neutral soils as a factor in reducing selenium uptake in plants. *Geering et al.* (1968) concluded that this combination occurs as a ferric oxide-selenite-adsorption complex and went

on to examine the conditions under which selenium may assume either higher or lower oxidation states. Both of these investigators determined that the redox potential (pe + pH) may indicate what to expect regarding the valence state of selenium in soil.

Elrashidi et al. (1987) used thermodynamic data in a purely theoretical study to develop equilibrium reactions and constants for selenium minerals and solution species that relate to soils and determined that the redox potential of soil is the major factor controlling the speciation of selenium in solution. The study determined that at high redox (pe + pH > 15.0) selenate is the major species in solution, whereas in the medium range (pe + pH > 7.5 - 15.0) selenite is dominant. At low redox (pe + pH < 7.5) selenide is the major species, particularly in alkaline environments. Solubility of the metal-selenate minerals is very high and in well-aerated, cultivated soils these are not stable in the solid phase. Selenite minerals also appear to be too soluble to persist in cultivated soils. It should be mentioned that this may be true in well-drained soils, however, at the soil surface, solubility limits of selenite and selenate minerals may be exceeded due to evaporative accumulation in a shallow water table environment such as exists at Kesterson. *Elrashidi et al.* also noted that, in general, selenide minerals are extremely insoluble under reducing conditions. In highly-reducing environments, therefore, they may act as a major inert sink for selenium present in the system. As long as conditions remain reducing, contamination of waters or soils by these minerals poses a minimal hazard of selenium toxicity. The presence of selenide minerals, however, is speculative and based on theoretical calculations only. Work done recently by personnel at Lawrence Berkeley Laboratory suggests that elemental selenium Se(O) is a major species under reducing conditions and may act as the dominant inert sink for selenium present at Kesterson Reservoir *(Weres,* Personal Communication).

The thermodynamic relationships discussed above are equilibrium relationships. The actual formation of these materials in soil depends on the kinetics of the reactions. Selenite, selenate, and organic selenides have been found to coexist in oxic seawater samples, suggesting the importance of kinetics in speciation *(Measures and Burton,* 1980). Experimental evidence

in the laboratory suggests that the selenate to selenite conversion and vice versa is relatively slow, whereas the selenite to elemental selenium reaction and vice-versa is rapid *(Rosenfeld and Beath,* 1964). Soil environments are generally non-equilibrium systems, and therefore it may be reasonable to expect selenium species, that are theoretically mutually exclusive, to coexist to some degree in solution.

2.1.3. Selenium Retention

Selenium availability to plants and mobility in the soil column is affected not only by redox controlled speciation and mineral formation but by the ability of soil to retain selenium, principally in the form of selenite, on the mineral surface through an adsorption process. Selenite is generally thought to adsorb by ligand-exchange *(Goldberg and Sposito,* 1984). Factors affecting adsorption include the degree of weathering, solution composition, soil composition, organic carbon content, calcium carbonate content, and pH. *John et al.* (1976) in a study involving 66 New Zealand soils found that as the degree of weathering increased, in general, so did selenite adsorption. Variations in ionic strength may affect selenite adsorption in the effect on the charge distribution on a solid surface, and in increased concentration of competing ions. *Singh et al.* (1981) observed dramatically reduced sorptive capacity of a soil with addition of sulfate and phosphate, however, other works have indicated little effect of variation in ionic strength *(Hingston,* 1981). *Neal et al.* (1987) in an experiment involving two soils from the San Joaquin Valley of California found no evidence for a relationship between selenite adsorption and the addition of chloride or sulfate. Phosphate, however, was found to reduce by ½ the amount of selenite adsorbed through the addition of 2 μmol *o*–phosphate/kg. Results obtained were supportive of a ligand-exchange mechanism.

Hamdy and Gissel-Nielsen (1977) showed selenite adsorption by iron oxides to be extensive, rapid, and reaching a maximum with pH between 3 and 5. Adsorption by clay minerals was affected more by pH than by layer type, although the 1:1 mineral kaolinite exhibited greater sorption than the 2:1 minerals vermiculite and montmorillonite. *Neal et al.* found adsorption to occur to the greatest extent in acidic soils. Under alkaline conditions adsorption of selenite

could be low and was independent of soil type. Below pH 6, however, the degree of adsorption varied with soil type and strongly correlated with the presence of solubilized Al, Fe, and Mn.

Yläranta (1983) demonstrated in a study involving two soils and a peat that organic C can be an important factor in selenite adsorption. The presence of organic matter reduces the amount of readily available fraction of selenium by chelation of selenite by organic compounds.

2.1.4. Oxidation-Reduction in Newly Flooded Soils

Reduction of the soil is the single most significant chemical change brought about by flooding, and it results directly from the exclusion of oxygen *(Ponnamperuma,* 1965). Upon flooding, consumption of oxygen proceeds rapidly as aerobic organisms convert organic matter to inorganic compounds. The demand of oxygen easily outpaces the supply which requires diffusion from the overlying soil and water column.

Depletion of oxygen and the establishment of anaerobic conditions can occur within 24-48 hours *(Takai,* 1956). During anaerobic respiration, inorganic compounds are utilized as electron receptors (they are reduced) in order to release the energy through oxidation stored in organic matter. Anaerobic bacteria, upon the exhaustion of available oxygen, utilize in a step-wise manner, and in accordance with thermodynamic predictions, nitrate, manganese, ferric iron, followed by sulfate and then carbon dioxide. The soils redox potential decreases. Reduced species accumulate either as soluble components or as precipitated compounds within the soil matrix *(Gunnison et al.,* 1985). In an experiment involving the addition of glucose to 4 lowland rice soils, *Yamane and Sato* (1968) observed Eh to drop rapidly within 8 hours of flooding. After 48 hours it had fallen from an initial value of 400 mV to approximately 0 mV. The addition of nitrate and cyanide was found to diminish the drop in Eh, however, sulfate had no influence. Nitrate probably acted as an alternate electron acceptor whereas cyanide addition led to the death of bacterial populations.

Several inherent difficulties are discussed by *Ponnamperuma et al.* (1967) in the quantitative treatment of redox equilibria in flooded soils: flooded soils are highly complex and dynamic systems especially in the early stages of flooding which prevents the establishment of true equilibrium; a large number of redox couples are influencing the system at any given time which can lead to uncertainty; and the coexistence of localized zones of differing redox potential, i.e. the interior of a soil aggregate as compared to a large pore, makes for uncertainty in measurements of the true potential of the system.

2.2. Lawrence Berkeley Laboratory Investigations

During the last two years, Lawrence Berkeley Laboratory (LBL) and the Sanitary Engineering and Environmental Health Research Laboratory (SEEHRL) at the University of California at Berkeley have been investigating the effects of selenium contamination and the mechanisms of selenium migration throughout geologic, plant and animal systems at Kesterson Reservoir. An intensive research effort has been undertaken to develop an understanding of the geochemical conditions and processes that determine to what extent selenium contamination of surface and groundwater will continue and can be controlled. It is the purpose of this section to briefly summarize major findings and conclusions of early work that dealt with issues of selenium mobility and transformation throughout soils of the Reservoir and that led to the Pond 1 experiment. In general, this section draws on work printed previously in the Lawrence Berkeley Laboratory Progress Reports 1 through 8 and the Lawrence Berkeley Laboratory Annual Report completed in December 1987. This material is reviewed and included because it constitutes a major literature source on important aspects of selenium chemistry and is necessary in order to understand the reason why the Pond 1 experiment was conducted.

The review of relevant literature and early observations of the distribution of selenium throughout the soils and groundwater at Kesterson guided much of the early research that was done at the Reservoir. As was mentioned in an earlier section, the chemistry of surface, interstitial and ground waters demonstrated evidence of direct communication through

similarities in salinity and the presence of trace elements, such as boron. However, in interstitial waters and groundwater, selenium was generally found in concentrations lower than 10 ppb while surface water ranged from approximately 200 to 400 ppb. In Figure 2.1 we see, in a large collection of data gathered from a diverse set of measurements, that the distribution throughout the soil profile at Kesterson has been highly skewed towards the accumulation of selenium in the near-surface sediments suggesting a mechanism that preferentially removes selenium from infiltrating pond water and precipitates it in shallow soils. The primary removal mechanism has been proposed to be the reduction of selenium species by bacterial activity to elemental and organic forms which are generally insoluble. An early question was whether selenium is metabolically reduced by anoxic reactions in bacteria or is inorganically reduced by microbially mediated processes *(Lawrence Berkeley Laboratory,* 1985 p. 4-10). In the case of selenate, however, there is now little doubt that the latter of the two proposed mechanisms does not occur, leaving metabolic reduction by microbes as the remaining possibility *(Weres,* Personal Communication).

Three distinct geochemical regimes have been characterized at Kesterson: surface waters, the shallow, organic-rich pond muds, and groundwater *(Lawrence Berkeley Laboratory,* 1986b p. 16). The water in the Reservoir is in contact with air and is therefore relatively rich in oxygen. Consistent with an oxidizing environment, most of the selenium present in surface water is in the form of the highly soluble and mobile selenate ion. The selenate/selenite ratio is in apparent equilibrium with oxygen saturation *(Weres et al.,* 1985).

Measurements made in the shallow pond sediments using a platinum electrode indicated conditions there can be much more reducing (-140 mV to -410 mV) than in the surface water (+80 to +310 mV) *(Lawrence Berkeley Laboratory,* 1985 p. 4-10). Further observations in interstitial waters indicated that high concentrations of hydrogen sulfide correlate with low Eh (Figure 2.2) and that soluble selenium is not found under mildly-reducing conditions (Figure 2.3).

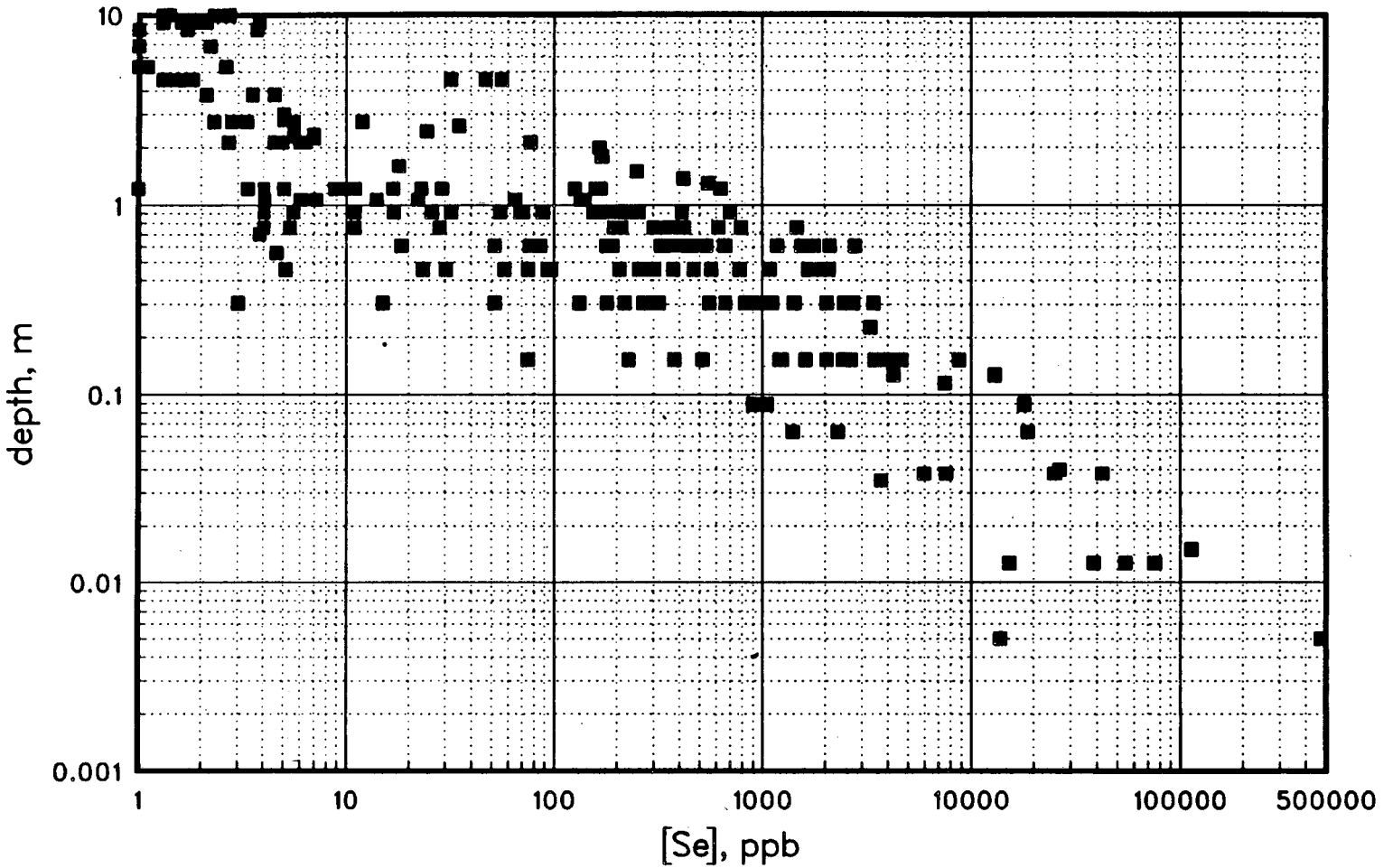

Figure 2.1 Vertical distribution of selenium in soils and groundwater at Kesterson.

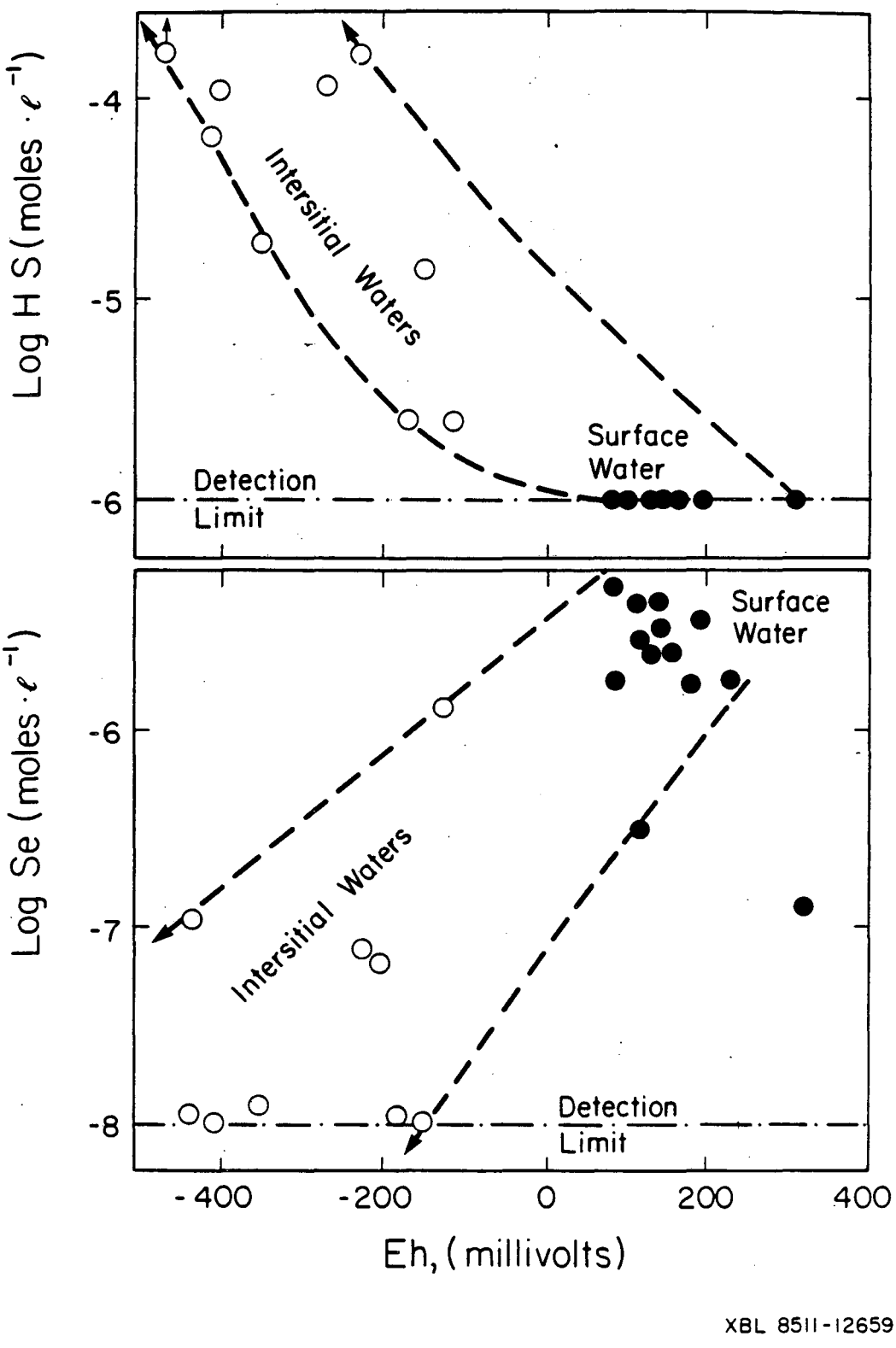

Figure 2.2 Relationships observed between total selenium, dissolved hydrogen sulfide, and Eh for surface and interstitial waters.

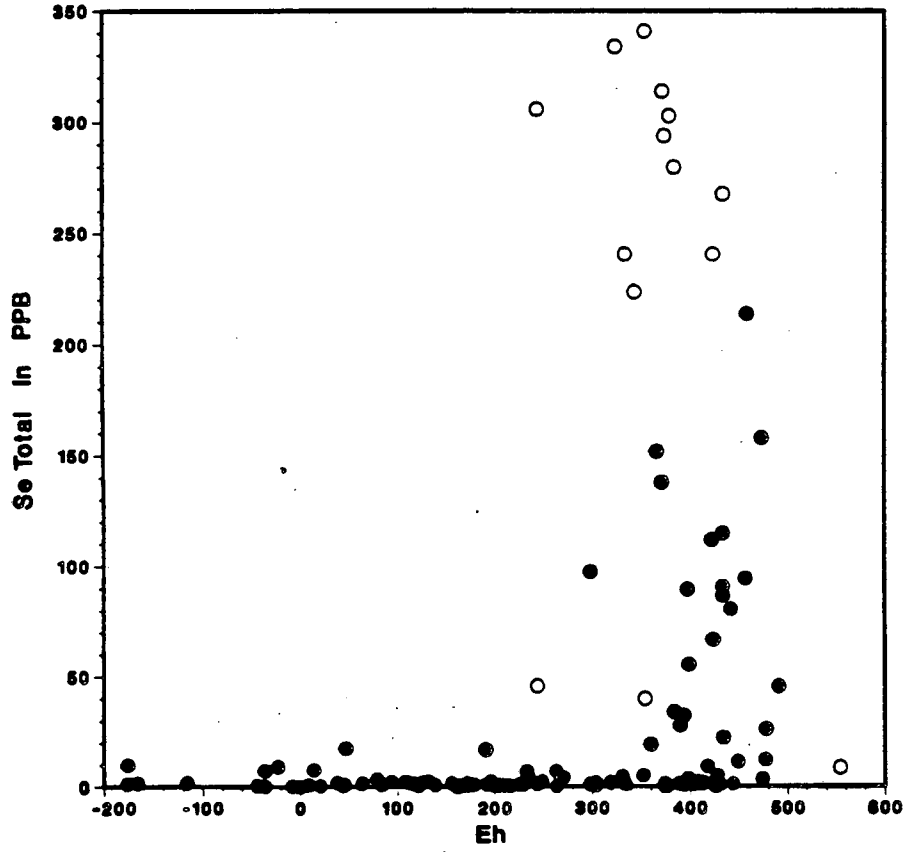

Figure 2.3 Total selenium concentration vs Eh for water samples collected at Kesterson. Open circles represent surface water and the closed circles groundwater.

In the muds, an abundance of organic matter causes H_2S to form. Reducing conditions in these shallow soils are controlled by the presence of H_2S produced through anaerobic activity. In groundwater, H_2S is generally absent suggesting a lack of significant organic content. Waters underneath the Reservoir, while containing little oxygen, are found to be actually neutral to slightly oxidizing. Mildly reducing environments, however, may also be microbially mediated, and are characterized by the presence of dissolved Fe^{+2} and Mn^{+2}. Experiments involving injection of selenium into native groundwater and infiltrated drain water demonstrated that selenium will not remain in a soluble form in the groundwater when nitrate is absent.

Soluble selenium is found at Kesterson at significant levels only when Eh $\geq$ 300 mV. H_2S and Fe^{+2} correlate strongly with low Eh, suggesting that the redox potential is controlled by the presence of these two ions *(Lawrence Berkeley Laboratory,* 1986a p. 46). Therefore, selenium is mutually exclusive relative to dissolved H_2S and Fe^{+2} (Figures 2.4 and 2.5). The presence of an oxidizing region in groundwater or soil water does not guarantee the presence of selenium, but in no instances has selenium been found in a zone of reducing conditions. Underneath the middle of Pond 2, even though drainage water has penetrated to a depth of 30.5 m (100 ft), the groundwater at that depth is low in selenium. Where selenium has migrated into the groundwater, the vertical distribution of selenium does not correlate with the maximum vertical penetration of pond water, however, it does correspond to the depth at which the groundwater becomes reducing *(Lawrence Berkeley Laboratory,* 1986a p. 50).

The presence of nitrate in water has been recognized as an inhibitor to the removal of selenium from water, probably through competition with selenate in the reduction process. Nitrate is an oxidant, and is utilized by microbes present in soil as an electron acceptor in the decomposition of organic matter after available oxygen has been depleted. Selenate is also utilized as an electron acceptor by bacteria, however, the energy gain in the electron transfer with selenate is low as compared to nitrate. Therefore, until available nitrate is depleted, selenate is not consumed. A significant correlation exists between the Eh of water and the

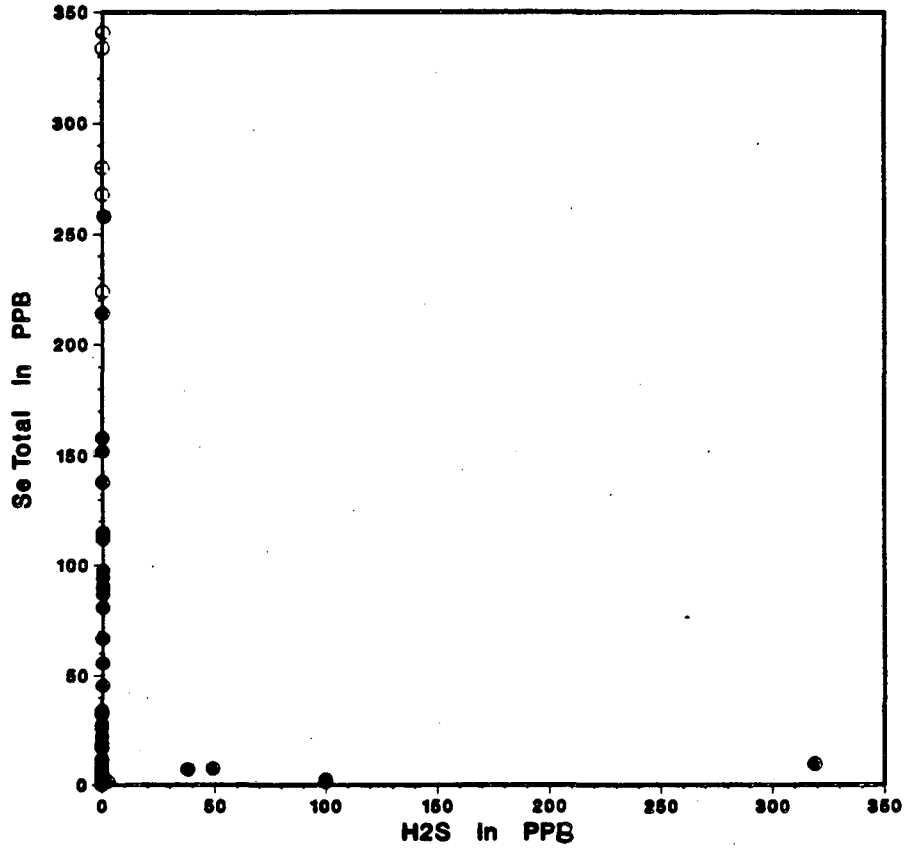

Figure 2.4 Total selenium vs dissolved hydrogen sulfide. Open circles represent surface water and the closed circles groundwater.

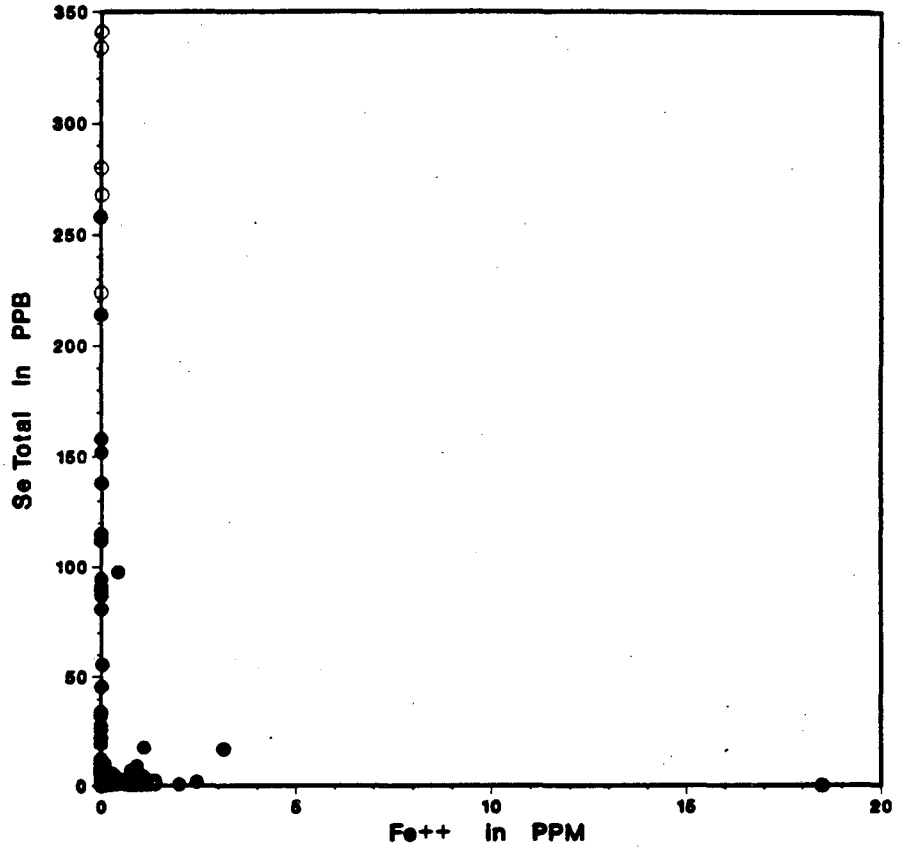

Figure 2.5 Total selenium vs ferrous iron. Open circles represent surface water and the closed circles groundwater.

presence of nitrate (Figure 2.6) *(Lawrence Berkeley Laboratory,* 1987a p. 17). Nitrate has been found to be mutually exclusive relative to Fe^{+2} (Figure 2.7). In places where nitrate has migrated into the aquifer, nitrate produces oxidizing conditions which cause Fe^{+2} to precipitate and selenium to remain in solution. Low nitrate in general corresponds to low selenium and vice versa.

In the pond bottom interstitial waters several potential mechanisms were identified for the removal of selenium: biological uptake in metabolic bacterial reactions as with sulfur, inorganic reactions with H_2S (applies only to selenite), and adsorption of selenite. Column experiments were performed on cores collected from surficial sediments of Pond 1. The removal of selenite appeared to be the result of sorption. Sterilization and the presence of nitrate did not affect its removal. The removal of selenate, however, required microbial activity. Sterilization completely blocked its removal. Selenate removal was inhibited by nitrate and by drying *(Lawrence Berkeley Laboratory,* 1987b p. 54)

It is fairly well established that as groundwaters become reducing, selenium is removed from solution, however, the mechanism is still not well understood. Potential selenium removal mechanisms in groundwater were identified as: reduction with dissolved ions such as ferrous iron and manganese, reactions at the surfaces of electrochemically active sites of minerals such as iron oxides, and possible reduction by microbes *(Lawrence Berkeley Laboratory,* 1987b p. 50). Laboratory studies indicate that selenite may be removed purely by adsorption. An experiment that involved extracting groundwater from the subsurface at two well locations, one located in a zone of reduced groundwater and the other screened in oxidizing groundwater, and then injecting the samples with known amounts of selenate and selenite indicated that aqueous reduction does not control selenium removal. Rather, the removal appeared to be related to the aquifer substrate itself, either through sorption or microbial reduction. Since selenate does not adsorb to any significant extent, selenate removal in groundwater is probably microbially mediated.

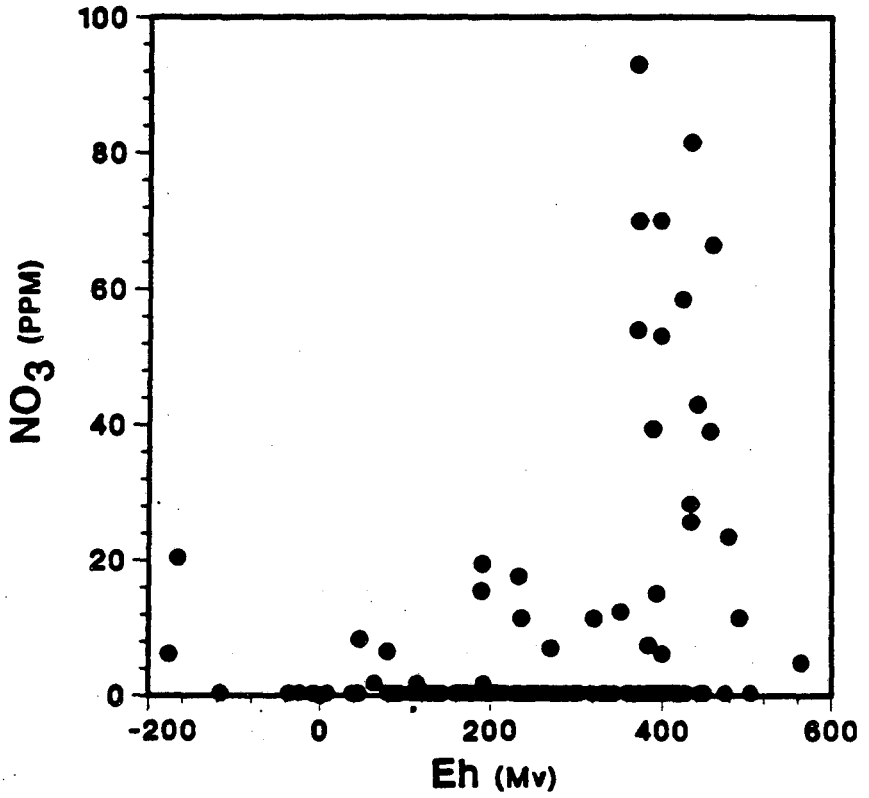

Figure 2.6 Eh vs nitrate in groundwater samples.

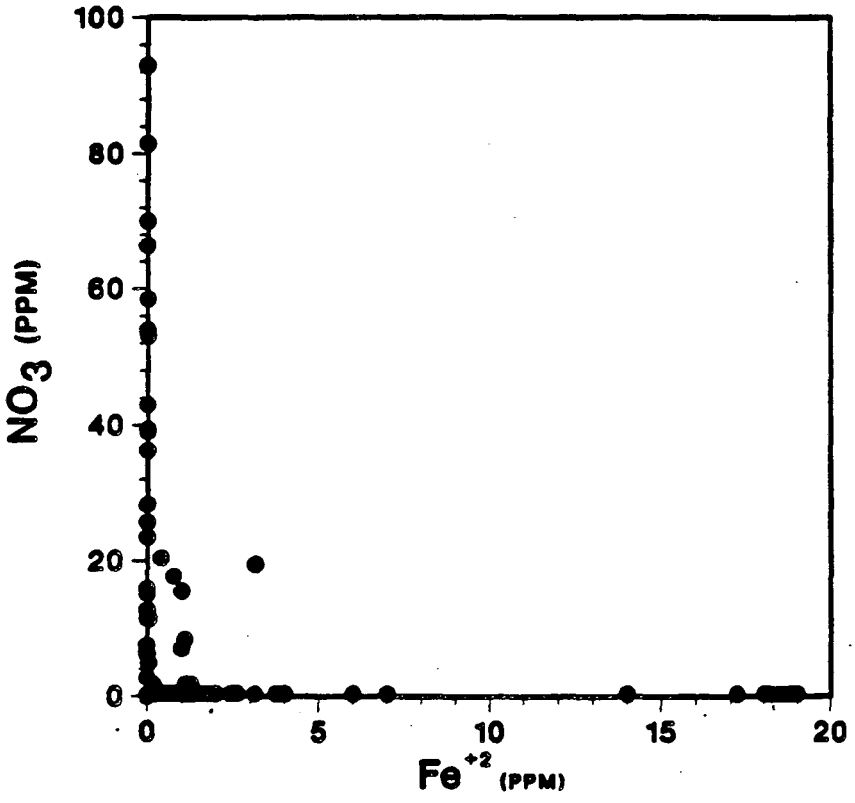

Figure 2.7 Ferrous iron vs nitrate in groundwater samples.

2.3. Remedial Measures Considered for Kesterson Clean-Up

Early results of research that took place at LBL in 1985 had important implications in the design of possible remedial strategies that the Bureau might consider at Kesterson Reservoir. There appeared to be features in the chemical behavior of selenium and certain conditions present in the shallow soils that could be taken advantage of in an innovative approach to reducing the mobility of selenium throughout the environment and the exposure to wildlife through food-chains. In Figure 2.8 we see a schematic that summarizes the conceptual model of selenium and sulfur geochemistry and mobility throughout the biosphere at Kesterson. Selenium in the surficial waters is in contact with oxygen and therefore is oxidized and highly mobile. By far the great majority of selenium in the pond water is in the form of the selenate ion. Within the organic rich sediments, anaerobic activity maintains a reducing environment, with little or no oxygen and high concentrations of hydrogen sulfide (H_2S). As water infiltrates through this region, selenium is removed and immobilized within the soil matrix. Any selenite ion present probably adsorbs onto organic detritus, clay minerals and/or iron hydroxides. The selenate ion, either directly or indirectly is reduced by microbial activity and precipitates as a trace constituent in sulfide minerals or as a selenide mineral or elemental selenium. Selenium that is present in solution is available to plants through root uptake where it is able to enter into the food chain. Sulfate, however, is not removed from infiltrating water nearly to the degree that selenate is. The groundwater contains a considerable amount of sulfate.

This conceptual model was the motivation for a remedial action plan called the Flexible Response Plan (FRP), which came to be called *Wet-Flex*, based on taking advantage of the biogeochemical conditions present in the Reservoir ponds. The southern ponds, where the majority of the drain water had been directed and which therefore had the highest concentrations of selenium, were to be continuously flooded with moderately saline and low selenium water (< 1 ppb). The selenium present in the soils would be immobilized by maintaining reducing conditions brought about by the decay of vegetation growing naturally in the ponds. The northern ponds, where less drainage water had been discharged, would be managed

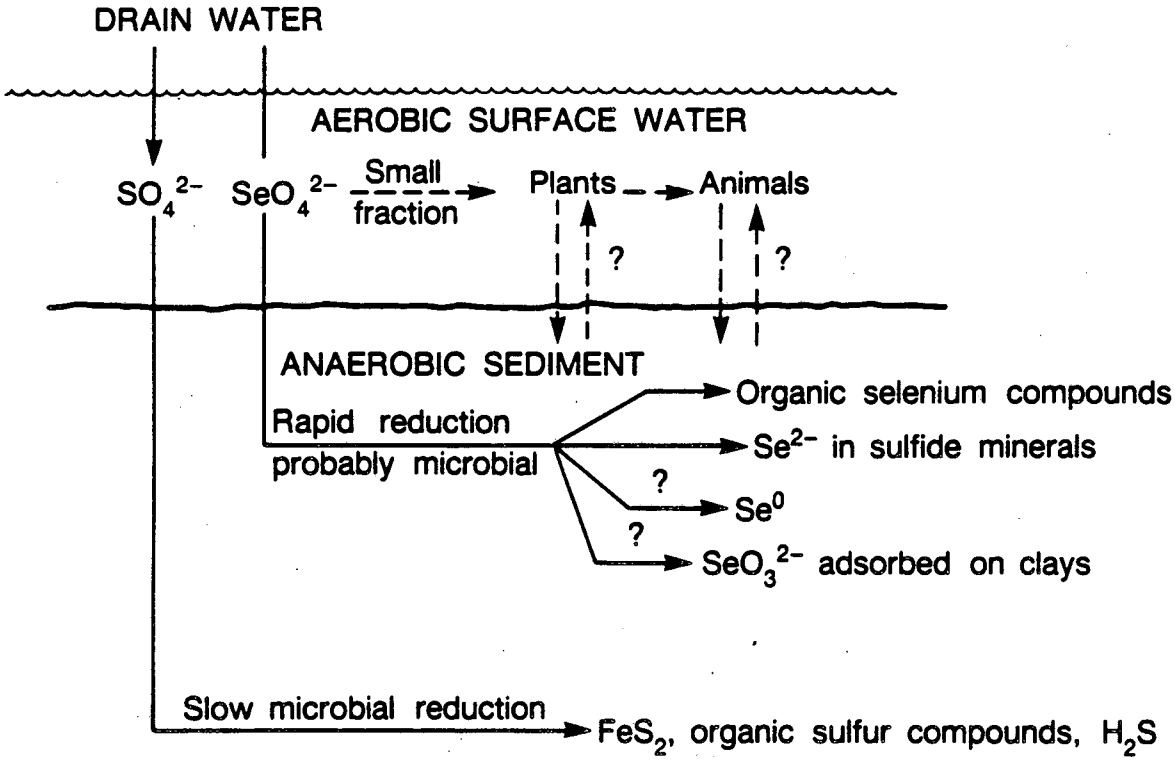

Figure 2.8 Schematic of the selenium and sulfur geochemical model at Kesterson Reservoir.

differently using some combination of tilling and harvesting.

If continued monitoring indicated that environmental goals were not being attained, then additional measures would be taken under the *Immobilization Plan.* This level of remediation was similar to the Flexible Response Plan but it involved extra features such as the harvesting and hauling of vegetation in the southern ponds and raising of pond water levels to discourage regrowth.

If monitoring indicated that wildlife was still not being adequately protected the *Onsite Disposal Plan* (ODP) would be implemented. This option involved drying the ponds, excavating the uppermost 0.15 m (0.5 ft) of soil from ponds 1 through 4, and excavating the remaining soils where selenium concentrations exceeded 4 ppm total selenium. All contaminated soils and vegetation would be stored in an engineered landfill located in the western portion of Pond 3. The entire Reservoir was then to be disced to a depth of 0.30 m (1 ft). An off-site disposal plan involving excavating 0.15 m (0.5 ft) Reservoir-wide was also considered at one time, however, the enormous cost involved precluded the plan from ever receiving serious attention.

The plan recommended by the Bureau was to be a phased approach, involving first the Flexible Response Plan and then the Immobilization and Onsite Disposal Plans if monitoring of surface water, groundwater, air, and wildlife indicated that certain environmental requirements were not being met. The goals were 2 to 5 ppb in pond water, 10 ppb in groundwater, and 3 ppm in food-chains.

3. POND 1 RESATURATION MONITORING

3.1. Purpose

Pond 1 Resaturation Monitoring was an experiment performed principally as a means of evaluating the effectiveness and risk-potential of the Phased Approach remedial action plan proposed for Kesterson Reservoir cleanup. Maintaining the Kesterson ponds in a permanently flooded condition as set-forth in the Wet-Flex plan would involve, at least, an initial flooding period, followed potentially at instances in the future, by additional periods of pond re-flooding due to potentially unavoidable or inadvertent periods of pond-drying. Most of the selenium present under the oxidizing conditions of the vadose zone, would be in the form of the selenate ion. There was some concern, based on the highly soluble and mobile nature of selenate, that the flooding of aerated pond bottom soils could drive unacceptably high concentrations of selenium downward to shallow water-bearing units. This experiment, therefore, was designed to monitor, during pond re-flooding, selenium fluxes through the near-surface sediments and into groundwater and to test for selenium removal from solution and subsequent immobilization into the soil matrix. Important questions to be addressed included: would the geochemical conditions of the shallow sediments promote selenium removal; to what extent would selenium removal occur and at what rate; would selenium immobilization be sufficiently effective to prevent contamination of groundwater; and what were the physical parameters that either enhanced or inhibited selenium removal.

3.2. Monitoring Site Installation

At nine sites in Pond 1 (UZ-1 to UZ-9), during the summer of 1986, a series of unsaturated and saturated zone monitoring devices were installed, including: soil water samplers, soil moisture tensiometers, and shallow groundwater monitoring wells. The instrumentation at each site comprised a monitoring package that provided depth profiles of soil suction and pore water chemistry. Refer to Figure 3.1 for the locations of sites UZ-1 through UZ-9.

The criteria used to locate the sites involved a loose consideration of several factors

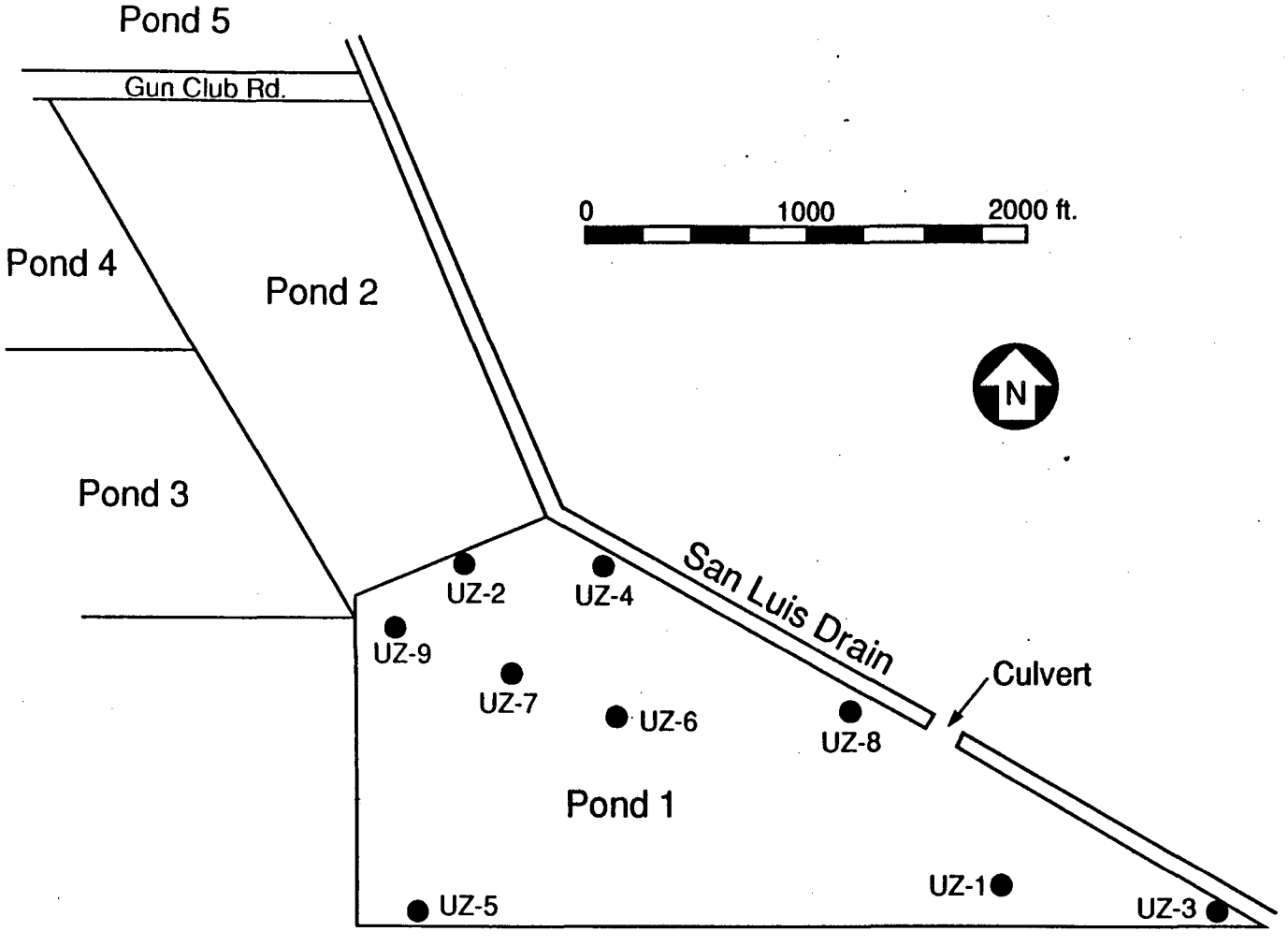

Figure 3.1 Pond 1 in plan view with the 9 UZ-series monitoring sites.

including expected clay thickness, elevation, and environment. An effort was made to position the sites so as to cover a range of clay thicknesses, differing elevations, and to include sites within the three major environments at Kesterson Reservoir, namely the playa, saltgrass, and cattail environments.

The monitoring packages at each site were nearly identical and included tensiometers and soil water samplers installed at depths of 0.15 m to 1.22 m (0.5 ft to 4 ft) at 0.15 m (0.5 ft) depth increments. The soil water samplers and tensiometers were supplied by Soil Moisture Equipment Co. of Santa Barbara, California. Some of the sites differed slightly in that, for reasons of instrument supply or delivery delays, the monitoring package was deficient a tensiometer. The instruments were arranged on a north-south orientated 2.7 m x 2.7 m (9 ft x 9 ft) grid. In order to prevent the water samplers from having an impact on tensiometer readings (during unsaturated conditions), tensiometers and water samplers of comparable depth were not located adjacent to one another. Refer to Figure 3.2 for a plan view of the configuration of the tensiometers and soil water samplers at each of the sites. Two of the sites, UZ-1 and -2 differed from this layout in that the instruments were positioned in a slightly different physical arrangement, however, the pond area that they extended over was essentially the same. Also, site UZ-2 was only equipped with 5 soil water samplers and tensiometers each, and they were installed to depths of 0.15 m (0.5 ft), 0.30 m (1.0 ft), 0.46 m (1.5 ft), 0.51 m (1.67 ft), and 0.71 m (2.33 m).

Installation of the tensiometers and soil water samplers was performed through the use of a gasoline-powered two-man auger. A 0.10 m (0.33 ft) diameter vertical hole was drilled to the appropriate depth and then backfilled with the instrument in place using the same material that was removed during drilling. The soil was compacted with a tamping rod around the instrument. Care was taken, especially in the case of the water samplers, to prevent any soil from the upper 0.15 m (0.5 ft) of sediments from being placed near the porous ceramic cup located at the tip of the instrument. An effort was made to place backfill to approximately its original depth. Figure 3.3 is a schematic illustration of an in-place soil water sampler.

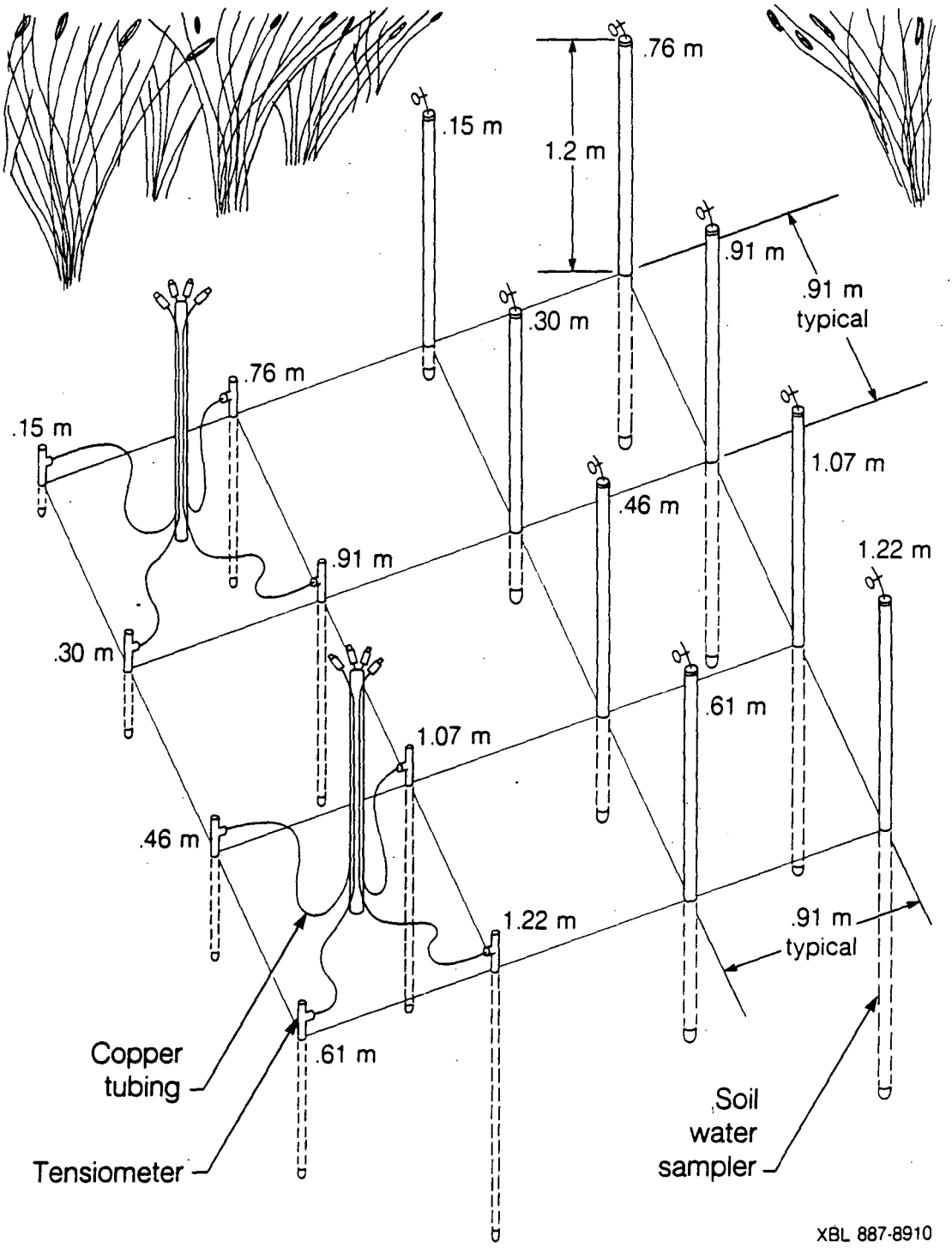

Figure 3.2 Plan view of a typical monitoring site layout.

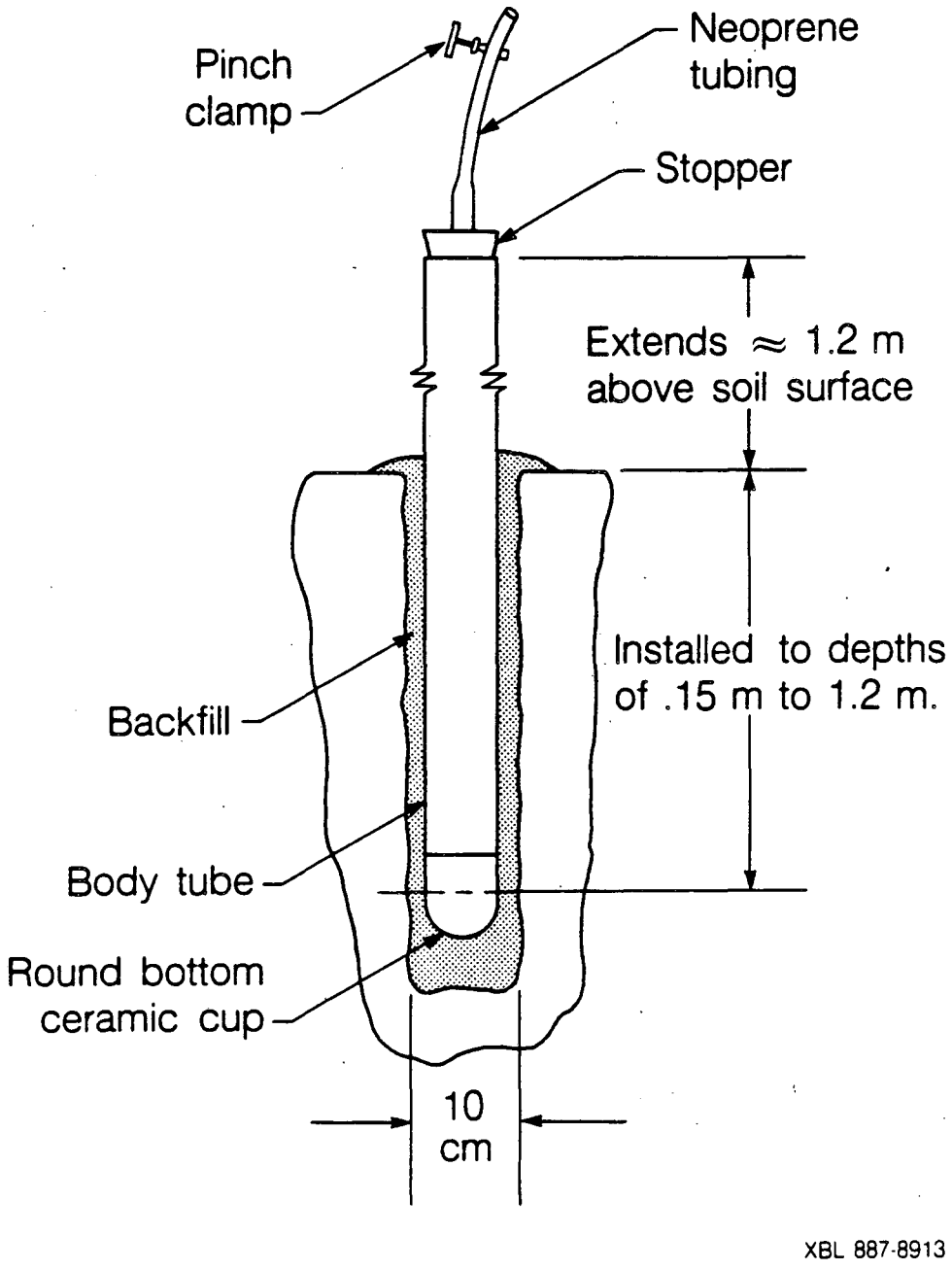

Figure 3.3 Soil water sampler schematic.

In addition to the instrumentation installed for measurements in the near-surface region, shallow groundwater monitoring wells were drilled and installed at each site for the collection of water samples from discrete intervals in the shallow aquifer. Each site was equipped with at least one well screened within the upper 0.6 m (2 ft) of the pre-flooding water table. At three sites, deeper nested wells were completed covering the interval from 3.0 m to 12.2 m (10 to 40 ft). These nests consist of six wells, screened from 3.0-4.6 m (10-15 ft), 4.6-6.1 m (15-20 ft), 6.1-7.6 m (20-25 ft), 7.6-9.1 m (25-30 ft), 9.1-10.7 m (30-35 ft), and 10.7-12.2 m (35-40 ft). During the drilling of these wells, undisturbed soil samples (Shelby Tube cores) from the ground surface to 3.0 m (10 ft) were collected and preserved for laboratory column experiments to be performed by others. Disturbed samples (Shelby Tube and split spoon) were collected from 3.0 to 12.2 m (10 to 40 ft) for lithologic classification and particle size analyses.

3.3. Data Collection

3.3.1. Sampling Frequency

Prior to flooding, monitoring packages installed in Pond 1 collected base line water quality and soil suction data in the unsaturated pond bottom sediments. Tensiometers were read weekly and samples of the soil water were collected every two weeks for chemical analyses. Flooding was initiated on October 27, 1986 through the opening of the culvert directly connecting San Luis Drain and Pond 1 along its northeastern edge. A flow of approximately 5 cfs was maintained for one week and then reduced roughly by a half. Water was allowed to flow into the pond at approximately this rate until late spring. Five sites (UZ-1, -3, -5, -6, and -8) were flooded within the first week to depths of approximately 0.1 to 0.5 m depending on the elevation of each site. Pond water increases then slowed considerably, varying gradually for the remainder of the experiment. Pond water depths at the 5 sites were maintained, in general, between 0.2 and 0.6 m, with a maximum pond water depth during the course of the experiment of 0.7 m. Four of the sites (UZ-2, -4, -7, and -9) were located at elevations above or just a few inches below the steady-state pond elevation and were never submerged by surface waters from above. The rise in the local groundwater elevation was

observed throughout the experiment, and at two sites, (UZ-2 and UZ-4), the water table rose to a level approximately equal to that of the ground surface. These sites were technically submerged, but not by surficial waters from above, and never by more than a few inches. Wetting at these two sites occurred over much longer time periods than at the five flooded sites, and it was difficult to determine the moment in time that they were actually flooded. These two sites then, though certainly of value in the examination of aspects of selenium mobility, did not necessarily lend themselves to an analysis like that performed on the other five sites and so were essentially excluded from consideration. Sites UZ-7 and UZ-9 were never flooded and remained dry for the duration of the experiment. Data collected at these two dry sites, as well, were not dealt with in this study since the experiment was specifically performed to evaluate the effects of pond flooding on selenium distributions throughout the soil and groundwater. Therefore, out of a total of 9 original sites, the discussion and analysis presented here are primarily restricted to data collected from the five wetted sites. Data from all of the sites, however, are presented in tabular form.

Water that was allowed to flow into Pond 1 was supplied from the San Luis Drain and was composed of a mixture of Delta-Mendota Canal water that had been present in the drain prior to flooding and groundwater. Groundwater was supplied from 10 wells located adjacent to the Drain in the northern portion of the Reservoir. Selenium analysis of samples collected from the water supply wells during the first flooding episode revealed that selenium concentrations in the groundwater were $\leq$ 3 ppb with most of the samples $\leq$ 1 ppb. Samples collected from the Drain at the weir into Pond 2 showed that selenium concentrations in drain water were slightly higher. Samples collected through the end of March 1987 contained selenium at concentrations $\leq$ 20 ppb whereas levels then dropped to $\leq$ 5 ppb. Electrical conductivity (EC) of the Drain water (uncorrected for temperature) ranged from 3 to 9 dS/m over the course of the first flooding episode with the higher values representing typical conditions during summer months.

After flooding Pond 1, an intensive sampling program was undertaken. Soil water samplers

at flooded sites were sampled at intervals of a few days to a week immediately following their submergence in order to monitor the rapidly changing solute distribution throughout the soil profile. Sample intervals were gradually reduced to two weeks and finally one month as conditions became less transient. Tensiometer measurements were made at intervals at least as frequent as the sampling intervals. Shallow groundwater monitoring wells, however, were sampled much more infrequently. Samples of groundwater underneath each site were collected roughly every 3 to 6 months.

Water was allowed to flow into Pond 1 from the SLD throughout the winter months. Due to increased evaporation in the late spring and summer, however, the drying of adjacent duck ponds, and insufficient water supply, large areas of the pond began to dry out in June and July of 1987. Two of the sites remained wet through August. Eventually, the entire pond dried out, and was then reflooded during November 1987 in a re-enactment of the original experiment. Even though data continued to be collected during the second flooding event, the presentation of data and the discussion of results reported in this study pertains primarily to the first flooding event only. Total experiment time-frames ranged from approximately 200 to 300 days. The unit of time used throughout this report for the presentation of temporal data is *days*. Day 1 was chosen arbitrarily as July 25, 1986. This is approximately when instrumentation first began to be installed in Pond 1. The time at which flooding occurred at the various sites for the two flooding episodes is included in Table 1 below along with the approximate day that each site returned to a dry condition prior to re-flooding in November, 1987. This information is useful when viewing plots of solute concentrations vs time or when examining the data in tabular form in Appendix II. The selection of specific instants in time when flooding and especially drying took place is not meant to imply that the events actually occurred so abruptly, but has been done out of a practical necessity to know, in general, when a particular site was under ponded conditions and when it was not.

Table 1. Wet/Dry Periods at Pond 1 Monitoring Sites

Site	Day of First Flooding	Approximate Day of Drying-Out	Day of Second Flooding
UZ-1	96.5	300	479.25
UZ-3	97.8	300	482.875
UZ-5	100	340	485.
UZ-6	97.5	400	482.04
UZ-8	95.5	400	477.625

Day 1 = July 25, 1986

3.3.2. Soil Water Sampling and Fluid Potential Measurement Procedures

The soil water samplers are 5 cm (1.9 in) diameter PVC tubes fitted at one end with a porous ceramic cup and at the other with a neoprene stopper and associated rubber tubing (Figure 3.3). In order for a sample of soil water to be collected, the fluid potential must be lower inside the sampler than outside. When the adjacent pore spaces are only partially saturated, this is accomplished by evacuating air from the soil water sampler with a hand held vacuum pump. The sampler is sealed with a pinch clamp and stopper, and a sample of the soil solution accumulates within the tube. The rate at which water enters the sampler depends on the unsaturated hydraulic conductivity of the soil, the soil moisture content, and the suction that has been applied to the sampler. In general, in this experiment, suction of 30 to 80 centibars was applied to the soil water sampler depending on the moisture conditions (depth). Time periods of a few hours to several days were often required to collect the minimum sample volume of ≈ 20 ml. During ponding, there was no need to apply a vacuum to the sampler, since the fluid potential of soil water under saturated conditions is slightly higher than that in an evacuated sampler.

In either case, after sufficient water for chemical analysis had collected in the sampler, the sampler was completely evacuated and a small sub-sample saved for analytical purposes. In this experiment this was accomplished by several methods. If the total quantity of sample in the sampler was small, i.e. $\simeq < \frac{1}{2}$ liter, a 100 ml plastic syringe connected to a hand vacuum pump was lowered into the sampler at the end of a 2.5 m (8 ft) length of Tygon tubing. Prior to lowering the syringe into each soil water sampler, the interior and exterior of the syringe as well as all tubing was thoroughly rinsed with distilled water. Before a sample was collected and saved for analysis, at least one syringe volume was withdrawn and discarded as a means of rinsing the syringe interior with soil water. The second or third syringe volume was retained as the sample. This method was performed during dry conditions when the amount of sample was often limited. During ponding, the amount of water collected in a soil water sampler was usually far in excess of that required for analysis. Complete evacuation of the sampler was required during each sample collection. The syringe method was simply too slow when the total evacuation volume was on the order of several liters. The large number of samplers involved in the experiment necessitated an efficient and rapid sampling procedure. Therefore, a Black and Decker hand operated peristaltic water pump was used in order to be able to quickly evacuate the sampler. The Tygon tubing, at one end, was equipped with a small check valve to prevent cross-contamination of samplers, and at the other, was attached to the peristaltic pump. The check valve and tubing were lowered down into each sampler. As with the syringe method, all materials that were lowered into a soil water sampler were thoroughly rinsed, inside and out, with distilled water. A considerable portion of the sampler volume was then pumped through the tubing and discarded prior to the collection of the sample in order to further rinse out the interior of the tubing and pump with sample water.

Eventually, a dedicated sampling system was constructed and installed at all of the sites that brought about a considerable savings of time and effort by eliminating the need for constant rinsing. This method did not involve any potential cross-contamination problems brought about by the the introduction of various objects into the samplers. The system was installed

just prior to the second flooding event. The sampling methods that were used throughout the first flooding event often seemed inefficient and time-consuming, and there was some potential for contamination of samples if adequate precautions failed to be taken. The procedure that was adopted, however, was standardized and strictly conformed to by all those involved in sampling. The consistency of the analytical results from sample to sample brought about by adherence to the decontamination procedure indicated that cross-contamination was not a significant problem in this experiment.

Soil suction tensiometers provided data on the distribution of hydraulic head throughout the soil column and the change of this distribution with time. Modifications were made to these devices, in a manner suggested by *Marthaler et al.* (1983) in order to allow measurements to be made during ponded conditions. In Figure 3.4 we see a schematic diagram of a tensiometer as it was used in this study. The sealed-Reservoir and Bourdon vacuum dial gauge were removed from the tensiometer body where they were attached some 0.15 m (0.5 ft) above the soil surface. An approximately 2.5 m (8 ft) long copper extension tube was fitted at the gauge port and supported vertically so that its opposite end was at an elevation above any anticipated pond level. A short ($\simeq$ 5 cm), piece of clear, 1 cm diameter lucite tubing was fitted to the end of the copper tubing with appropriate couplings. The tensiometer, including the 1.22 m long copper extension, was then filled with water. A septum stopper, like ones commonly used in medical infusion systems, was fitted to the lucite tube, sealing the upper end of the tensiometer and leaving a small air-pocket, visible through the lucite, just below the septum stopper. A pressure transducer, with attached syringe needle and digital readout was used to make the tensiometer measurements. The needle is inserted through the septum where it reads the pressure in the air-pocket which is in equilibrium with the water in the tensiometer. Septum stoppers form air-tight seals during and after insertion of syringe needles.

The commercially available pressure transducer was acquired through Soil Measurement Systems, of Las Cruces, New Mexico. Briefly, the transducer consists of a steel enclosure with a

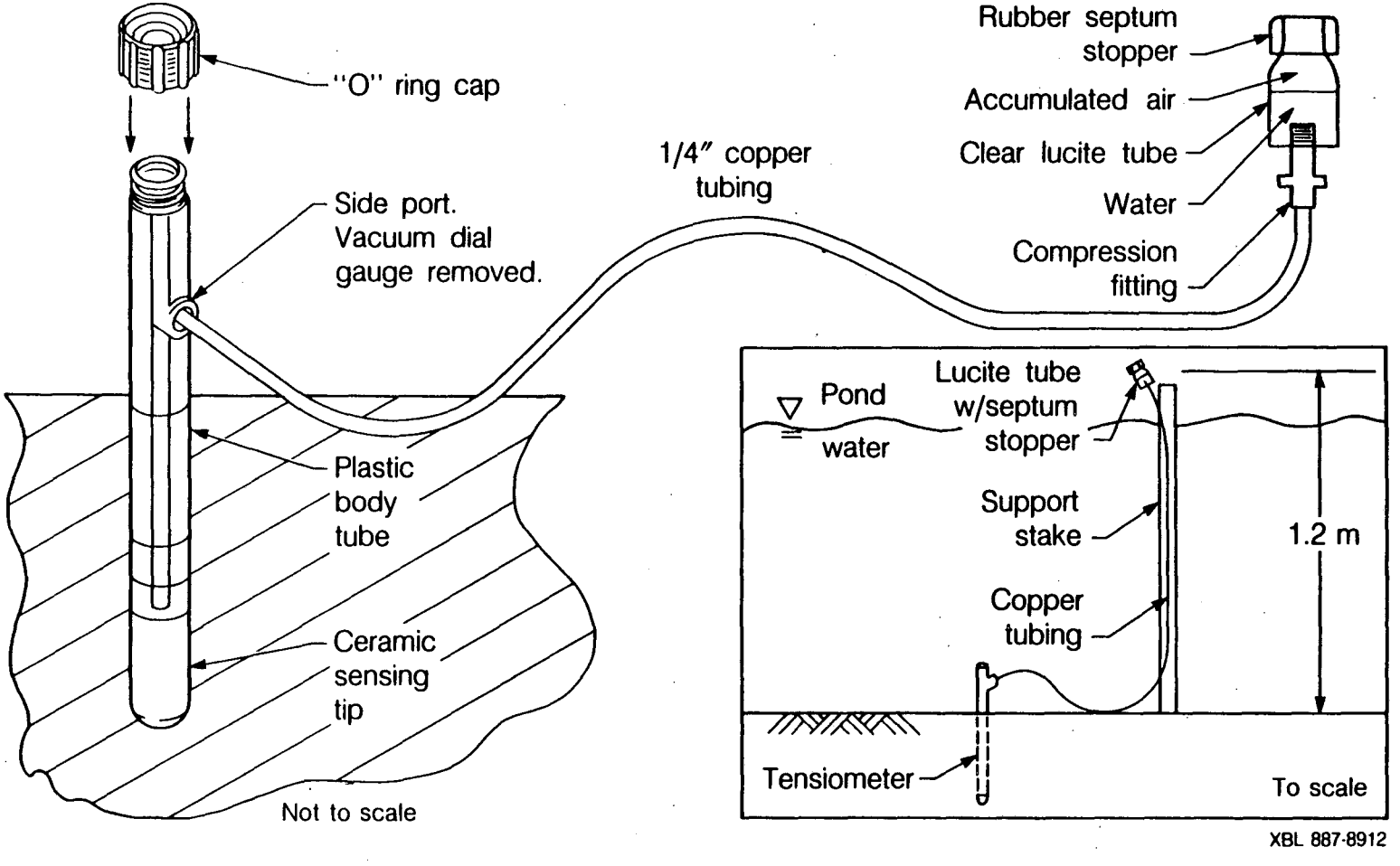

Figure 3.4 Diagram of a soil suction tensiometer indicating modifications that allowed for use under ponded conditions.

transducer membrane separating the enclosure into two chambers, the upper of which is at atmospheric pressure. Through the syringe needle, air pressure in the tensiometer equilibrates with the pressure in the lower chamber, thereby causing a small deflection of the transducer membrane and a change in the resistance of silicon semiconductors embedded in the membrane. A constant current source, pocket-sized resistivity meter with liquid crystal display and zero adjustment, reads directly in either millibars or centibars of water. An evaluation of the accuracy of this system by *Marthaler et al.* (1983) concluded that there is an excellent relationship between mercury manometer readings and the pressure transducer readings. The measurement procedure consisted of adjusting the meter to read 0 (atmospheric pressure) and then inserting the syringe needle through the septum stopper into the small air void above the tensiometer water. The reading was allowed to stabilize and was then recorded. To calculate the soil suction in meters of water with reference to the ground surface (z=0 at the ground surface) the height of water in the 1.22 m (4 ft) extension tube was subtracted from the resistivity meter reading and then converted from millibars to meters of water. With the following conversion factors:

$$1 \text{ millibar} = 10^3 \frac{\text{dyne}}{\text{cm}^2}$$

$$1 \frac{\text{dyne}}{\text{cm}^2} = 1.0198 \times 10^{-3} \text{ cm of } H_2O$$

The factor that converts millibars to head units is calculated as:

$$\frac{1.0198 \times 10^{-3} \text{ cm of } H_2O}{\frac{\text{dyne}}{\text{cm}^2}} \cdot \frac{10^3 \frac{\text{dyne}}{\text{cm}^2}}{\text{millibar}} =$$

$$= 1.0198 \frac{\text{cm } H_2O}{\text{millibar}}$$

$$= .010198 \frac{\text{m } H_2O}{\text{millibar}}$$

Therefore the stem height (1.22 m of H_2O) corresponds to the following millibar quantity:

$$1.22 \text{ m } H_2O \cdot .010198 \frac{\text{m } H_2O}{\text{millibar}} \approx 120 \text{ millibars}$$

and the fluid potential with reference to the ground surface is calculated from the meter readings with the following equation:

$$\text{fluid potential, m } H_2O = \left[\text{ reading + 120 mb}\right] \cdot \left[\frac{.010198 \text{ m } H_2O}{\text{millibar}}\right] \qquad (2)$$

3.4. Sample Analysis

3.4.1. Selenium

Analysis of selenium was performed by personnel in LBL's Earth Science Division Analytical Chemistry lab. The method used is based on hydride generation followed by atomic absorption spectroscopy. After filtering to eliminate interference by colloidal matter and without any further sample preparation, selenite is determined directly. In the determination of selenate, the sample is first treated to convert all the species to the selenite form and then analyzed as for selenite, resulting in a total selenium determination. The difference between the total selenium result and selenite is taken as the selenate, however, organic forms of selenium may also comprise some portion of this difference.

To convert the selenate ion to selenite prior to hydride generation, 5 ml of 12N HCl is mixed with an equal volume of sample and with 0.2 ml 2% ammonium persulfate in a screw-capped culture tube. The mixture is then heated in a boiling water bath for 10 minutes and allowed to cool before analysis by hydride generator AA.

Reducing agents in the water may mask inorganic selenium, producing low readings for total selenium. The ammonium persulfate removes interference by reducing agents, but may also oxidize some of the organic selenium compounds, causing some additional contribution to the total selenium determination and therefore the selenate concentration. If the sample is cloudy, smelly or otherwise suspect of being high in organics, hydrogen peroxide is used to remove all reducing agents and to fully oxidize the organic selenium *(Lawrence Berkeley Laboratory*, 1986b p. 22).

3.4.2. Chloride

For the chloride determination, two analytical methods were employed. The Mohr Titration method as discussed in *Skoog and West* (1963) was used for all samples analysed at LBL. In this method, a known quantity of sample (1 to 10 ml) is titrated with a silver nitrate ($AgNO_3$) solution of known concentration in the presence of chromate ion. The solubility of silver chromate is significantly greater than that of silver chloride. Therefore, the presence of the red silver chromate precipitate indicates the first excess of silver ion and the chloride endpoint. The silver nitrate solution is standardized against a sodium chloride standard. Attention must be paid to the acidity of the medium. The method will provide acceptable results only for solutions of nearly neutral pH (pH 7-10). For acidified samples, a few drops of sodium hydroxide (NaOH) were added to adjust the pH.

Because of the large number of samples requiring analysis, it became necessary to send out approximately 1/3 (400) of the samples chosen for chloride analysis to a private analytical laboratory - Soil and Plant Laboratory of Santa Clara, California. QuickChem Method No. 10-117-07-1-D was used with these samples. Chloride reacts with mercuric thiocyanate to form a strong, covalent complex which displaces thiocyanate. The free thiocyanate so produced reacts with aqueous iron(III) to produce red hexacyanoferrate(III). This ion absorbs strongly at 480 nm. A 1:10 dilution factor was required for nearly all of the samples analysed with this method. Potential interferents include substances which reduce iron(III) and mercury(III), and other halides (e.g. Br, and I) which also form strong complexes with mercuric ion. Approximately 50 samples analysed at LBL by Mohr Titration were included in the batch sent to Soil and Plant Lab in order to compare the results of the two methods. Very close agreement was observed, with the QuickChem method consistently resulting in chloride estimates that were from 95 to 100 % of those obtained by Mohr titration.

3.5. Redox Measurements

3.5.1. Electrode Construction and Installation

A dominant mechanism governing selenium solubility and immobilization in soil has been identified in the literature and by more recent investigators at LBL to be the redox potential. Therefore, a natural aim of an investigation into selenium removal is to examine the relationship between observed levels of soluble selenium and this parameter. In the present investigation, an attempt has been made to make measurements of Eh in the shallow pond sediments in the time period before and during a flooding episode. A *portable-type* Eh electrode was constructed in order to allow for field measurements to be made in shallow sediments quickly and at a variety of locations throughout the pond. *Permanent-type* electrodes were also installed at one site to monitor the temporal and spatial variation in Eh. Platinum was used as the inert electrode material because of its high degree of response to changes in redox conditions *(Bohn et al.,* 1985).

The portable-type electrode was constructed by machining a small diameter hole lengthwise through an approximately 1.22 m (4 ft) long 1.3 cm (0.5 in) diameter fiberglass rod. The rod was fitted with a sharpened tip to allow easy penetration into soil. A 4 cm (1.5 in) long piece of 0.06 cm (0.025 in) diameter platinum wire protruded through the drilled hole in the tip. The wire was glued along the side of the tip so that when the electrode penetrated into the soil, it remained secure from damage. Copper wire soldered to the platinum electrode ran through the inner portion of the rod and out the top where it was fitted with a banana plug for attachment to a voltmeter.

Four permanent-type electrodes similar to those described in *Blanchar and Marshall* (1981) were constructed and installed at UZ-3 (Figure 3.5), each with a platinum tip positioned at depths of 0.15 m (0.5 ft), 0.30 m (1.0 ft), 0.46 m (1.5 ft), and 0.61 m (2.0 ft). These electrodes were constructed from 1.9 cm (0.75 in) schedule 80 PVC. Small holes were drilled into the side of the tube at the specified depths and were then fitted with approximately 4 cm

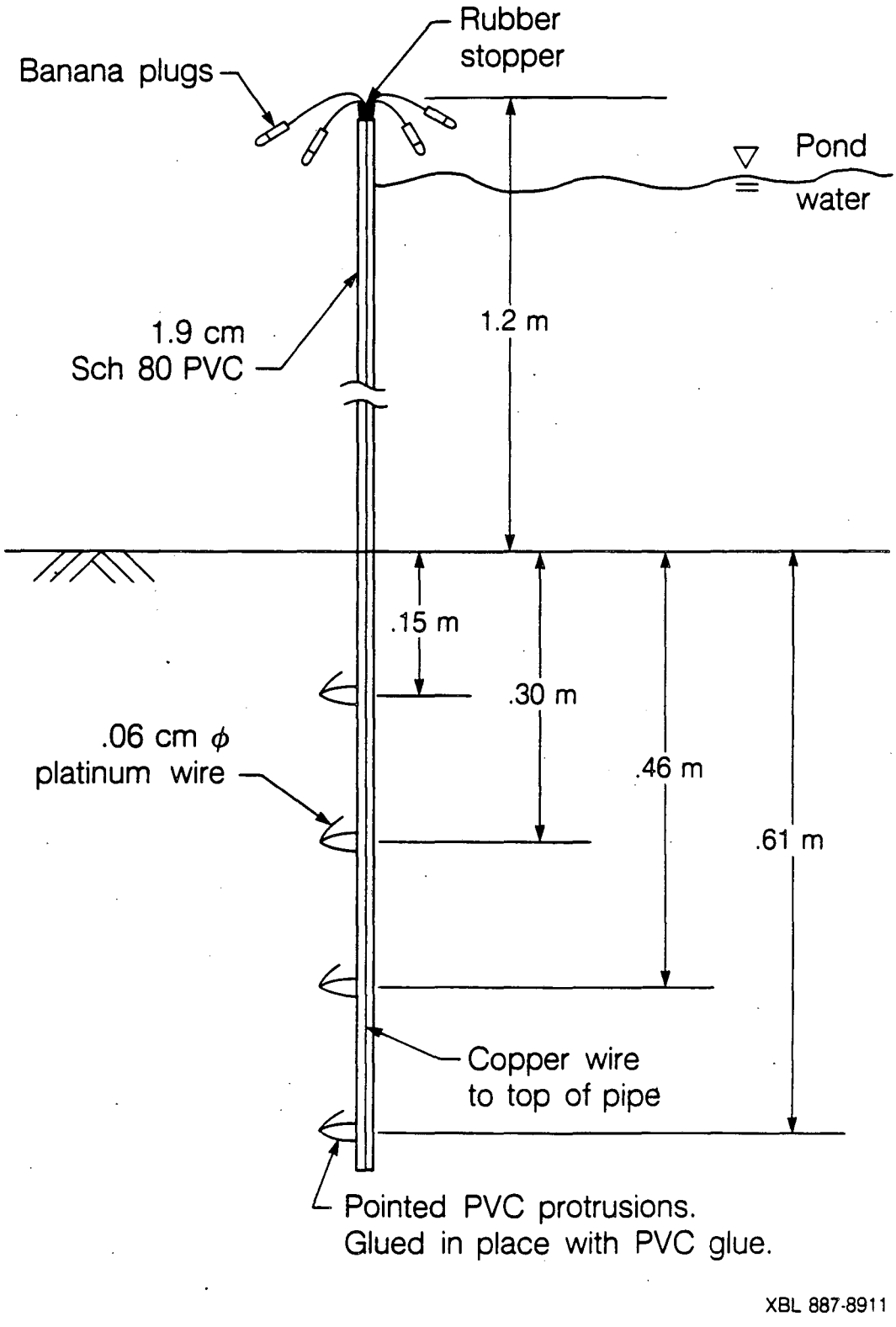

Figure 3.5 Permanent-type Eh electrode.

(1.5 in) long pointed PVC protrusions out of which 4 cm long platinum wires extended. Copper wire, soldered to the short section of platinum, then ran through the interior of the pipe and out through a sealed rubber stopper where they were then fitted with banana plugs. After the platinum wires were inserted through the pointed tips, each tip was filled with waterproofing silicon sealant to prevent water from leaking into the interior of each electrode.

Four 5 cm (2 in) diameter holes were dug with a slide-hammer punch device. The permanent Eh electrodes were then placed into the 0.61 m (2 ft) deep holes and forced up against the hole wall to push the PVC protrusions into undisturbed soil. The holes were then backfilled with original material. The four PVC tubes stood unsupported approximately 1.22 m (4 ft) tall, above any anticipated pond water level, and were positioned approximately 0.9 m (3 ft) from one another within the confines of site UZ-3.

3.5.2. Measurement Procedure

Measurements were made with a platinum electrode, a reference electrode (Calomel), and a potentiometer (voltmeter). The platinum electrode does not require standardization, however, performance checks were performed with prepared solutions of standard Eh. To convert the platinum electrode readings to Eh, a correction factor of +245 mV was added to account for the offset from the calomel reference electrode potential to the standard hydrogen electrode potential. This conversion factor is slightly temperature dependent, however, it has been neglected due to the rather large degree of uncertainty already associated with the measurement.

The measurement procedure in the case of the portable electrode involved dipping the calomel electrode into pond water, and inserting the platinum tip approximately 0.15 m (0.5 ft) into the soil. With the permanent electrodes, the reference electrode was dipped in water that had collected in an adjacent soil water sampler. Readings were recorded at 30 s or 1 min intervals up to a total time of 1 to 6 min. At the four sites without the permanent set-up, measurements were made at 5 to 10 random locations within the general vicinity of a given

site at intervals of a few days to a week after the pond was flooded. No attempt was made to return to the exact same locations over time at these four sites. The permanent site was monitored at approximately the same intervals.

Measurements were made with two different types of voltmeter models, a Fluke 77 Multimeter and Cole-Palmer Model 5996 pH Meter. The Fluke device, however, was used for nearly all of the measurements, especially during the early period of Eh monitoring just after flooding. The two meters were repeatable and returned similar results for a particular electrode placement, however, individual measurements with both meters demonstrated considerable drift, often continuing to change by as much as 5 mV units per minute after 5 minutes. In Figure 3.6 we see an example, in two separate measurements with each meter, of typical drift that was encountered. (The measurements shown were each made at separate locations, i.e. 4 different positions within the pond. It is not intended to show in the figure a comparison of the two meters at identical locations in the soil.) Among the measurements made with the portable Eh electrode, both meters exhibited a similar tendency to drift. At site UZ-3, however, where the platinum electrodes remained permanently fixed in the soil, the Cole-Palmer meter returned very stable readings while the Fluke meter continued to exhibit drift. The stable Cole-Palmer reading was very close to the initial reading made with the Fluke. While the explanation is speculative, it may be that the Fluke meter is an inappropriate potentiometer for this purpose due to its relatively low impedance. The drift observed with the portable arrangement in both meters may be related to a lack of equilibrium between the platinum electrode and the soil solution as compared to that in the permanent electrode set-up. Throughout the experiment, due to a failure to adopt a standard measurement procedure, the length of time spent collecting a single measurement varied from 1 to 5 minutes. Especially at the beginning of flooding, one minute readings were often the rule. Steady-state mV readings generally were not achieved during a particular measurement.

The question is raised, therefore - which value recorded (1 minute? 2 minute?) is most appropriate and how valid of an Eh estimate is being made? For reasons discussed in a

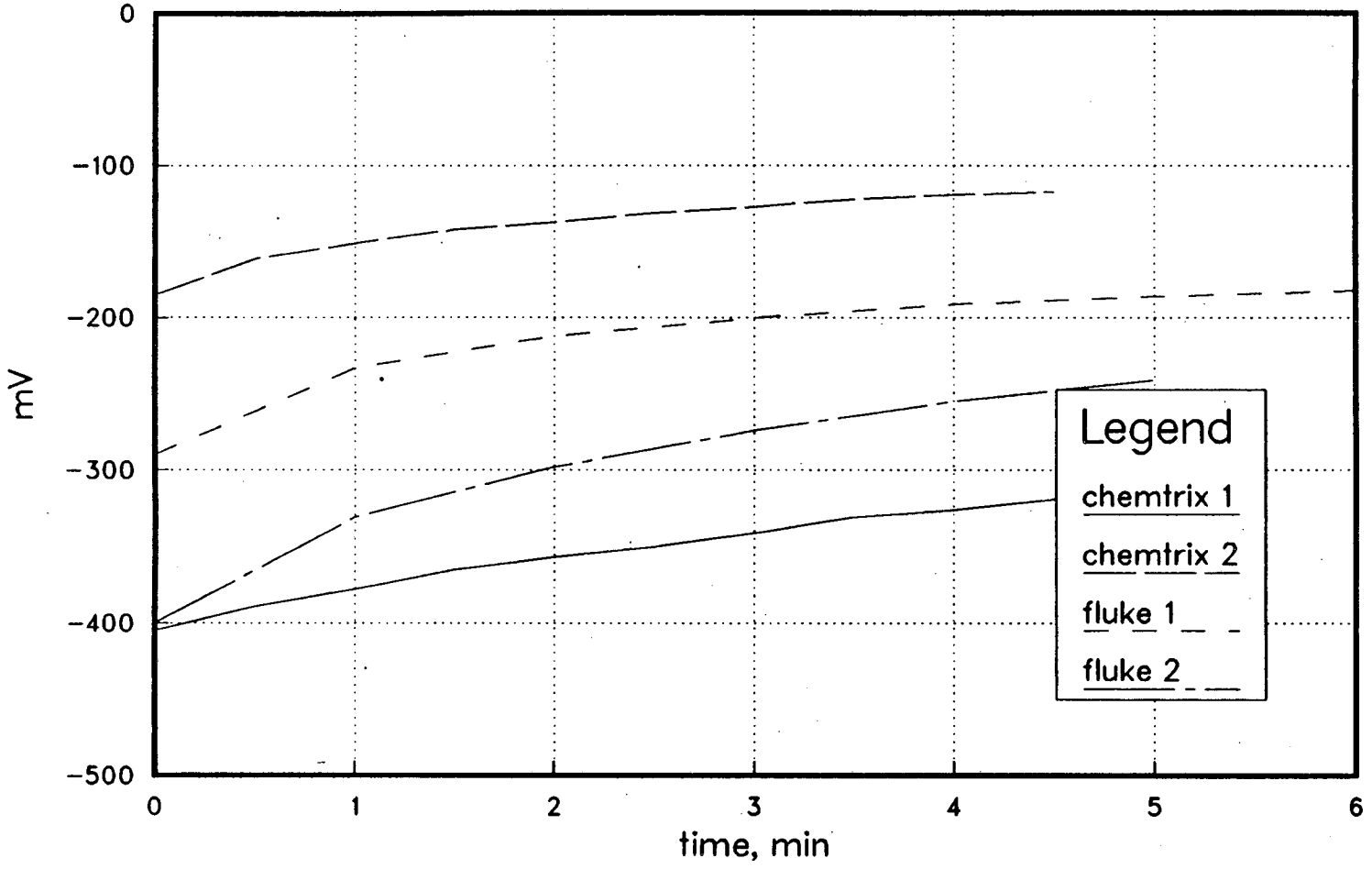

Figure 3.6 Typical drift that was observed in the two voltmeters used for measuring Eh. Four separate and distinct measurements are shown.

previous section on the difficulties associated with quantitative treatment of redox equilibria in flooded soils (Section 2.1.4), the information aimed for in this exercise could only be of a qualitative nature. The detection of general trends in Eh conditions with time was considered sufficient justification for making this effort. It was not the intent to attempt to make thermodynamic predictions of selenium speciation based on these measurements. The goal was to observe pre-flooding Eh conditions, in a general sense, and the rate and approximate magnitude of any Eh shift during flooding. Based on this purely qualitative goal and the necessity to choose some standard manner of picking the Eh values, it has been considered appropriate to choose a criterion that may not result in absolutely the *best* Eh value but that will be consistent so that individual measurements are meaningful relative to each other. Therefore, at the four sites without the permanent electrode arrangement, the value that is presented represents a one minute reading obtained with the Fluke device. While this value may not represent the most stable value, it is necessary so that data collected early in the experiment, when only the one minute readings were taken, can be compared to later data. Relative change is the goal and not absolute estimates of Eh.

At site UZ-3, the permanent electrodes returned fairly stable mV readings with the Cole-Palmer meter. On the one occasion when the two meters were compared at this site, the stable Cole-Palmer readings were very close to initial readings (the first value indicated or 0 minute reading) made with the Fluke, which was the meter used for essentially all of the measurements. Initial Fluke readings were therefore chosen as the Eh values to present for site UZ-3.

3.6. Chloride as a Tracer

Chloride (Cl^-) has been used extensively in the determination of groundwater and soil water velocity in tracer tests *(Biggar and Nielsen,* 1962; *Miller et al.,* 1965; *Kissel et al.,* 1973; *McMahon and Thomas,* 1974 and *Saffigna et al.,* 1977) due to its ease of analysis, high water solubility, mobility, low cost, and invulnerability to chemical transformations. Because chloride is negatively charged, it can be repelled slightly from the surface of clay platelets in

a process known as anion repulsion and can move deeper into the soil than would be calculated using the assumption that it was moving with the water *(Thomas and Swoboda,* 1970). Anion repulsion results in an effectively reduced pore volume available for flow which leads to an overestimation of the average pore water velocity. The degree to which anions are excluded is related to, among other factors, the anion valence and concentration, and to the nature of the mineral surface and its exchangeable cations *(Bohn et al.,* 1985). This effect on the rate of chloride movement is greatest with dilute solutions in soils that possess a high negative charge. In general, however, the effect is quite small. *Bresler* (1973) examined the importance of anion exclusion in the transport of anions during infiltration and observed that only about 10% of the anions were excluded. *Van De Pol et al.* (1977) conducted batch-type shaking experiments and observed a small amount of exclusion at chloride concentrations below 4 meq/liter. Above 26 meq/liter anion exclusion was virtually zero. Evidently, higher concentration solutions result in a depression of the double layer which increases the volume of mobile water. The minimum chloride concentration of soil water samples in the present study was approximately 1000 mg/liter = 28 meq/liter. Sulfate, however, was present as well, and at levels at least as high as those of chloride. The total anion concentration was therefore considerably higher than the 26 meq/liter value. In addition, the clay content of the upper 1 to 2 m of Kesterson pond soils is only 20 to 30% by weight. This effect, therefore, has been neglected in the present study.

3.7. Issues of Soil Water Sample Validity

Porous cup devices, first described by *Briggs and McCall* (1904), are simple and versatile instruments that extract water from soil by forming a hydrodynamic sink. A particularly complete review of the different types of soil solution samplers with discussion of their relative advantages and limitations is included in *Litaor* (1988). Their primary advantage lies in the ability to conveniently and continuously monitor the distribution of solutes within the soil profile. The devices have been widely used in water pollution studies to collect water from partially saturated soils for chemical analysis. Concerns over the representativeness of the sample, however, may lead to questions regarding sample validity. *Hansen and Harris*

(1975) performed laboratory and field tests to determine if porous ceramic cups collect representative samples of nitrate and phosphorus in soil water. Between-cup variability and inherent biases in sampling were examined and identified. Sources of bias included, leaching, diffusion, sorption and screening of phosphate ion by the cup walls. Leaching and diffusion were found to be minor and sorption was significant only if the sorptive capacity of the cup was significantly greater than that of the surrounding soil. Sample variability was influenced by factors that affect the timing of sampling (the duration of sampling), and included, a range of intake rates due to variations in cup wall thickness, plugging, sample depth and vacuum level. Intake rate was one of the most important sampler-related variables that affected sample concentration. Plugging and vacuum level both affected intake rate. These factors produced as much as a 60% range in sample concentration from eight samplers installed in a small plot. Recommendations made to minimize this variability emphasized procedures that would result in uniform intake rates between samplers such as using the same initial vacuum for samplers, using a uniform sampler length and selecting samplers that had similar permeability.

In addition to concerns that result from inherent bias of the devices and from their operation, problems relating to the adequacy of soil solution sampling arise from the heterogeneous nature of soil and from the fact that the composition and concentration of soil solutions are not homogeneous. Macropores may have significantly different solute concentrations than those in smaller pores. Depending on the positioning within the structure of the soil, macropores may circumvent the solution samplers. Hence, soil solution samplers may only represent point samples and may not adequately integrate for soil spatial variability *(Amoozegar-Fard et al.,* 1982). Therefore, a dense network of samplers may be required to adequately characterize the spatially variable soil solution chemistry and soil hydraulic properties.

A potentially major problem in investigations involving redox dependent ions is the application of a vacuum to the sampling device. Various redox dependent species such as iron,

manganese and ammonia have been shown to be oxidized in a relatively short time *(Stumm and Morgan,* 1981). This is not seen to be a problem in the present study because any oxidation that would occur in the soil water sampler would not result in selenium loss from solution, but rather, in an increase in the selenium solubility. Diffusion of oxygen, however, from the air in the soil water sampler, into the surrounding soil material, conceivably could lead to the development of a zone where conditions were more oxidizing than in material some distance away from the sampler. Evidence for this behavior has not been observed at Kesterson nor have any theoretical studies of its potential been undertaken at LBL. If this process did occur, however, then the extensive selenium immobilization that was observed in the Pond 1 experiment, and which is discussed fully in the chapters ahead, would represent a conservative estimate of actual immobilization quantities.

The discussion included above is an attempt to provide a modest level of awareness regarding potential limitations in porous cup sampler use. This study, however, does not attempt to examine or resolve any of these issues. The question of what a soil water sampler collects is highly relevant and one that is difficult to answer. There is much work that could be done in this area. Unfortunately though, limitations of time and effort dictate that these interesting problems be left for others to pursue.

4. SELENIUM MOBILIZATION DUE TO POND FLOODING

4.1. Solute Distributions under Vadose Conditions

Soil water samplers and tensiometers installed prior to flooding gathered baseline information under vadose zone conditions on the distribution of solutes and hydraulic head throughout the soil profile. Appendix II includes a complete list in tabular form of chemical data (selenium and chloride) collected at each of the nine sites throughout the entire experiment. In Figures 4.1 to 4.5 we see profiles of selenium and chloride observed at the various sites in Pond 1 while they were still dry. These concentrations are expressed in terms of mass of selenium per unit mass of soil solution. Typically, concentrations of soluble selenium were in the 1000's of ppb near the surface dropping to 10's of ppb at a depth of 1.22 m (4 ft). Maximum observed values at the 0.15 m (0.5 ft) level were in the range of 4000 to 5000 ppb. In Table 2 we see that samples of ground water collected in wells screened in the 1.8 to 12.2 m (6 to 40 ft) range commonly were below 10 ppb.

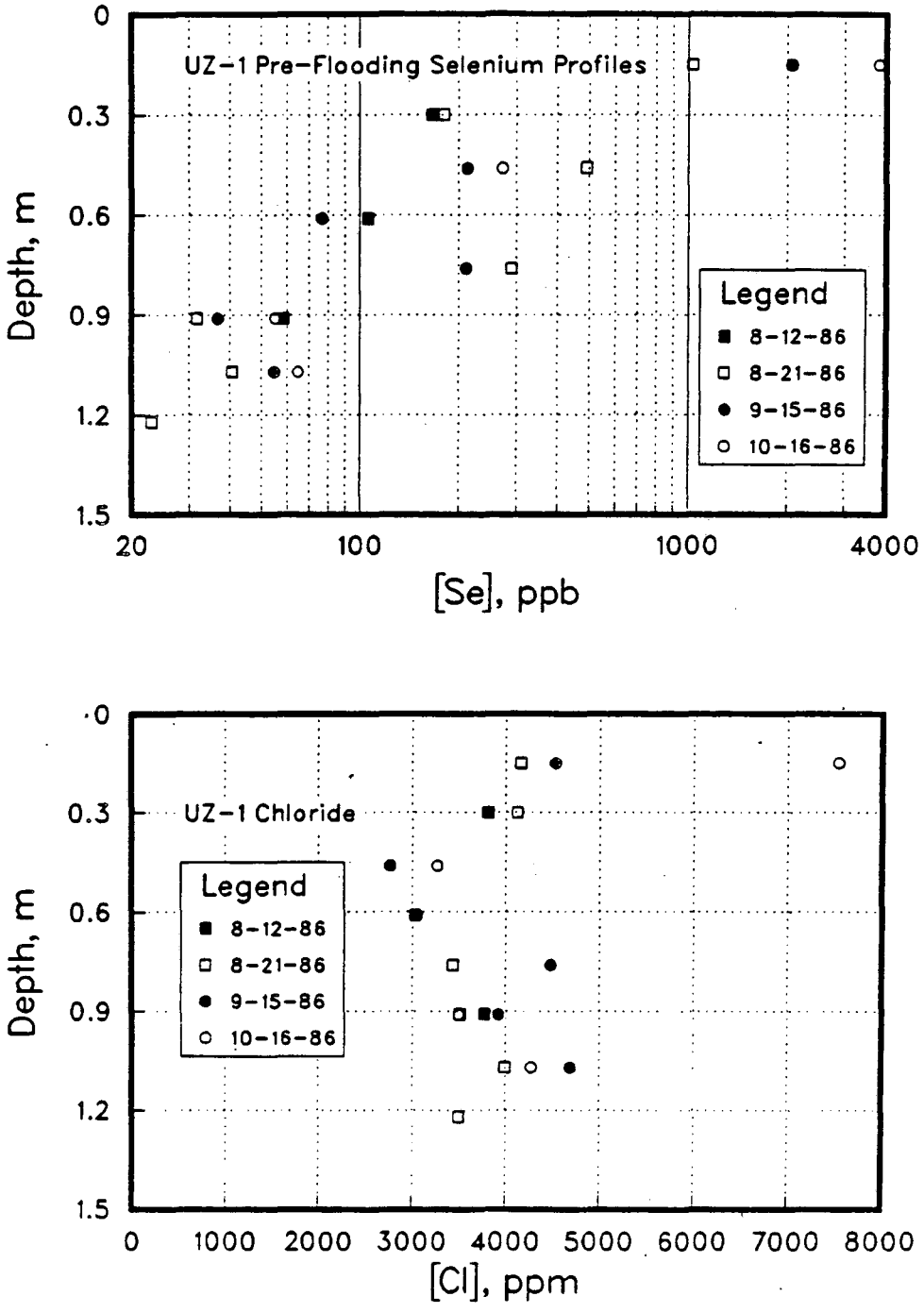

Figure 4.1 Pre-flooding selenium and chloride profiles at UZ-1.

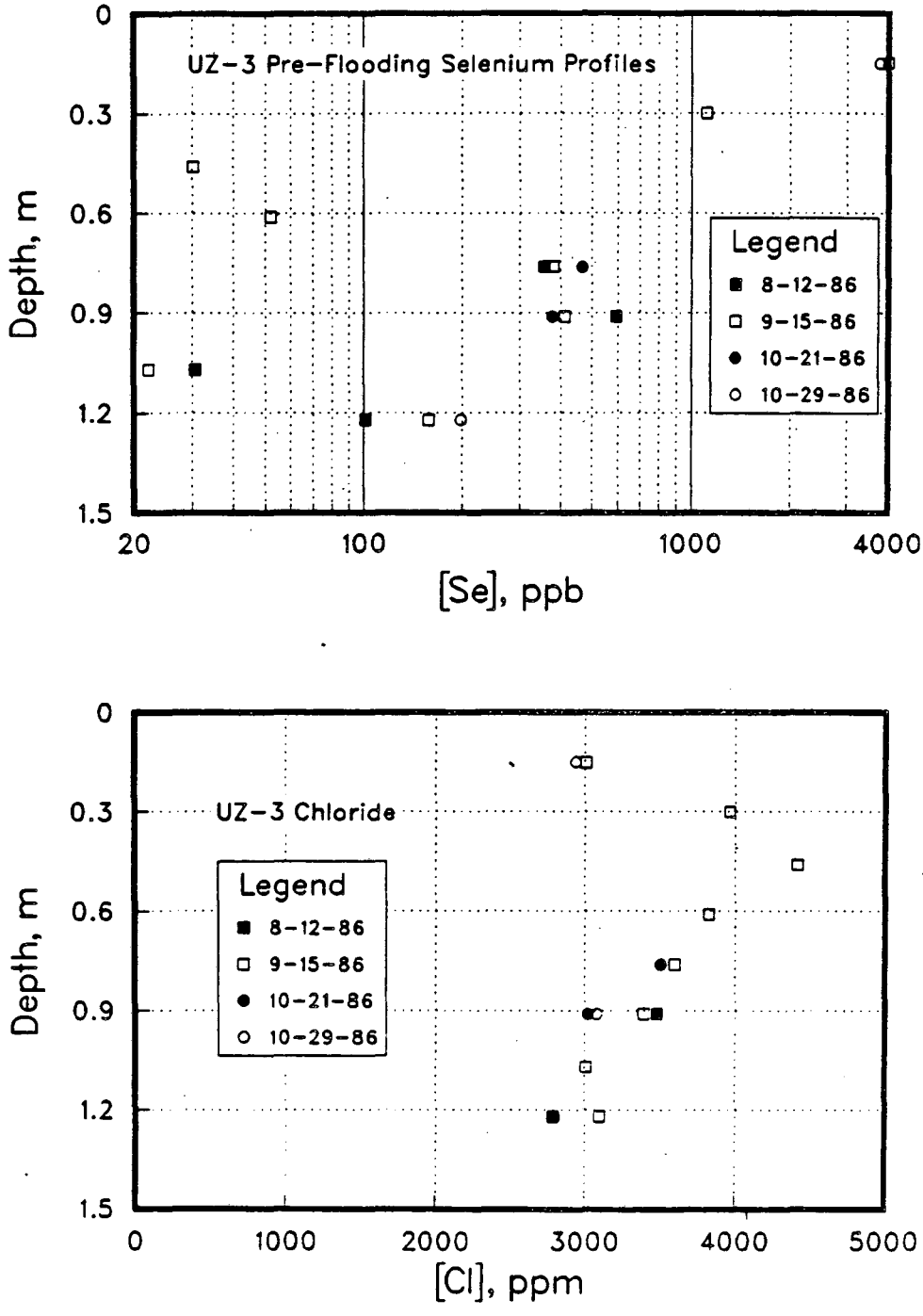

Figure 4.2 Pre-flooding selenium and chloride profiles at UZ-3.

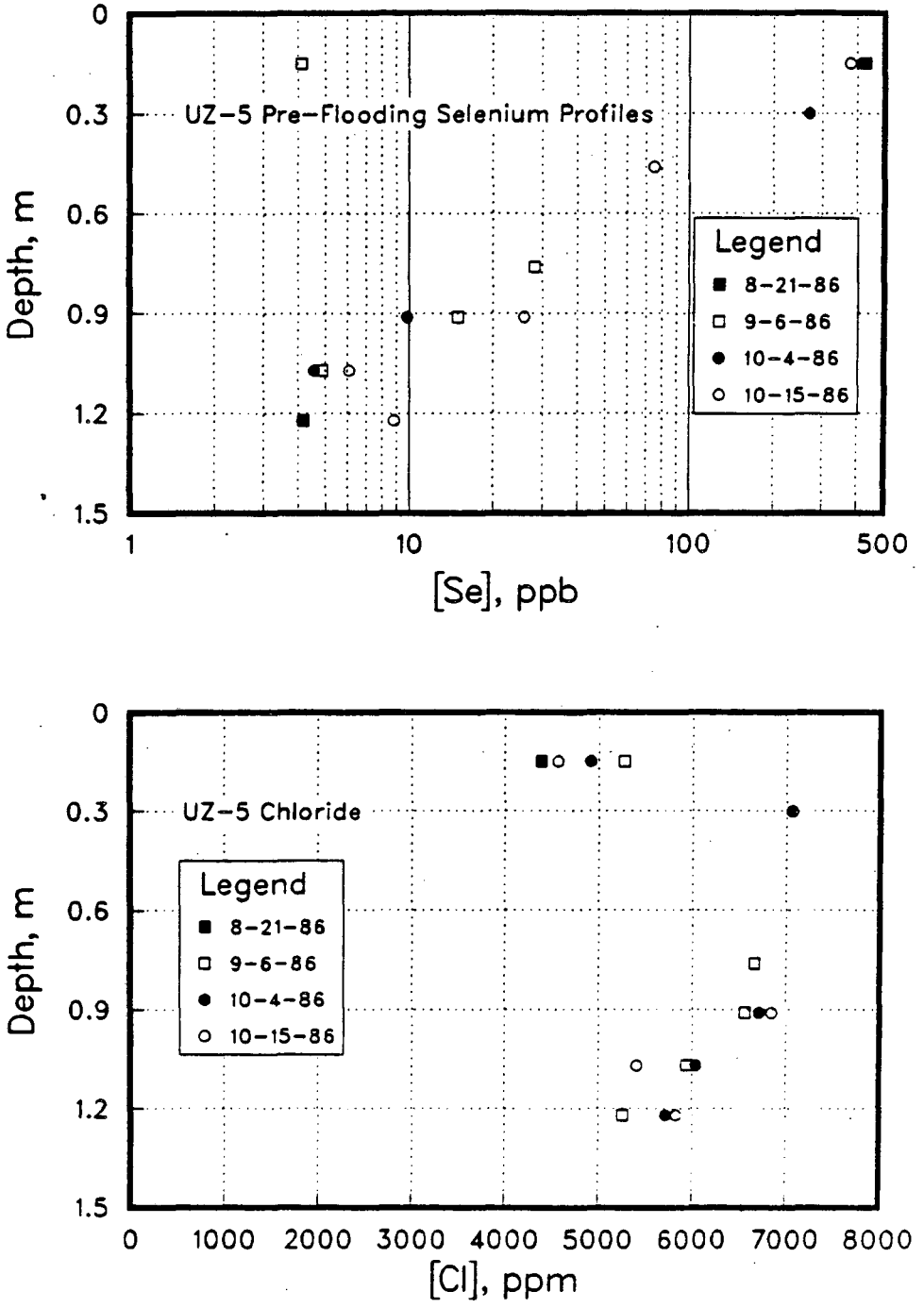

Figure 4.3 Pre-flooding selenium and chloride profiles at UZ-5.

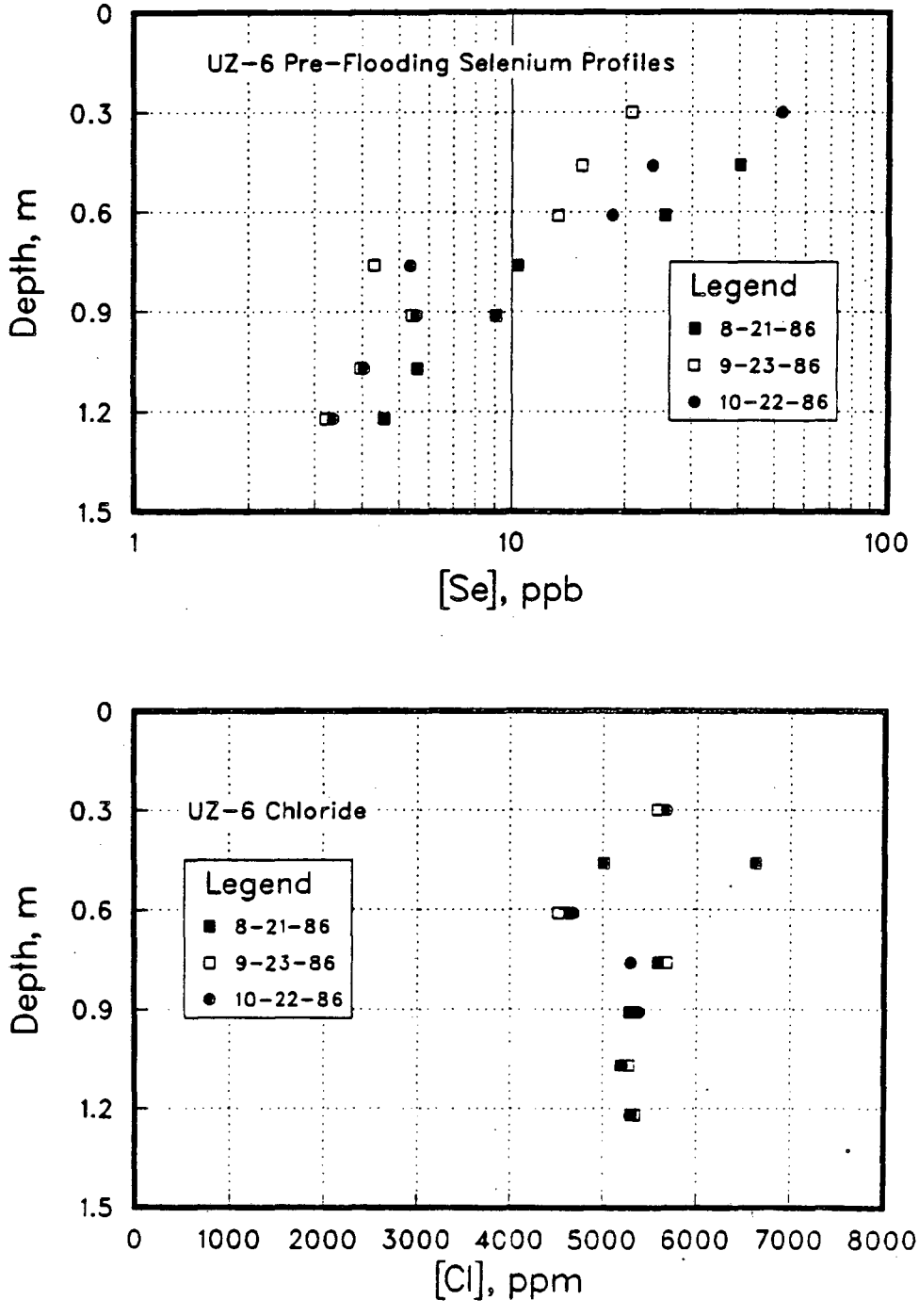

Figure 4.4 Pre-flooding selenium and chloride profiles at UZ-6.

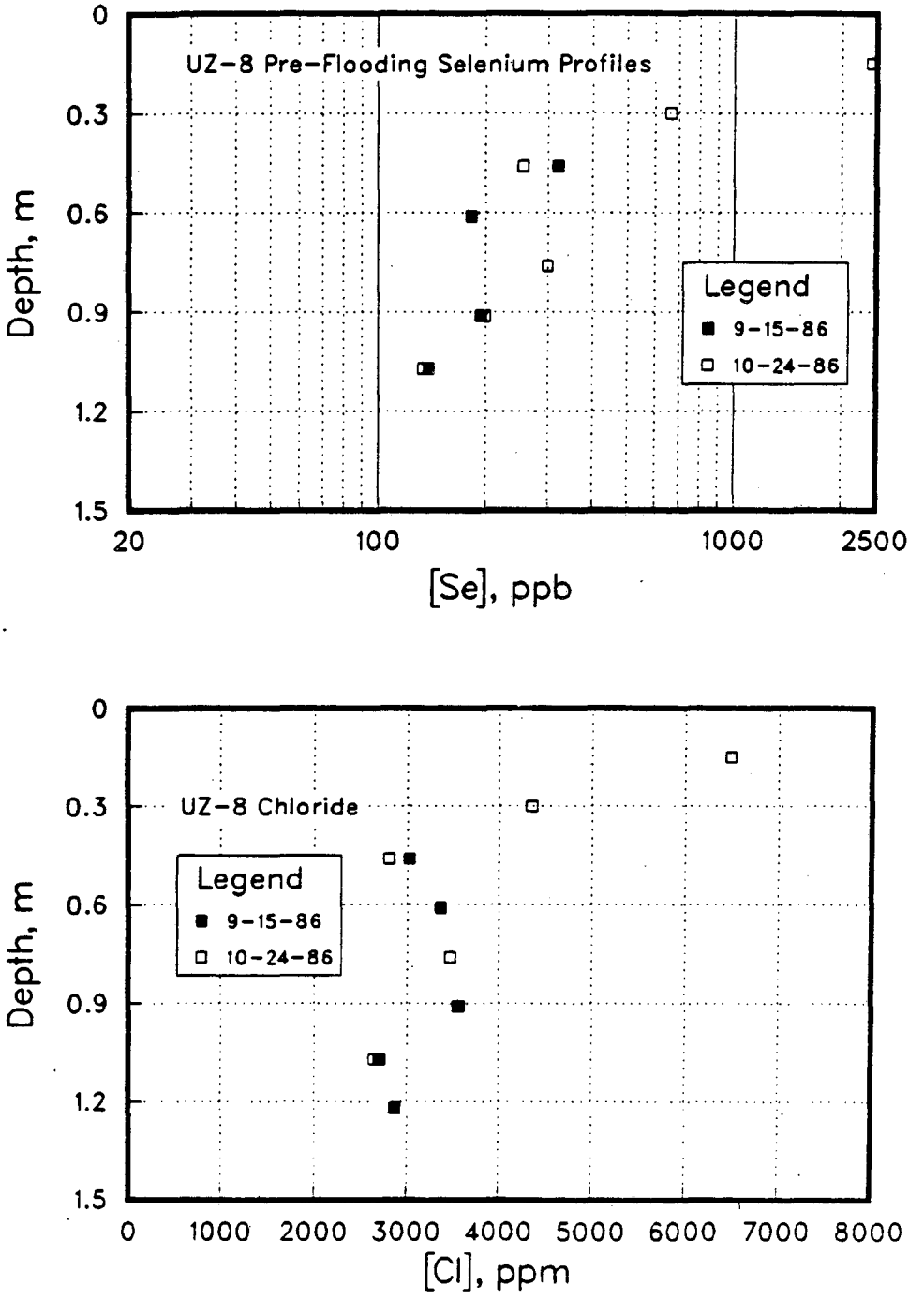

Figure 4.5 Pre-flooding selenium and chloride profiles at UZ-8.

Table 2. Pond 1 Pre-flooding Selenium Levels in Groundwater

Site	Screened Interval, m	Selenium Concentration, ppb	Site	Screened Interval, m	Selenium Concentration, ppb
UZ-1	3.0-4.6	2.1	UZ-5	1.8-2.4	4.9
	4.6-6.1	1.1	UZ-6	1.8-2.4	n/a
	6.1-7.6	1.0		2.4-3.0	n/a
	7.6-9.1	1.0	UZ-7	3.0-4.6	3.5
	9.1-10.7	1.3		4.6-6.1	0.8
	10.7-12.2	1.4		6.1-7.6	0.8
UZ-2	1.8-2.4	6.3		7.6-9.1	1.7
	2.4-3.0	5.6		9.1-10.7	2.3
UZ-3	1.8-2.4	n/a	UZ-8	1.8-2.4	n/a
	2.4-3.0	n/a		2.4-3.0	n/a
UZ-4	2.4-3.0	5.6	UZ-9	1.8-3.0	24.6
	3.0-4.6	4.3			
	4.6-6.1	2.6			
	6.1-7.6	2.2			
	7.6-9.1	3.7			
	9.1-10.7	2.7			
	10.7-12.2	2.7			

n/a - indicates no pre-flooding data are available

Similar data reflecting order of magnitude selenium decreases with depth have been observed in test plots at other locations within the Reservoir *(Lawrence Berkeley Laboratory,* 1987c p. 59), and this trend of generally decreasing selenium concentrations with depth can be

considered a typical one. However, not all observed profiles exhibited this trend. In Figure 4.2 (UZ-3) we see an example of extreme depth variation where a local maxima is located at a depth of 0.91 m (3 ft) below the surface, illustrating the complex nature of selenium transport.

A significant degree of variability is evident in the pre-flooding profiles throughout Pond 1 with regard to selenium inventories. Some sites, i.e. UZ-1, -3, -4, -7, -8, and -9 are characterized by very high concentrations (1000's of ppb) in the shallowest samples. At UZ-5 and UZ-6, however, maximum levels of 100's and 10's of ppb near the surface, are exhibited. This may be a manifestation of spatial variability in flow and transport parameters and/or the result of some complex mechanism or combination of physical mechanisms which are not very well understood. Possibilities include low hydraulic conductivity which may have limited the flux of selenium through the soil, low organic content which may have inhibited selenium accumulation through immobilization, or enhanced selenium volatilization.

Hydraulic head profiles typical of pre-flooding conditions in Pond 1 soils are presented in Figures 4.6 and 4.7. A complete list of hydraulic head data collected is included in Appendix II. Evaporative soil water loss is apparent from these tensiometer measurements of hydraulic head variations in the soil column. Certainly a partial explanation for apparent preferential selenium accumulation near the soil surface is the strong evaporative gradient. However, this alone cannot account for the order of magnitude variations observed in the soluble selenium distribution. As noted in *Lawrence Berkeley Laboratory* (1987c p. 60) soil water content variations in Reservoir core samples indicate that seasonal fluctuations in water content are only in the range of 2-fold. Data comparing the temporal variations in soluble selenium and electrical conductivity (EC) profiles at various sites show that selenium is accumulated in surficial material to a much greater extent than the other salts *(Lawrence Berkeley Laboratory*, 1987b p. 25). The chloride profiles in Figures 4.1 to 4.5 clearly demonstrate that even though there is some degree of variation in solute concentration with depth, the distribution does not exhibit distinct maxima, suggesting a mechanism which preferentially precipitates

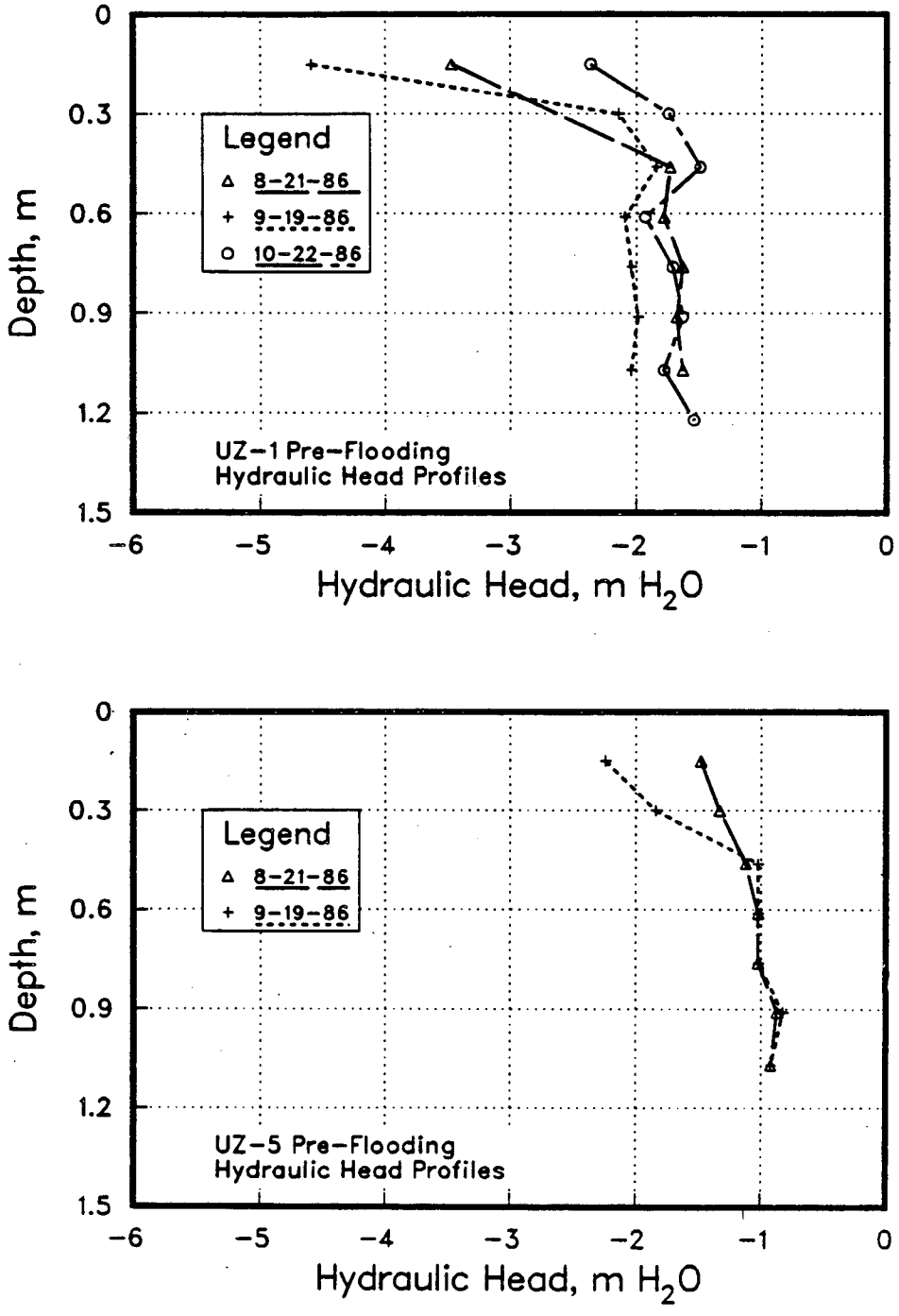

Figure 4.6 Pre-flooding hydraulic head profiles at sites UZ-1 and UZ-5. Measurements are made with reference to the ground surface.

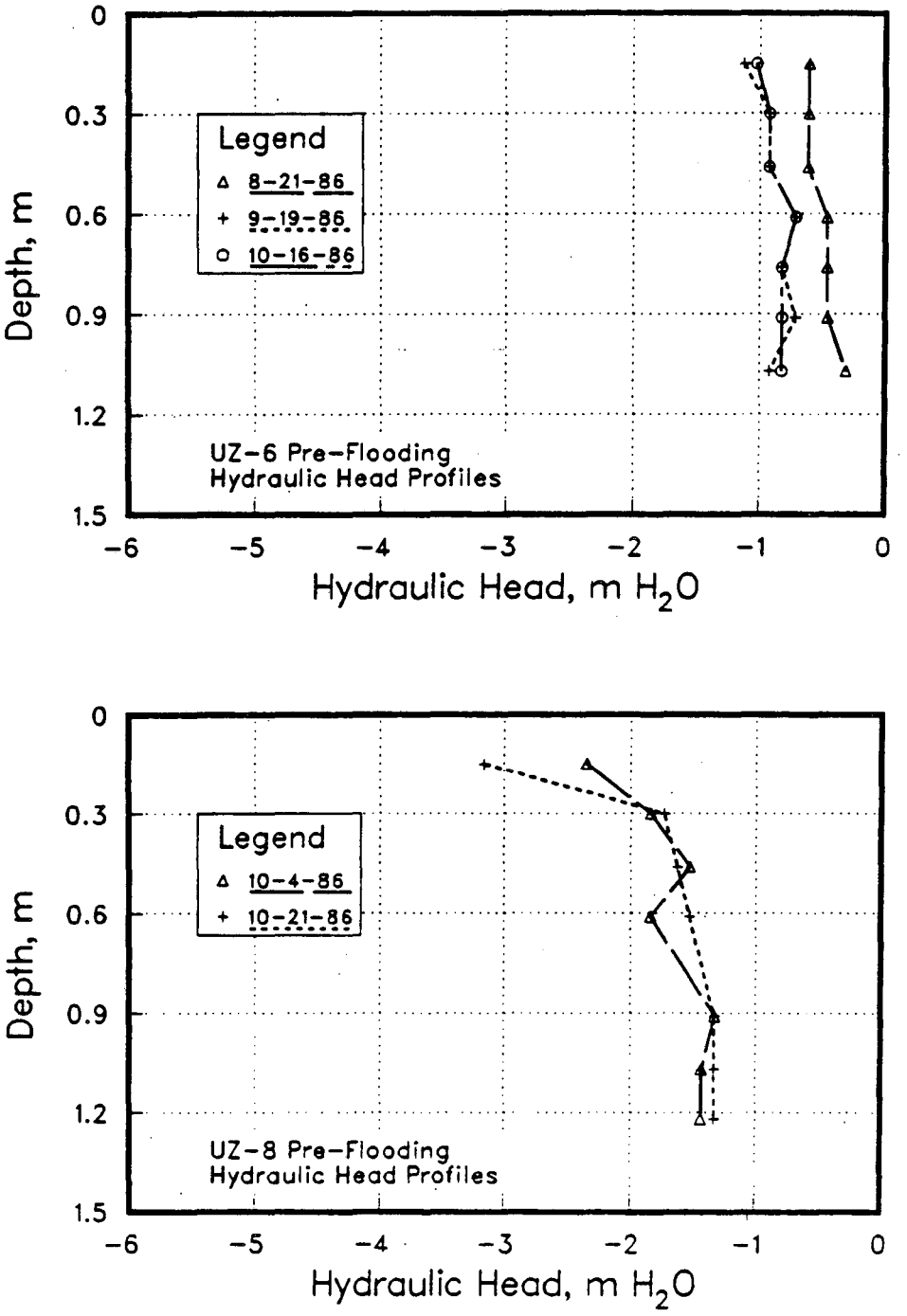

Figure 4.7 Pre-flooding hydraulic head profiles at sites UZ-6 and UZ-8. Measurements are made with reference to the ground surface.

selenium within the upper few inches of the soil surface. This observed general depth trend has been suggested to be the result of the low solubility and resulting precipitation of selenium in anoxic pond bottom sediments when the Reservoir was flooded with seleniferous drainage waters *(Weres et al., 1985).*

4.2. Solute Breakthrough due to Pond Flooding

Figures 4.8 to 4.17 are plots of solute breakthrough following pond flooding observed at the 8 depth locations within each of the 5 flooded sites. Data are presented for total selenium, chloride, and the selenate and selenite species. Appendix II contains a complete list for all the sites of chemical data collected. Data collected for both flooding episodes are included in these figures. The intensive monitoring during and after flooding revealed that, at some sites, flooding lead to increased total selenium concentrations in soil water, even at the deeper depths. Soil water total selenium concentrations jumped dramatically within many soil water samplers immediately after the flooding episode, commonly by 100's of % and in some cases by an order of magnitude or more. At three sites, UZ-1, UZ-3 an UZ-8, concentrations exceeded 1000 ppb below 0.61 m (2 ft) after flooding. The highest concentration observed at the 1.22 m depth was 1300 ppb, observed 4 days after flooding at UZ-3. At two sites, UZ-5 and UZ-6, no increase was observed in samplers below 0.61 m (2 ft). The selenate ion was present in much higher concentrations than selenite prior to and immediately after flooding. Concentrations of selenite anywhere in the soil column never exceeded 300 ppb. Selenate concentrations, however, were in the 1000's of ppb near the soil surface just following flooding and exceeded 4000 ppb in extreme cases. Chloride levels also increased due to flooding, however, not to the extent that was observed with total selenium and selenate. Chloride increases in individual soil water samplers were generally less than 100%.

In Figures 4.18 to 4.22 are plotted curves of *average* concentrations with time of solute levels observed in the 8 soil water samplers at a particular site. These data are also included in Tabular form in Appendix II. Average concentration plots have been prepared of the average total selenium, average chloride, average selenate and selenite levels. Only data from the first

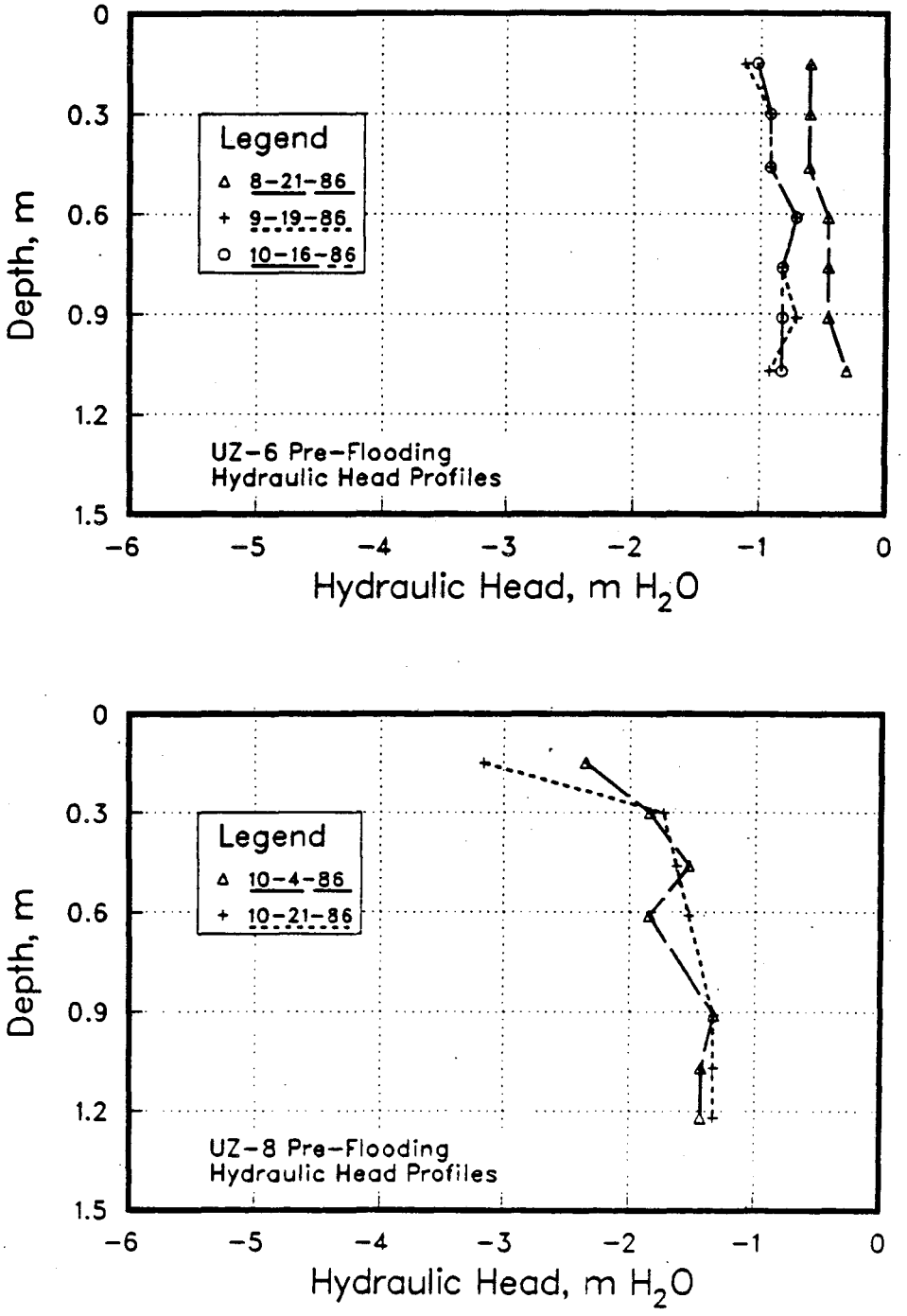

Figure 4.7 Pre-flooding hydraulic head profiles at sites UZ-6 and UZ-8. Measurements are made with reference to the ground surface.

selenium within the upper few inches of the soil surface. This observed general depth trend has been suggested to be the result of the low solubility and resulting precipitation of selenium in anoxic pond bottom sediments when the Reservoir was flooded with seleniferous drainage waters *(Weres et al., 1985).*

4.2. Solute Breakthrough due to Pond Flooding

Figures 4.8 to 4.17 are plots of solute breakthrough following pond flooding observed at the 8 depth locations within each of the 5 flooded sites. Data are presented for total selenium, chloride, and the selenate and selenite species. Appendix II contains a complete list for all the sites of chemical data collected. Data collected for both flooding episodes are included in these figures. The intensive monitoring during and after flooding revealed that, at some sites, flooding lead to increased total selenium concentrations in soil water, even at the deeper depths. Soil water total selenium concentrations jumped dramatically within many soil water samplers immediately after the flooding episode, commonly by 100's of % and in some cases by an order of magnitude or more. At three sites, UZ-1, UZ-3 an UZ-8, concentrations exceeded 1000 ppb below 0.61 m (2 ft) after flooding. The highest concentration observed at the 1.22 m depth was 1300 ppb, observed 4 days after flooding at UZ-3. At two sites, UZ-5 and UZ-6, no increase was observed in samplers below 0.61 m (2 ft). The selenate ion was present in much higher concentrations than selenite prior to and immediately after flooding. Concentrations of selenite anywhere in the soil column never exceeded 300 ppb. Selenate concentrations, however, were in the 1000's of ppb near the soil surface just following flooding and exceeded 4000 ppb in extreme cases. Chloride levels also increased due to flooding, however, not to the extent that was observed with total selenium and selenate. Chloride increases in individual soil water samplers were generally less than 100%.

In Figures 4.18 to 4.22 are plotted curves of *average* concentrations with time of solute levels observed in the 8 soil water samplers at a particular site. These data are also included in Tabular form in Appendix II. Average concentration plots have been prepared of the average total selenium, average chloride, average selenate and selenite levels. Only data from the first

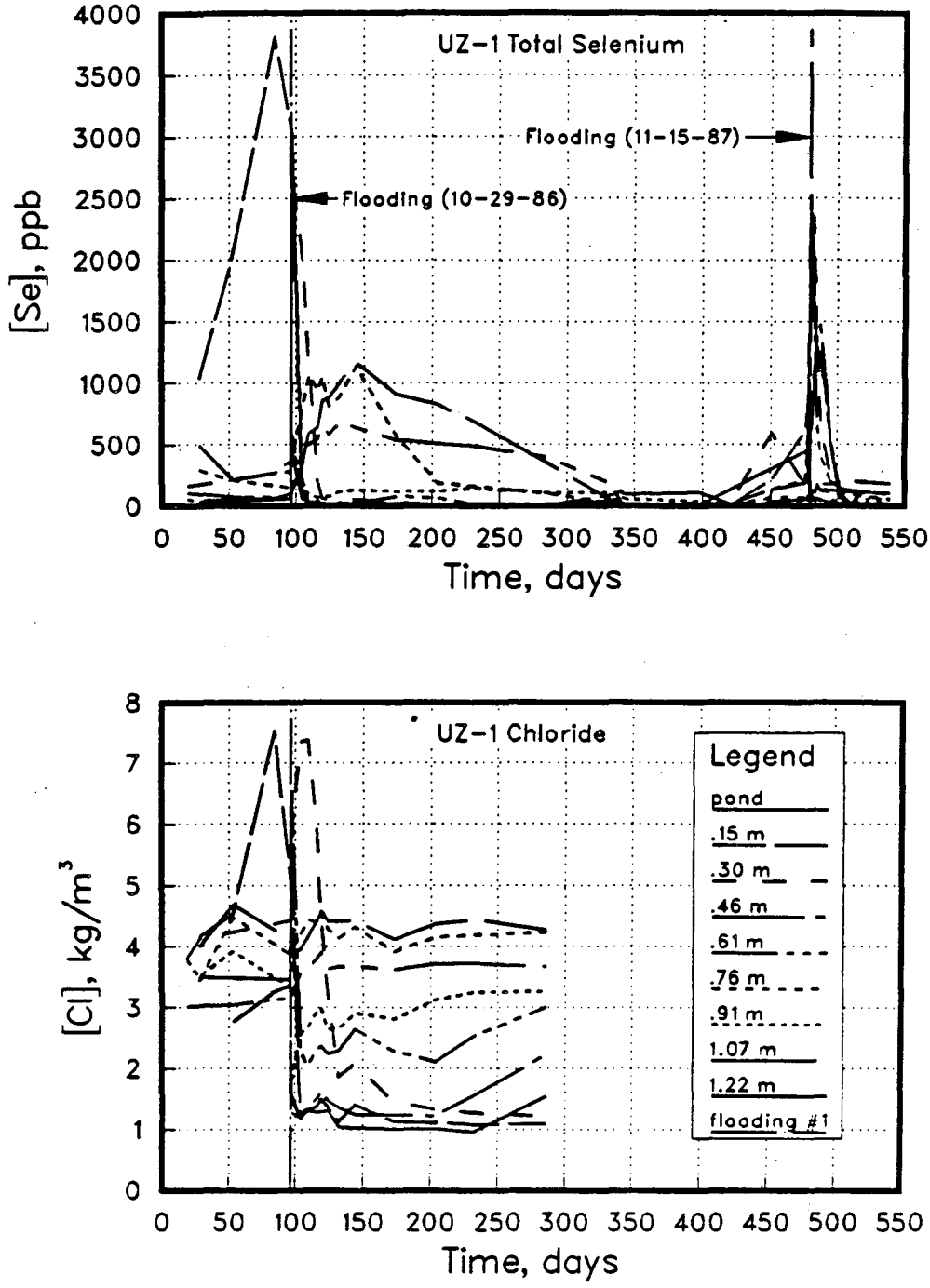

Figure 4.8 Total selenium and chloride concentrations of soil water samples collected throughout the experiment time period at site UZ-1.

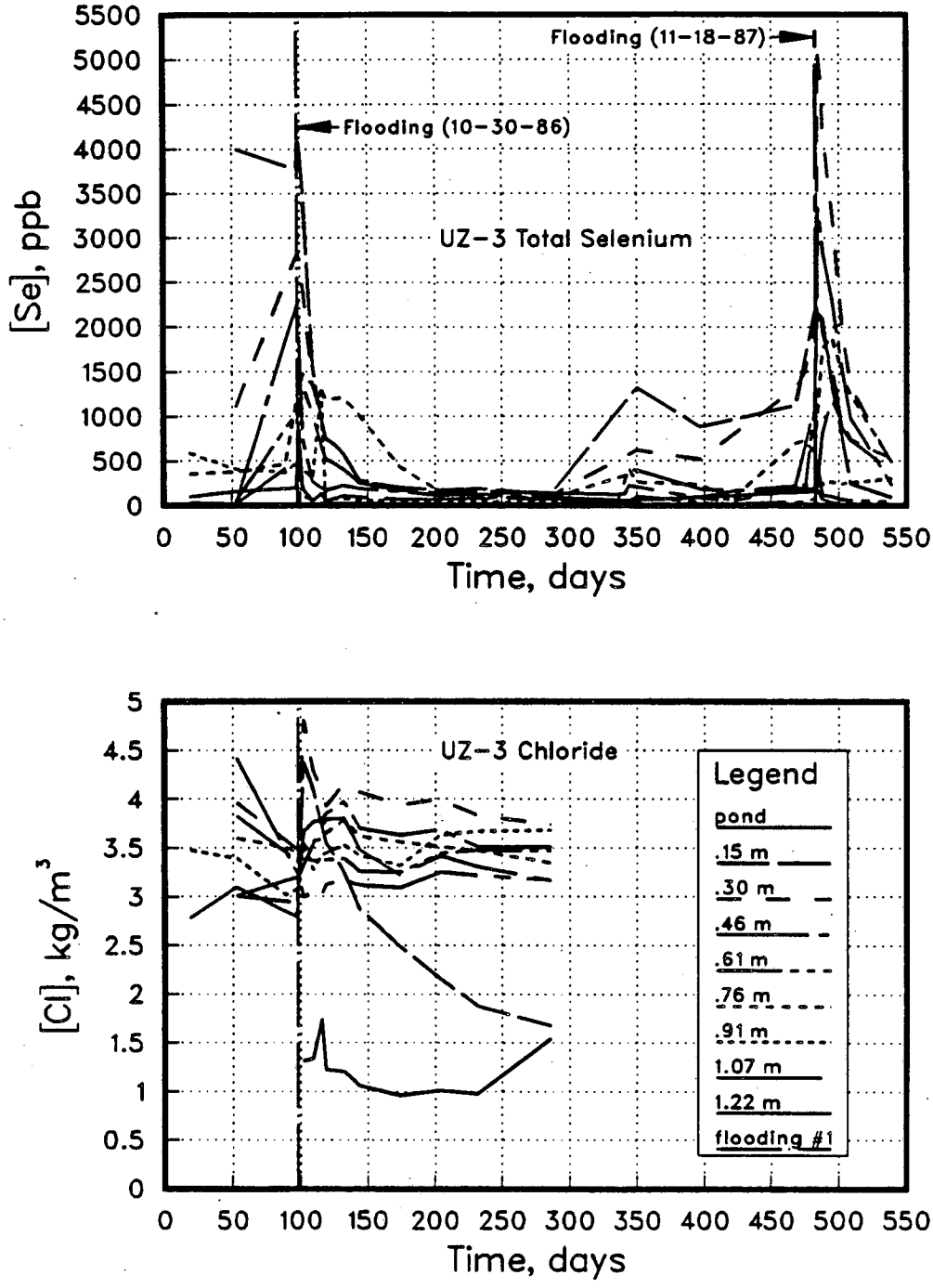

Figure 4.9 Total selenium and chloride concentrations of soil water samples collected throughout the experiment time period at site UZ-3.

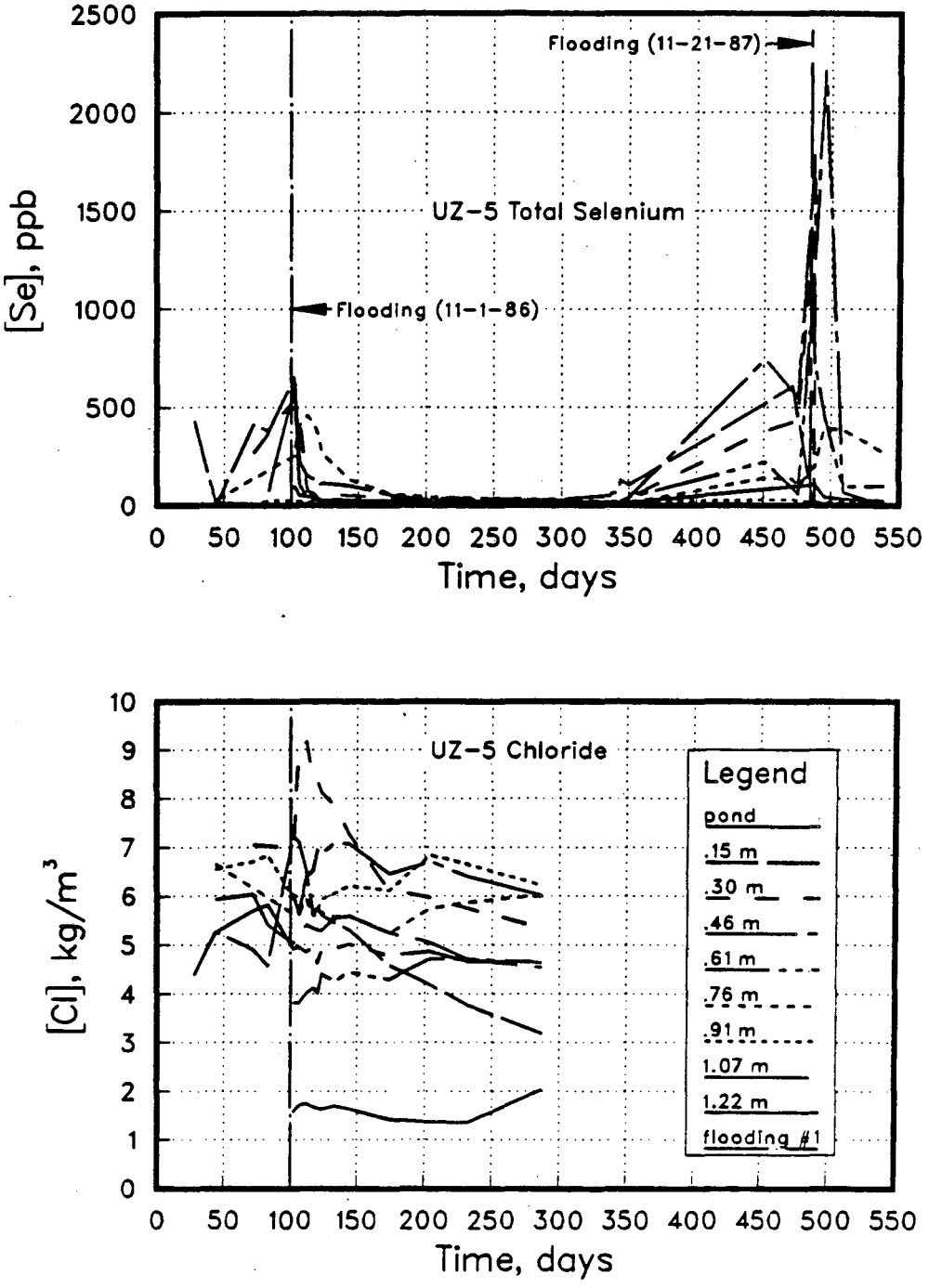

Figure 4.10 Total selenium and chloride concentrations of soil water samples collected throughout the experiment time period at site UZ-5.

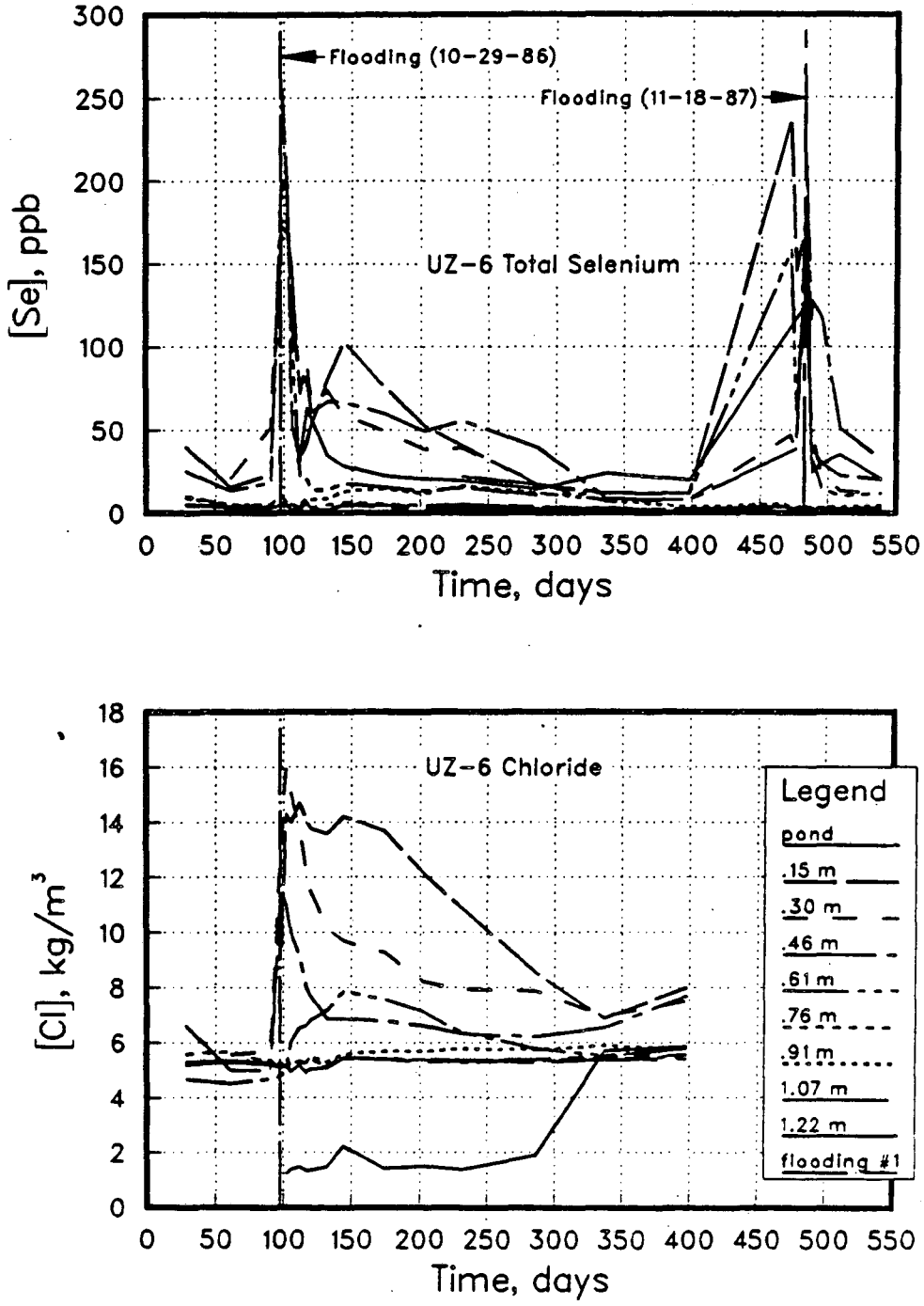

Figure 4.11 Total selenium and chloride concentrations of soil water samples collected throughout the experiment time period at site UZ-6.

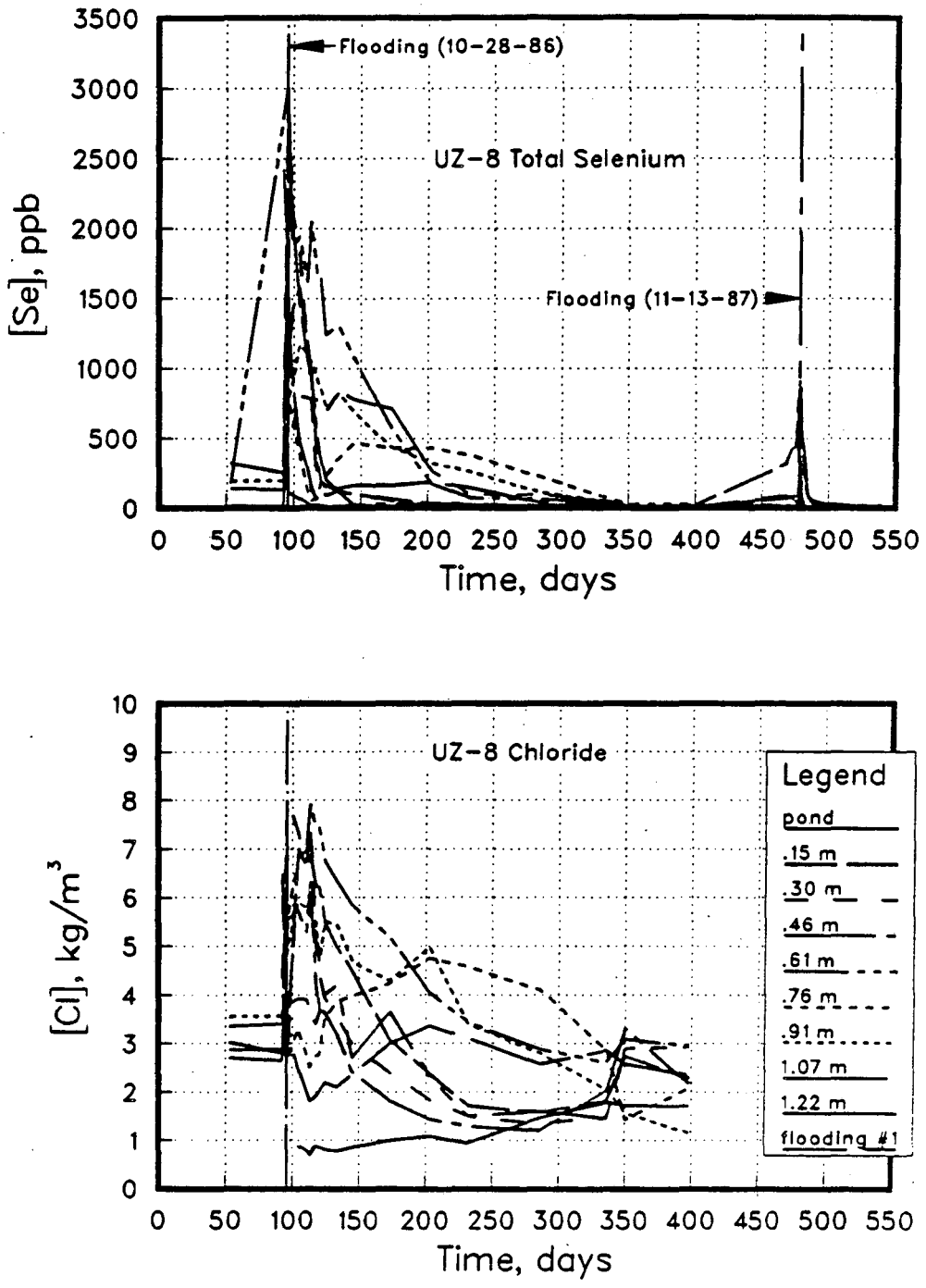

Figure 4.12 Total selenium and chloride concentrations of soil water samples collected throughout the experiment time period at site UZ-8.

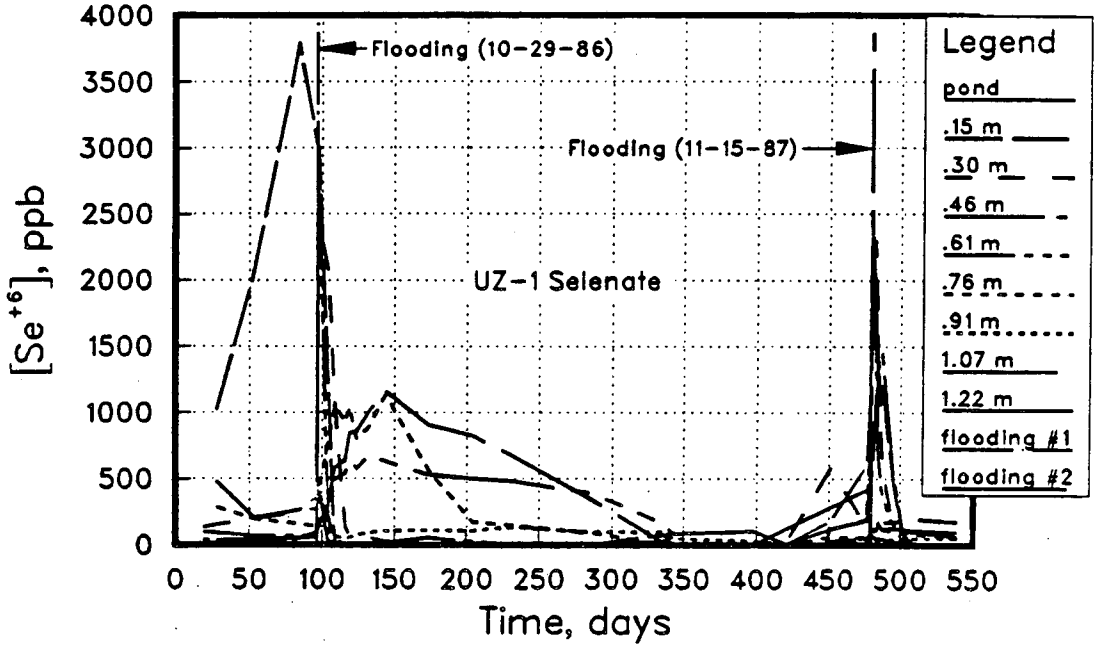

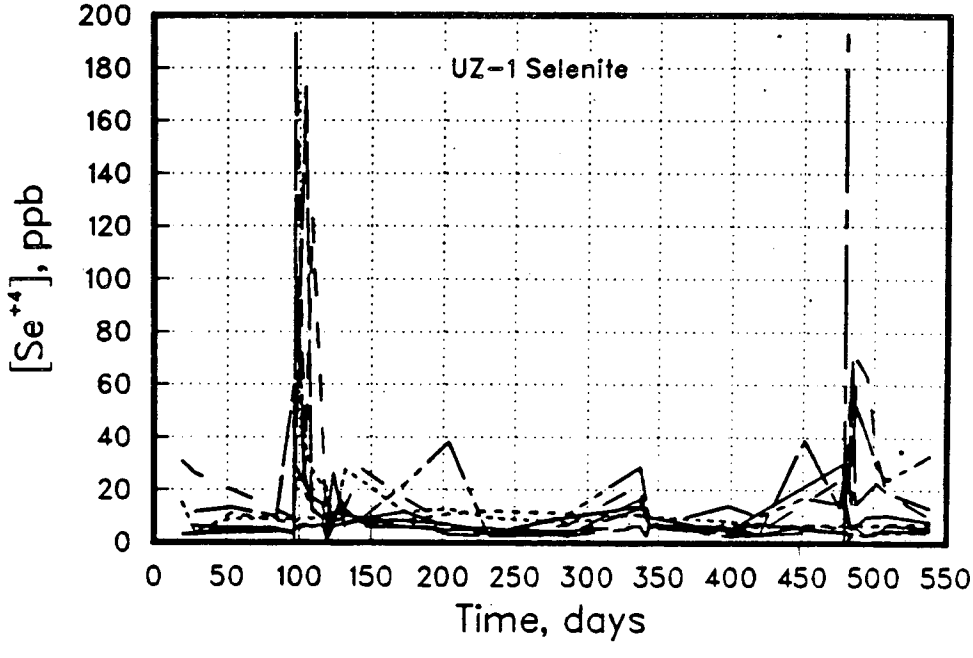

Figure 4.13 Selenate and selenite concentrations of soil water samples collected throughout the experiment time period at site UZ-1.

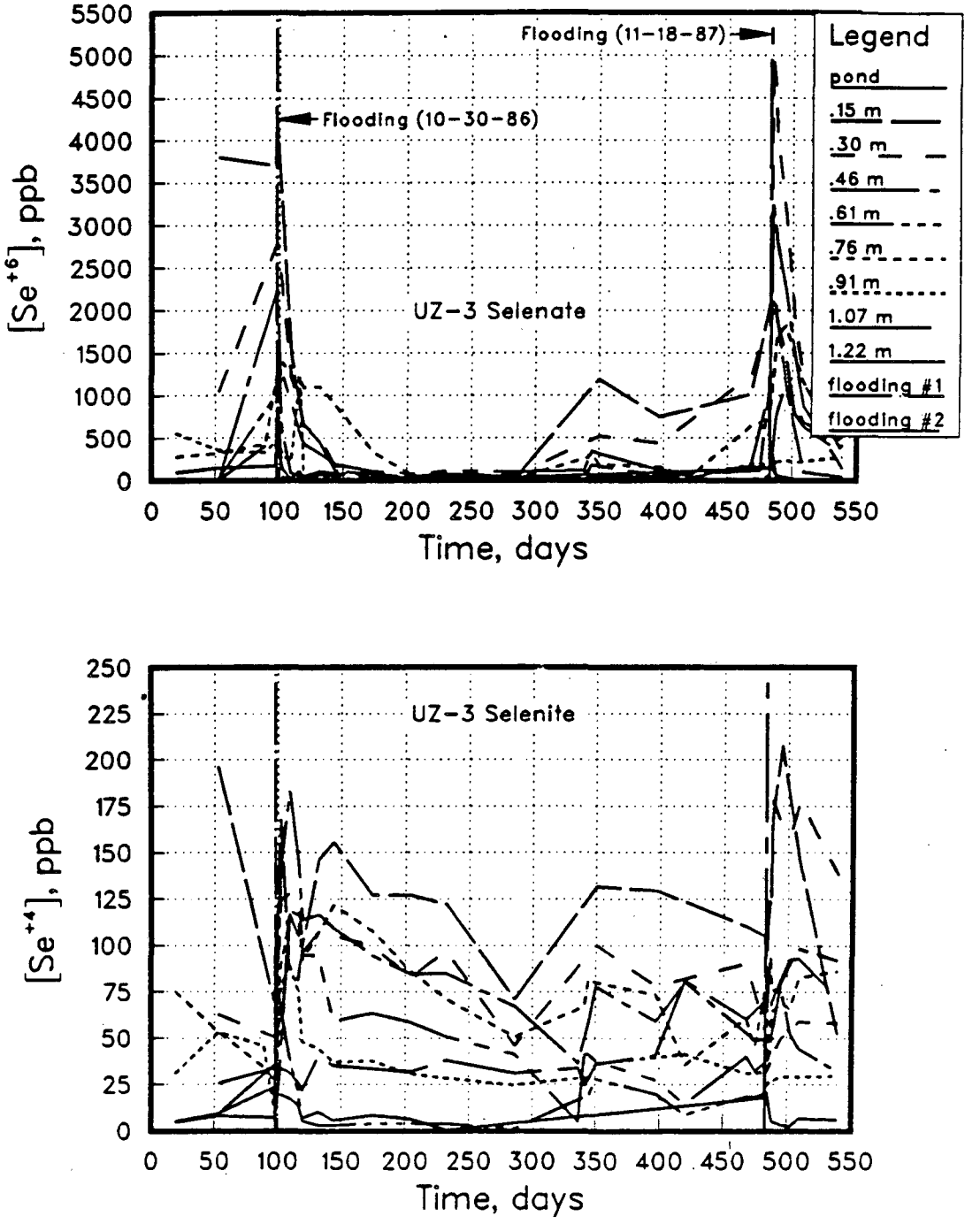

Figure 4.14 Selenate and selenite concentrations of soil water samples collected throughout the experiment time period at site UZ-3.

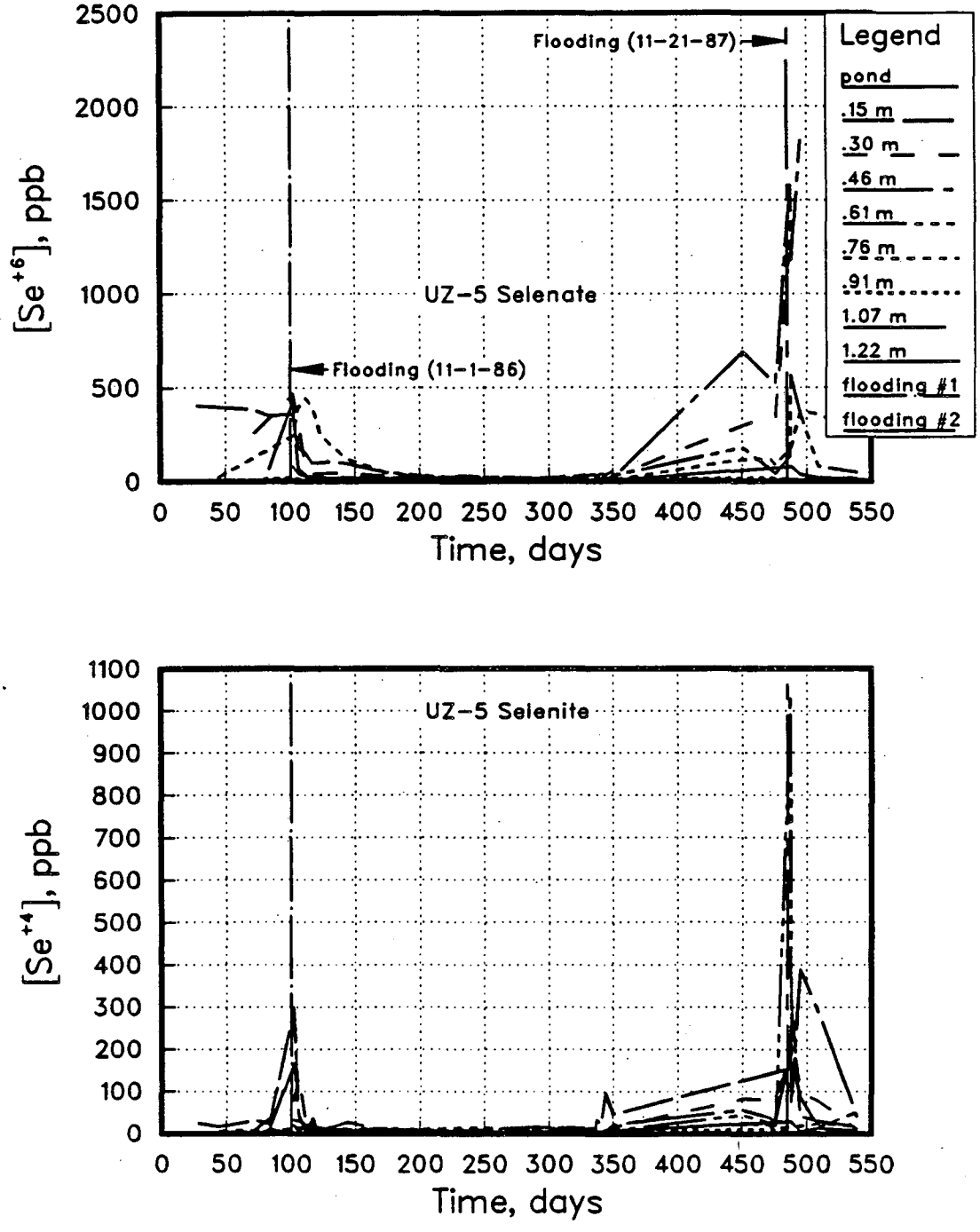

Figure 4.15 Selenate and selenite concentrations of soil water samples collected throughout the experiment time period at site UZ-5.

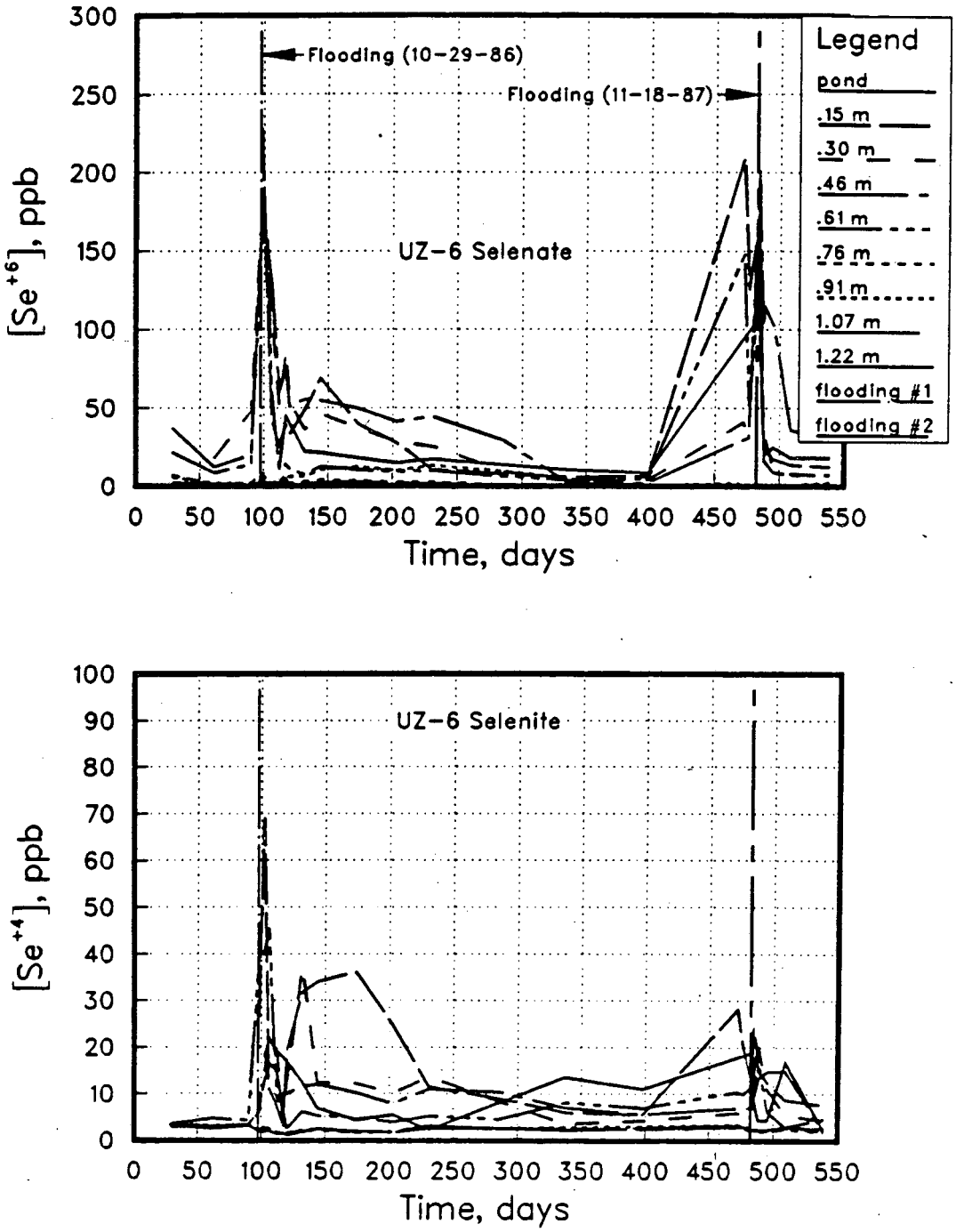

Figure 4.16 Selenate and selenite concentrations of soil water samples collected throughout the experiment time period at site UZ-6.

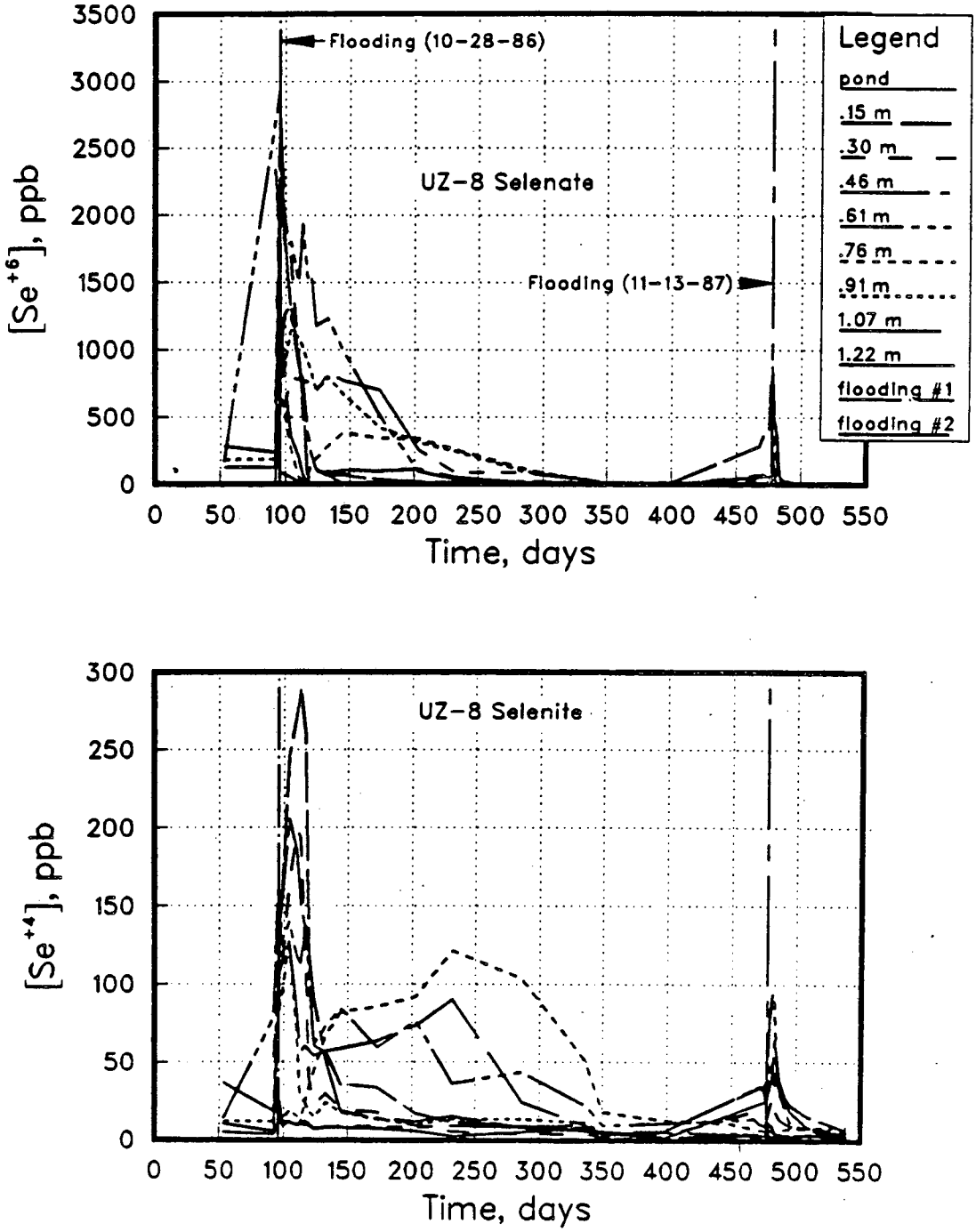

Figure 4.17 Selenate and selenite concentrations of soil water samples collected throughout the experiment time period at site UZ-8.

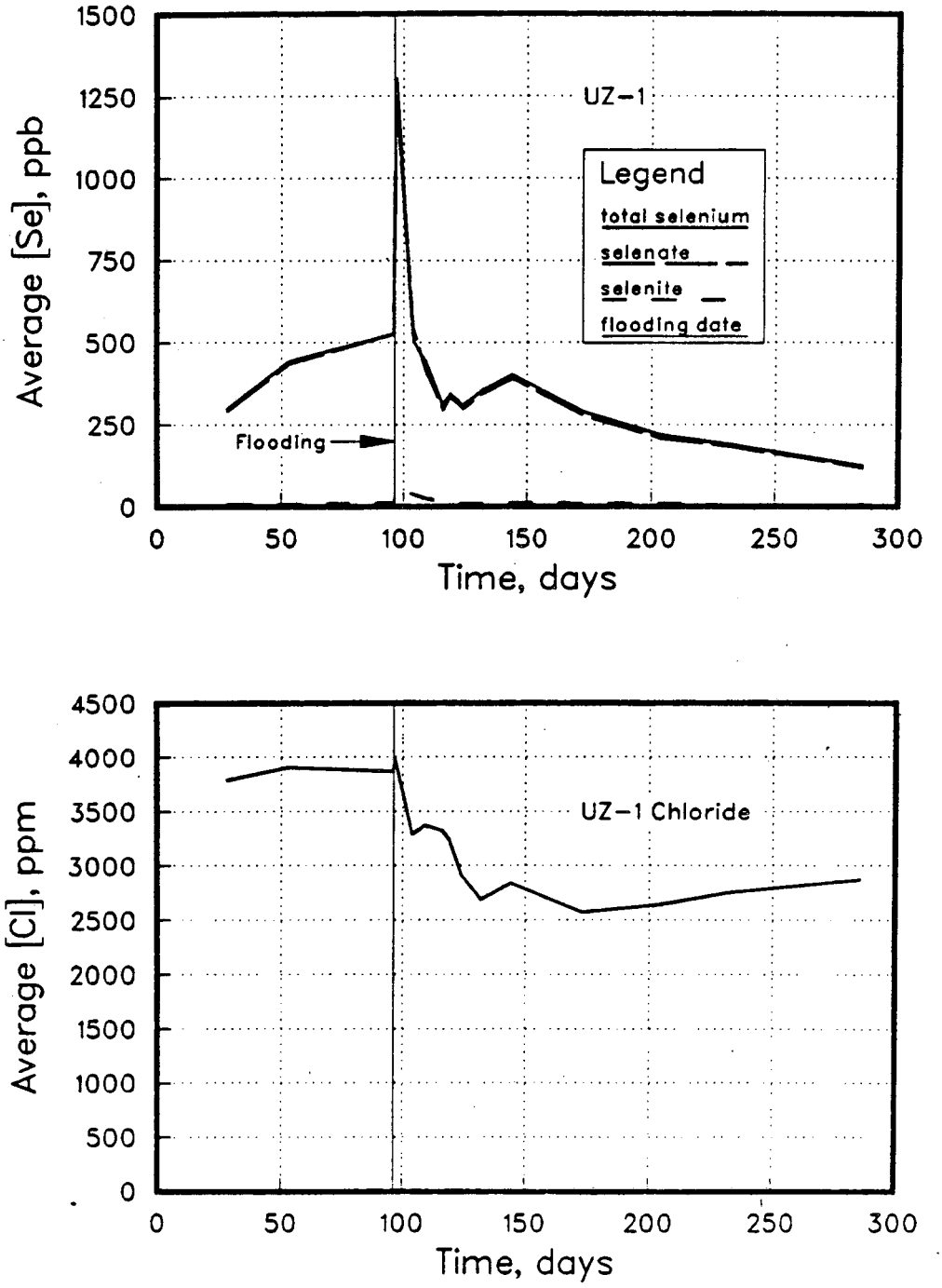

Figure 4.18 Average selenium and chloride concentrations of the 8 soil water samplers vs time at site UZ-1.

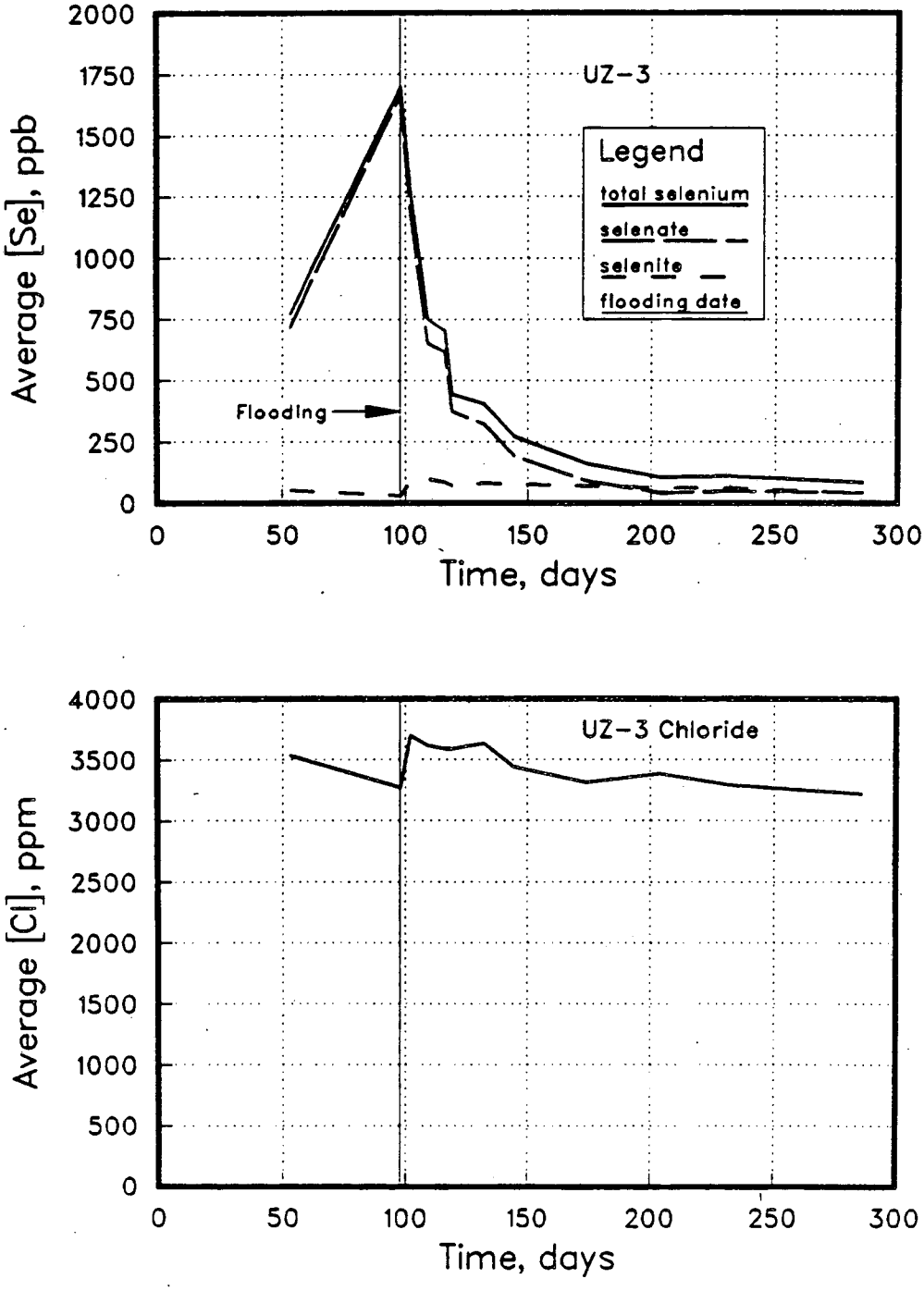

Figure 4.19 Average selenium and chloride concentrations of the 8 soil water samplers vs time at site UZ-3.

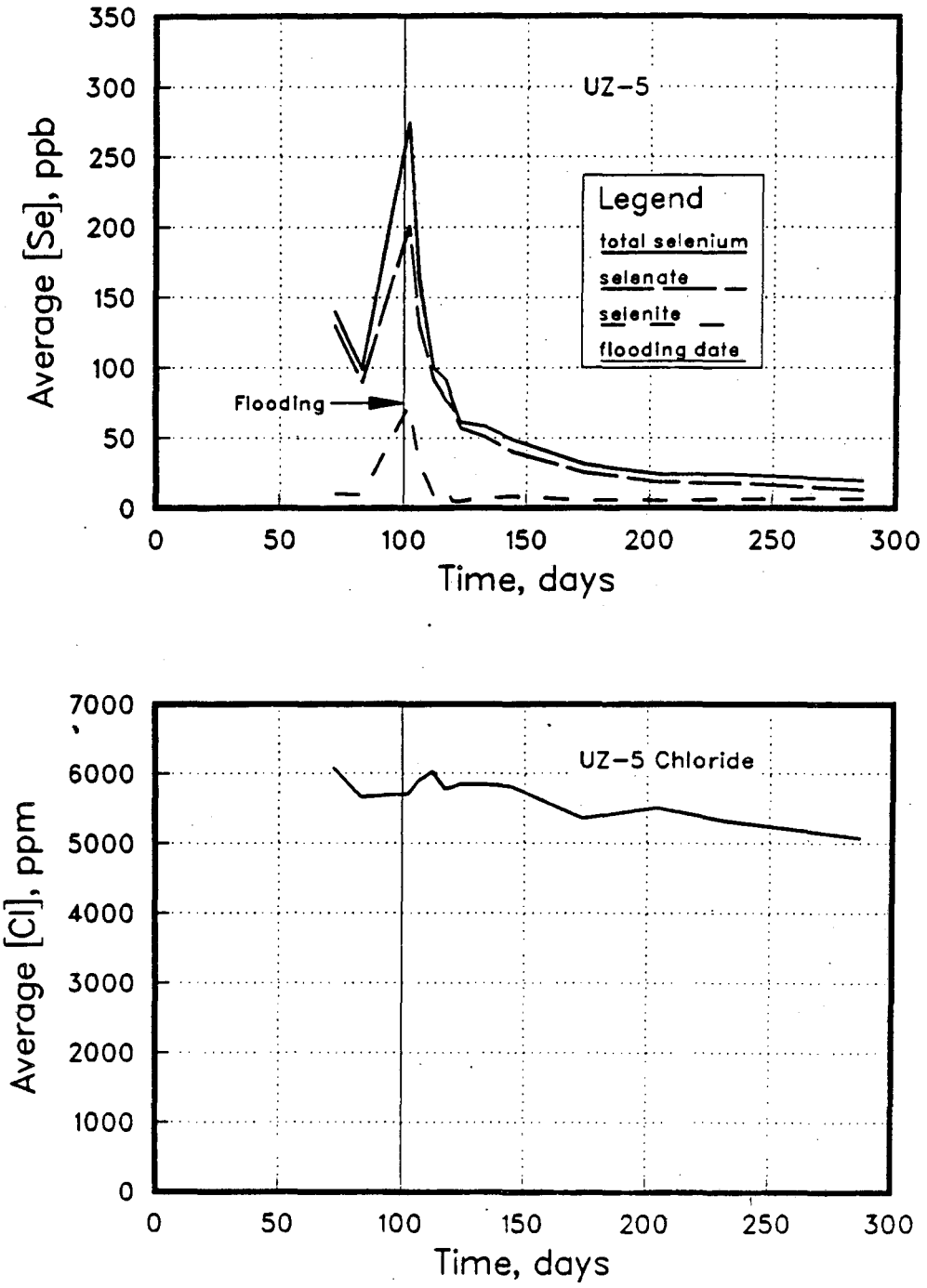

Figure 4.20 Average selenium and chloride concentrations of the 8 soil water samplers vs time at site UZ-5.

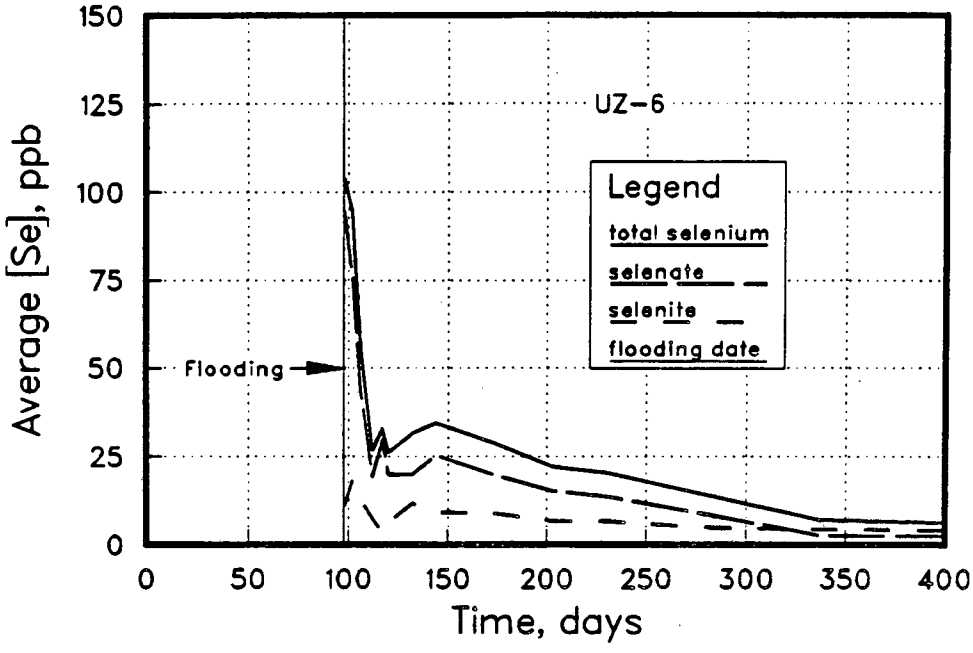

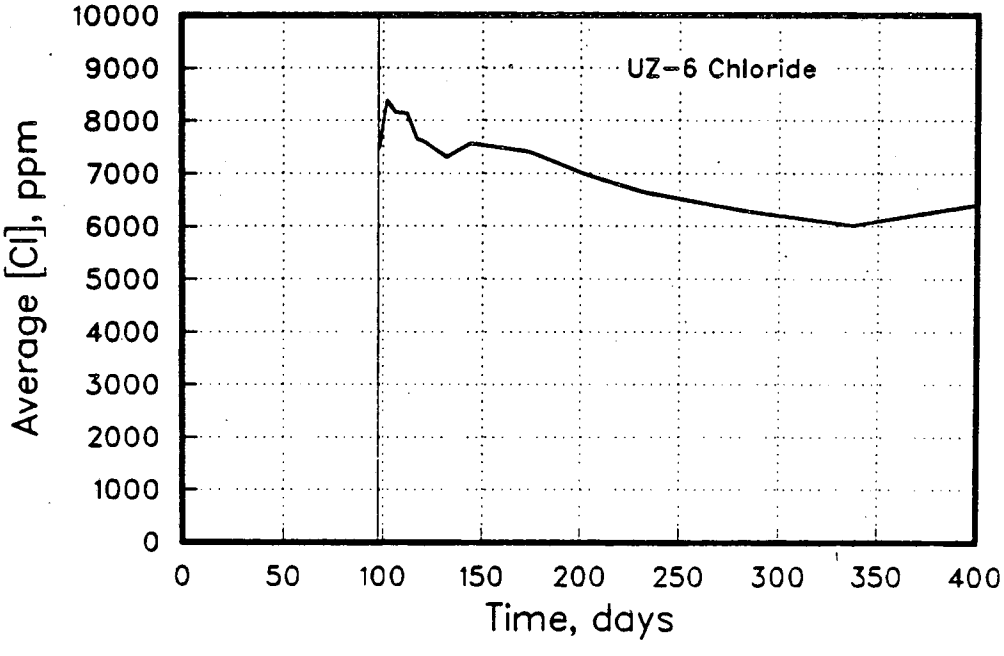

Figure 4.21 Average selenium and chloride concentrations of the 8 soil water samplers vs time at site UZ-6.

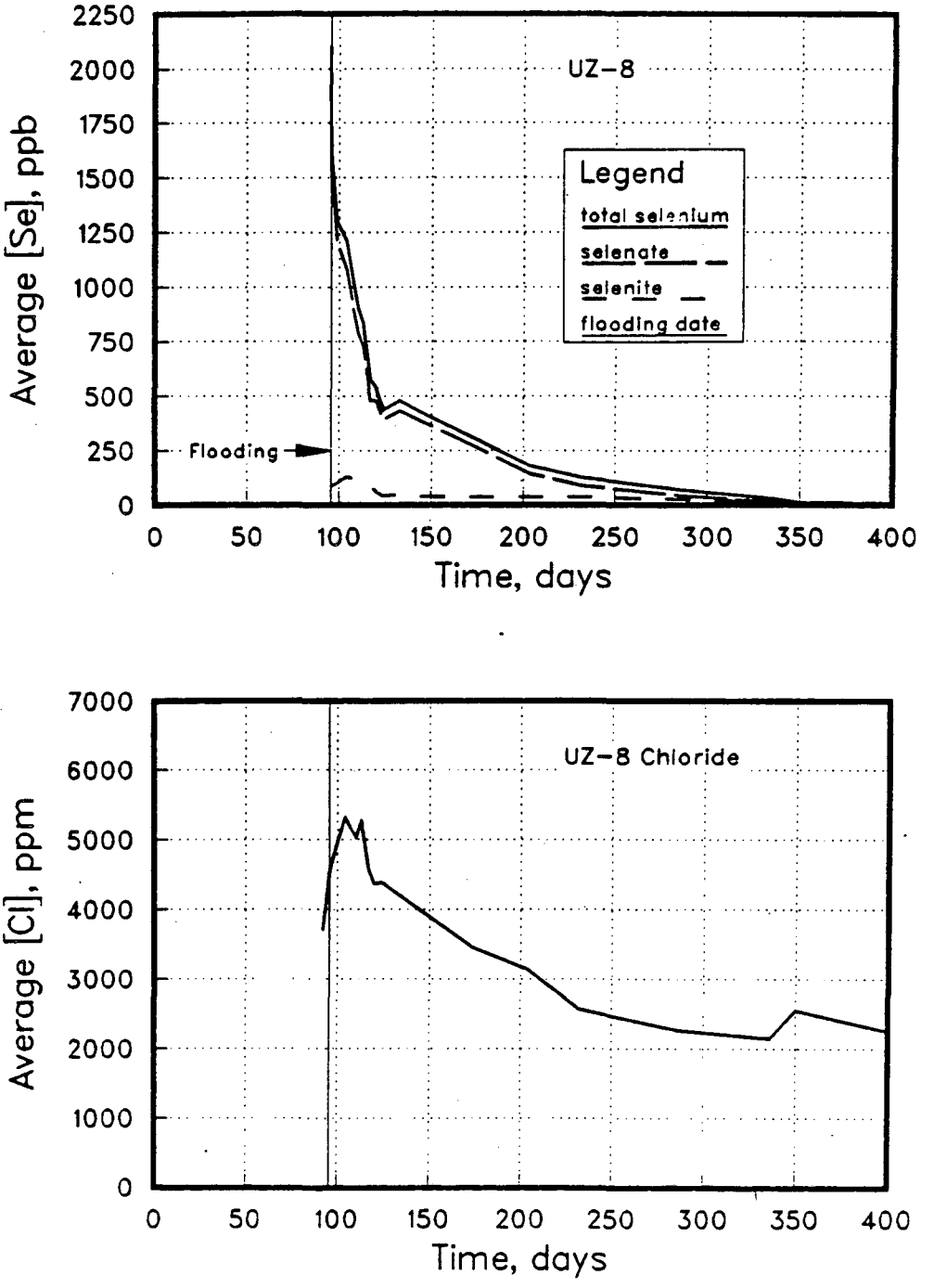

Figure 4.22 Average selenium and chloride concentrations of the 8 soil water samplers vs time at site UZ-8.

flooding event have been included. Because it is an average over the monitoring zone, these data represent estimates of the temporal variation of total mass of the particular solute within the 1.22 m thick study zone. We see that, in general, total selenium, selenate and selenite concentrations measured just after flooding represent maximum levels observed throughout the experiment. Selenate was the dominant species of soluble selenium immediately after flooding, however, as the experiment proceeds the two ions approach equal concentrations. Chloride levels also reached a maximum value soon after flooding, however, the subsequent decline was generally much slower than that observed for total selenium and selenate.

Analysis of groundwater samples collected periodically over the approximately one year-long experiment indicated that flooding Pond 1 did not create widespread elevated concentrations of selenium in the shallow aquifer. Refer to Figure 4.23 for total selenium and chloride in shallow groundwater monitoring wells and to Appendix II for a complete list of groundwater quality data. Prior to flooding, levels in groundwater underneath Pond 1 monitoring sites were generally less than 10 ppb (Table 2). Even though levels in overlying soil water samples were in the 100's to 1000's ppb range, concentrations of soluble selenium in groundwater remained relatively low. At one site, UZ-8, an increase in total selenium was observed to 322 ppb some 4 ½ months after flooding before returning to 16 ppb approximately 8 months later. Groundwater at UZ-1 reached a high of 20 ppb. Samples collected at the remaining 3 sites never exceeded 5 ppb.

4.3. Qualitative Discussion of Selenium Distributions resulting from Seasonal Flooding

As mentioned previously, the resaturation experiment actually involved two separate flooding events separated by a period when the pond soils were allowed to dry. This section will draw on data collected throughout the wetting/drying/wetting cycle in order to qualitatively discuss the effect of seasonal wetland management practices on selenium levels in soil water and pond water.

In Figure 4.24, we see a time trend for a site in Pond 1 of total selenium levels in soil water

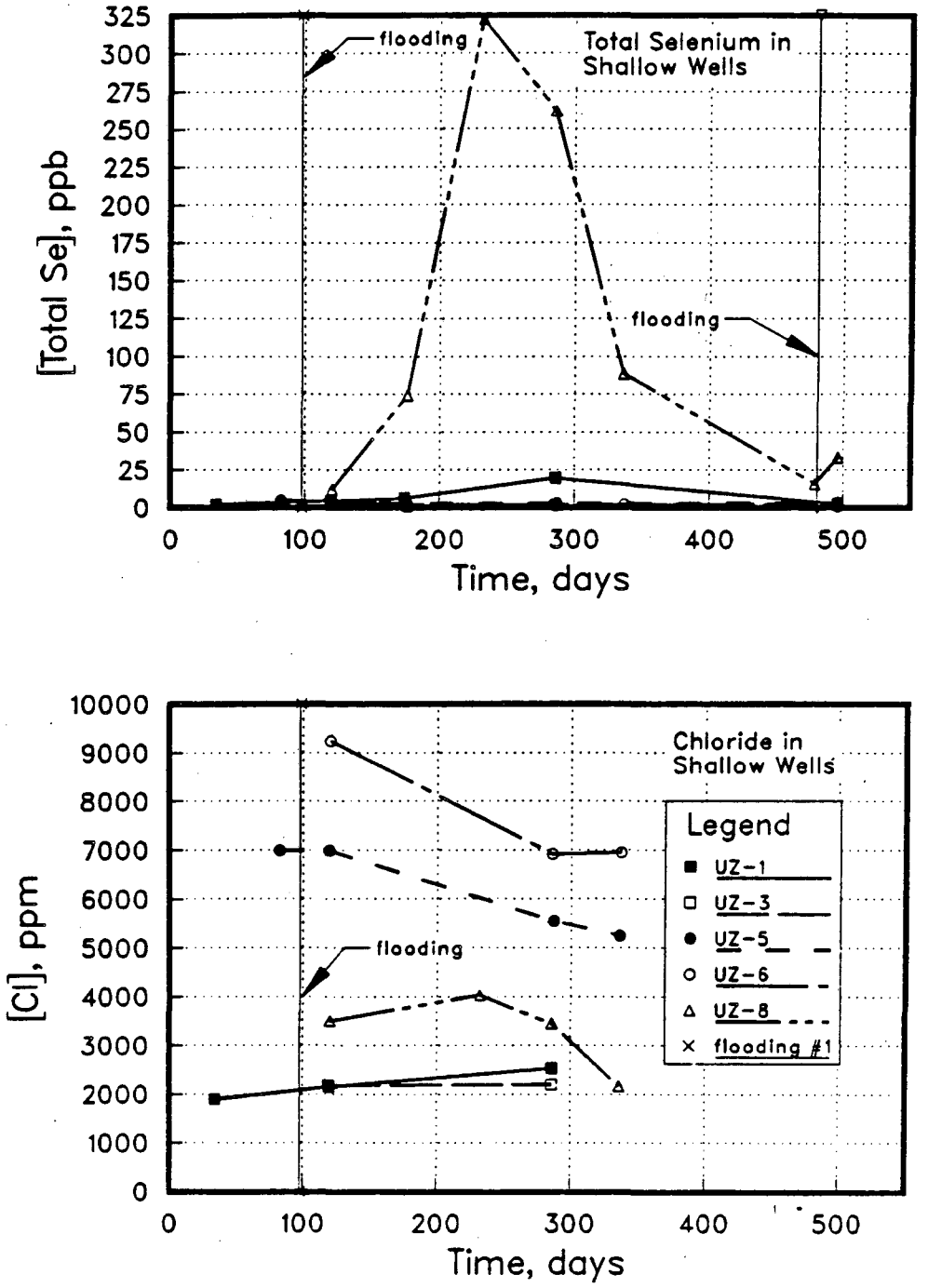

Figure 4.23 Total selenium and chloride concentrations vs time in shallow groundwater samples collected throughout the experiment at the five flooded sites.

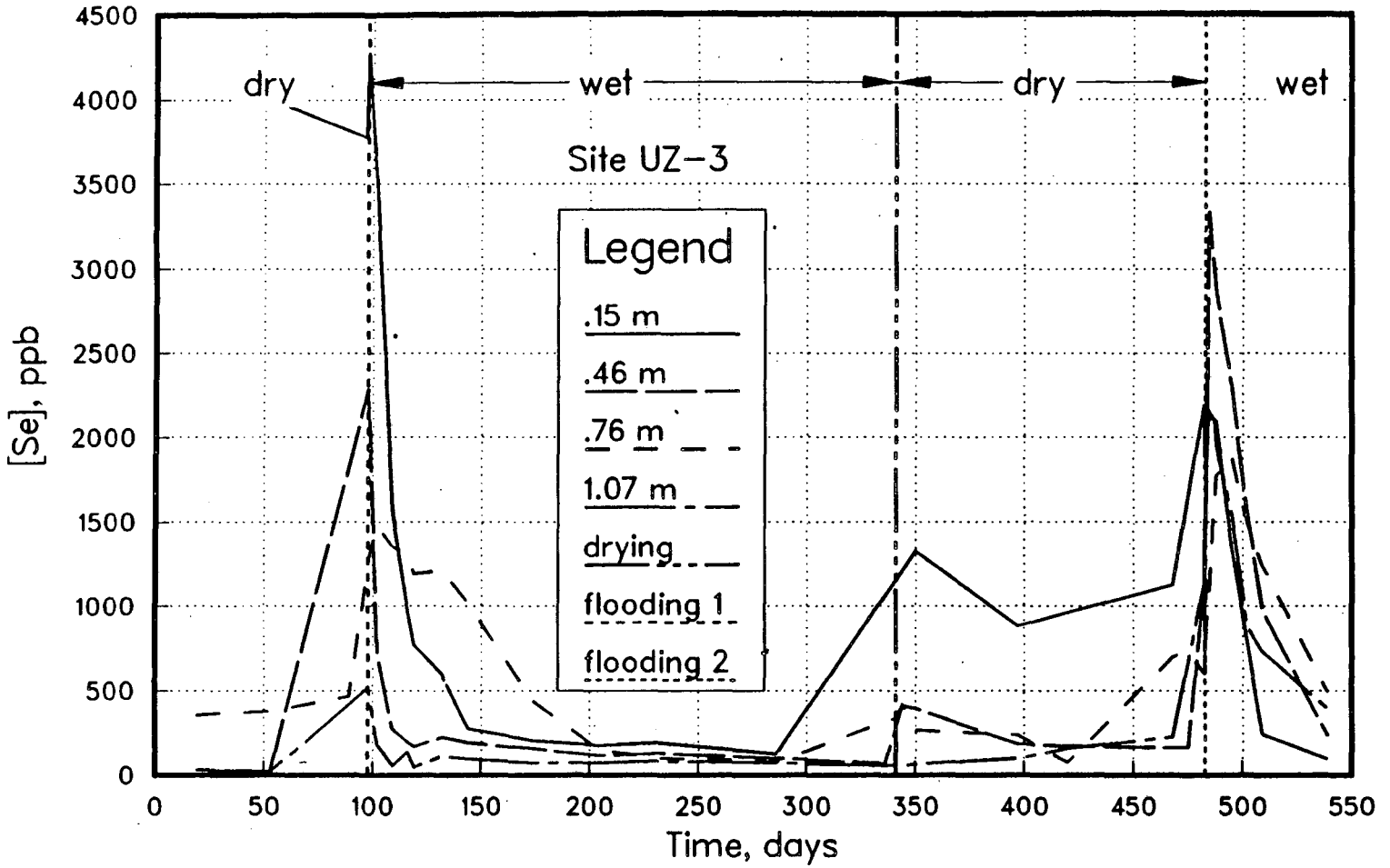

Figure 4.24 The evolution of soil solution total selenium concentrations with time at site UZ-3 in response to periodic wetting and drying.

collected at four depths. The general trends demonstrated by the figure can be considered typical of the five Pond 1 sites. Periods of ponded and un-ponded conditions have been indicated on the figure. The onset of flooding around day = 100 led to increases in the selenium concentration even at the deepest depth where the level increased from a pre-flooding value of 22 ppb to 514 ppb. The observed increases resulted largely from the dissolution of selenate mineral phases contained in a surficial evaporite mineral crust and the downward movement of seleniferous pore waters from the surface. Another possibility includes the oxidation and subsequent dissolution of reduced selenium mineral phases.

Following the sudden rise, selenium concentrations declined rapidly, at a rate much more rapid than in the case of chloride, both when individual soil water samplers and average concentration responses are examined. Assuming chloride to behave conservatively (Section 3.6), selenium therefore appears to have undergone a rapid chemical transformation that selectively removed it from the aqueous phase. Chapter 5 will include a quantitative analysis of selenium immobilization.

Referring again to Figure 4.24, we see that with continuous flooding, selenium concentrations at all depths fell to ≤ 150 ppb and continued to slowly decline. Selenium concentrations in the soil water at the wet sites in Pond 1 were low in comparison to areas in the Reservoir where, in general, the water table was below the ground surface *(Lawrence Berkeley Laboratory*, 1987c p. 84). Similarly with pond water, we see in Figure 4.25, that after an initial period of relatively high concentrations, selenium levels stabilized at ≤ 25 ppb. Drying out the pond led to an increase again in soil water total selenium concentration, especially at the shallowest depth, to levels that approached the pre-flooding values. At sites UZ-3 and UZ-4 selenium concentrations exceeding 1000 ppb re-occurred within a period of a few weeks of drying out. A possible explanation is that aeration of pond soil exposed reduced forms of selenium to oxygen, thereby converting them to more soluble forms. Evaporative fluxes also probably led to increased selenium levels in near-surface soil water. Flooding the pond a second time was again accompanied by a large increase and subsequent rapid decrease.

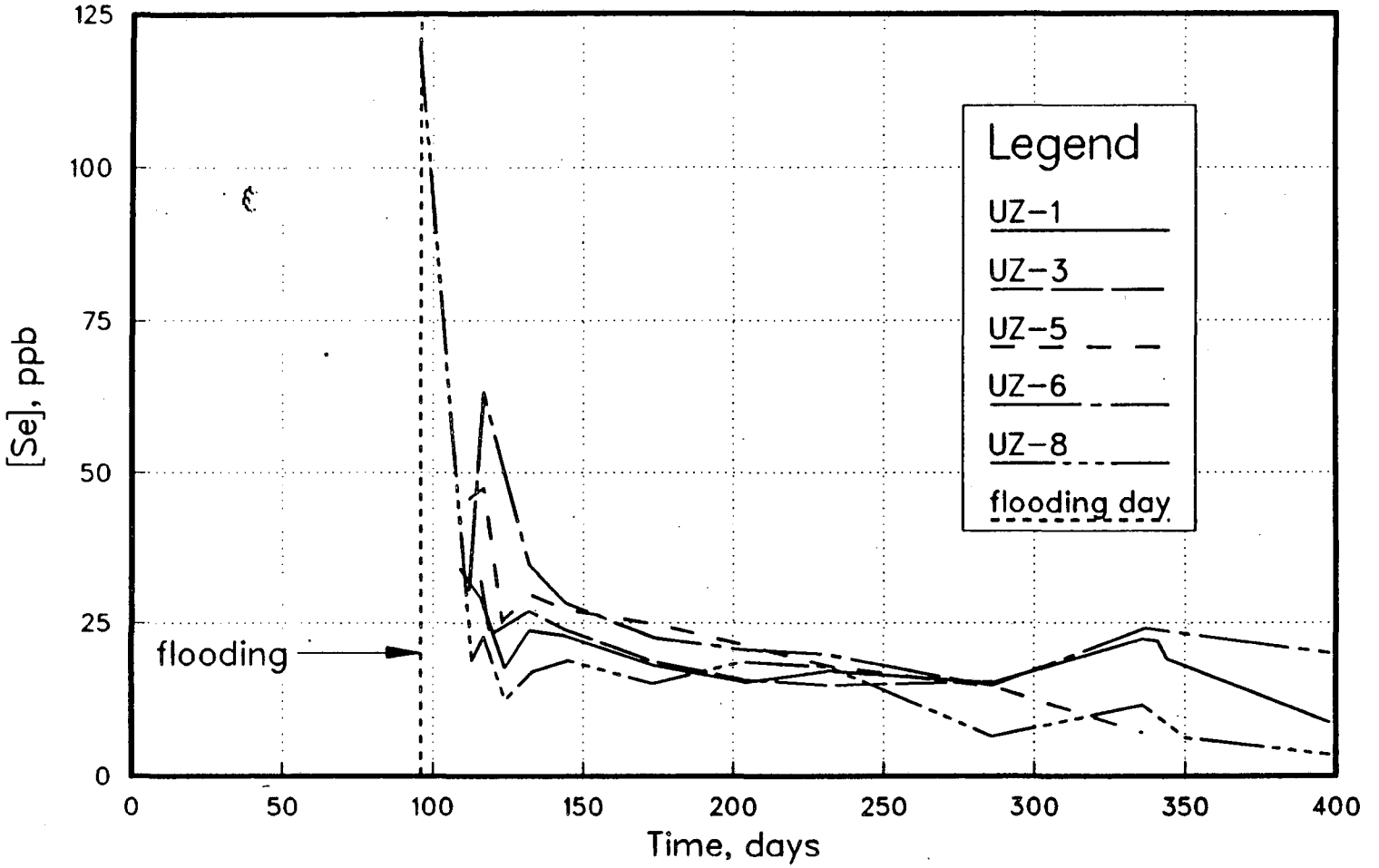

Figure 4.25 Pond 1 surface water total selenium concentrations with time.

These same type of observations are evident in Figure 4.26 where we see the temporal variation in a selenium *profile* throughout the same cyclic flooding episodes.

In Figures 4.27 to 4.29 the selenate to selenite concentration ratio has been plotted for 4 depths at each of the sites. Refer to Appendix II for a complete listing of ratios calculated for all 8 depth locations and pond water. Both flooding events are included in these figures. A number of observations are possible from an examination of these curves:

(1) Reflecting the predominantly oxidizing conditions that existed in the pond sediment under unsaturated conditions, selenate to selenite ratios prior to flooding were typically much greater than 1. In the the deeper samples ratios were generally in the 1's to 10's range while near the surface ratios in the 10's to 100's were more typical. At sites UZ-5 and UZ-6, however, ratios as low as .02 were observed in deeper soil water, indicating a possible lack of atmospheric oxygen at depth.

(2) At nearly all of the soil water sampler locations, the flooding episodes led to an increase in the selenate to selenite ratio, indicating that selenium was remobilized preferentially in the form of selenate by the oxidizing pond waters. Ratios increased immediately with flooding and by factors from approximately 2 to 30. Even in the shallow soil water (0.15 m and 0.30 m depths), already characterized by relatively high ratios (10's and 100's), increases were observed (during the second flooding event).

(3) The increase often was very short-lived, especially in the shallow soil water. Selenate to selenite ratios quickly dropped in only a few days after flooding as immobilization occurred, eventually stabilizing at some sites at values ≤ 1. The large apparent selenium immobilization, therefore, occurred primarily with the selenate ion.

(4) The absolute magnitude of the ratio values observed varied between sites and appeared to coincide with site total selenium inventories. Sites with high selenium (UZ-1, UZ-3, and UZ-8) inventories exhibited higher values of the selenate to selenite ratio. Sites UZ-5 and UZ-6, however, which have shown to have relatively lower total selenium inventories also demonstrated lower ratios.

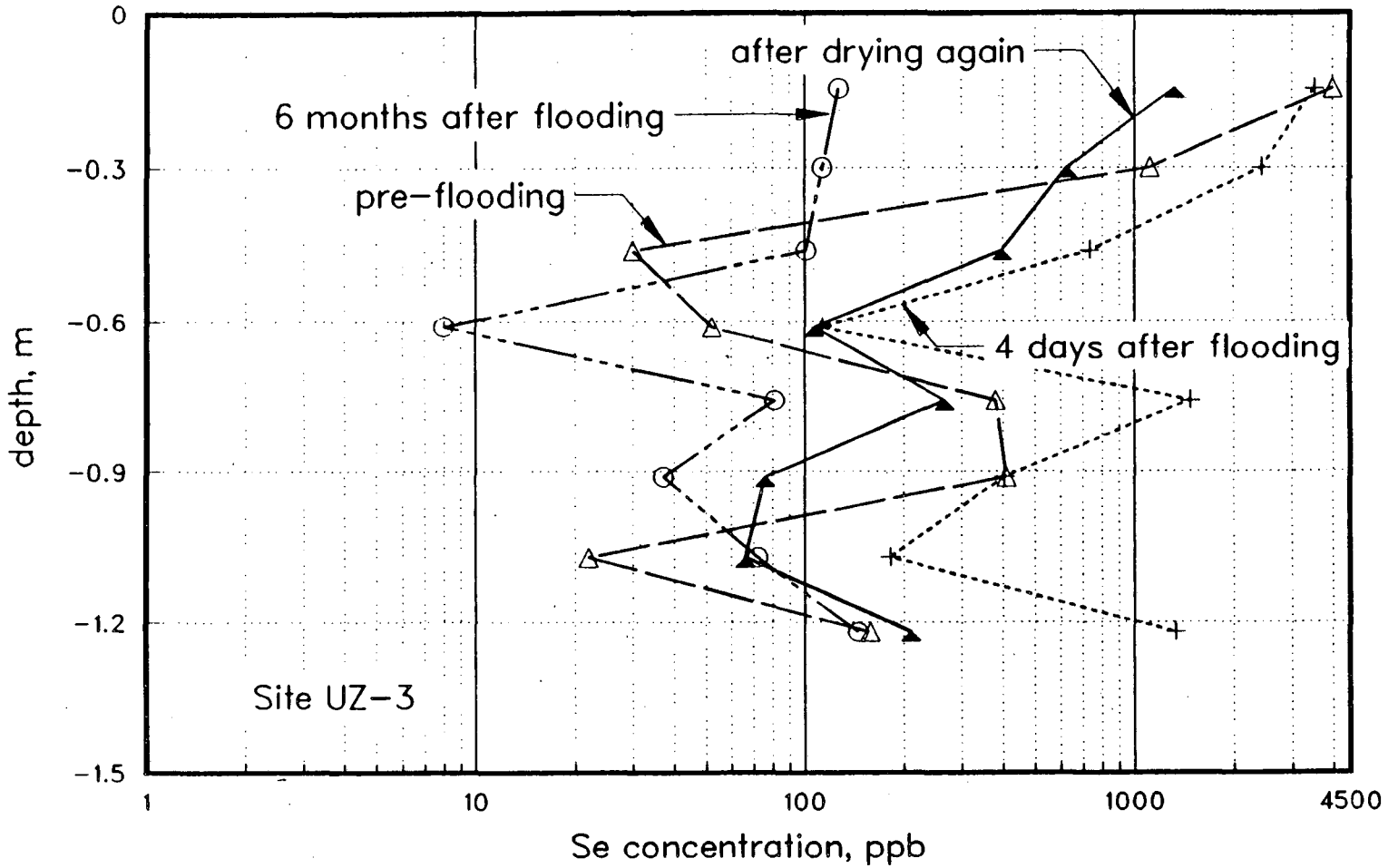

Figure 4.26 Soil solution total selenium concentration depth profiles with time at site UZ-3 in response to periodic wetting and drying.

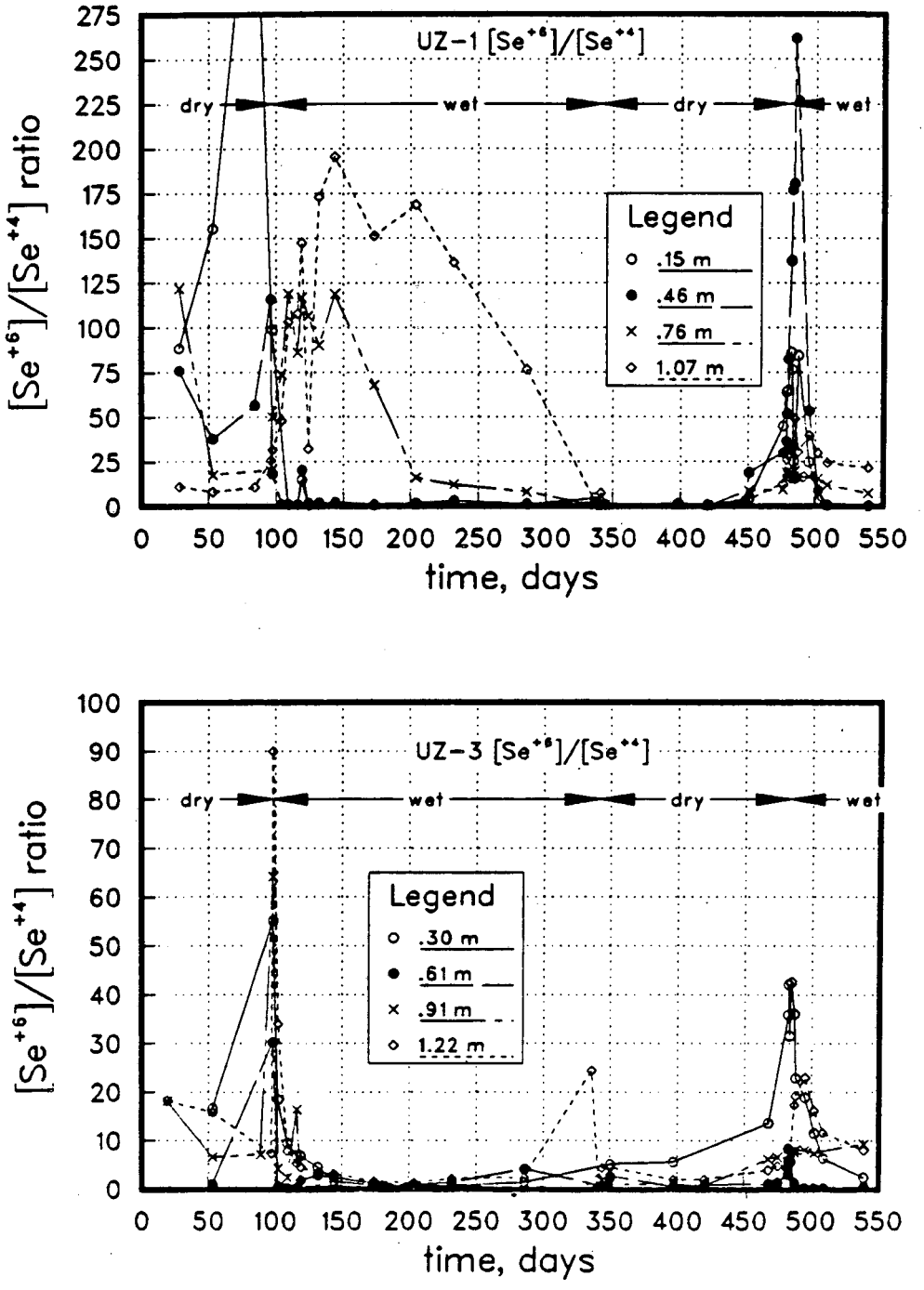

Figure 4.27 Selenate to selenite ratios of samples collected throughout flooding for sites UZ-1 and UZ-3.

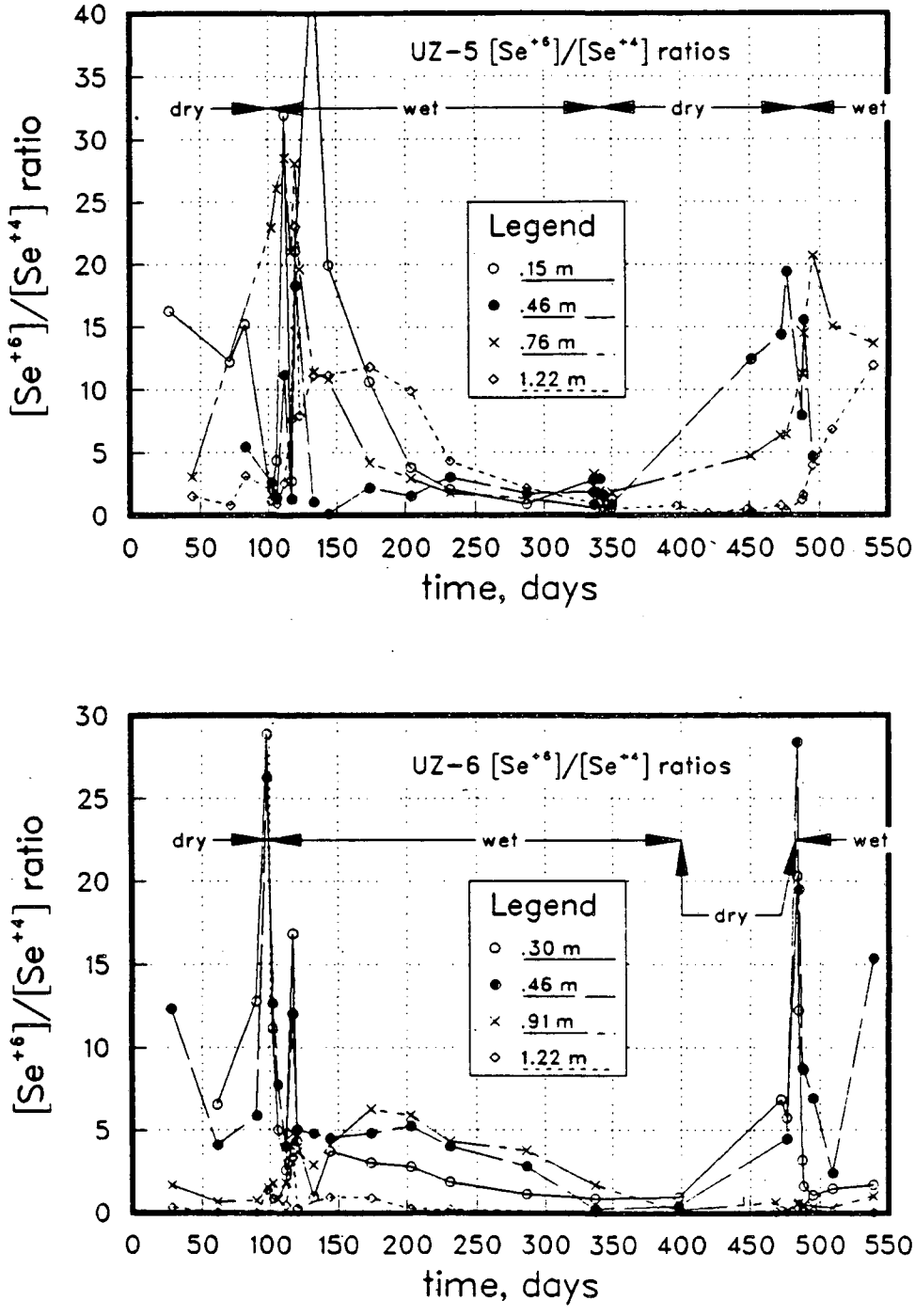

Figure 4.28 Selenate to selenite ratios of samples collected throughout flooding for sites UZ-5 and UZ-6.

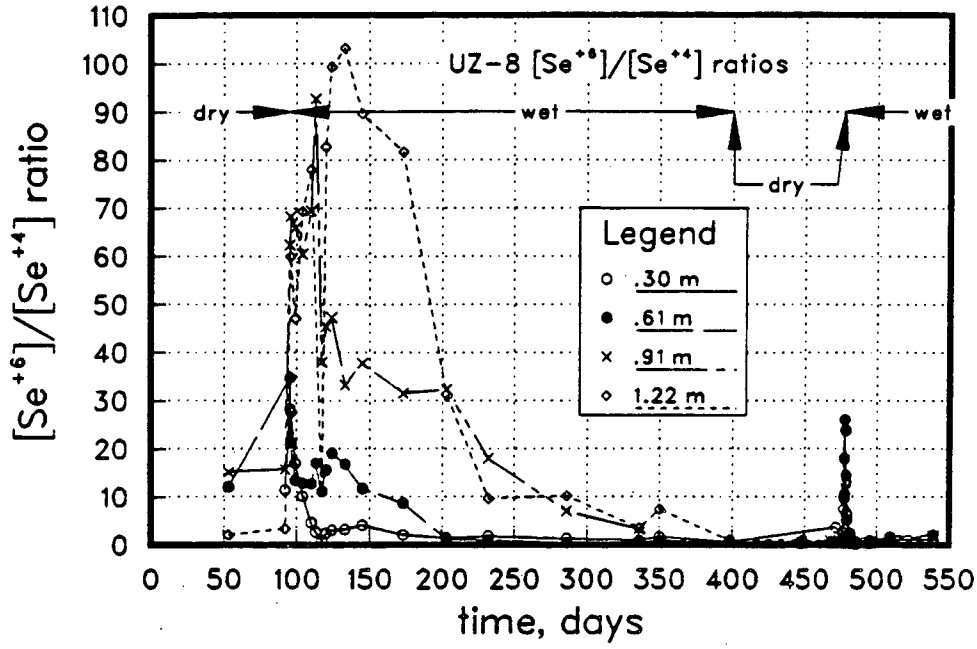

Figure 4.29 Selenate to selenite ratios of samples collected throughout flooding for site UZ-8.

(5) At three sites - UZ-1, UZ-5, and UZ-8, the rate of the ratio decline appeared to be related somewhat to depth. Deeper soil water maintained a high value of the ratio for longer time periods, possibly indicating that reducing conditions were established more quickly at the shallower depths. Infiltration by low ratio pond water could also account for this more rapid decline in the shallow area.

(6) In the shallow soil water, pond drying coincided with a return to values greater than 1 (Appendix II - UZ-3) as sediment exposure to the air led to variations in the redox status of the soil and probable conversion of reduced selenium species to more soluble forms.

(7) Pond water ratios (Appendix II) remained nearly constant over time in the approximate range of .5 to 3.5.

4.4. Importance of Macropore Flow

Strong evidence has been provided in the solute breakthrough data (Figures 4.8 to 4.17) for the establishment of preferential flow paths and bypass through part of the wetted space during the hours immediately following flooding. In general, theories describing miscible fluid displacement in uniform soil predict the appearance of a non-adsorbed solute at the outflow end of a saturated soil column after the application of one-pore volume of fluid. Experiments involving the transport of solutes in field situations, however, have often demonstrated quite different behavior. Many investigators have examined the importance of large soil voids and have observed that macropores can significantly increase the rate at which solutes and water move through field soils. *Beven and German* (1982) provide a particularly complete review and documentation of experimental evidence. *Aubertin* (1971) used flouresceine dye in a study involving percolation through a forest soil and observed that water may move very rapidly through the soil macropores and not contribute to the wetting of the soil mass. *Kissel et al.* (1973) also demonstrated that large continuous soil cracks were important pathways of transport in swelling clay soils with a solution of chloride and fluorescein dye. fluorescein and chloride were found to have moved quite rapidly through soil cracks whereas in nearby areas little or no fluorescein was found. *Godfrey* (1964) determined that remnants of shrinkage cracks resulting from long term dessication cracking may persist as natural fissures in

swelling clay soil.

In the present study, the transport of solutes in the period immediately following flooding occurred much more quickly than would be predicted based on available saturated hydraulic conductivity data and uniform infiltration. Saturated hydraulic conductivities at the five sites, based on harmonic mean values of *in situ* conductivity profiles, range from 1 to 20 m/year (3.3 to 65.6 ft/year), clearly much to low to be able to account for the nearly instantaneous selenium and chloride concentration increases observed. At Kesterson, large pores, channels and cracks have been observed on the soil surface. Clay shrinkage during hot summer months and subsequent dessication cracking probably account for a majority of these macropores. The possibility that macropores could act as local conduits for rapid vertical migration to groundwater certainly exists. However, selenium levels in shallow groundwater suggest that even though macropores may allow some amount of water to travel deeper into the soil profile before immobilization removes selenium from soil water, overall, selenium migration into the shallow aquifer is substantially inhibited.

In addition to the existence of macropores, the possibility exists that leakage along the walls of soil water samplers could have contributed to the observed apparent bypass of the soil matrix. It is most likely that annular flow would have occurred, if at all, during the earliest periods of flooding when the soil was still not fully water saturated. During soil water sampler installation, a considerable amount of care was taken to tamp soil firmly and closely around the sides of the sampler wall (Section 3.2). Clay shrinkage, however, could potentially have occurred due to summer conditions and created a small annular region along the sides of the sampler tube. This annular space would behave as additional macropore volume. If an annular space was created due to shrinkage, resaturation of the soil during flooding would likely cause the soil to swell and reseal the flow path. If annular flow continued to occur throughout the course of the experiment, levels of chloride in soil water samples would quickly approach pond water chloride concentrations.

By assuming that the entire change in chloride concentration at a particular soil water sampler was due to dilution with annular pond water, a worst case estimate of the magnitude of the annular flow contribution can be made in a simple calculation. By comparing the chloride concentration in a soil water sample at a particular instant with that observed at the beginning of flooding (Appendix II), the percentage of soil water that was made up of pond water can be determined, based on the following equation:

$$x \cdot C_o + y \cdot C_a = C_t \qquad (3)$$

where x and y are the percentages of original soil water and pond water, respectively, that have mixed and $x + y = 1$. C_o is the concentration of original soil water - soil water collected just prior to or after flooding, C_a is the concentration of annular pond water, and C_t is the soil water chloride concentration that results from the mixing. C_t was taken as the last measured chloride concentration with time for the purposes of this calculation. The chloride concentration of pond water was observed to be fairly constant at approximately 1000 ppm throughout Pond 1 (C_a = 1000 ppm). Among the 1.22 m (4 ft) soil water samplers, the largest value of y, the annular flow percentage, was 35% at UZ-8. The other 4 sites were all below 7.5% with 3 below 3.5%. Since this calculation neglects any contribution from matrix infiltration, the actual annular flow contributions were less than these estimates. The issue of annular flow will largely remain unresolved, however, the results of this conservative estimate suggest that, at least after soils became fully saturated, annular flow contributions were probably not significant in the temporal solute variations that were observed.

5. SELENIUM IMMOBILIZATION ESTIMATES

The previous section consisted of a presentation and qualitative description of data relating to the impact of flooding on selenium distributions in pond bottom sediments and the quality of shallow groundwater underneath Pond 1. This chapter consists of a quantitative evaluation of selenium immobilization. A series of calculations have been performed utilizing the average chloride concentration data and the concept of mass balance to determine the amount of selenium that was transported out of the 1.22 m (4 ft) thick study zone and the extent to which selenium was removed from solution. All results and calculations presented pertain only to the 1.22 m thick monitoring zone. For purposes of definition, "discharged" refers to the mass of water or of soluble total selenium that was transported out through the bottom of the study block. "Immobilized" refers to that portion of soluble total selenium that was converted through some chemical or biological process to a non-soluble or sorbed form of selenium within the study block. Such processes include adsorption and precipitation. Volatilization may also have accounted for some small percentage of the observed selenium immobilization.

5.1. Calculation Methodology and Assumptions

The immobilization calculations include the following series of assumptions:

(1) The dissolution of selenium and chloride is assumed to be essentially instantaneous and complete, so that all of the potentially available solute enters into solution within a very short time following wetting - possibly within a few hours. Kinetic limitations to dissolution are not considered. Therefore, solutes are not being introduced into the study block, after the initial flooding episode, other than by migration of infiltrating waters. The assumption of instantaneous and complete dissolution allows the post-flooding high concentrations to represent the initial inventories in the system of the two solutes. Quantities measured at later dates are normalized to these post-flooding highs.

(2) Diffusion of solutes from within the interior of soil aggregates to the soil water sampler cup surface is assumed to be negligible. The observed chloride response is therefore indicative only of advective movement and does not also represent a source term of this sort.

(3) Saturation of the system is assumed to occur essentially instantaneously. This assumption is not strictly correct, however, computer modeling of the saturation process indicates that the minimum saturation within the soil column is at least 90% within the first day after the ground surface is flooded. This prediction is corroborated by tensiometer data.

(4) As discussed in Section 3.6, chloride can be assumed to behave conservatively. Therefore, after the initial rise in concentration brought on through the dissolution of material near the soil surface, chloride removal or addition to the aqueous phase does not occur. Chloride can only be removed from the soluble inventory of the study block through advective transport in water. If we assume that ρ_f, the fluid density, and ϕ, the porosity of the saturated medium, are constant throughout the study block, then the *average* chloride concentration is directly equatable to the total mass of chloride present, M_{Cl} (kg), in the study block by the equation:

$$M_{Cl} = \rho_f \cdot \phi \cdot V \cdot C_{Cl,ave} \tag{4}$$

where $C_{Cl,ave}$ (kg Cl·(kg fluid)$^{-1}$) represents the average chloride concentration of soil water collected in the 8 soil water samplers and V (m^3) is the bulk volume of the 1.22 m deep soil column (assume a unit surface area). The temporal variation in $C_{Cl,ave}$ (Figures 4.18 to 4.22) can therefore be used as an indication of the rate at which water seeps through the soil profile. Selenium, on the other hand, is released into solution at the initiation of flooding, by dissolution and the oxidation of reduced forms by aerated waters, and is then subject to various chemical and/or biological mechanisms that may cause immobilization.

(5) The average pore water velocity of fluid that infiltrated through the 1.22 m thick study block throughout the duration of flooding is treated as a constant in the calculation procedure. This assumption is surely not correct in the strictest sense, but was deemed satisfactory for the purposes of these calculations. It is not the intent to imply that the average pore water velocities determined depict actual fluid velocities but that they represent spatially and temporally averaged effective values. The actual velocities were probably higher during early and late stages of flooding, and lower during the middle period. The

presence of macropores and the heterogeneous nature of the soil profile probably led to the situation where localized zones were characterized by fluid velocities considerably variant from the mean value. Within the interior of aggregates, fluid velocities were considerably less than those in larger, well-connected pore spaces.

In order to understand the motivation behind the use of the constant fluid velocity assumption, it is helpful to examine measurements of fluid potential that were made with tensiometers installed at each site prior to flooding. The measured hydraulic heads at various depths within the five flooded sites are plotted in Figures 5.1 to 5.3. While the resolution of such fluid potential data is probably insufficient to distinguish gradients within the soil column, it can be used as a general indicator of the degree to which fluid potentials and therefore fluid velocities were changing within the soil profile with time. In the figures we see that the fluid potential responses over time at the five flooded sites were relatively flat and constant. Hydraulic heads began to vary considerably only near the end of the experiment when the pond was drying out. It is these data that implied that the constant velocity assumption might be appropriate. A discussion of the validity of this assumption and others used in the calculation method is included at the end of this section.

In order to calculate the rate of seepage from the pond, a simple mass balance is performed on chloride within the study block. The mass of chloride present in the study block with time, $M_{Cl,t}$ (kg), can be represented by the following equation:

$$M_{Cl,t} = M_{Cl,o} + M_{Cl,in} - M_{Cl,out} \tag{5}$$

where $M_{Cl,o}$ (kg) is the initial mass in the system (the above mentioned post-flooding high), $M_{Cl,in}$ (kg) is the cumulative mass that has flowed into the study block with infiltrating waters since the initiation of flooding, and $M_{Cl,out}$ (kg) is the cumulative mass outflow that has occurred out of the bottom. These quantities are defined as follows:

$$M_{Cl,in} = \rho_f \cdot v \cdot \phi \cdot A \cdot C_{Cl,in} \cdot \Delta t \tag{6}$$

$$M_{Cl,out} = \rho_f \cdot v \cdot \phi \cdot A \cdot C_{Cl,out} \cdot \Delta t \tag{7}$$

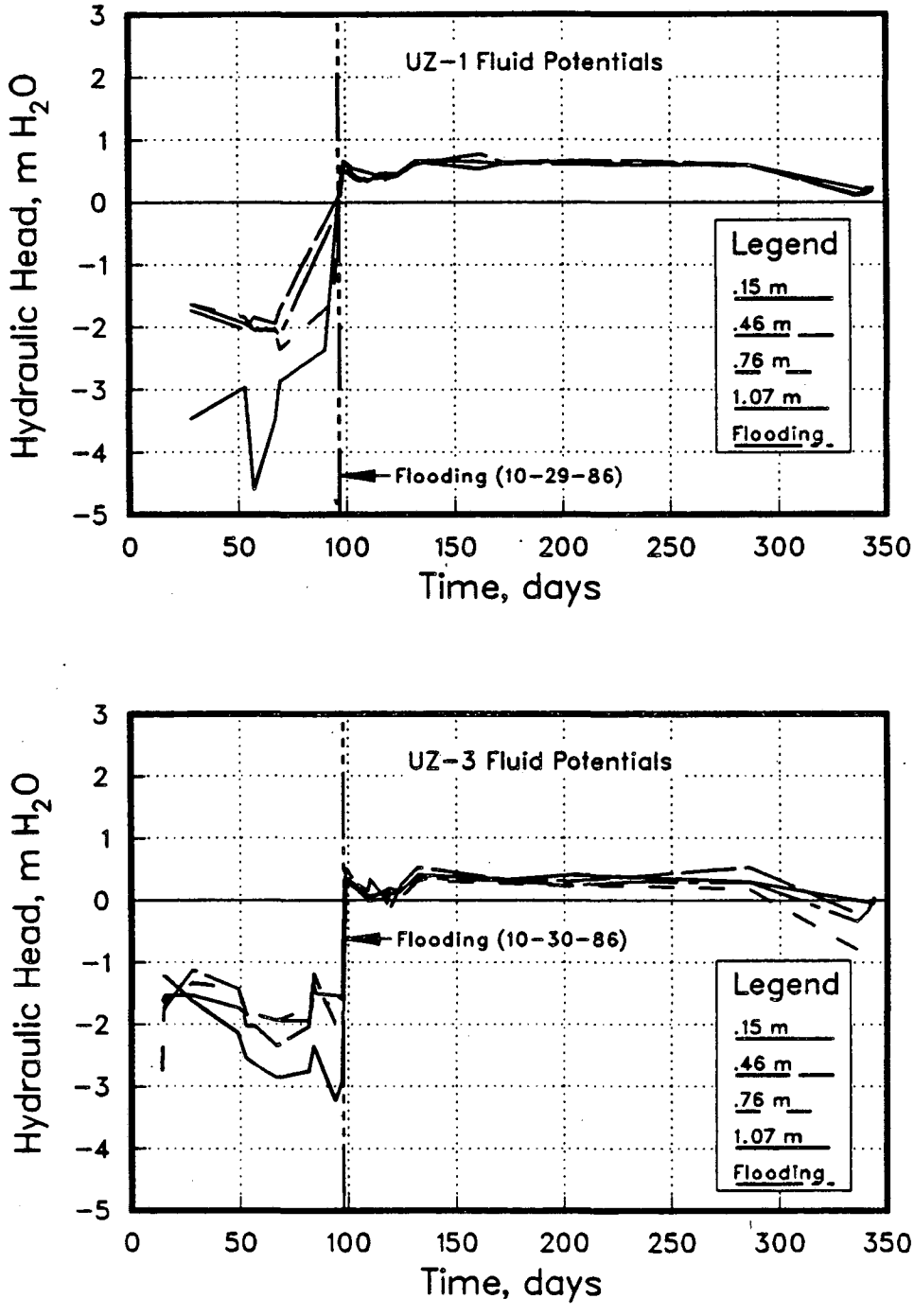

Figure 5.1 Tensiometer measurements of hydraulic head made throughout flooding for sites UZ-1 and UZ-3.

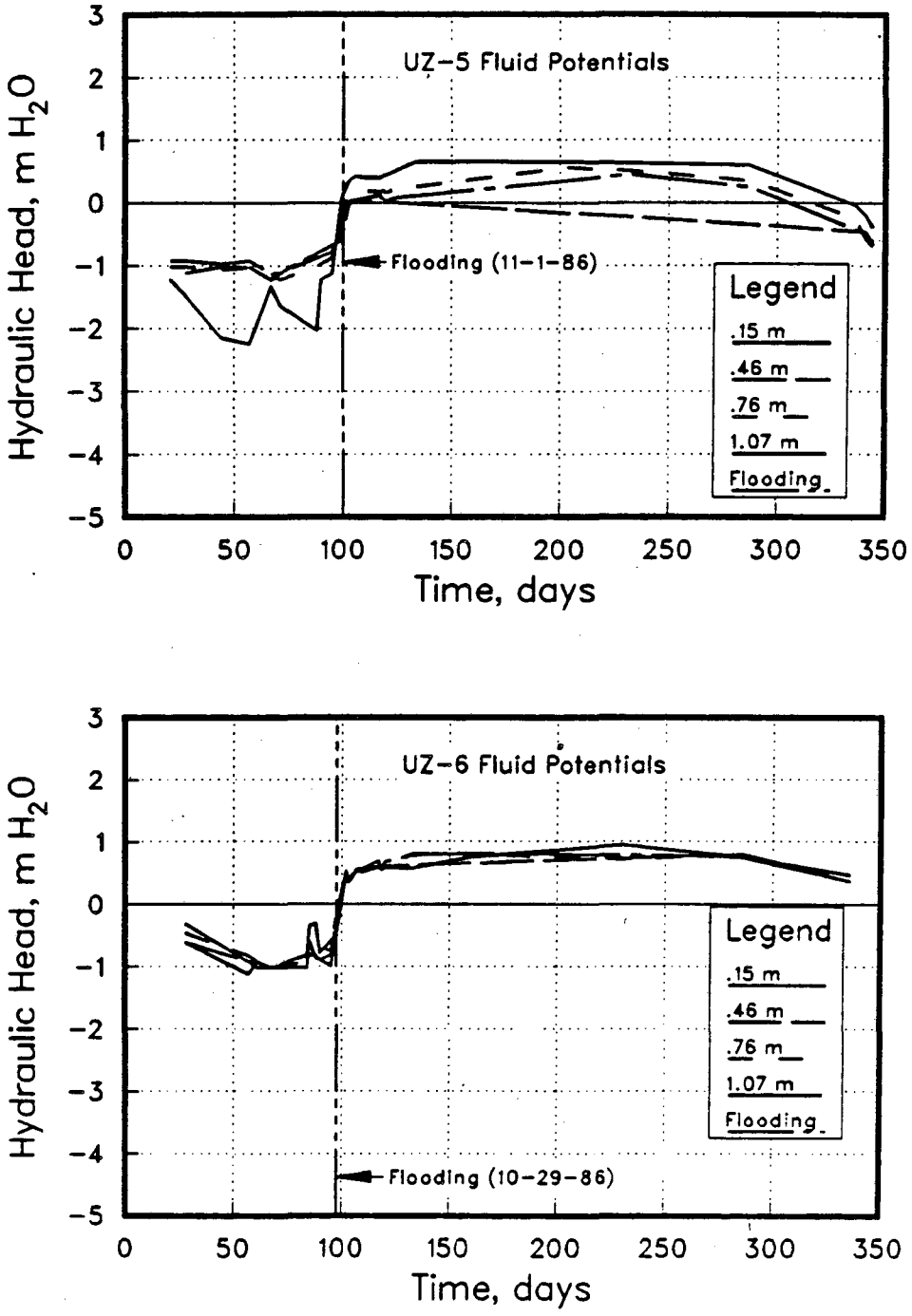

Figure 5.2 Tensiometer measurements of hydraulic head made throughout flooding for sites UZ-5 and UZ-6.

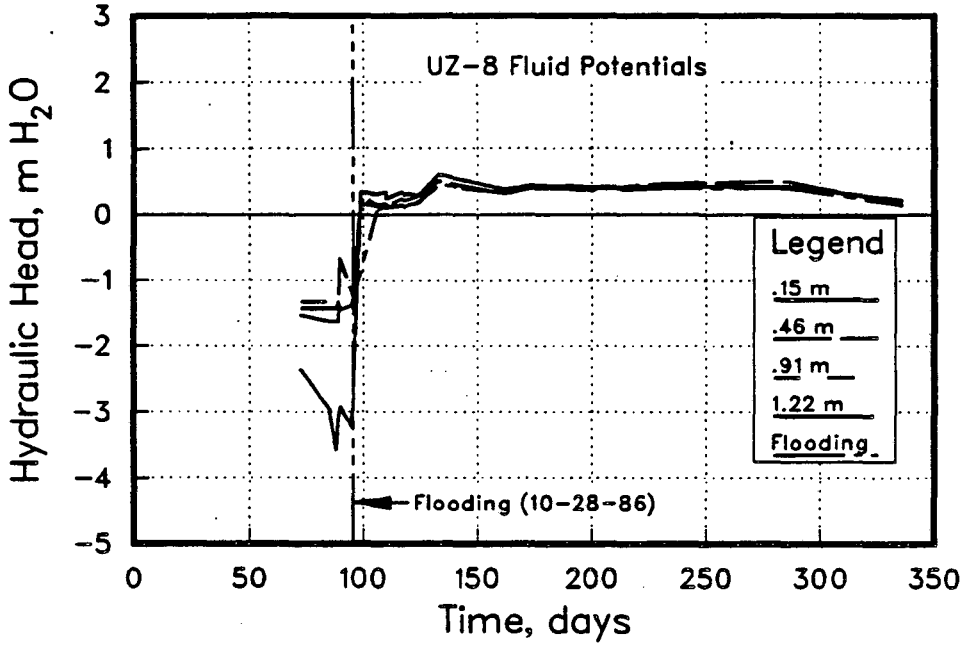

Figure 5.3 Tensiometer measurements of hydraulic head made throughout flooding for site UZ-8.

where,

ρ_f = fluid density, (kg water·m^{-3})

v = average pore velocity, (m·day^{-1})

ϕ = porosity (= 0.4)

A = cross-sectional area (= 1 m^2)

$C_{Cl,in}$, $C_{Cl,out}$ = Cl concentration of waters entering and exiting the monitoring zone, respectively, (kg Cl·(kg fluid)$^{-1}$).

Δt = interval between sample collection (time step), days

For the purposes of the estimates, $C_{Cl,out}$ is defined as the chloride concentration of waters collected from the sampler at the 1.22 m (4 ft) depth, and $C_{Cl,in}$ is set equal to pond water chloride concentrations. The observed value of Cl in the study block with time, $M_{Cl,t}$, is determined simply by multiplying the observed average chloride concentration (Figures 4.18 to 4.22) by the total volume of water present in the 1.22 m zone. A porosity of 0.4, an area of 1 m^2, a fluid density of 1000 kg·m^{-3}, and a depth of 1.295 m (4.25 ft) are assumed for these calculations at each of the sites. The only unknown quantity in Eq. (5) is v, the average pore water velocity. Through a trial and error procedure that compares an estimated chloride study block content with the observed value, based on Eq. (4-7), an average pore water velocity is determined. The most satisfactory match possessed the minimum *percent* difference between the estimated and observed chloride versus time concentrations.

In Figures 5.4 to 5.6 we see the observed and calculated chloride contents based on the optimized value of average pore water velocities determined at each site. Table 3 shows the extent of deviation in percent between the predicted values and observed values. These percentages were calculated for each time step over which the calculation was performed. The time steps correspond to time intervals between sample collection. The maximum deviation is

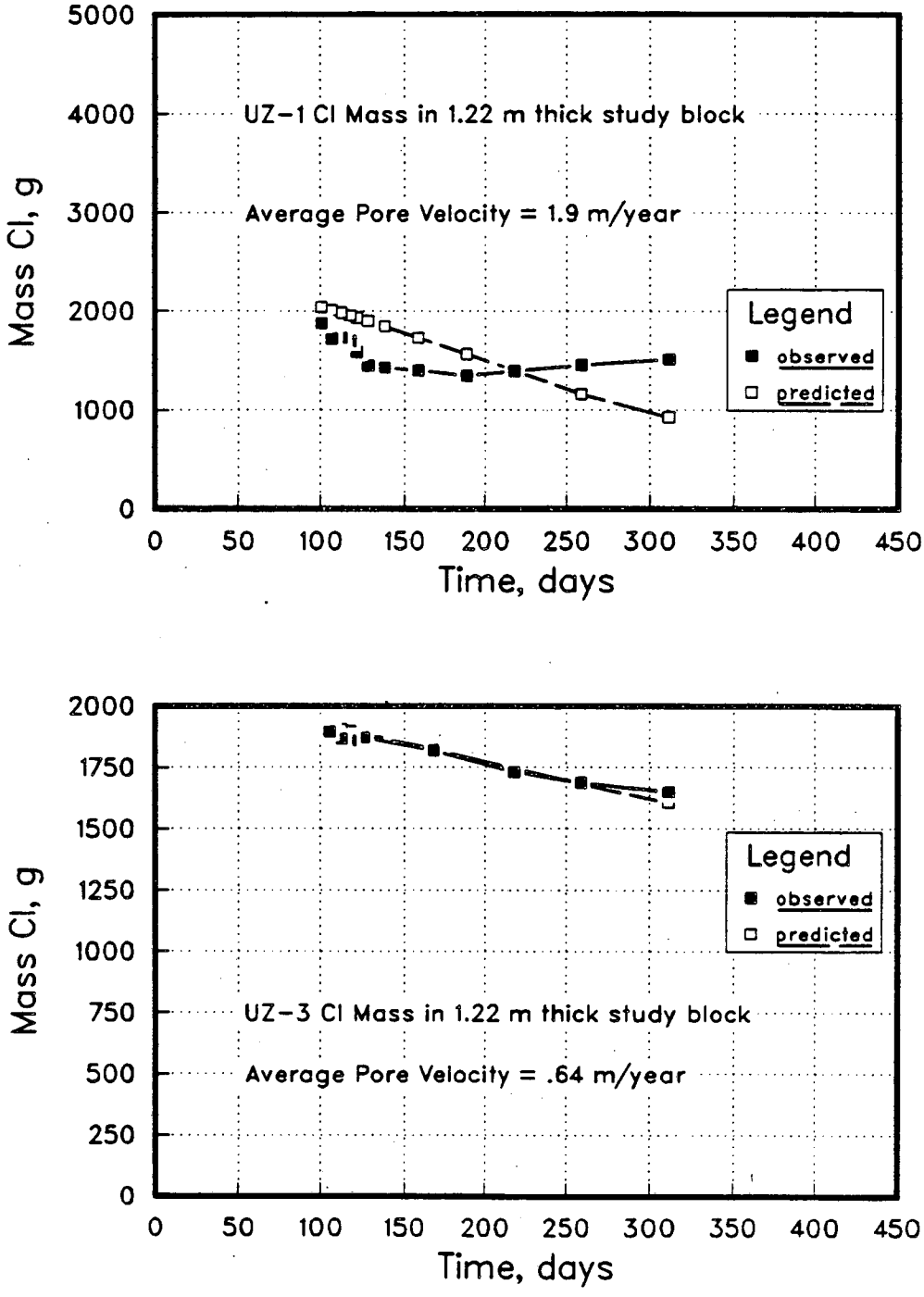

Figure 5.4 Predicted and observed study block chloride contents at sites UZ-1 and UZ-3 based on the optimized average pore water velocity.

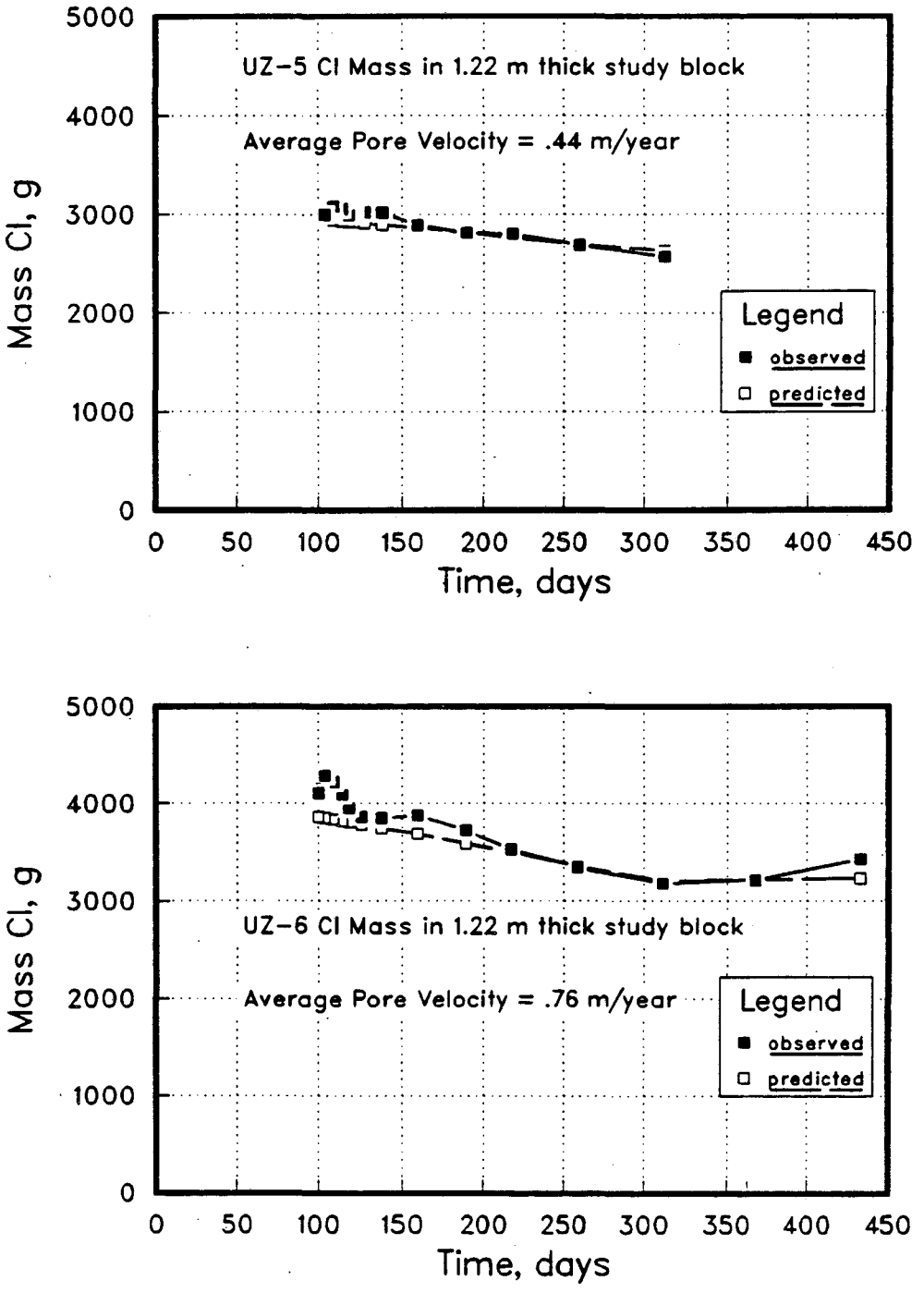

Figure 5.5 Predicted and observed study block chloride contents at sites UZ-5 and UZ-6 based on the optimized average pore water velocity.

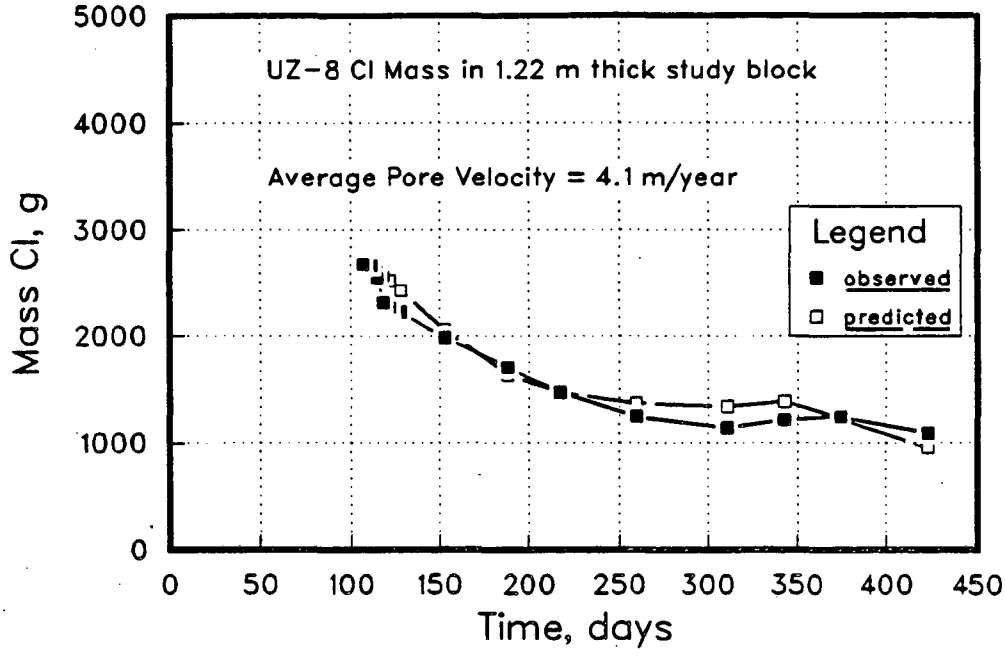

Figure 5.6 Predicted and observed study block chloride contents at site UZ-8 based on the optimized average pore water velocity.

simply the maximum percent difference that occurred between any time step while the average deviation is the average, at a particular site, of the individual time step deviations. The maximum deviation (38.6%) and maximum average deviation (19.7%) both occurred at site UZ-1. As is evident in the figures and the table, the other sites demonstrated much closer agreement.

Table 3. Percent Deviation Between Estimated and Observed Study Block Cl Contents based on the Optimized Average Pore Water Velocity

Site	Maximum Deviation,%	Average Deviation,%
UZ-1	38.6	19.7
UZ-3	5.3	2.0
UZ-5	4.5	2.3
UZ-6	10.1	4.0
UZ-8	17.5	7.0

For selenium, a similar mass balance procedure is performed, however, an extra term, M_{Imm} (kg), is added to the mass balance Eq. (5), to account for the transformation and immobilization of selenium from solution. The mass balance equation takes the form,

$$M_{Se,t} = M_{Se,o} + M_{Se,in} - M_{Se,out} - M_{imm} \tag{8}$$

where,

$$M_{Se,in} = \rho_f \cdot v \cdot \phi \cdot A \cdot C_{Se,in} \cdot \Delta t \tag{9}$$

$$M_{Se,out} = \rho_f \cdot v \cdot \phi \cdot A \cdot C_{Se,out} \cdot \Delta t \tag{10}$$

and ρ_f, v, ϕ, A, and Δt are as above for chloride. $M_{Se,o}$ (kg) is the initial mass of selenium in

the system and is determined from the post-flooding high of average selenium concentration. $C_{Se,in}$ (kg Se·(kg fluid)$^{-1}$) is set equal to the selenium concentrations measured in infiltrating pond waters and $C_{Se,out}$ to concentrations measured in waters collected from the 1.22 m soil water sampler. Since the velocity is determined from the analysis of the chloride data and $M_{Se,t}$ is the observed mass of selenium in the system, the only unknown is M_{imm}. The difference between the initial inventory ($M_{Se,o}$) and the sum of the fluxes crossing the monitoring zone boundaries is the quantity that has been immobilized (M_{imm}).

The apparent ability of the simple predictive model to match average chloride concentrations (Figures 5.4 to 5.6) does not necessarily confirm a valid description of system behavior. Nor does it necessarily justify various assumptions that were made, including the choice of a *constant* average pore water velocity. There are a combination of factors, such as the other basic assumptions made in the calculation method, that conceivably contributed to the match. There is an element of non-uniqueness that must be dealt with before it can be said that the apparent ability of the predictive model to match chloride concentrations verifies the fluid velocity predictions. Therefore, a discussion follows of the relative merit of the first three assumptions and their potential for introducing uncertainty into the calculation procedure.

(1) The dissolution of soluble forms of selenium and chloride mineral phases was assumed to be instantaneous and complete. Selenate and selenite (in oxic waters) and chloride are all highly soluble. The relevant question is whether there were kinetic limitations to dissolution such that selenium and chloride continued to enter into the aqueous phase after the initial soluble inventories were calculated. As is discussed in the next section, selenium immobilization was initiated within a few days following flooding. A source of soluble selenium, therefore, does not appear to be likely since this would imply simultaneous dissolution and immobilization. The discussion below is concerned with possible kinetic limitations to chloride dissolution and potential effects on the average pore water velocity estimates.

At Kesterson, chloride exists in the solid phase in evaporite minerals. The dominant

chloride bearing mineral in Kesterson pond soils has been identified as halite (NaCl) *(Lawrence Berkeley Laboratory,* 1988). *Jurinak et al.* (1977) in batch experiments examining dissolution kinetics of various salts, including gypsum, calcite and halite, with a weathered, shale-derived saline soil, observed that salt dissolution could be described by three, diffusion controlled, first-order reactions. The first reaction was rapid and was completed within the initial 0.5 min of contact with water. It was suggested that this rapid dissolution reaction involved highly soluble salts such as halite. The succeeding slower reactions indicated the presence of relatively slow dissolving salts such as gypsum and calcite. These reactions required roughly 72 hours to attain equilibrium. The release of salt, therefore, was found to be a slow continuous process, but that the highly soluble salts quickly were dissolved and moved through the soil profile in an early, initial pulse.

If halite existed in the interior of soil aggregates, characterized by extremely slow fluid velocities, its dissolution and entrance into the advective stream could potentially be limited to diffusion. Soil water samples collected during unsaturated conditions, however, do not indicate that the solubility limit of chloride was approached within the soil profile. Subsurface halite, therefore, can be discounted, and it is reasonable to suggest that soluble chloride present in the solid phase is not to be found to any significant extent below the soil surface. The very high solubility of surficial halite and its prompt exposure to flooding waters suggests that it underwent rapid dissolution.

(2) The available information does not suggest any kinetic limitations to chloride dissolution in this system. A somewhat related issue, however, may produce a similar effect. Already solubilized chloride within the interior of soil aggregates could be transport limited by slow diffusion outward to the aggregate boundary, thereby providing a chloride source term to the advective stream. For this to occur, a concentration gradient would be required between soil water within the aggregate and soil water at the aggregate surface. If we consider a worst case scenario - one in which the soil water samplers were positioned adjacent to aggregate surfaces and collected water primarily representative of macropore porosity but with a diffusive chloride source term from the aggregate interior,

we can observe the magnitude of any such gradient by comparing the chloride levels after flooding with pre-flooding chloride concentrations. If the opposite case was true, that is, if the soil water samplers were actually positioned within aggregates, then the observed chloride response would be indicative of essentially only advective contributions rather than some additional unknown diffusive component. The pre-flooding chloride levels should give an indication of the approximate chloride concentrations of soil water within aggregates. Examination of chloride breakthrough data in individual soil water samplers (Figures 4.8 to 4.12 and Appendix II) reveals that, after the post-flooding maximums, chloride levels did not decline very rapidly and did not vary to a large extent from the preflooding levels . At the end of the first flooding period, the average chloride concentration at each of the five sites was at least 73% of the initial chloride inventory (except for site UZ-8 which had declined to 43% of the initial inventory). It does not appear that the chloride concentration at the aggregate surface (or at least at the sampler cup surface) was appreciably different from that within the aggregate, and that therefore, diffusive fluxes out of the aggregate would have been small. If chloride did continue to be released into the advective stream, however, after the onset of flooding, due to diffusion from within the interior of soil aggregates, the actual fluid velocities would have been larger than those that were estimated. How much larger would depend on a whole series of factors, including the size of the aggregates, the apparent diffusion coefficient of chloride in soil, the pore water velocity within the aggregates, the degree of communication between soil water sampler and macropore/aggregate porosities, etc.. Larger fluid velocities would result in less immobilization and greater discharge estimates at sites where the concentration of selenium at the discharge end of the study block was greater than that at the inflow end (3 of 5 sites).

(3) The assumption of instantaneous and complete saturation of the soil column was made on the basis of computer modeling of the infiltration process and tensiometer measurements made in the field. Complete saturation ($\geq$ 95%) certainly occurred at some point in the experiment soon after flooding. The critical issue, however, is whether the soil column was indeed saturated when the initial inventory quantities of selenium and chloride were

measured which was just after flooding. These inventory amounts are important in that the immobilization quantities were normalized to the selenium initial inventory, and that they represented components of the mass balance calculations. If saturation was some quantity less than 100%, then the initial soluble inventories were overestimated. As mentioned before, computer modeling indicated that the minimum saturation in the soil profile was roughly 90% after approximately one day. Since a large proportion of the soil column was indeed 100% saturated in the modeling study, the maximum error in calculating the initial solute inventories assuming 100% saturation was < 10%. Overestimating the initial soluble inventory of chloride in the study block would result in the overestimation of average pore water velocity in the chloride mass balance calculations. At two sites, UZ-1 and UZ-8, the mass balance calculation was repeated for chloride with the initial chloride inventories ($M_{Cl,o}$) reduced by 10%. This resulted in new average pore water velocity estimates that were 30% and 20%, respectively, lower than the original estimates. These new average pore water velocities resulted in negligibly different selenium immobilization quantities.

(4) The treatment of chloride as a conservative solute was discussed in Section 3.6. Chloride is highly soluble and non-reactive. Anion exclusion of chloride was concluded to be essentially zero at the concentrations commonly observed in this experiment. Therefore, the potential error from this assumption is considered to be negligible.

The degree of uncertainty associated with the four assumptions discussed above has been shown to be relatively small. Therefore it seems reasonable to assert that the apparent ability of the mass balance calculation to closely predict the observed concentrations of chloride suggests that the assumption of a constant average pore water velocity is an acceptable component of the physical model.

5.2. Immobilization Results

Immobilization and migration of the inventory of soluble selenium have been calculated for each of the flooded sites (UZ-1, UZ-3, UZ-5, UZ-6, UZ-8). Refer to Figures 5.7 to 5.9 for the plots of quantity of selenium that was immobilized or discharged during the flooded portion of the experiment. The data plotted have been normalized to the initial mass of total selenium present in the system, $M_{Se,o}$ - the post-flooding high. It should be noted that it was possible to calculate ratios greater than unity since some selenium was added to the system with infiltrating pond water. This water, however, was low in total selenium (10-40 ppb), and yet, at sites with low initial inventories, the mass of selenium inflow could be significant.

Table 4 summarizes the results of the soluble selenium mass balance calculations in the 1.22 m zone at each of the five sites. The calculations have been performed for the period that began with the first flooding event and ended, for each site, when ponded water was no longer present. This length of time varied from roughly 200 to 300 days, depending on the site (Table 1). The quantities listed include percentages of the initial selenium inventory that were immobilized in and discharged below the 1.22 m zone. We see that immobilization quantities ranged from 66 to 108%, whereas estimates of the mass of selenium discharged ranged from 1 to 47%. The average pore water velocities determined in the chloride mass balances and applied in the selenium immobilization estimates also are presented.

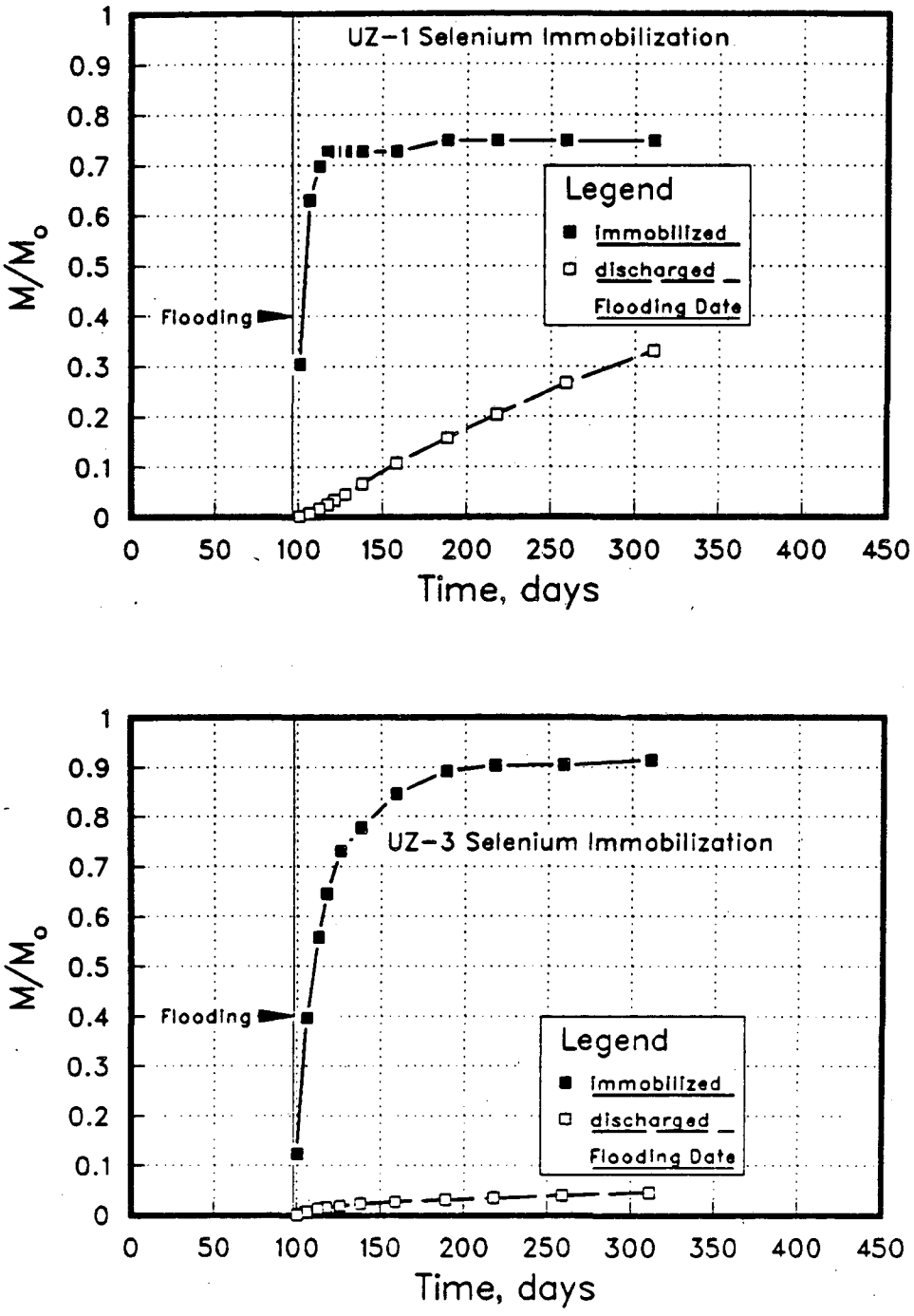

Figure 5.7 Results of the selenium immobilization calculations at sites UZ-1 and UZ-3. Quantities plotted are normalized to the initial inventory of soluble selenium, M_o, in the 1.22 m thick study block.

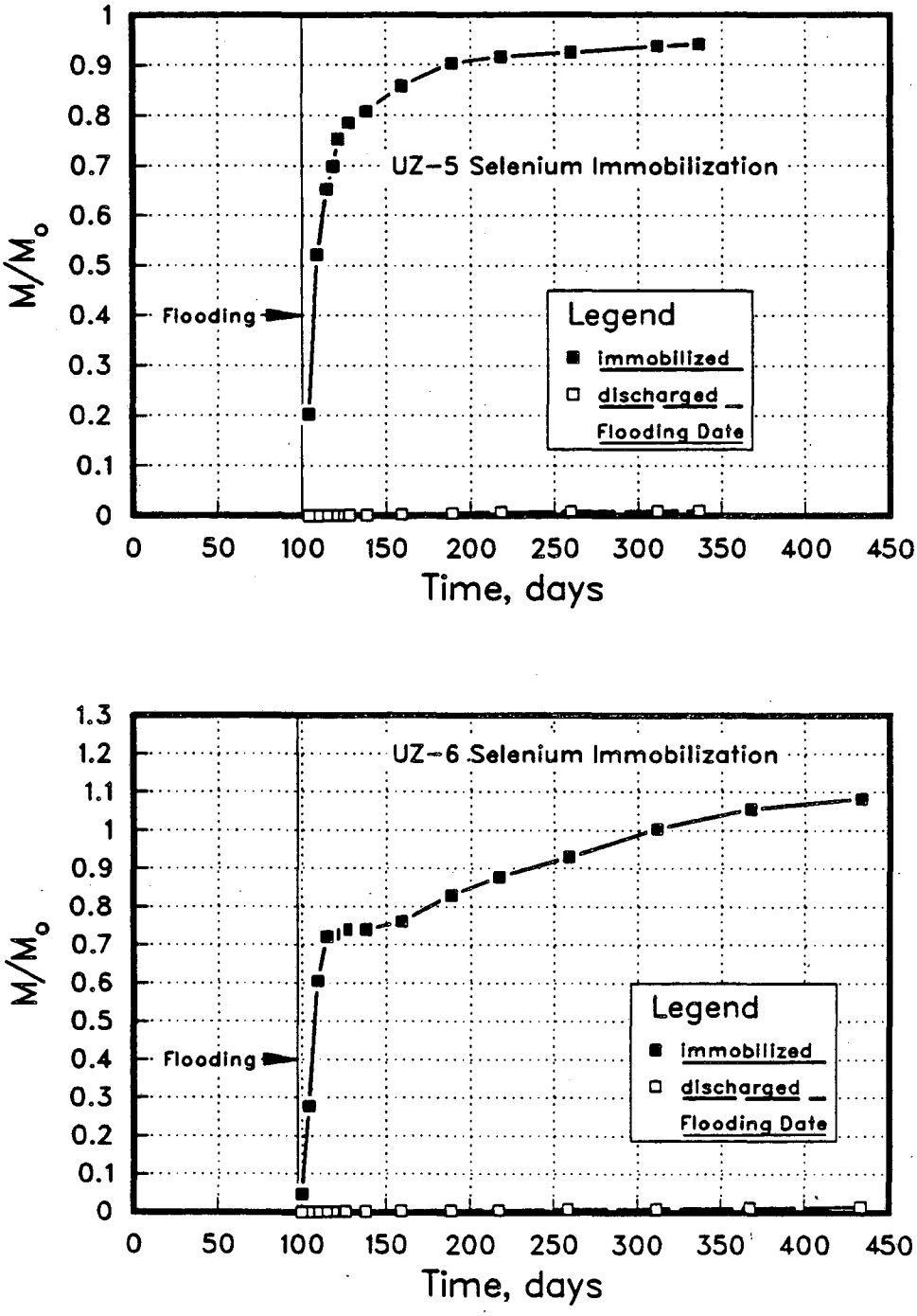

Figure 5.8 Results of the selenium immobilization calculations at sites UZ-5 and UZ-6. Quantities plotted are normalized to the initial inventory of soluble selenium, M_o, in the 1.22 m thick study block.

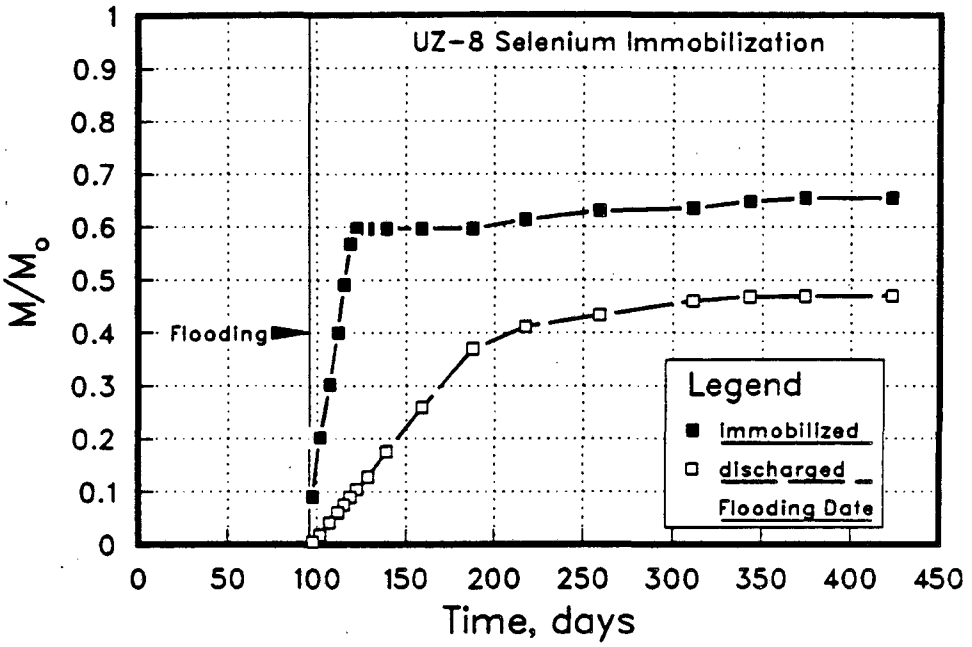

Figure 5.9 Results of the selenium immobilization calculations at site UZ-8. Quantities plotted are normalized to the initial inventory of soluble selenium, M_o, in the 1.22 m thick study block.

Table 4. Selenium Discharge/Immobilization during First Flooding Episode

Site	Average Pore Water Velocity, m/year	Initial Mass of Soluble Se g/m^2	Discharged		Immobilized	
			% of Initial Mass	Mass, g/m^2	% of Initial Mass	Mass, g/m^2
UZ-1	1.92	.675	33	.224	75	.506
UZ-3	.64	.88	5	.046	91	.804
UZ-5	.44	.14	1	.001	94	.134
UZ-6	.76	.05	1.5	.001	108	.058
UZ-8	4.08	.833	47	.39	66	.55
Average		.52		.13		.41

The validity of these calculations is supported by observations of soluble selenium concentrations in shallow groundwater monitoring wells (1.8 to 12.2 m) located in Pond 1. Elevated selenium concentrations were detected at only 2 of the 5 sites, UZ-1 and UZ-8. Levels at UZ-1 rose only very slightly to nearly 20 ppb, however, in Figure 4.23 we see that at UZ-8 a concentration of 322 ppb was observed approximately 4 ½ months after flooding, before returning to 16 ppb after an additional 8 months, in a well screened from 2.4 to 3.0 m (8 to 10 ft). This is consistent with the estimates above that 0.224 and 0.39 g/m^2 migrated out of the 1.22 m (4 ft) thick monitoring zone below sites UZ-1 and UZ-8, respectively. This corresponds to 33 and 47% of the initial quantity of soluble selenium at each of the two sites. At all of the other sites, where elevated levels of selenium were not detected, less than 0.05 g/m^2 (5%) of the soluble selenium was estimated to have migrated out of the monitoring zone. The reason why the selenium level in groundwater at UZ-1 was not higher, based on a discharge quantity nearly equal to that of UZ-8, may be related to the fact that the shallow well at UZ-1 is at 3.0 to 4.6 m (10 to 15 ft) while the well at UZ-8 is only at 2.4 to 3.0

m (8 to 10 ft). It should be remembered that the processes that lead to immobilization in the shallow zone can continue to take place below the 1.22 m (4 ft) depth.

In Figure 5.10 the average pore water velocities from Table 4 have been plotted vs the corresponding % discharged and % immobilized quantities for each site. At sites with relatively low pore water velocities, the greatest degree of immobilization appears to have occurred while the least amount of selenium migrated out of the study block. On the other hand, the highest quantity of discharge and lowest of removal are associated with the site possessing the maximum average pore water velocity. The figure suggests a correlation between the effectiveness of the selenium removal mechanism and fluid velocity. Such a relationship has been reported in *U.C. Salinity/Drainage Task Force* (1987) where selenate reduction was examined in batch studies in the presence of a carbon source and was shown to be time-dependent. Soil column leaching experiments performed in *Lawrence Berkeley Laboratory* (1987a) demonstrated that Darcy flow rates over the range of 7 to 0.91 $m \cdot year^{-1}$ exerted a significant effect on Se mobilization, suggesting a time-dependent Se immobilization process. Columns characterized by higher flow rates produced higher total Se concentrations in outflow solutions over the course of the experiments. Regions in the Kesterson pond bottoms where the thin veneer of fine-grained material is absent or meager may have sustained higher than average pore water velocities during past Reservoir operation, allowing infiltrating pond water to pass through the reducing layer without the necessary residence time to allow for effective selenium removal. The mechanism(s) governing selenium breakthrough is probably a composite of at least several physical parameters, including the level of microbial activity, the presence of organic matter, and the concentration of nitrate, however, results from this experiment clearly indicate that higher-than-average seepage rates may also be an important factor.

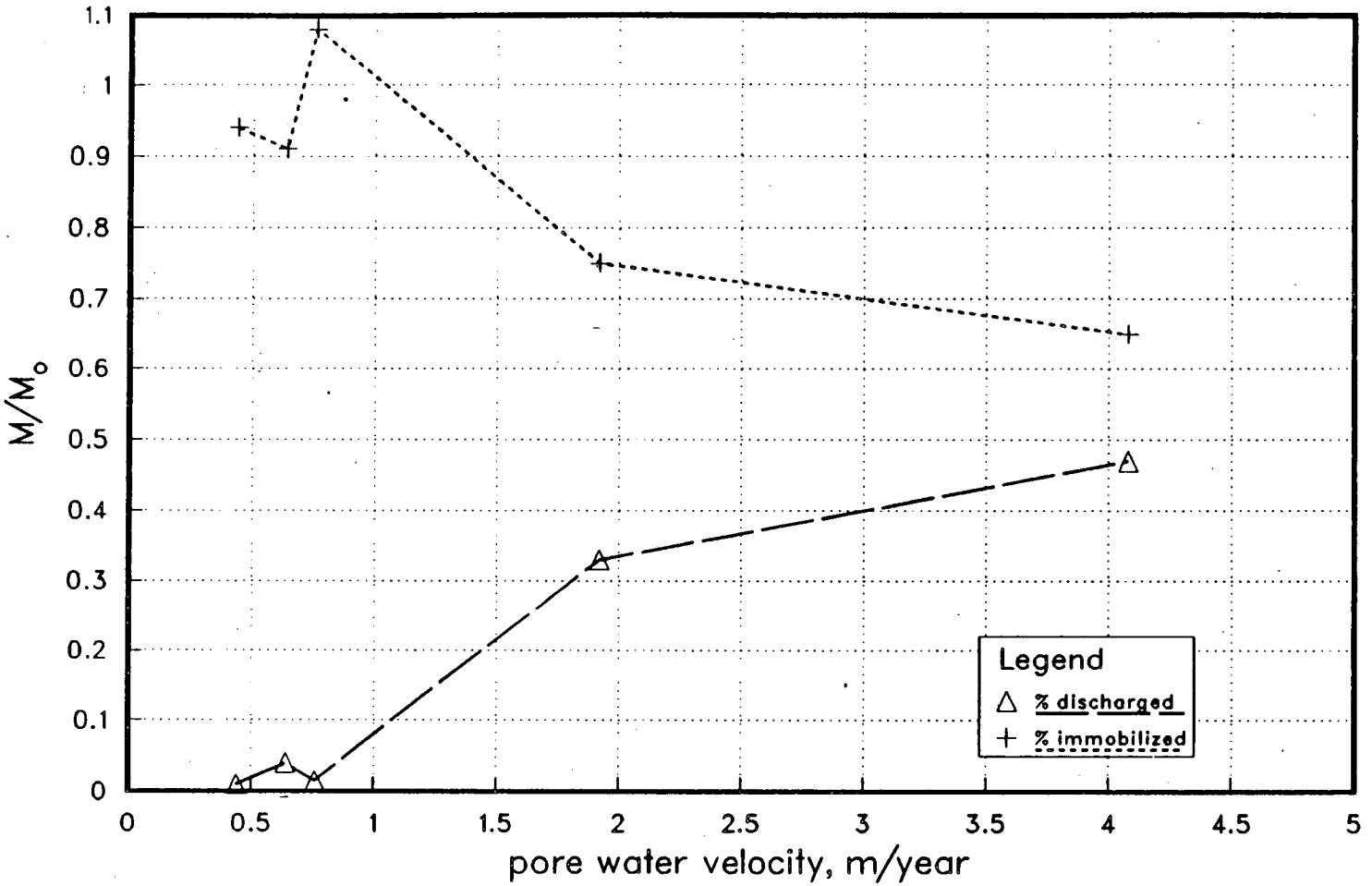

Figure 5.10 The relationship observed between average pore water velocity and the degree of selenium immobilization and discharge.

5.3. Redox Measurements

The redox measurements presented here were made during the second Pond 1 flooding event which began in November 1987. Selenium immobilization estimates were not performed on data collected during the second period of flooding, and therefore it is not possible to correlate actual immobilization rates or quantities to any observed redox shift. In general, however, similar behavior was observed in the two experiments, i.e. that of rapid apparent selenium immobilization following flooding. It is interesting, therefore, to examine the redox measurements in order to see if the observed selenium removal may have been accompanied by a corresponding shift of sufficient rate and magnitude in the oxidation-reduction conditions of the pond bottom sediments.

In Figures 5.11 to 5.14 the measurements of redox variation are plotted that were made at the five wetted sites. Values are plotted for pond water and soil water. Refer to Section 3.5 for a discussion of the measurement method. Several observations are possible upon an examination of these data:

(1) Before flooding, at site UZ-3, Eh values at all the locations were thoroughly oxidizing. Eh's measured during this time ranged from +400 to +500 mV.

(2) With the onset of flooding, Eh decreases occurred quickly. The permanent-type electrodes, fairly consistently, reflected an approximately 200 mV drop within the first few days, a time period as short as those observed to have resulted in fairly extensive selenium immobilization. Whether the magnitude of the decline was sufficient to result in selenium removal is essentially not known, however, data presented in *Lawrence Berkeley Laboratory* (1986a p. 46) suggest that soluble selenium does not occur in significant quantities when Eh $\leq$ 300 mV.

(3) Data from the portable-type electrodes also indicated rapid drops in Eh, however, the data exhibited scatter. On any particular day, Eh was shown to vary over 100's of mV's. The coexistence of localized reducing zones and oxidizing zones at the scale of soil aggregates is very commonly observed *(Smith,* 1977). These data could be interpreted as an indication that localized zones of reducing conditions can develop rather

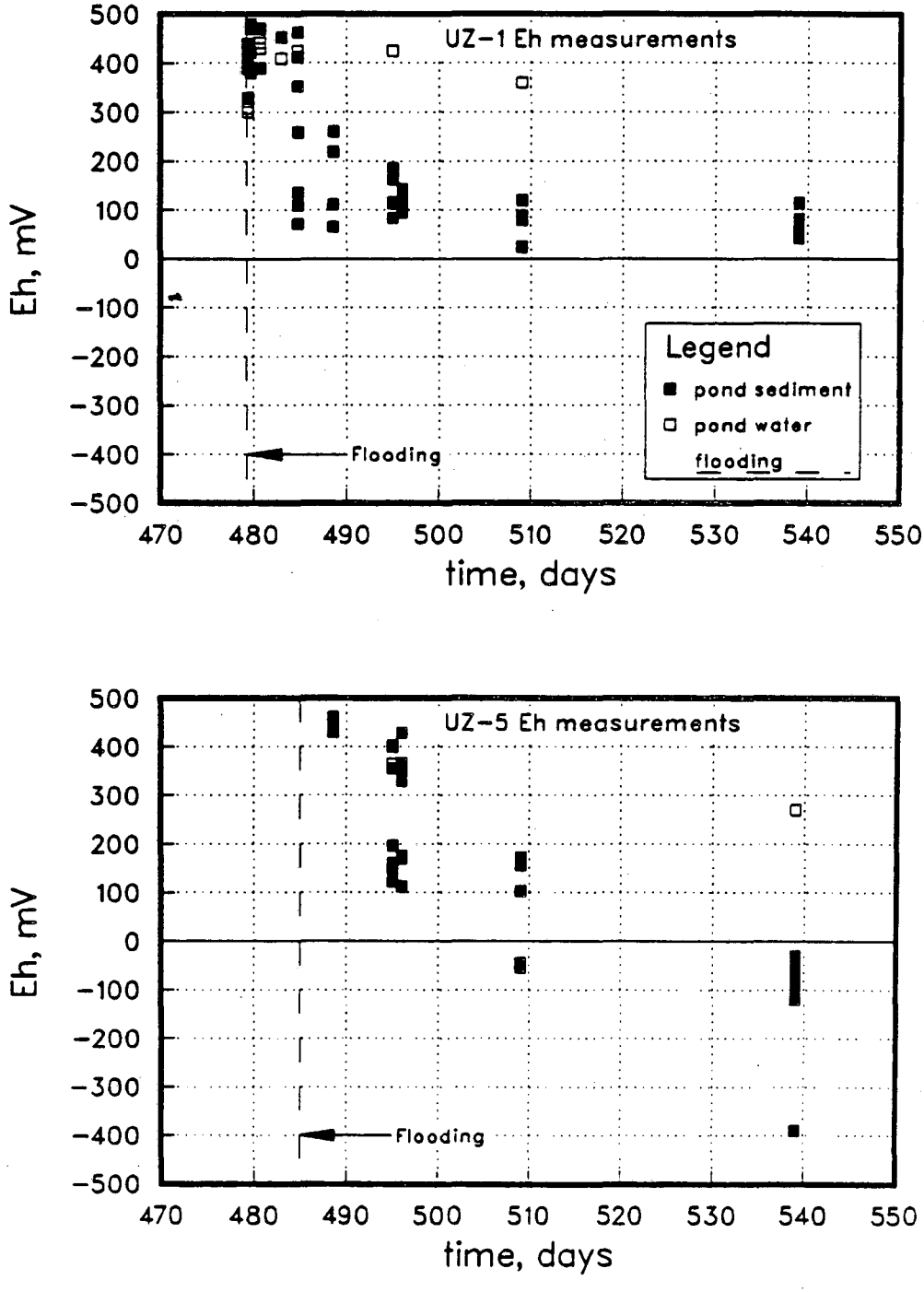

Figure 5.11 Eh measurements made following pond-flooding at sites UZ-1 and UZ-5 with the portable-type Eh electrode.

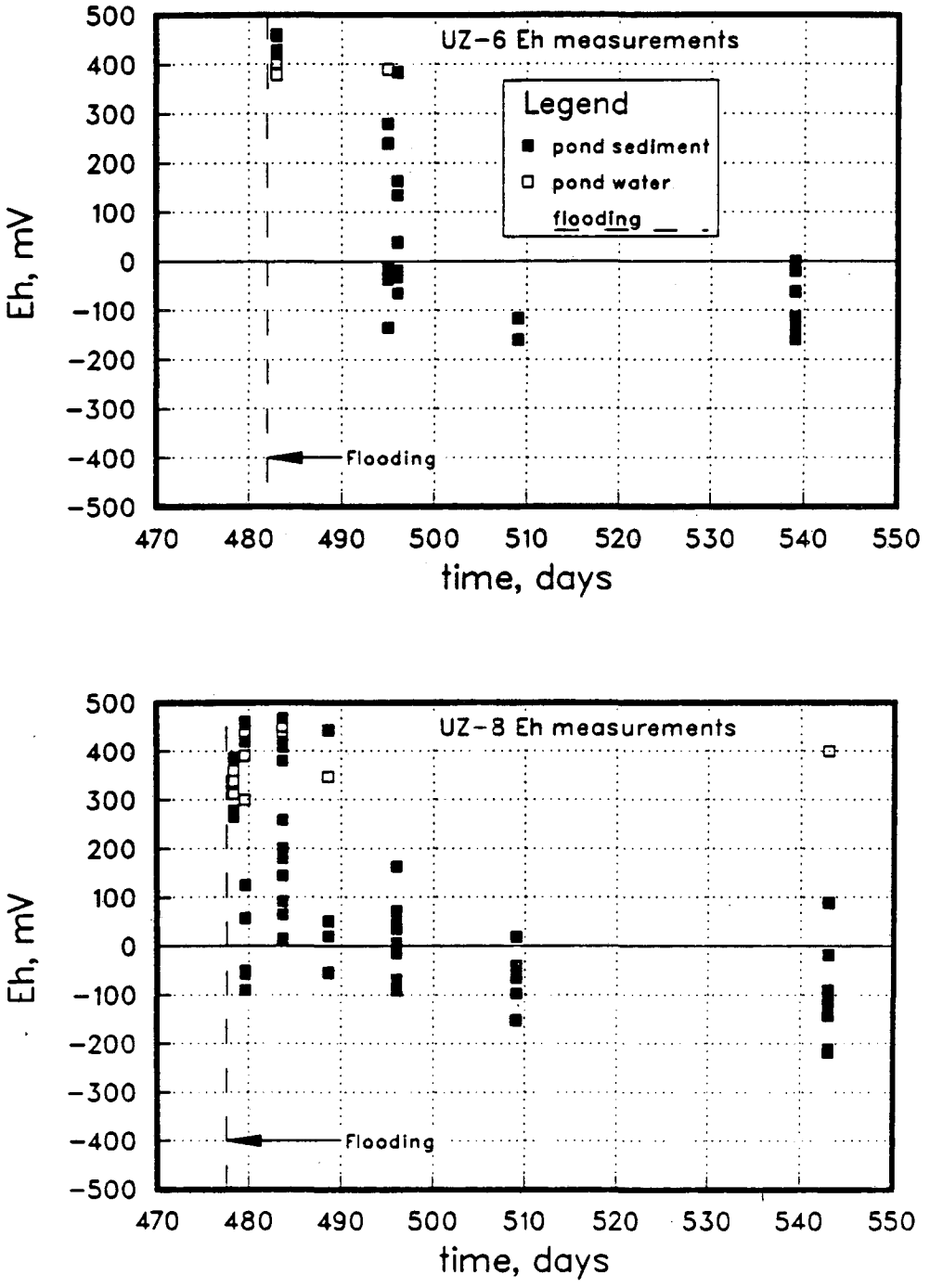

Figure 5.12 Eh measurements made following pond-flooding at sites UZ-6 and UZ-8 with the portable-type Eh electrode.

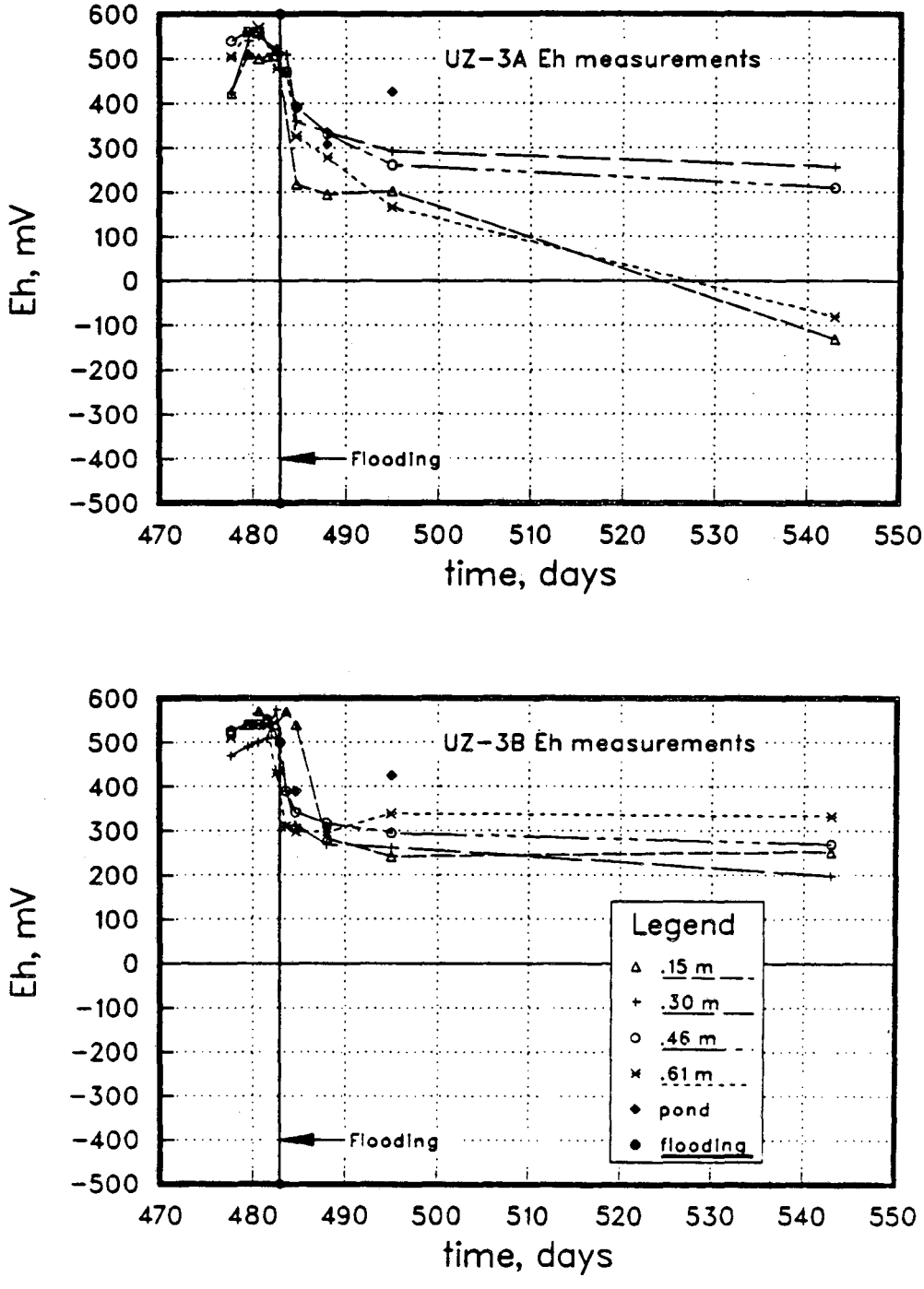

Figure 5.13 Eh profiles measured prior to and following pond-flooding at locations A and B adjacent to site UZ-3.

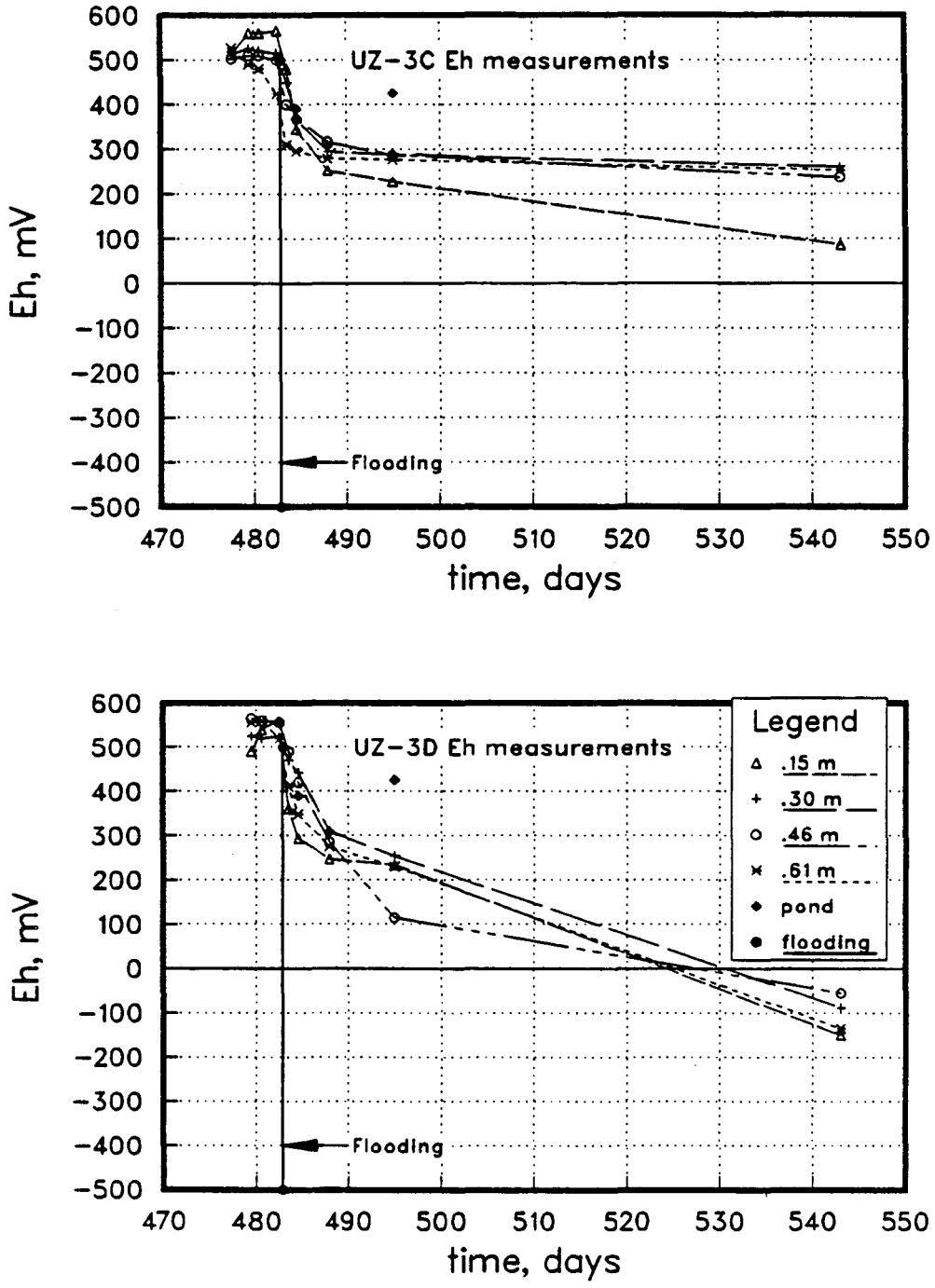

Figure 5.14 Eh profiles measured prior to and following pond-flooding at locations C and D adjacent to site UZ-3.

quickly, but that portions of the soil bulk may remain relatively oxidizing for longer periods of time. The soil matrix during the early stages of flooding may therefore be characterized as a heterogeneous system of spatially variable redox conditions.

(4) This spatial variability is indicated by a comparison of measurements made at identical depths at UZ-3 in the permanent electrodes (Figures 5.13 and 5.14). Between the four replicate electrode bundles A through D, we see that at any particular depth, Eh estimates varied by 100's of mV's.

(5) Pond water remained oxidizing while soil water underwent an Eh decline. Pond water Eh remained near +400 mV during the entire period.

(6) There is a weak indication of a relationship between depth and Eh. Again referring to Figures 5.13 and 5.14, we see that for two of the four electrodes at UZ-3, the 0.15 m (0.5 ft) electrode definitely reflected the most reducing conditions, however, beyond this depth the depth relationship was unclear. It is very likely that the resolution of the measurement system is incapable of resolving an Eh gradient, or that one simply did not exist.

(7) Based on data collected with the portable electrode, it seemed to take between 20 and 30 days for reducing conditions to become fully established throughout the soil matrix (Eh $\leq$ 0 mV). The permanent electrodes suggest that even longer time periods were required. Based on this information, if the lowering of Eh was indeed responsible for the rapid and extensive selenium removal observed, then Eh reductions down to relatively low levels (i.e. Eh $\leq$ 0 mV) were not required. This statement is consistent with observations made previously in *Lawrence Berkeley Laboratory* (1986a p. 46) that no selenium is observed in waters with Eh $\leq$ 300 mV.

It should be emphasized again that the above measurements are by no means intended to represent quantitative evaluations of electrode potential, but are only presented as qualitative information regarding general redox trends. Application of an equilibrium oxidation-reduction model in species prediction requires knowledge of the electrode potential. In an ideal situation, an inert electrode should take on a potential corresponding to the electron availability of

the system. Redox potentials, however, often vary considerably from electrode potentials. These reasons include the fact that redox reactions in soils are often in nonequilibria, and that redox couples do not necessarily transfer electrons irreversibly with platinum. The potential of the platinum electrode in a mixture of nonequilibrium redox couples is only a poorly defined average of the potentials of all the redox couples present *(Bohn et al.,* 1985). The potential that is measured is a mixed potential. In addition to these theoretical sources of uncertainty, previously discussed deficiencies in the measurement procedure may add to the qualitative nature of the results. The possibility that redox potential may exhibit a high degree of spatial variability further complicates matters. Even though these measurements may not provide data sufficiently accurate to quantitatively determine selenium speciation, they are useful in the indication that conditions in the soils at Kesterson may have become reducing rapidly enough to account for the observed selenium immobilization.

5.4. Application of a First-Order Decay Term

The selenium removal estimates presented in Section 5.2 indicate that the immobilization process occurred most rapidly soon after flooding and thereafter proceeded at a slower rate. Examination of the immobilization curves (Figures 5.7 to 5.9) suggests that it may be possible to describe the removal mechanism by a first-order reaction, a reaction in which the rate depends on the first power of the concentration of the reactant (a concentration-dependent sink). In an attempt to provide insight into the nature of the removal mechanism, Eq. (5) has been modified to incorporate a first-order reaction term. Calculations have been performed that examine the rate of the observed selenium immobilization process based on a first-order assumption.

The loss of reactant mass from a batch solution over a given time increment, Δt, is

$$-k_d \cdot M_{Se} \cdot \Delta t \qquad (11)$$

where k_d ($days^{-1}$) is the first-order reaction constant, and M_{Se} (kg) is an average mass quantity of selenium present in the reactor volume over the time increment. Substituting Eq. (9-11) into Eq. (8) and dropping the M_{Imm} term yields

$$M_{Se,t} = M_{Se,o} + \rho_f \cdot v \cdot \phi \cdot A \cdot C_{Se,in} \cdot \Delta t + \rho_f \cdot v \cdot \phi \cdot A \cdot C_{Se,out} \cdot \Delta t - k_d \cdot M_{Se} \cdot \Delta t \qquad (12)$$

where the various terms are all as described above.

This equation, as with those above, has been applied to the 1.22 m (4 ft) thick study block as if it can be treated as a reactor vessel, and as if the average selenium concentration measured within each site is representative of average conditions within the reactor vessel. The inflow and outflow concentrations are defined as in the previous calculations, by selenium concentrations measured in pond water and by selenium levels in soil water collected at the bottom of the monitoring zone. The average pore water velocity determined above, using the average chloride concentration, was again used to calculate the mass flux of selenium into and out of the control volume. The parameter k_d was adjusted as the only remaining unknown in a trial and error procedure designed to produce the closest possible match between a predicted average selenium concentration and the observed level. The most satisfactory fit was defined as the match that produced the minimum *percent* difference between the estimated and observed selenium vs time concentrations. The same assumptions apply as in the immobilization estimates. The values of k_d determined represent average rate terms over the entire study block depth. The possibility that immobilization could be occurring at greater rates within certain portions of the study block was also examined in a similar set of calculations associated with only the 0.15 m (0.5 ft) soil water sampler.

In Figures 5.15 to 5.17 are plotted the results of the first-order decay calculations applied to the study block as a whole. For each site the observed average selenium concentration is plotted along with two predicted response curves - one derived with the decay term included and another without decay. In the figures, we see that the large differences between the predicted responses (without decay) curves and the observed responses clearly indicates the presence of a transformation mechanism. The predicted response (with decay) much more closely approximates the data, however, it consistently overpredicts average selenium concentration at early times and at late times often predicts a 0 concentration, indicating that a first-order decay cannot fully describe the data. The rate constants determined range from a low

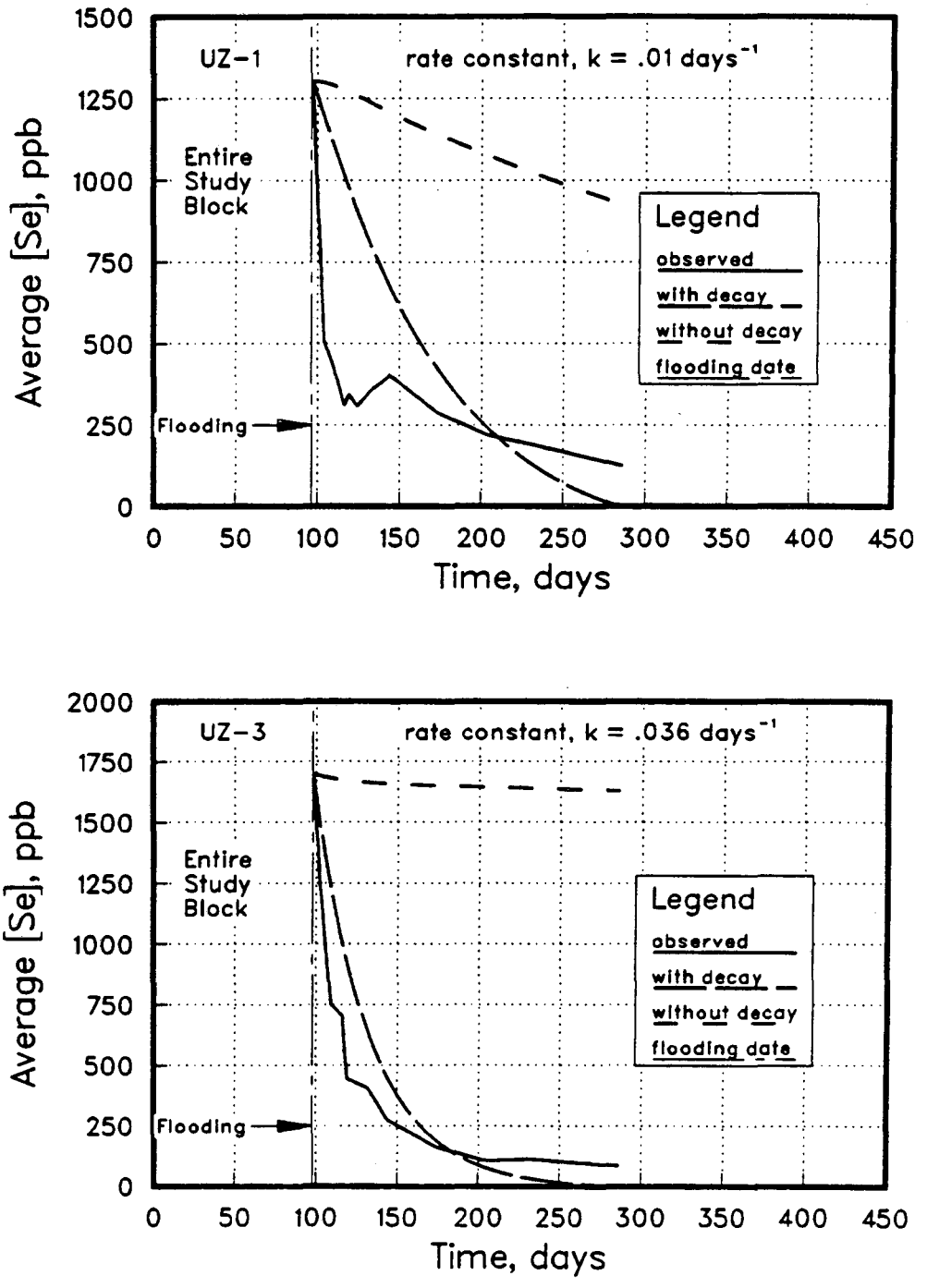

Figure 5.15 Application of a first-order decay term, k_d, to the chloride mass balance calculation performed over the entire 1.22 m thick study block at sites UZ-1 and UZ-3.

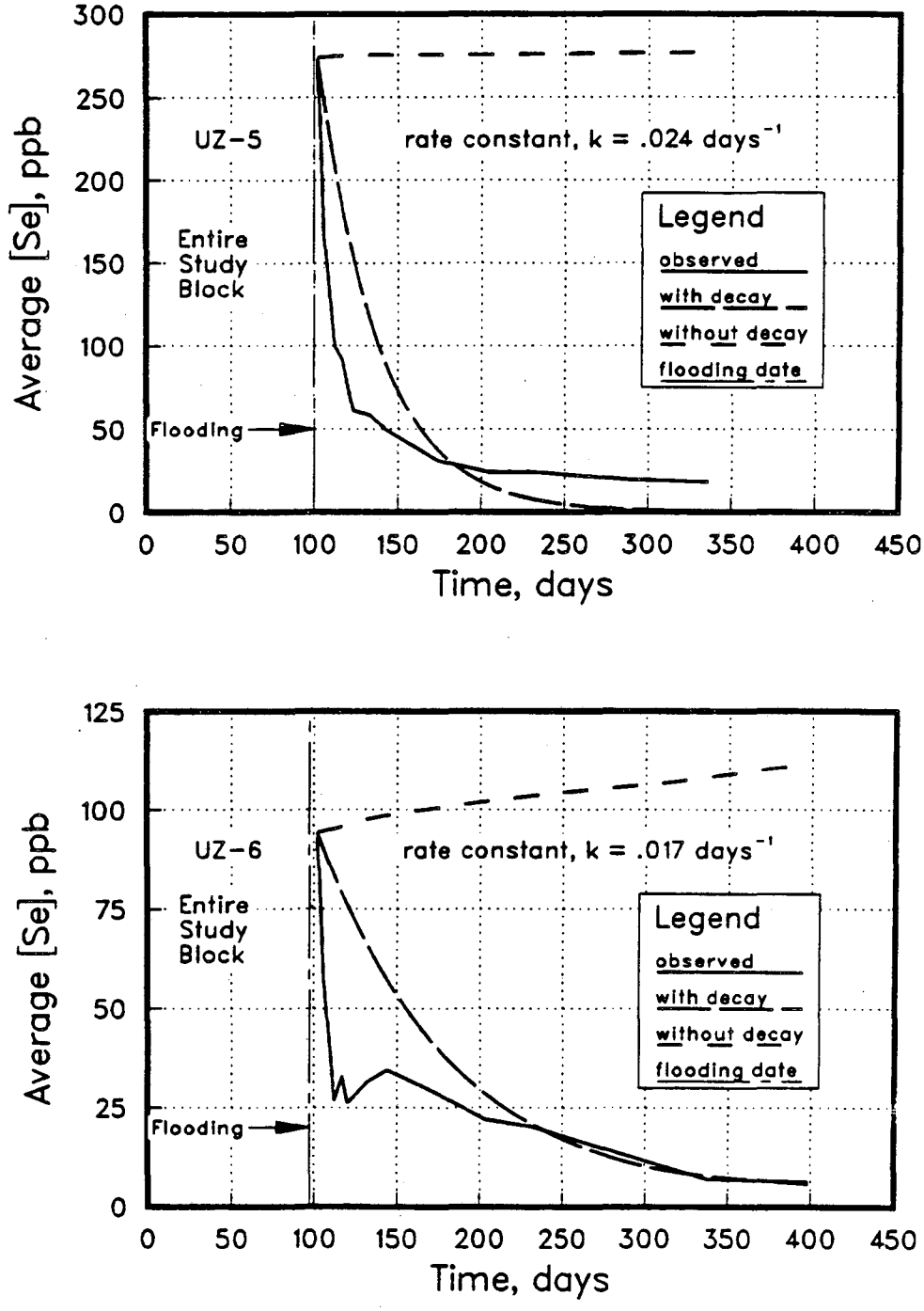

Figure 5.16 Application of a first-order decay term, k_d, to the chloride mass balance calculation performed over the entire 1.22 m thick study block at sites UZ-5 and UZ-6.

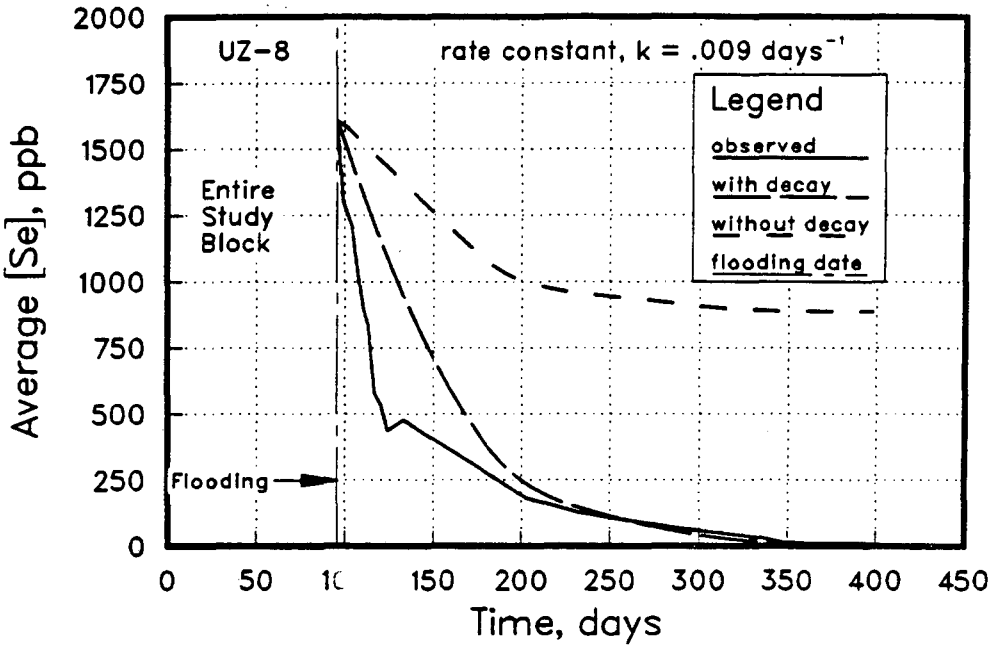

Figure 5.17 Application of a first-order decay term, k_d, to the chloride mass balance calculation performed over the entire 1.22 m thick study block at site UZ-8.

of .009 day^{-1} to .036 day^{-1}. Interestingly, the two sites that had the greatest selenium discharge (least immobilization), UZ-1 and UZ-8, also had the lowest rate constants, .009 day^{-1} and .012 day^{-1}, respectively. However, UZ-6 also is estimated to have one of the lower rate constants with $k_d = .017$ day^{-1}, and yet immobilization was greater than at any other site. The identical calculations were performed on the selenate data (rather than on total selenium) and very similar results were obtained with no improvement obtained in the history-matches.

In order to examine the possibility that immobilization occurred at greater rates in the shallowest sediments, breakthrough curves from the 0.15 m (0.5 ft) soil water sampler depths were analyzed as above using Eq. (12) to determine a rate constant, k_d, that applied only over the shallow zone from 0 to 15 cm (6 in). Rather than using the previously determined average pore water velocities, based on chloride concentration data representative of the entire 1.22 m thick study block, new average pore water velocities were determined prior to the rate constant determination using chloride breakthrough data from the appropriate 0.15 m soil water sampler. The inflowing concentrations again were taken to be pond water solute concentrations. The outflowing solute concentrations were set equal to the concentrations observed in the 0.15 m deep soil water sampler. Figures 5.18 and 5.19 present the results of the history-matching of the shallow soil water sampler data at 4 of the sites. The match between calculated and observed concentrations is similar to that observed in the case of the whole study block treatment. The analysis was not performed at UZ-1 due to insufficient data in the experiment period soon after flooding.

The rate constants determined over the two soil depths, the near-surface zone and the entire study block, are summarized in Table 5 below. Average pore water velocities used in the two analyses are listed as well. These data or calculations are not intended to argue that the selenium removal mechanism is in fact governed by a first order reaction. Controlled experiments in the lab would be required before being able to make that assertion. The primary purpose of this section has been to provide estimates of the rates at which the removal

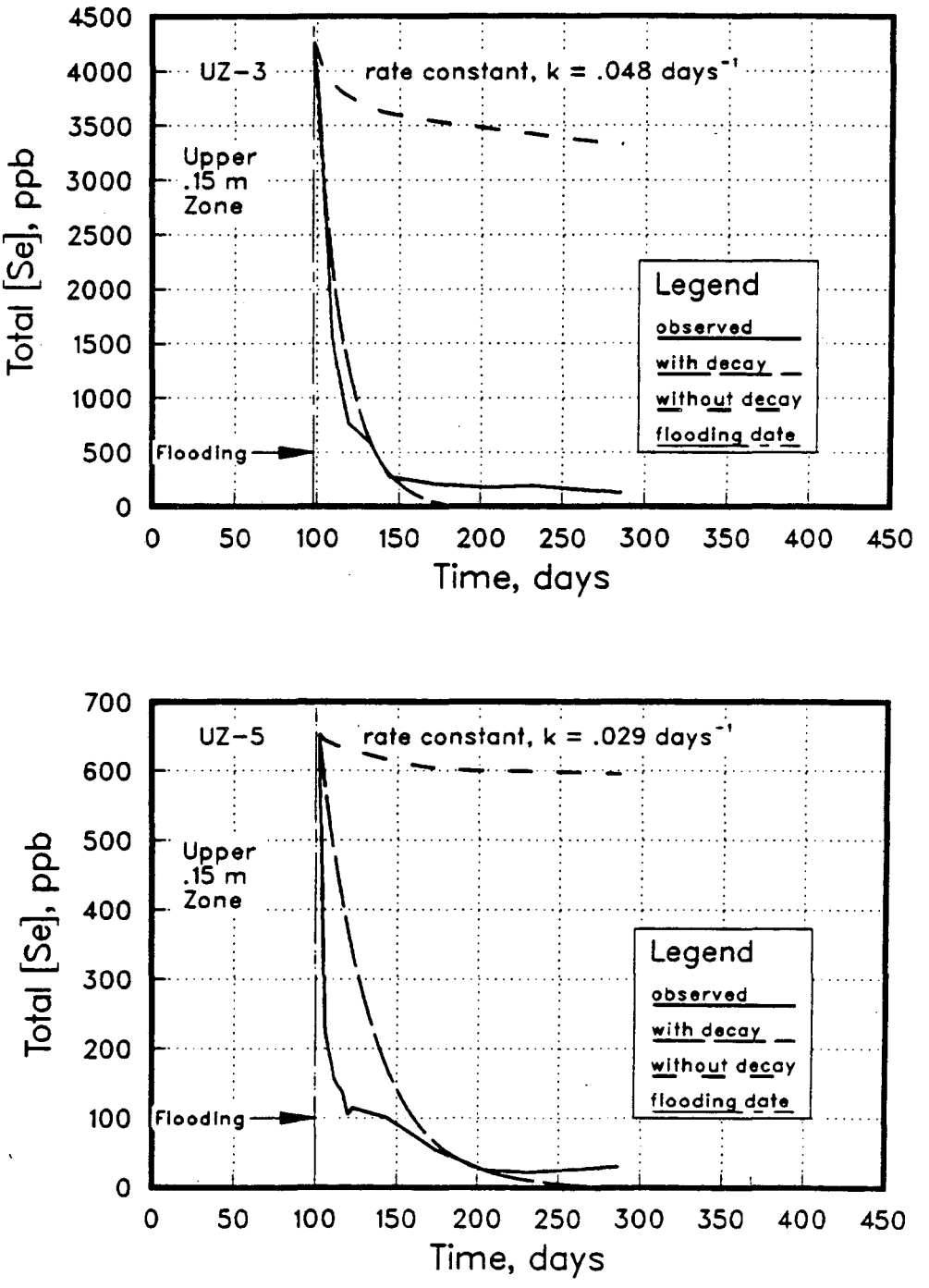

Figure 5.18 Application of a first-order decay term, k_d, to the chloride mass balance calculation performed only within the upper .15 m at sites UZ-3 and UZ-5.

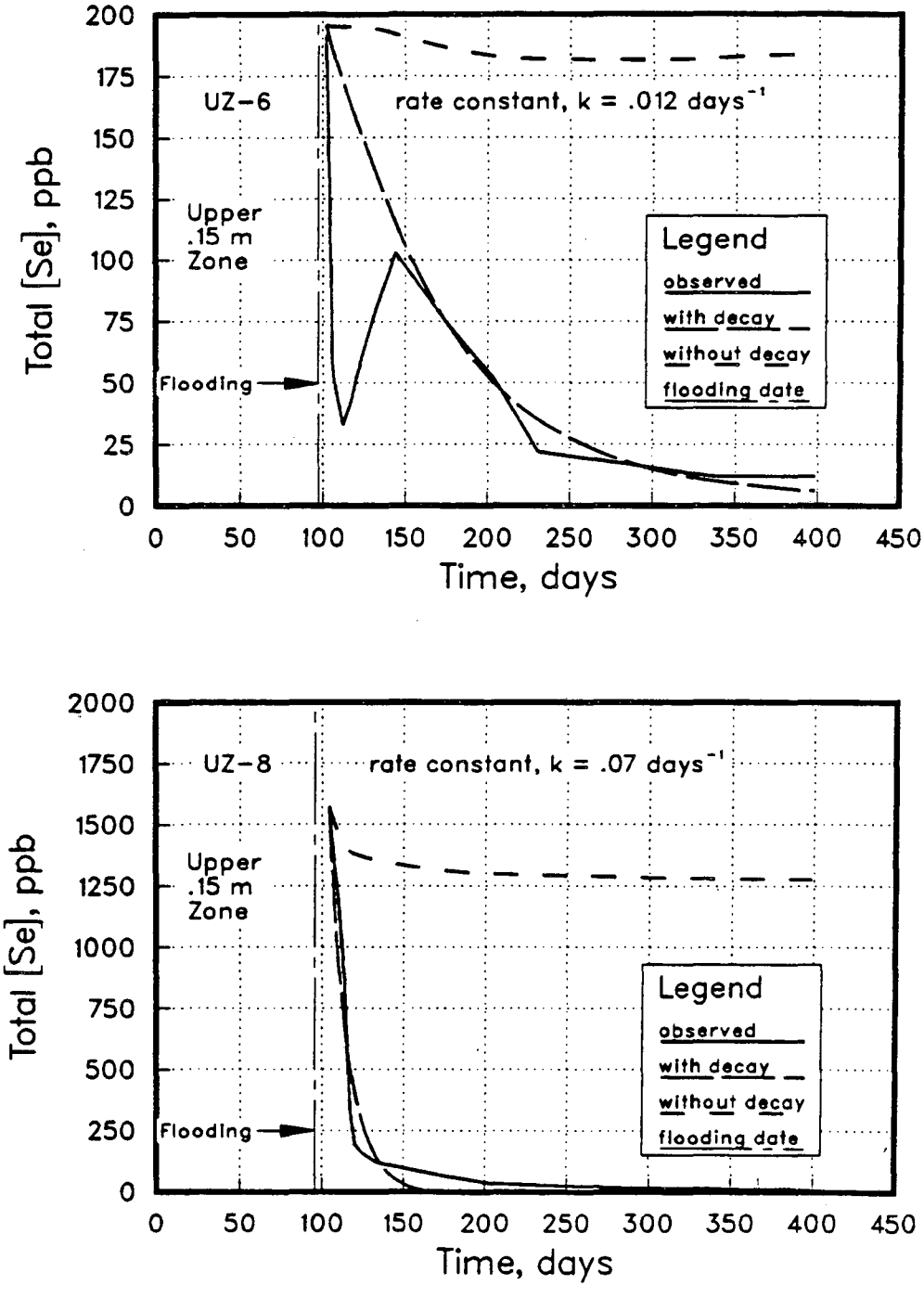

Figure 5.19 Application of a first-order decay term, k_d, to the chloride mass balance calculation performed only within the upper .15 m at sites UZ-6 and UZ-8.

reactions occurred, to examine the possibility that the mechanism occurred at different rates within different portions of the soil column, and to attempt to identify a relationship between removal rate and average pore water velocity.

Table 5. k_d Estimates for the Entire Study Block and Upper 15 cm Zones

Site	Entire Study Block % Immobilized	Entire Study Block		0.15 m Zone Only	
		pore velocity, m/year	k_d, days^{-1}	pore velocity, m/year	k_d, days^{-1}
UZ-1	75	1.92	.012		
UZ-3	91	.64	.036	.64	.048
UZ-5	94	.44	.024	.44	.029
UZ-6	108	.76	.017	.16	.012
UZ-8	66	4.08	.009	.76	.07

In the table above, we see that for the entire study block treatment, k_d was lowest for the sites with the highest average pore velocities. Site UZ-8, with the largest average pore water velocity, 4.08 m/year, had the smallest rate constant, .009 days^{-1}, and but for one exception, the trend of increasing k_d with decreasing pore water velocity was adhered to at the other sites. These data support the notion suggested in Section 5.2 that the ability of the soil medium to geochemically remove selenium from infiltrating water is inhibited by increases in the fluid velocity. Fluid velocity increases shorten the residence time of the water in the "reactor vessel", and possibly limit the effectiveness or completeness of the kinetically dependent removal processes.

Only at site UZ-8 did the value of k_d change significantly when the calculation was performed over the shallow zone only. k_d increased from a value of .009 days^{-1}, representative

of the 1.22 m thick study block, to .76 $days^{-1}$ for the zone from the ground surface to 15 cm. Interestingly, the new average pore water velocity estimate at UZ-8, based on the chloride breakthrough data observed at the 0.15 m soil water sampler rather than on the average chloride data, also was significantly different from the original average pore water velocity estimate, and in fact, it decreased significantly from 4.08 m/year to .76 m/year. UZ-6 also demonstrated a reduction in pore water velocity with the shallow zone calculation, yet no corresponding increase in the rate constant was observed as in UZ-8. At the remaining two sites, identical average pore water velocity estimates were obtained over the two soil depths.

In general, therefore, evidence has not been provided to support the notion that selenium removal may occur at greater rates in the near-surface area as compared to deeper soil zones. This is not to say that removal may not occur in greater quantities near the surface due to greater available soluble selenium, but that the soil from 0 to 1.22 m seems to possess an equal capacity throughout its profile to remove selenium from solution. In the table above, we see that the parameter which had the greatest effect on the value of the rate constant was not depth, but average pore water velocity. When the calculation was performed over the two different depths at one site and resulted in similar pore water velocities estimates (UZ-3 and UZ-5), the value of k_d remained essentially constant. But when the average pore water velocity decreased (UZ-8), a corresponding increase was observed in k_d. This result is consistent with the observation above of a velocity dependent rate constant. Additional support is provided, therefore, for the hypothesis of velocity dependent selenium immobilization insofar as k_d increased at a site with an observed decrease in the average pore water velocity estimate. The behavior at UZ-6, however, did not conform to this observed trend. A velocity decrease was not accompanied by an increase in k_d. At this site, the average pore water velocity based on the entire study block treatment already was relatively low, and it may have been that any additional immobilization due to velocity reduction may simply not have been possible.

PART II. TRANSPORT OF A CONSERVATIVE SOLUTE THROUGH A SHALLOW POND SEDIMENT

Part II of the thesis has been undertaken in order to provide supporting evidence for the fluid velocity determinations that were obtained through chloride mass balance calculations in previous sections. Attention is shifted, in the following chapters, away from the consideration of data pertaining to selenium and towards a numerical analysis of the chloride breakthrough data. Estimates of the velocity of pore fluids during ponding have been obtained by numerically modeling the observed transport of chloride at each of the flooded soil water sampler locations. The primary purpose of these calculations was to perform a more rigorous evaluation of the pore fluid velocities than was performed earlier as one means of verifying the original estimates. As the process progressed, however, other issues of interest, related primarily to the field of solute transport, evolved and have been investigated. Therefore, the following chapters may appear to be somewhat disconnected to what has gone before them. Hopefully, the change in subject matter is not too unsettling or confusing to the reader, and I apologize if it is so, however, during this rather extended aside, the reader should remain confident that the original purpose of this section will be addressed.

6. INTRODUCTION

Interest has risen markedly in recent years in improving our ability to make accurate estimates of solute and water fluxes through systems of porous media. The need to quantify movement of chemical constituents through soils arises in a variety of situations, including the use of fertilizers and pesticides in agricultural applications, the disposal of industrial and municipal wastes in landfills, and the leaching of salts during soil reclamation. Technologists wish to improve their understanding of the physical processes that govern transport so that they are better able to predict the fate of contaminants in the subsurface and their potential impact on water resources. Concern over adverse environmental impacts through agriculture and land disposal of wastes has been reflected in increased governmental regulation and in

the current high level of research occurring presently in the fields of waste isolation and contaminant fate prediction. Ultimately, the ability to assess impacts on groundwater quality depends on the use of reliable models and methods that are able to describe water and solute fluxes over large field systems. This includes the ability to estimate not only average properties and processes but the potential for the occurrence of extreme behavior.

The determination of *average* solute and water fluxes, however, is made difficult by the extreme spatial and temporal variability exhibited in soil water and solute transport properties. The use of deterministic treatments in water and solute movement investigations is complicated by the very nature of soils as heterogeneous systems. Properties applied uniformly in a macroscopic model may vary tremendously over the microscopic scale. Models that treat the porous medium as a representative continuum may be highly simplifying and inappropriate if the scale of model application is not at least as large as a representative elemental volume. Several investigators have examined issues of spatial variability of soil properties, and these investigations have elucidated difficulties for the transport modeler. *Biggar and Nielsen* (1976), in a steady-state study of chloride movement during ponding among 20 sites within a 150-ha field, fitted observed data to a one-dimensional analytical solution to the advection-dispersion equation through the variation of two parameters - apparent dispersion coefficient (D_h) and average pore water velocity *(v)*. Statistical analysis of D_h and v showed them to be log-normally distributed. D_h and v were observed to vary by an order of magnitude within a plot. *Van De Pol et al.* (1977) and *Kies* (1981) in an experiment involving unsaturated transport fitted apparent dispersion coefficients and average pore water velocities in a similar fashion and observed that some breakthrough curves indicated solute arrival at deeper depths before shallower depths. D_h and v were again found to be log-normally distributed. *Misra and Mishra* (1977), in an experiment involving the leaching of a chloride pulse through a field-plot, observed that even though the soil was completely water saturated, the majority of flow appeared to be occurring through only a small fraction of the total pore space. *Kissel et al.* (1973) demonstrated with a solution of chloride and fluorescein dye that relatively large continuous soil cracks were important pathways of transport in saturated

swelling clay soils. fluorescein and chloride were found to move quite rapidly through soil cracks whereas in nearby areas little or no fluorescein was found.

With the eventual analysis of the reactive chemical transport of selenium in mind, a primary objective of this work has been to characterize the physical properties governing flow and transport through the pond bottom sediment. If such a characterization is to provide accurate information for the prediction of solute fluxes, it must include not only an estimate of average properties but an understanding of the spatial variability of the soil properties. Therefore, values of permeability and apparent dispersion coefficient have been determined at a number of locations throughout the pond and are analyzed for type of distribution and degree of heterogeneity. A comparison is included of average pore water velocities determined in the modeling effort to those estimated in earlier chapters through a chloride mass balance calculation, and any implications for the selenium immobilization estimates are examined. An integrated finite difference method numerical code is used for the solute transport simulations. Discussion is included of the equations used and the modeling methodology, including choice of boundary and initial conditions. Several related issues, such as a possible functional relation between average pore water velocity and apparent dispersion coefficient, and an examination of the effect of sample number on parameter estimation are also presented.

A second purpose of this section involves the determination of the longitudinal dispersivity of the pond sediment. Hydrodynamic dispersion is a key process that determines the fate of contaminant plumes. At present, only a few tens of field tracer tests are reported in the literature involving the determination of field-scale dispersivities and only five were judged to be of high reliability in a recent literature review that was performed on the subject *(Gelhar et al.*, 1985). Clearly, a need exists for the generation of reliable field-scale dispersivity data to fill the present gap. Reliable data on field-scale hydraulic transport parameters are required for the development of accurate models for predicting the transport of contaminants by groundwater. With the performance of additional experiments in the field will come a better understanding of the processes and mechanisms of flow and transport at the field scale, as

well as more of a consensus as to what methods of measurement are most appropriate. Numerous determinations have been made of dispersivity through the analysis of tracer breakthrough in laboratory columns, yet dispersivities calculated in this manner are generally felt to provide little insight to the field-scale values. Therefore, calculated dispersivities are presented and a few potential correlations are examined with subsurface environmental parameters, such as travel distance and pore water velocity.

7. THEORY

7.1. Flow of Water

For isothermal, steady-state flow in an isotropic porous medium, the following empirical equation, as later amended by Richards (1931) to include conditions of unsaturated flow, was proposed by Henri Darcy (1856),

$$\vec{q} = -\vec{K}(\Psi)\cdot\vec{\nabla}h \tag{13}$$

where $\vec{q}$ is the soil water flux ($L\cdot T^{-1}$), $\vec{K}$ is the soil hydraulic conductivity ($L\cdot T^{-1}$), h (L) represents the hydraulic head (h = elevation head (z) + pressure head (Ψ)) and ∇ is the standard differential operator. The equation states that $\vec{q}$ is proportional to the spatial gradient of hydraulic head, through a 'constant' of proportionality, K, which for unsaturated soils, has been found to be a strong function of the soil water matric potential, Ψ. Only the elevation and pressure components to the hydraulic head are included in these expressions. The component due to gradients in solute concentration is small and for this study was neglected. In deriving the differential equations governing soil water flow, the law of mass conservation, or the continuity equation, is employed, which states that the net flow of water into and out of an elemental volume must be balanced by a change in storage of fluid in that volume element. Substituting Eq. (13) for q into the equation of continuity,

$$\frac{\partial\theta}{\partial t} = \nabla\cdot\vec{q} \tag{14}$$

where θ is the volumetric water content and t (T) is time, yields what is often called the *Richard's Equation:*

$$\frac{\partial\theta}{\partial t} = \nabla\cdot\left[\vec{K}(\Psi)\cdot\vec{\nabla}h\right] \tag{15}$$

which is valid for multi-dimensional flow in heterogeneous, anisotropic soil. This equation is used most often in unsaturated soils. Considering only one dimension, z, reduces Eq. (15) to:

$$\frac{\partial\theta}{\partial t} = \frac{\partial}{\partial z}\left[K(\Psi)\frac{\partial\Psi}{\partial z}\right] - \frac{\partial\left[K(\Psi)\right]}{\partial z} \tag{16}$$

The dependence of K on the soil water matric potential, Ψ, makes this equation highly non-linear and therefore analytical solutions to Eq. (16) are not available except for highly-idealized problems involving simple initial and boundary conditions. For a fully-saturated, isotropic soil, K is no longer a function of matric potential or space and Eq. (16) further simplifies to the diffusion equation:

$$\frac{\partial^2 h}{\partial z^2} = \frac{S_s}{K}\frac{\partial h}{\partial t} \tag{17}$$

which is a linear differential equation. S_s (L^{-1}) is the specific storage or the volume of fluid released for an elemental volume per unit change in hydraulic head. Eq. (17) is a differential equation governing the transient movement of subsurface fluids in one-dimension without source/sink terms.

Alternately, the governing equation can be expressed in terms of an integral equation *(Narasimhan and Witherspoon,* 1977) which expresses the conservation of fluid mass in an elemental volume. For a volume element, the equation of mass balance can be written as the algebraic sum of fluxes entering and exiting the system. Dividing the element into L segments, and denoting $\vec{n}_l$ to be the outer normal to the surface segment l, we write

$$\sum_{l}^{L} \rho_f \vec{q}_l \cdot \vec{n}_l d\Gamma_l \tag{18}$$

where $d\Gamma_l$ is the surface area of the segment and ρ_f is the fluid density. The quantity $\vec{q}_l \cdot \vec{n}_l d\Gamma_l$ represents the rate of fluid flux across the surface segment. Setting Eq. (18) equal to the rate at which fluid mass, $M_{f,l}$, is accumulating in the volume element we have:

$$\sum_{l}^{L} \rho_f \vec{q}_l \cdot \vec{n}_l d\Gamma_l = \frac{\Delta M_{f,l}}{\Delta t} \tag{19}$$

Substituting the Darcy expression for $\vec{q}$,

$$\vec{q} = -K[\nabla z + \nabla \Psi] \tag{20}$$

and letting the number of segments $L \rightarrow \infty$ and the time interval $\Delta t \rightarrow 0$, we may write the continuity equation in integral form:

$$\int \rho_f K[\nabla z + \nabla \Psi] \cdot \vec{n} d\Gamma = M_{c,l} \frac{d\Psi}{dt} \tag{21}$$

where $M_{c,l}$, the *fluid mass capacity*, represents the change in fluid mass in the volume element due to a unit change in the value of Ψ, and is defined as,

$$M_{c,l} = \frac{\Delta M_{f,l}}{\Delta \Psi} = \frac{\Delta(\rho_f \theta V)}{\Delta \Psi} \tag{22}$$

The differential equation Eq. (17) which is expressed with reference to an infinitesimal volume can be derived from the integral form by dividing Eq. (21) by the bulk volume, $V_{b,l}$ and letting $V_{b,l} \rightarrow 0$.

The application of Eq. (21) in numerical models involves dividing the flow regime into a grid of elemental volumes and applying in a systematic manner to each element the law of mass conservation in the form of the integral equation. The complete formulation includes boundary elements, source/sink terms and is subject to boundary/initial conditions through which the system interacts with the outside world. The resulting set of equations is assembled into a matrix which then must be solved by one of many available matrix solution methods.

7.2. Solute Transport

The transport of solutes in soil is in response to the advective movement of the fluid stream, and to molecular diffusion. Mechanical dispersion, a mixing process similar in effect to diffusion, results from spatial variations in advection. For saturated systems, the mass of solute flowing through a unit cross-sectional area of soil per unit time due to the advective process can be represented by:

$$J_a = \vec{q}C = \vec{v}\phi C \tag{23}$$

where $\vec{v}$ is the average pore water velocity ($L \cdot T^{-1}$), ϕ is the porosity, and C is the solute concentration (M solute$\cdot M^{-1}$ fluid). The mass flux per unit time due to diffusion only across a unit cross-sectional area can be described in the following manner by Fick's first law:

$$J_D = -D_e \phi \vec{\nabla} C \tag{24}$$

where D_e ($L^2 \cdot T^{-1}$) is the effective coefficient of molecular diffusion. $D_e = \tau D_o$, where D_o is the coefficient of molecular diffusion of the solute in pure water, and τ is a dimensionless property of the porous medium that includes effects of tortuosity in the flow paths. Experimental results have found it to vary between .5 and .01 *(Freeze and Cherry,* 1979).

Due to variations in fluid velocity, the advective term creates a dispersion of the solute. In some cases dispersion has been found to conform, in an empirical sense, to an equation of the same form as that of diffusion, but which is the result of entirely different processes occurring at different scales. The mass flux of solute crossing a unit cross-sectional area per unit time J_m is generally described in an analogous manner with diffusion:

$$J_m = -D_m \phi \vec{\nabla} C \tag{25}$$

where D_m is the coefficient of mechanical dispersion ($L^2 \cdot T^{-1}$). The effect of dispersion appears mechanistically similar to diffusion but the processes are not related. Dispersion results from the heterogeneous nature of soil water flow including velocity variations within individual pores, variably distributed pore sizes, and the tortuous nature of flow paths. The fact that the two processes can be described by similar equations has led researchers to lump them together additively in mathematical treatments and to consider them as if they were one mechanism. This leads to the use of a single coefficient, the apparent dispersion coefficient, D_h, that incorporates both effective molecular diffusion (D_e) and mechanical mixing (D_m),

$$D_h = D_e + D_m \tag{26}$$

Eq. (24) can then be restated as:

$$J_h = -D_h \phi \vec{\nabla} C \tag{27}$$

Combining Eq. (23) and (27) with the governing differential equation of fluid flow Eq. (17), yields the following form of the advection-dispersion equation for transient, one-dimensional solute transport in fully-saturated, homogeneous, isotropic media:

$$\frac{\partial C}{\partial t} = \frac{\partial}{\partial z}\left[D_h \frac{\partial C}{\partial z} - v C \right] \tag{28}$$

The solution to Eq. (28) provides solute concentration as a function of space and time. Many analytical solutions are available for problems involving simple geometries, well-defined initial/boundary conditions, and steady flow. The application of Eq. (28) to problems of practical interest has been investigated by various researchers and the equation has been thoroughly tested in the laboratory under conditions of steady-state and transient water flow. The work of *Danckwerts* (1953), *Day* (1956), and *Nielsen and Biggar* (1961,62) demonstrated the utility of the physically-based model in columns of uniform glass beads, clean sands, and sieved loams. In aggregated soils, the use of Eq. (28) has also been justified in the work of *Passioura* (1971), *Rao et al.* (1976, 1980), and *Nkedi-Kizza et al.* (1983). Its application, though, has often required a scaling-up of the relatively small dispersion coefficients measured in the lab to larger values observed from field-scale experiments.

In highly-structured soils or unsaturated soils, the use of Eq. (28) has been less successful, and evidence from a number of researchers *(Biggar and Nielsen,* 1962; *Green et al.,* 1972; *Gupta et al.,* 1973 and *Rao et al.,* 1974) suggests that the application of a physically-based model may be inappropriate for describing the movement of water and solutes at large field sites exhibiting a high degree of spatial heterogeneity with regard to fluid flow and transport properties. Several new approaches have been developed in an effort to try and cope with the extreme lateral and vertical variability in soil water hydraulic properties and with the concern that the advection-dispersion equation is an inappropriate approximation to solute transport description in the field. *Coats and Smith* (1964), *van Genuchten and Wierenga* (1976), and *Wierenga* (1982), partition the soil water into mobile and immobile phases. Solute movement between the two phases is purely by diffusion while transport in the mobile phase is by a more conventional deterministic process.

Most of the alternate approaches use stochastic methods to describe the inherent statistical distributions of the pertinent properties. Variations in velocity are explicitly included to account for solute spreading rather than the use of large dispersion coefficients. *Jury* (1982) proposes the use of a transfer function for simulating solute transport under field conditions,

beginning with the assumption that soils are so spatially variable as to make any representative measurement of soil water hydraulic properties impossible. Solute dispersion is ascribed to spatially-varying, log-normally distributed pore water velocities without any reference to physical mechanisms that contribute to the velocity variations. Measurements are made of the distribution of travel times to a particular depth, and then using this distribution it is possible to estimate the solute concentrations at any depth. A possible weakness of this model is that it assumes the measured distribution of travel times, made at one particular depth, is representative of all depths over which it is applied.

Scaling theory *(Peck et al.,* 1977; *Warrick and Amoozegar-Fard,* 1979 and *Dagan and Bresler,* 1979) is another newly proposed approximate procedure that incorporates a description of the variable nature of soil water properties but that still retains deterministic considerations as well. Dispersion on the macroscopic scale is considered to be a process related to the spatial variability of the hydraulic conductivity and other water and solute transport characteristics. A standard set of measurements is made at one point in a field, allowing for the determination of a distribution of transport parameters. Different regions of the field are related to each through a characteristic scaling factor, or length factor. Knowledge of the scaling factor distribution allows for the calculation of laterally-variable water and solute movement through a series or bundle of vertical, parallel, non-interacting flow regions each with its own set of independent flow and transport parameters. Simulation results are then averaged to determine mean field behavior.

In this study, rather than attempting to verify or compare particular models, a deterministic approach is taken in an attempt to make local measurements of flow and solute transport properties and to gain an understanding of the type of statistical variability that exists in the Kesterson soils. In many field situations, however, as in this study, initial and boundary conditions are such that analytical solutions to the advection-dispersion equation are not available. For problems of this type and for others where the geometry of the flow regime is arbitrary and where heterogeneity and anisotropy are to be dealt with, numerical approaches

are often required. One such approach is suggested in alternately expressing Eq. (28) in an integral form, as in the case of fluid flow, where the conservation of fluid and solute mass are applied to an elemental volume. This is the method found in CHAMP *(Narasimhan et al.*, 1985), the numerical code that has been used throughout this study for the analysis of the solute transport problem. For an arbitrary volume element V, which is fully enclosed by the closed surface Γ_V, the equation of mass balance can be written as the sum of fluxes entering and exiting the system. Dividing the element into L segments, we write for non-reactive fully-saturated solute transport:

$$-\sum_{1}^{L}\vec{q}\cdot\vec{n}C\ \Delta\Gamma+\sum_{1}^{L}\phi D_h\nabla C\cdot\vec{n}_V\ \Delta\Gamma = V_w\frac{\Delta C_V}{\Delta t} \tag{29}$$

where ϕ is porosity, and V_w is the volume of water in the element. This formulation assumes that the flow problem has already been solved. The basic philosophy of this procedure was demonstrated in *Narasimhan and Witherspoon* (1977) in a numerical code TRUST for the solution of saturated-unsaturated flow problems in deformable porous media. CHAMP has been developed directly from this code to include the transport of solutes and incorporates the same basic calculational model and solution method. A mixed explicit-implicit iterative scheme is used for matrix solution. This manner of mathematically describing the fluid flow and solute transport processes possesses considerable utility with the advent in recent years of fast, inexpensive digital computers that allow for the performance of the intensely repetitious calculations. The primary advantage lies in the ability to solve problems of arbitrary shape and boundary conditions for which closed-form or analytic solutions are not available, in other words, for most problems of practical interest.

8. MODELING METHODOLOGY

8.1. Model Verification

Prior to the modeling effort, an attempt was made to verify that internally CHAMP was functioning correctly and consistently by applying it in simple problems for which closed-form solutions exist. Numerous well known solutions are available in the literature to the one-dimensional form of the advection-dispersion equation. For steady flow in a homogeneous, isotropic, fully-saturated porous medium, with no production or decay, and with linear adsorption, the following equation applies:

$$R\frac{\partial C}{\partial t} = D_h\frac{\partial^2 C}{\partial z^2} - v\frac{\partial C}{\partial z} \tag{30}$$

where D_h is the apparent dispersion coefficient in the longitudinal direction, z, R is the retardation factor, and the other terms are defined above. Based on the following boundary and initial conditions,

$$C(z,0) = C_i$$

$$C(0,t) = C_o \quad 0 < t \le t_o$$

$$= 0 \quad t > t_o$$

$$\frac{\partial C}{\partial z}(\infty,t) = 0$$

a solution to Eq. (30) is *(Lapidus and Amundson,* 1952; *Ogata and Banks,* 1961):

$$C(z,t) = C_i + (C_o - C_i)\, A(z,t) \tag{31}$$

$$= C_i + (C_o - C_i)\, A(z,t) - C_o\, A(z,t-t_o)$$

where,

$$A(z,t) = \tfrac{1}{2}\,\mathrm{erfc}\left[\frac{Rz - vt}{2(D_h R t)^{1/2}}\right] + \tfrac{1}{2}\exp(vz/D_h)\,\mathrm{erfc}\left[\frac{Rz + vt}{2(D_h R t)^{1/2}}\right]$$

The Peclet number is a measure of the relative magnitude of advective solute fluxes to those

due to dispersion. In numerical modeling of solute transport, knowledge of its value is important in determining the degree to which the numerical procedure itself is introducing error into the solute transport calculations. In the determination of the advective solute fluxes, an estimate of concentration is required at the interface of element surfaces. Concentration values are associated with nodal points, therefore the interface concentration is determined by linearly interpolating between nodal points. In advectivelly dominated systems, where the advancing solute front may be sharply defined , this approximation can be significantly in error. The propogation of this error is often called numerical dispersion. If hydrodynamic dispersion is already present in the system, the error introduced may be small, and it may be possible to be convinced that the error is not significant. Therefore, the Peclet number is defined as a means of determining if a system can be considered to be advectivelly dominated. For the purposes of CHAMP, the Peclet number for the element, l, is defined as the sum of upstream advectances, F, divided by the element's total chemical conductance, Y:

$$Pe_l = \frac{\sum_{m}^{upstream} F_{l,m}}{\sum_{m} Y_{l,m}} \qquad (32)$$

$$= \sum_{l}^{m} \rho_f K_{l,m} \frac{\Delta\Gamma_{l,m}}{d_{l,m}}$$

where ρ_f is fluid density, $\Delta\Gamma_{l,m}$ is the surface area of the interface between elements l and m, and $d_{l,m}$ represents the distance between nodal points. For one-dimensional flow, Eq. (32) reduces to:

$$Pe_l = \frac{\frac{1}{2}\, v\, \Delta z}{D_h} \qquad (33)$$

The common practice in numerical studies involving solute transport is to be concerned with numerical dispersion only if $Pe_l \geq 2$.

Solute breakthrough curves have been calculated based on the solution to Eq. (30) and from

application of the code, CHAMP, and are plotted in Figure 8.1 for two values of the Pe_l, .025 and 2.5. We see that for the two depths, CHAMP appears to be providing the correct solution, and that even for the larger Pe_l the deviation from the exact solution is small. Pe_l values for the history-matching cases run in this study have been calculated and are presented in Table 6.

8.2. Method and Assumptions

The ability of the deterministic model to history-match observed transport during the *resaturation* period in this and similar experiments is in all likelihood extremely limited, partly due to limitations of the model and partly due to manner in which the experiment was performed. The deterministic model can be extremely valuable, however, in theoretical studies where the effects of hypothetical properties or conditions wish to be analyzed in idealized settings. Immediately following the flooding event, conditions were highly transient with the occurrence of preferential flow and bypass of the soil matrix, resaturation, chloride dissolution and subsequent redistribution throughout the soil profile. The three-dimensional network of soil macropores, including dessication cracks, root holes, worm holes, etc is probably beyond description and yet it is of primary importance in the spatial and temporal response of solutes. Solute movement was occurring at a rate greater than that which could have been resolved in space or time by the frequency of soil water sampling carried out in this experiment. In a practical vein, the rapid pore water velocities in soil fractures and the highly transient nature of this type of problem incur serious difficulties of stability and accuracy in the numerical solution of the flow and transport equations which also happen to be non-linear. Boundary and initial conditions would have been extremely difficult to define without an unreasonable degree of instrumentation and complexity. The water application rate and the initial rate of chloride mobilization were essentially unquantifiable. Therefore, no attempt was made to model this early period of partially-saturated flow. The modeling effort begins several days after flooding, after fully water saturated conditions were established. It was felt that during this time the data that had been collected were suited to a successful modeling effort. Boundary conditions of fluid potential and concentration had been directly

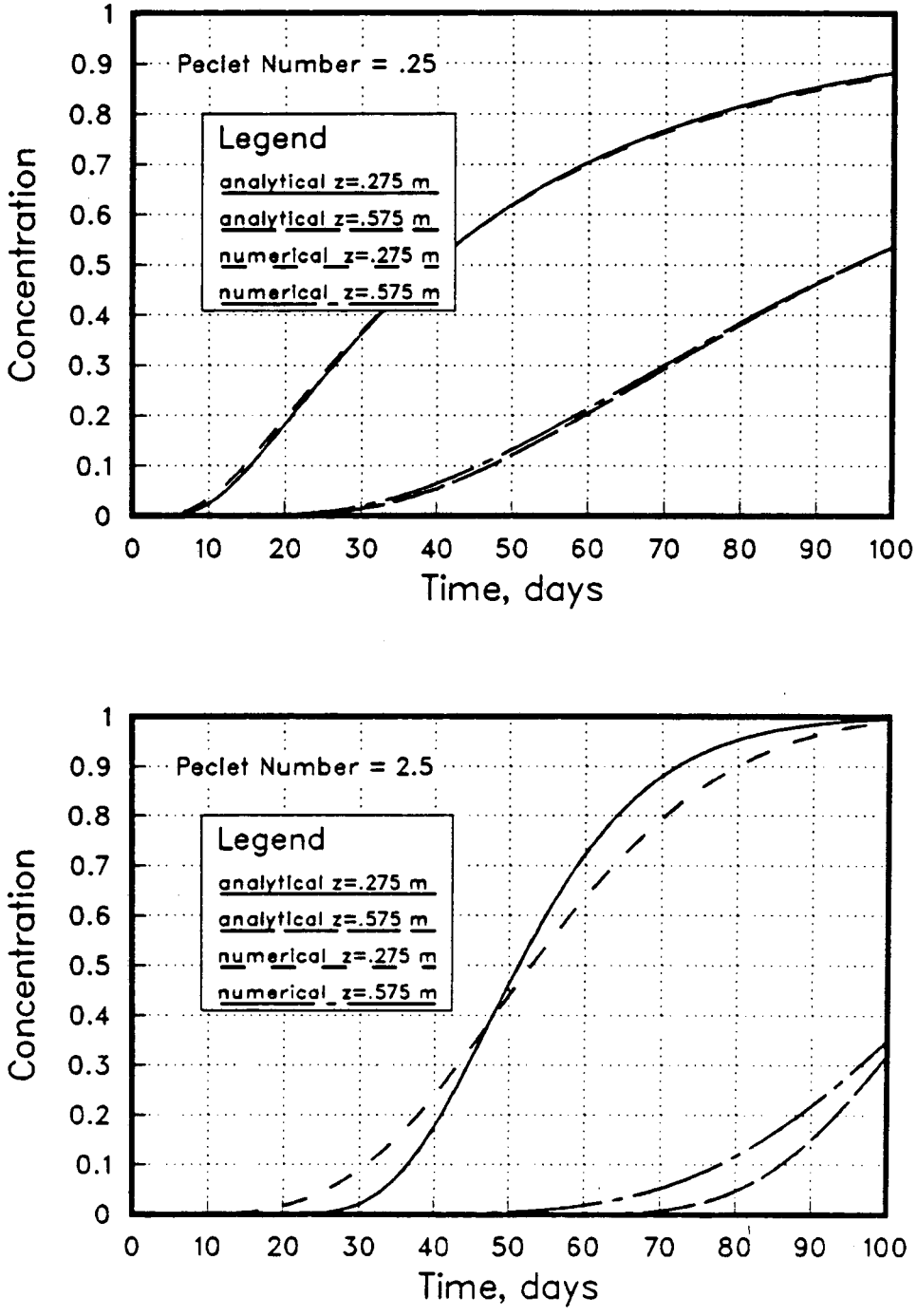

Figure 8.1 Comparison of the computer code CHAMP with an analytical solution for 1-dimensional fully-saturated solute transport. Cases are run for two values of the Peclet number - .25 and 2.5.

measured, knowledge of unsaturated hydraulic conductivities was not required, and the sampling intervals had been sufficient to adequately resolve the movement of the solute.

Chloride concentrations and fluid potentials were monitored at each of the plots from the pond surface to a depth of approximately 2.75 m (9 ft). A one-dimensional grid of 55 5 cm (1.97 in) thick elements was constructed to discretize the 2.75 m flow region. The top element represented the ground surface, and the bottom element coincided with the mid-point of the shallow well screened interval. For site UZ-1, the shallowest well was screened from 3.0 to 4.6 m (10 to 15 ft), thereby extending the grid to 76 elements and a depth of 3.80 m (12.5 ft). For the upper boundary, measured pond water depths served as a prescribed potential boundary while measured chloride concentrations provided a prescribed concentration boundary condition. For the bottom boundary, in a similar manner, hydraulic head values measured in monitoring wells were input directly as the potential condition and observed chloride concentrations in groundwater served as the concentration boundary condition. The complete listing of concentration and potential boundary conditions used at each of the five sites is included in Figures 8.2 to 8.11.

At each site, an instant T_o some few days after flooding was chosen to be the time from which history-matching of solute breakthrough would begin. T_o, depending on the site, ranged from 4 to 19 days after flooding. The solute concentration profile measured at each site at this time was utilized as the initial concentration for the site grids (Figures 8.7 to 8.11). For initial chloride concentrations of elements located between soil water sampler depths, values were chosen by a simple linear interpolation between concentrations observed in soil water samplers directly above and below them in depth. For the fluid potential initial condition, a linear interpolation between the potentials measured at the surface and in the shallow well at T_o was used.

It is important to mention several key assumptions that were made in the analytical procedure and possible resulting limitations.

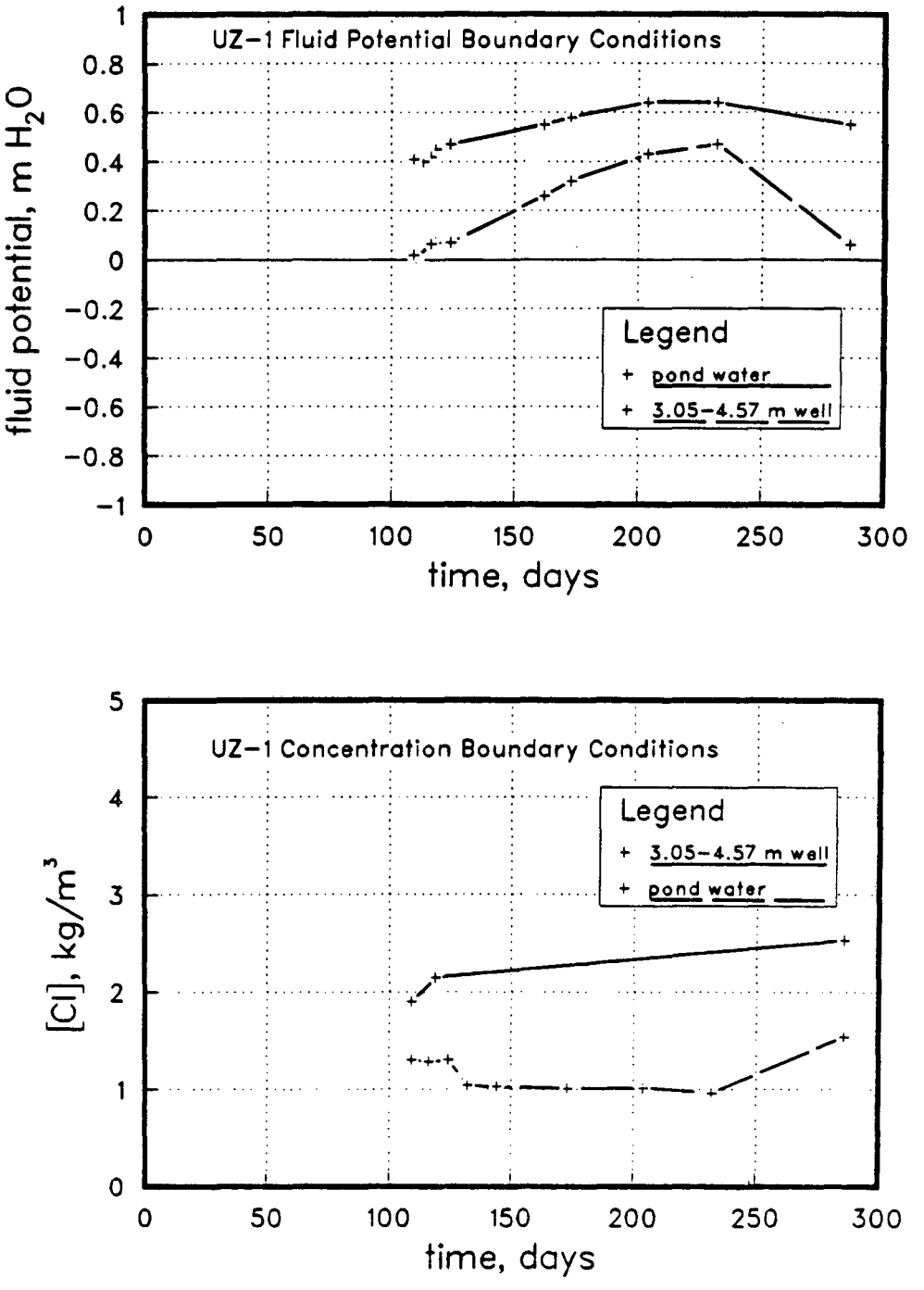

Figure 8.2 Fluid potential and chloride concentration boundary conditions used in the modeling effort at site UZ-1. Pond water data was applied to the upper boundary and the data from shallow groundwater monitoring wells was applied to the bottom boundary.

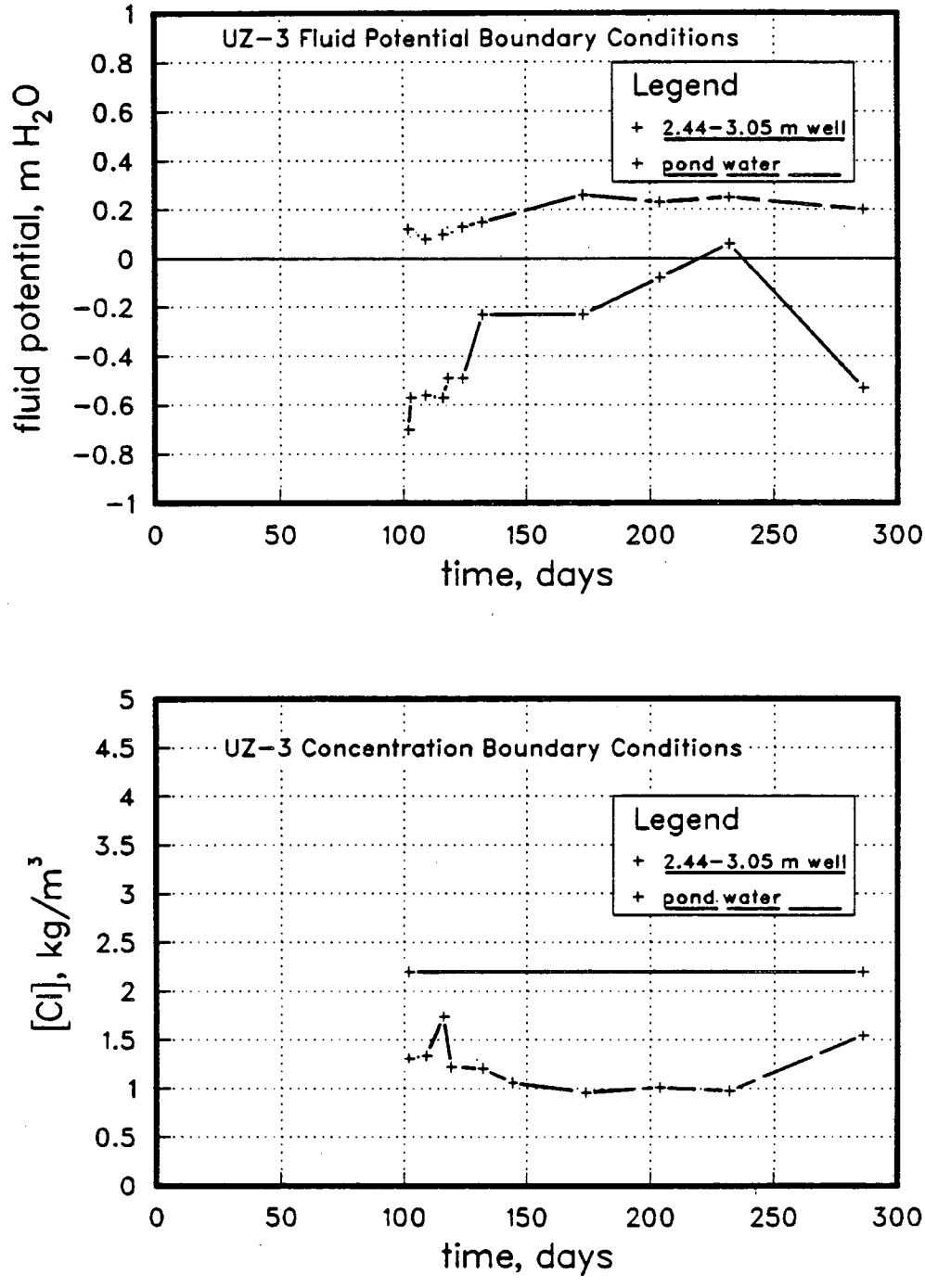

Figure 8.3 Fluid potential and chloride concentration boundary conditions used in the modeling effort at site UZ-3.

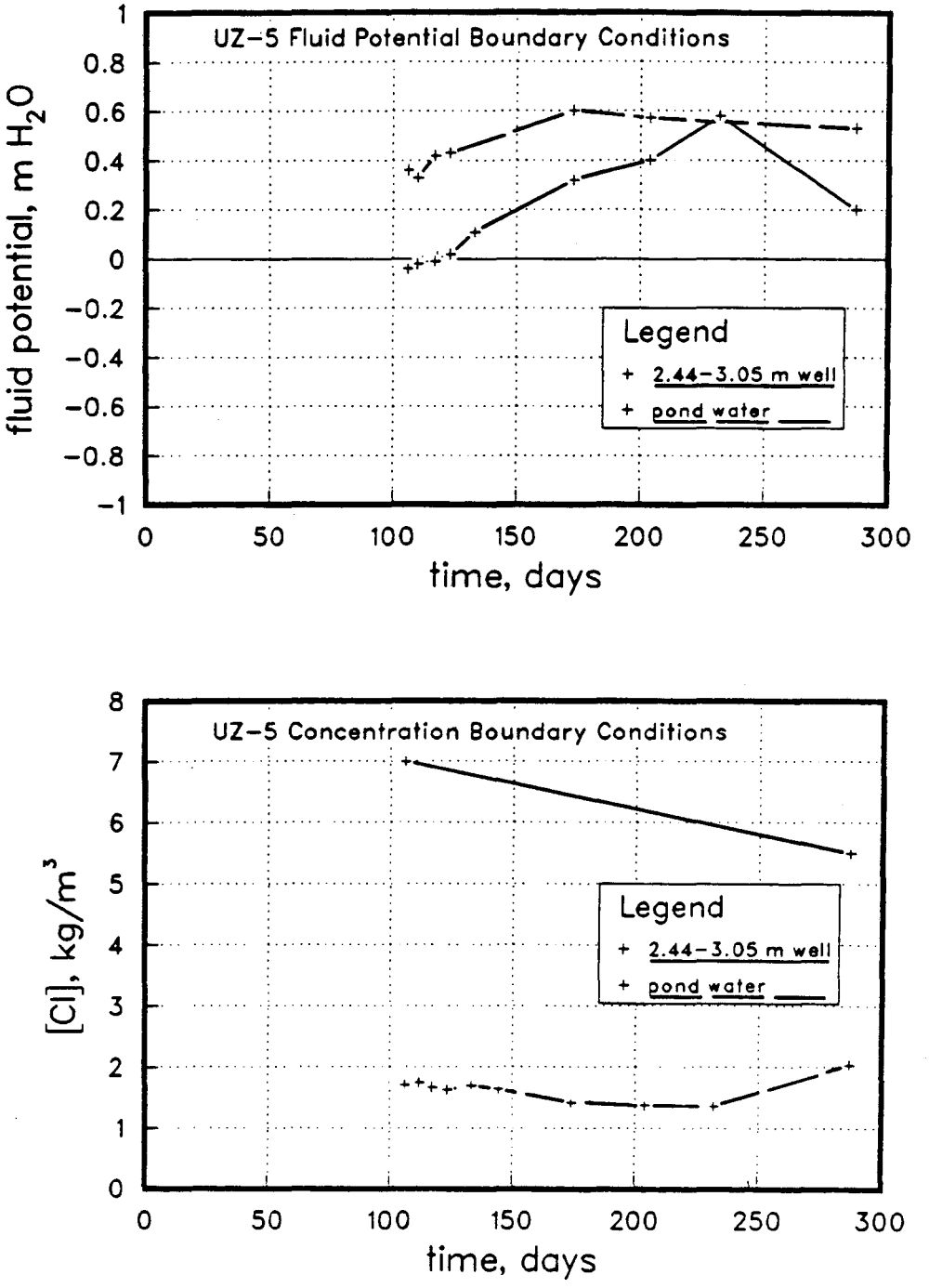

Figure 8.4 Fluid potential and chloride concentration boundary conditions used in the modeling effort at site UZ-5.

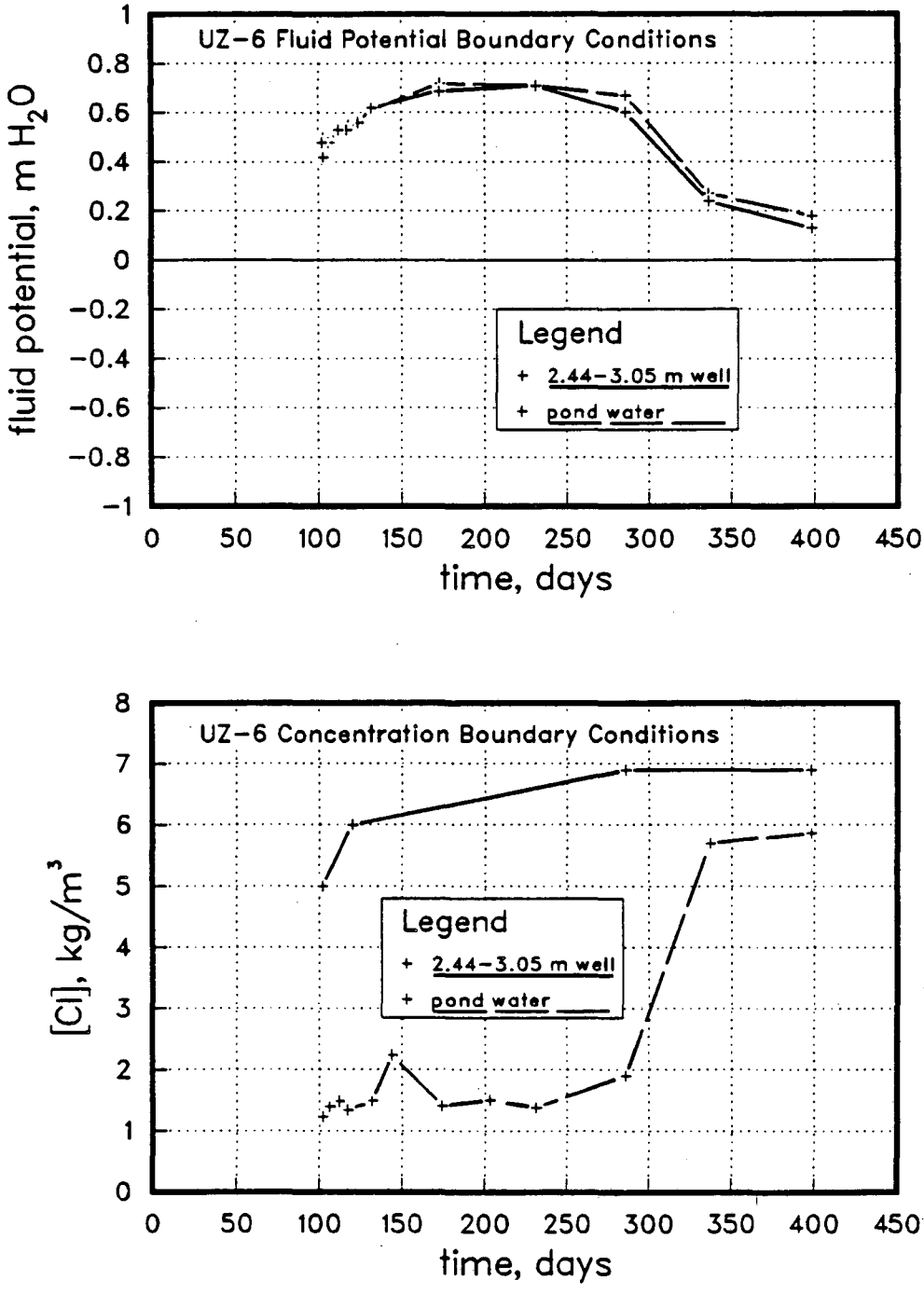

Figure 8.5 Fluid potential and chloride concentration boundary conditions used in the modeling effort at site UZ-6.

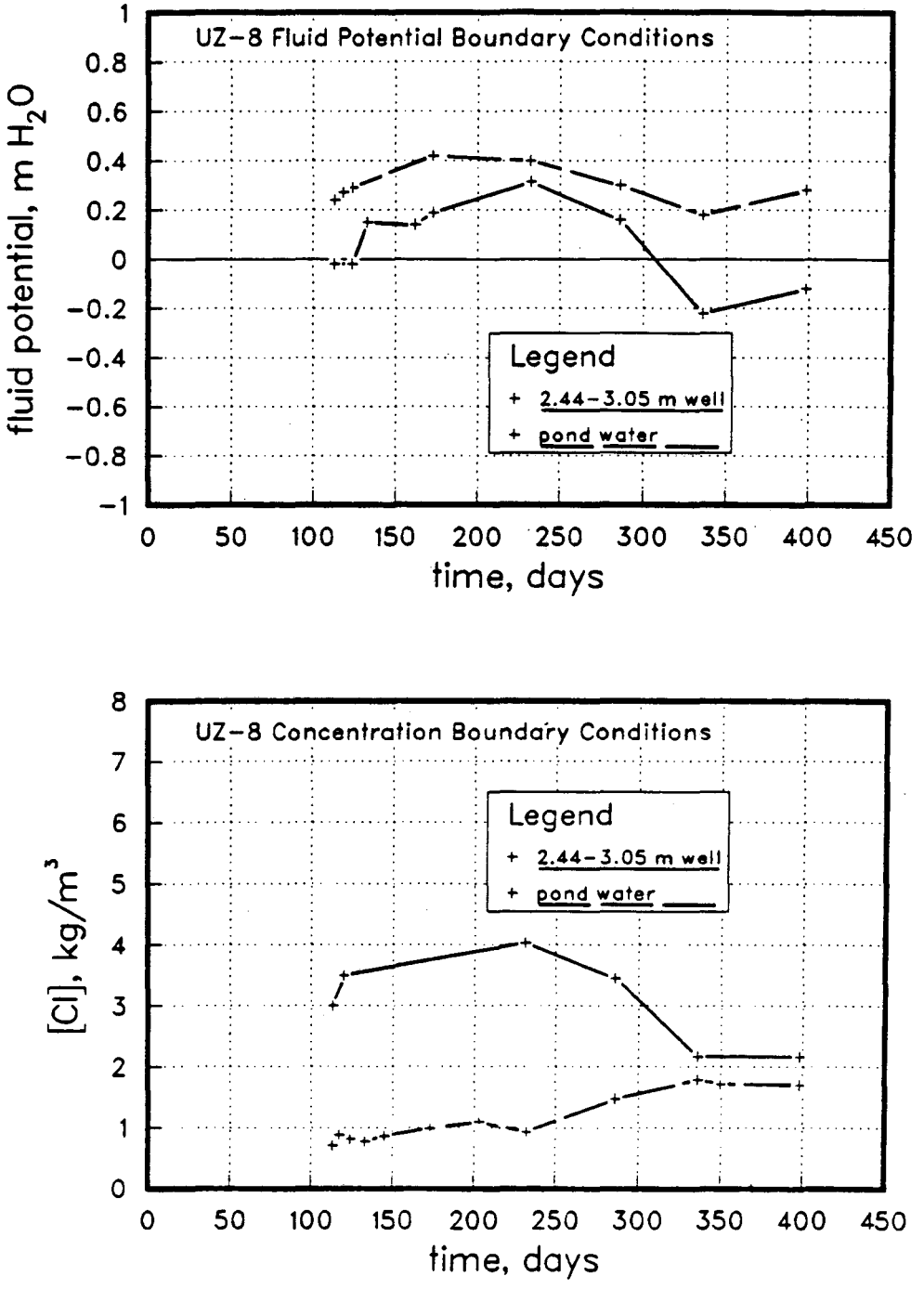

Figure 8.6 Fluid potential and chloride concentration boundary conditions used in the modeling effort at site UZ-8.

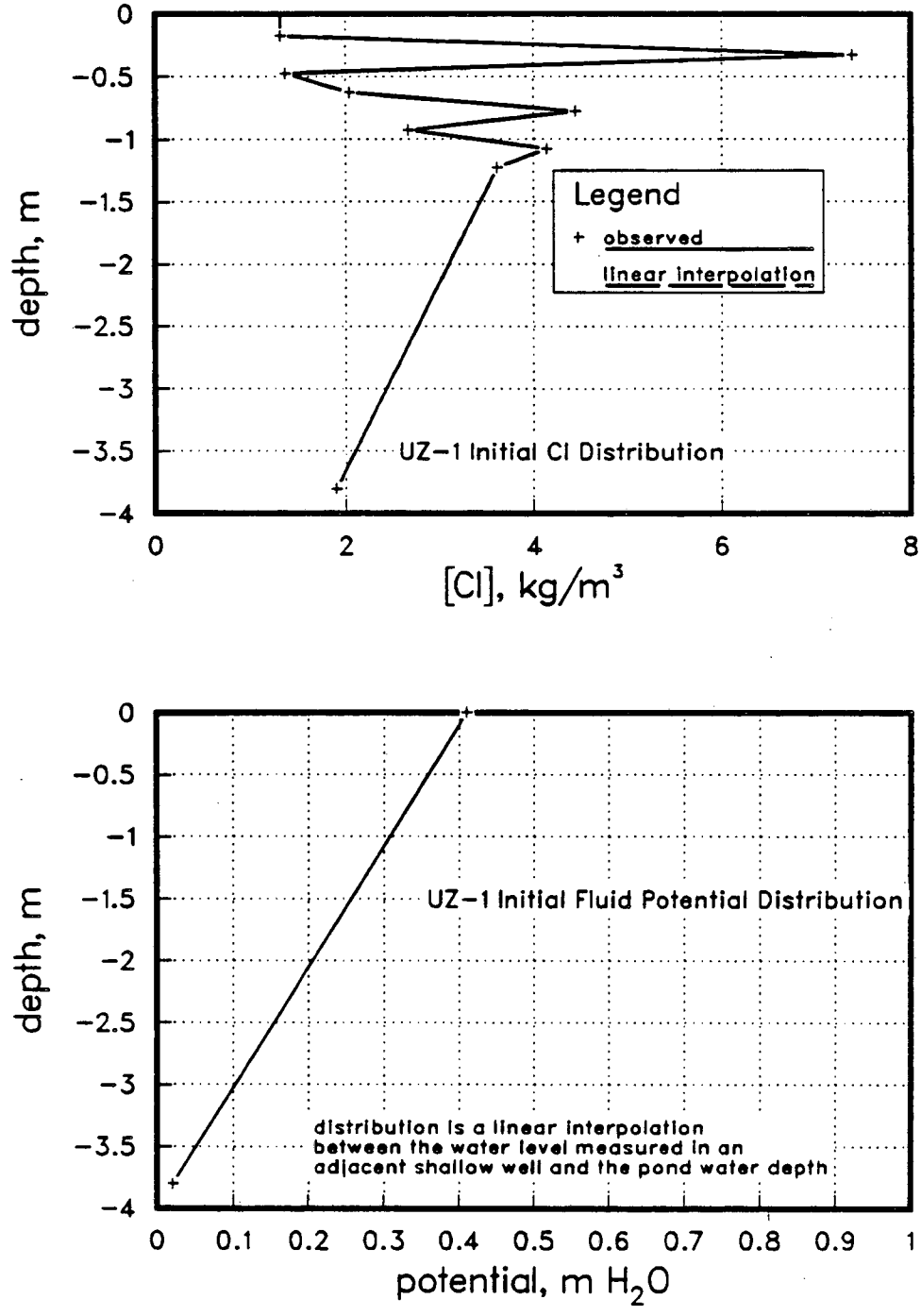

Figure 8.7 Initial conditions of fluid potential and chloride concentration measured at site UZ-1 and applied in the modeling effort.

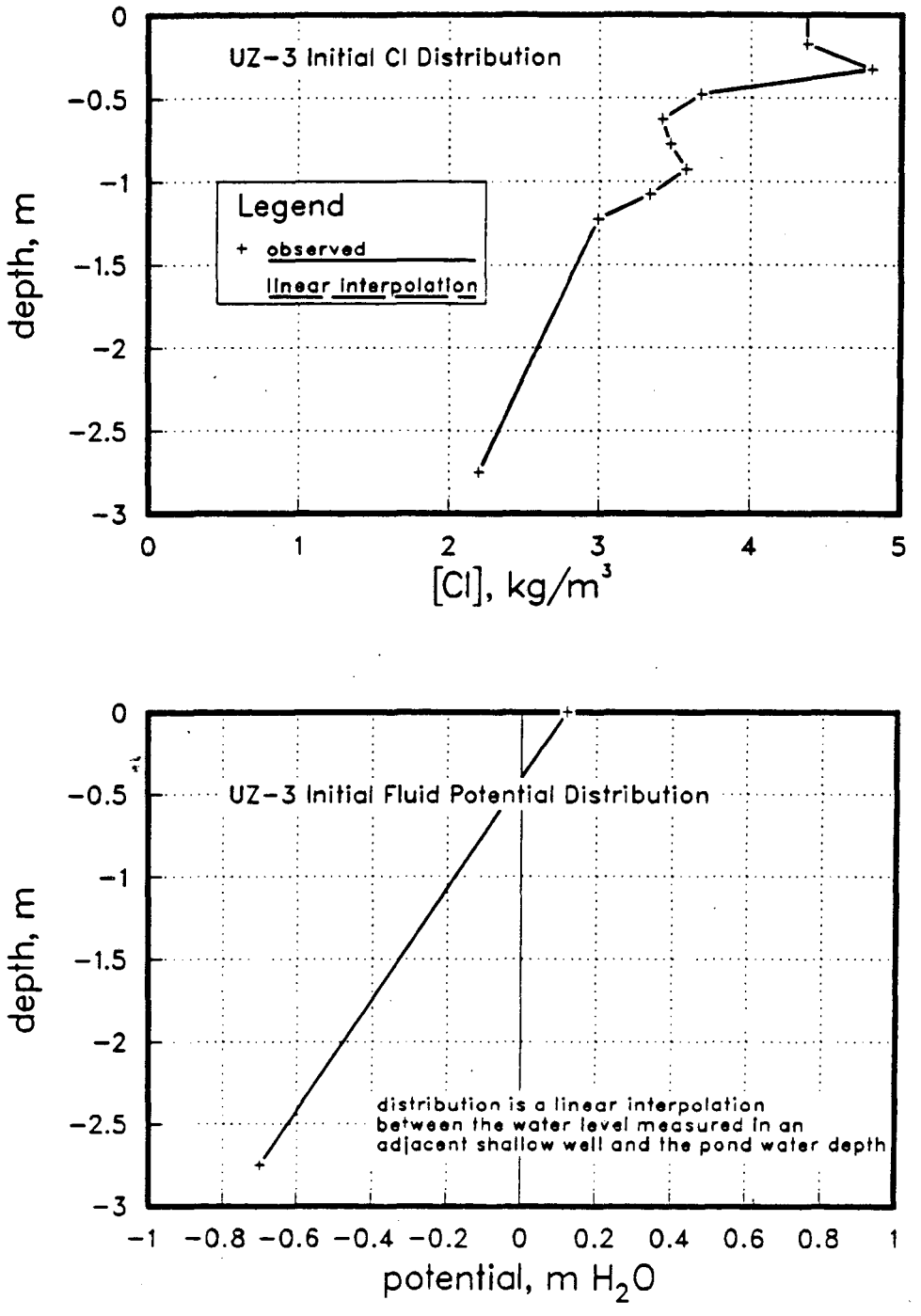

Figure 8.8 Initial conditions of fluid potential and chloride concentration measured at site UZ-3 and applied in the modeling effort.

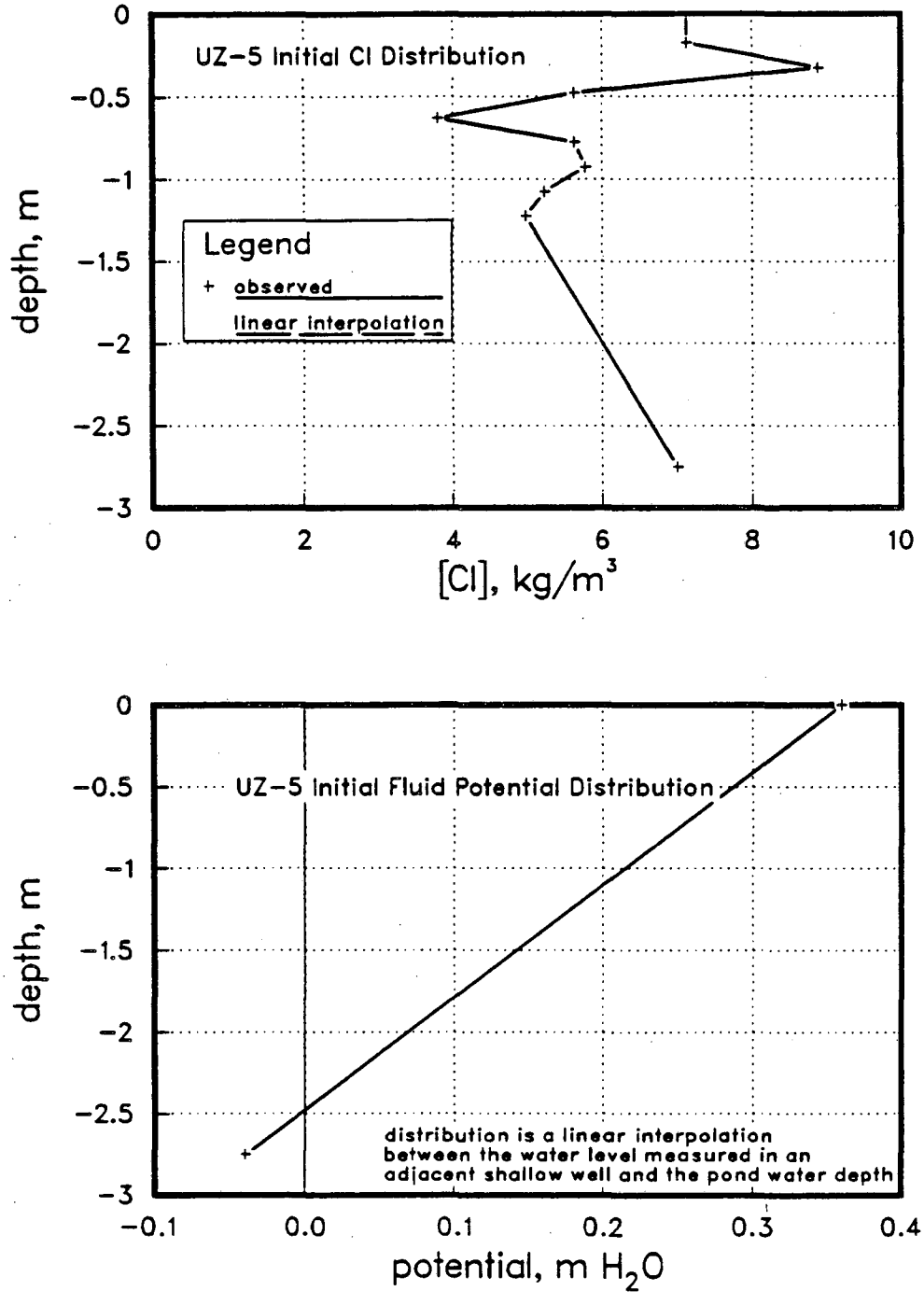

Figure 8.9 Initial conditions of fluid potential and chloride concentration measured at site UZ-5 and applied in the modeling effort.

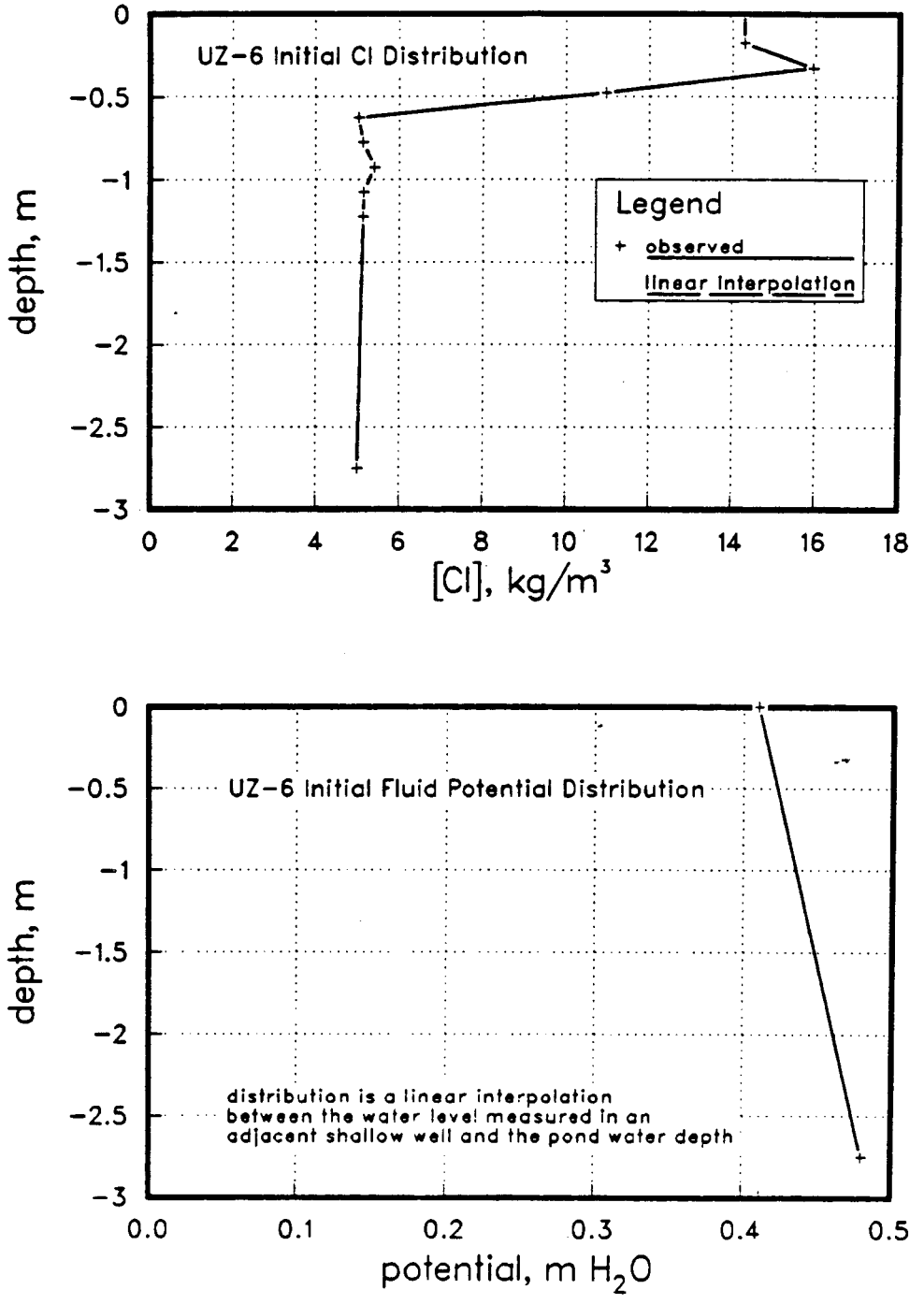

Figure 8.10 Initial conditions of fluid potential and chloride concentration measured at site UZ-6 and applied in the modeling effort.

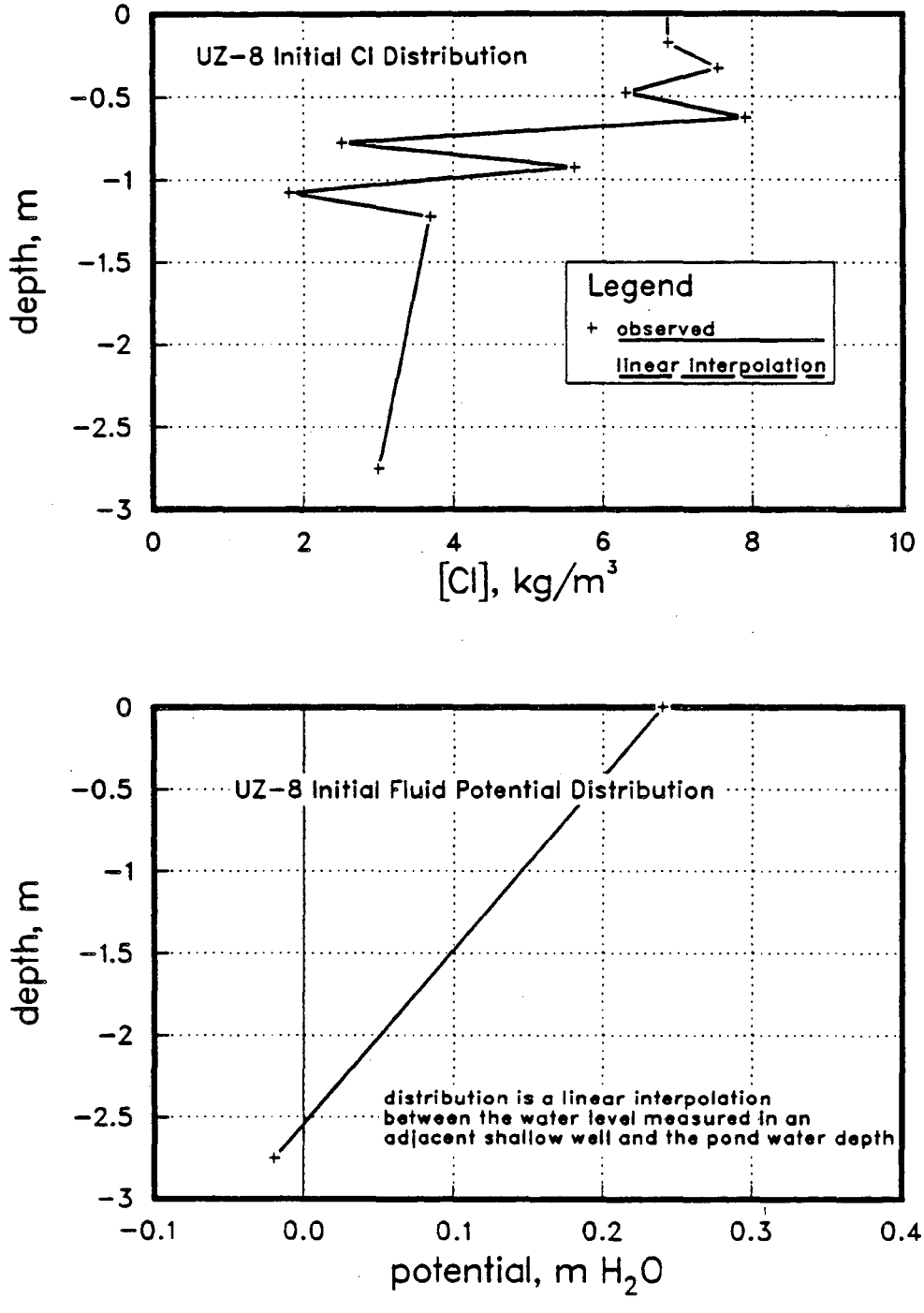

Figure 8.11 Initial conditions of fluid potential and chloride concentration measured at site UZ-8 and applied in the modeling effort.

(1) The flow regime was modeled as a fully-saturated medium. As is discussed in Section 5.1, actual saturation at T_o may have been slightly less than this due to the presence of entrapped air, however, tensiometer data collected during the experiment, and modeling of the infiltration process indicated that it was very likely that by this time the soils were at least 90-95% saturated.

(2) It was assumed that the dissolution of chloride was complete at the commencement of modeling, i.e. that there was no chloride source within the flow region during the modeling time frame. This issue has been discussed previously in this report. The reader is referred to Section 5.1 for a more complete discussion.

(3) Chloride measurements were assumed to provide representative estimates of average conditions at the particular depth or location from which they were collected, i.e. pond water and well water samples were considered to adequately define the upper and lower boundary conditions, and that chloride levels measured in soil water samplers were indicative of processes and transport occurring in the interval adjacent to the soil water sampler.

(4) The chloride profile used as the initial condition was constructed from soil water samples collected laterally throughout each plot. Due to the extreme lateral variability that is often evidenced in soils, these conditions used may not have been representative of initial conditions throughout the test plot. The extent to which uncertainty in the initial conditions would affect interpretation of results is a function of the degree to which lateral heterogeneity is exhibited in the solute profiles. Sensitivity studies have been performed to address this issue and are included in Appendix I.

(5) The modeling was performed assuming one-dimensional vertical flow. A two-dimensional effort would have lead to an unwarranted degree of complexity. With the addition of a large number of variables and parameters, a highly arbitrary history-matching procedure would have resulted. However, the large spatial variations in soil hydraulic parameters that have often been observed in soils, can lead to possible 2- and 3-dimensional flow effects which have been neglected in this study. An attempt has been made, the results of which are included in Appendix I, to evaluate for some simple forms of soil heterogeneity, the extent to which water may flow laterally during infiltration.

In modeling performed at a particular site, one site-specific set of boundary and initial conditions was applied to the eight individual locations, however, history-matching of the chloride concentration was performed separately at each soil water sampler (at each depth) as if it possessed its own set of parameters representing a vertical, independent, non-interacting flow region. No attempt was made to match chloride concentration *profiles* during the experiment.The results therefore represent spot measurements of properties at discrete points where each parameter is an effective value over the entire 2.75 m (9 ft) soil column. History-matching involved making numerous iterative runs of CHAMP and systematically varying the parameters, permeability, k (L^2), and apparent dispersion coefficient, D_h, in an attempt to produce the best possible match, determined visually, to the observed data. The parameters were applied uniformly over the grid, and a constant porosity of .45, based on an average value obtained from laboratory measurements, was assumed for all the sites. The final results of the history-matching at the 40 locations, produced with the best possible combination of parameters, are presented in Figures 8.12 to 8.31.

It was often possible, based purely on the closeness of the two curves, for a range of parameter values to match the data almost equally well. This range at times was confined to less than one order of magnitude, however, at times this degree of variance was exceeded. In Figures 8.32 to 8.39, for all 8 soil water samplers at one site (UZ-3), is illustrated the relative effect of property variations on model output, and we see that it is possible to subjectively determine a range of possible values of k and D_h that could result in potentially *good* matches. Good matches, however, could often be made with the choice of physically unrealistic combinations of parameters or the choice of values that were considered unlikely based on previous measurements made in the laboratory and at Kesterson. The purely visual determination lacks any degree of physical appreciation of what is possible and what is reasonable. An element of discretion was therefore introduced into the history-matching procedure by systematically constraining D_h and k. Dispersion coefficients were adjusted so as to result in dispersivity values that were consistent with the scale of the experiment and which were within range of values reported elsewhere in the literature. Permeabilities were chosen with

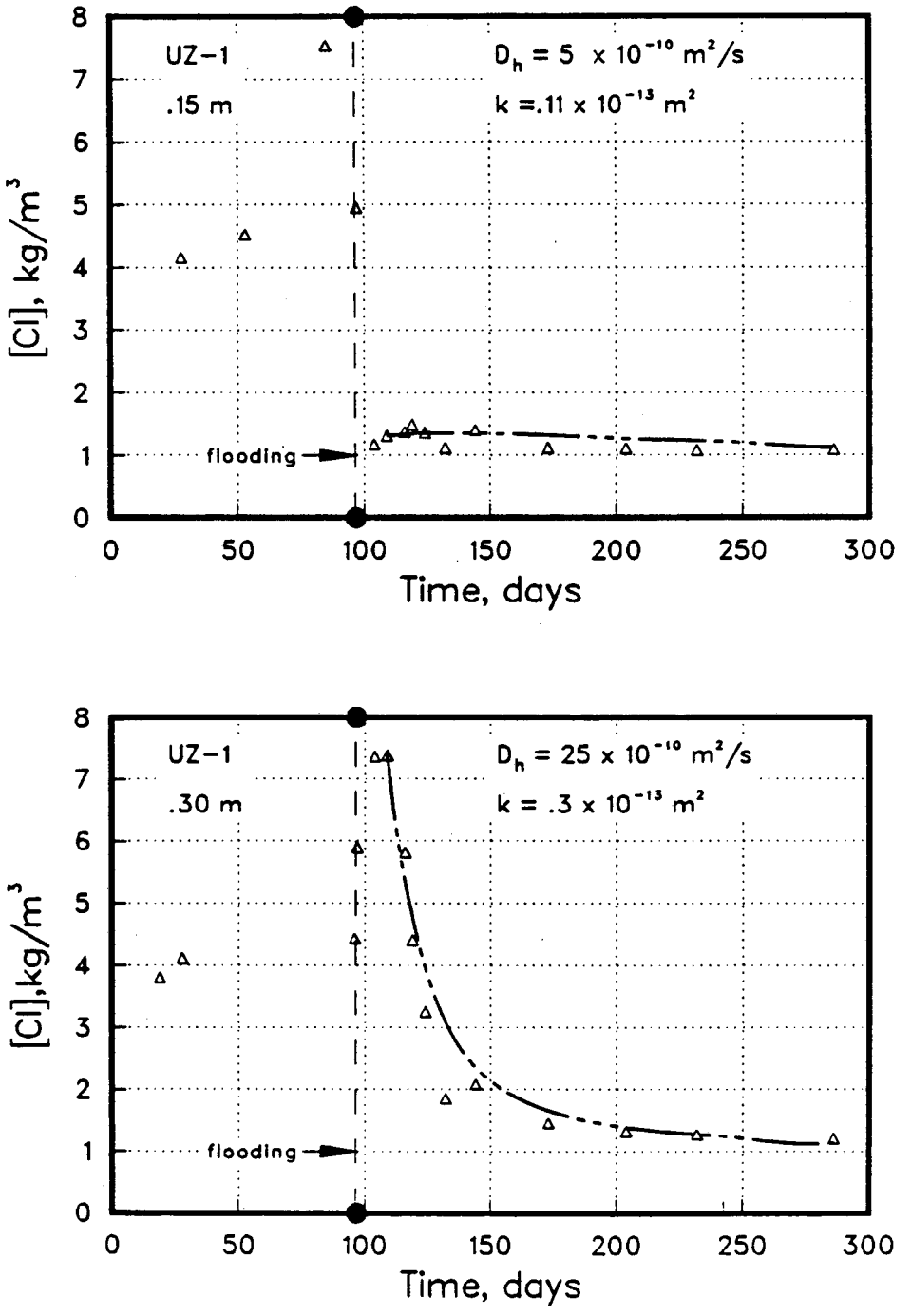

Figure 8.12 The results of the history-matching. Open triangles represent the observed data while the dashed line is model output.

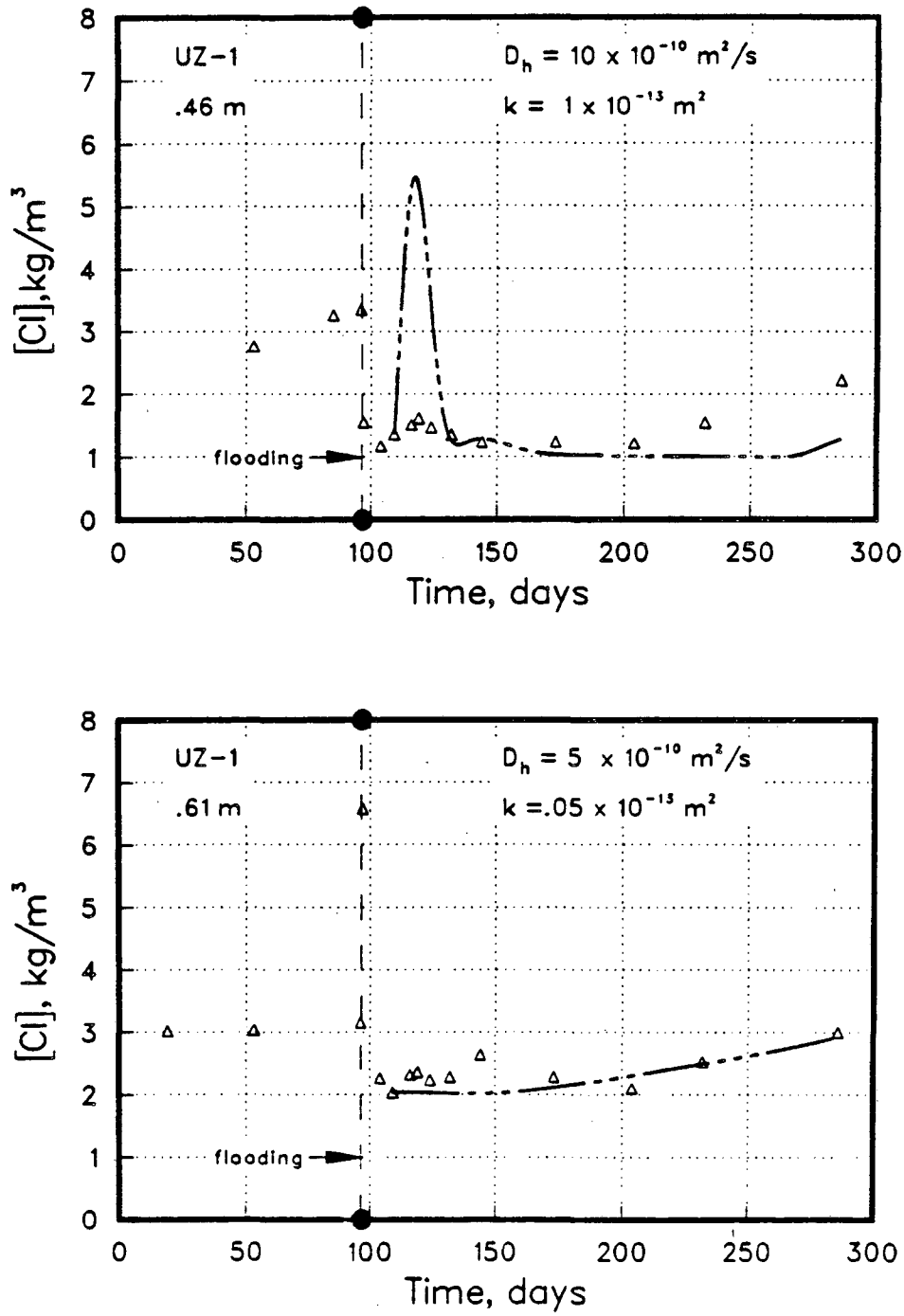

Figure 8.13 The results of the history-matching. Open triangles represent the observed data while the dashed line is model output.

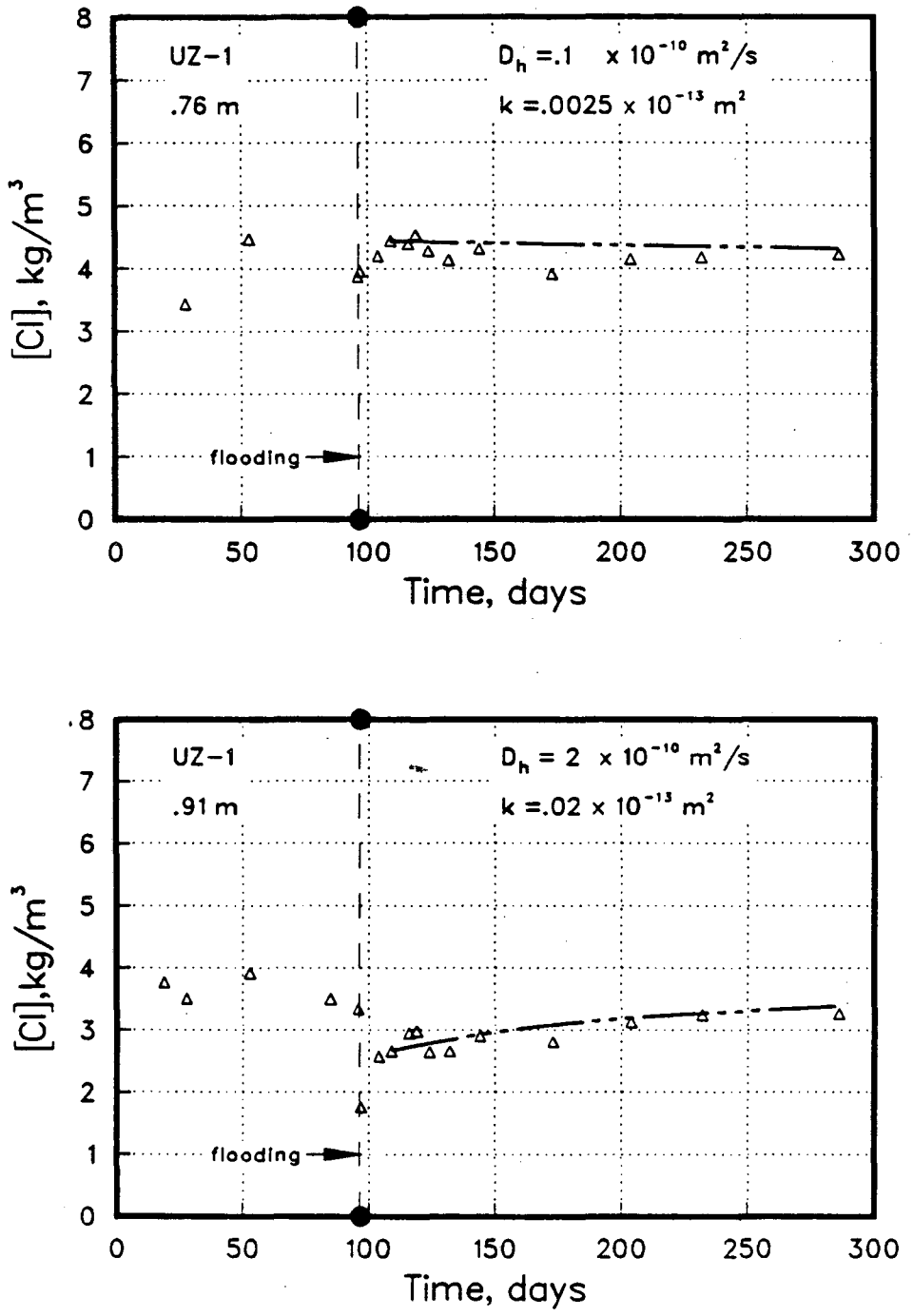

Figure 8.14 The results of the history-matching. Open triangles represent the observed data while the dashed line is model output.

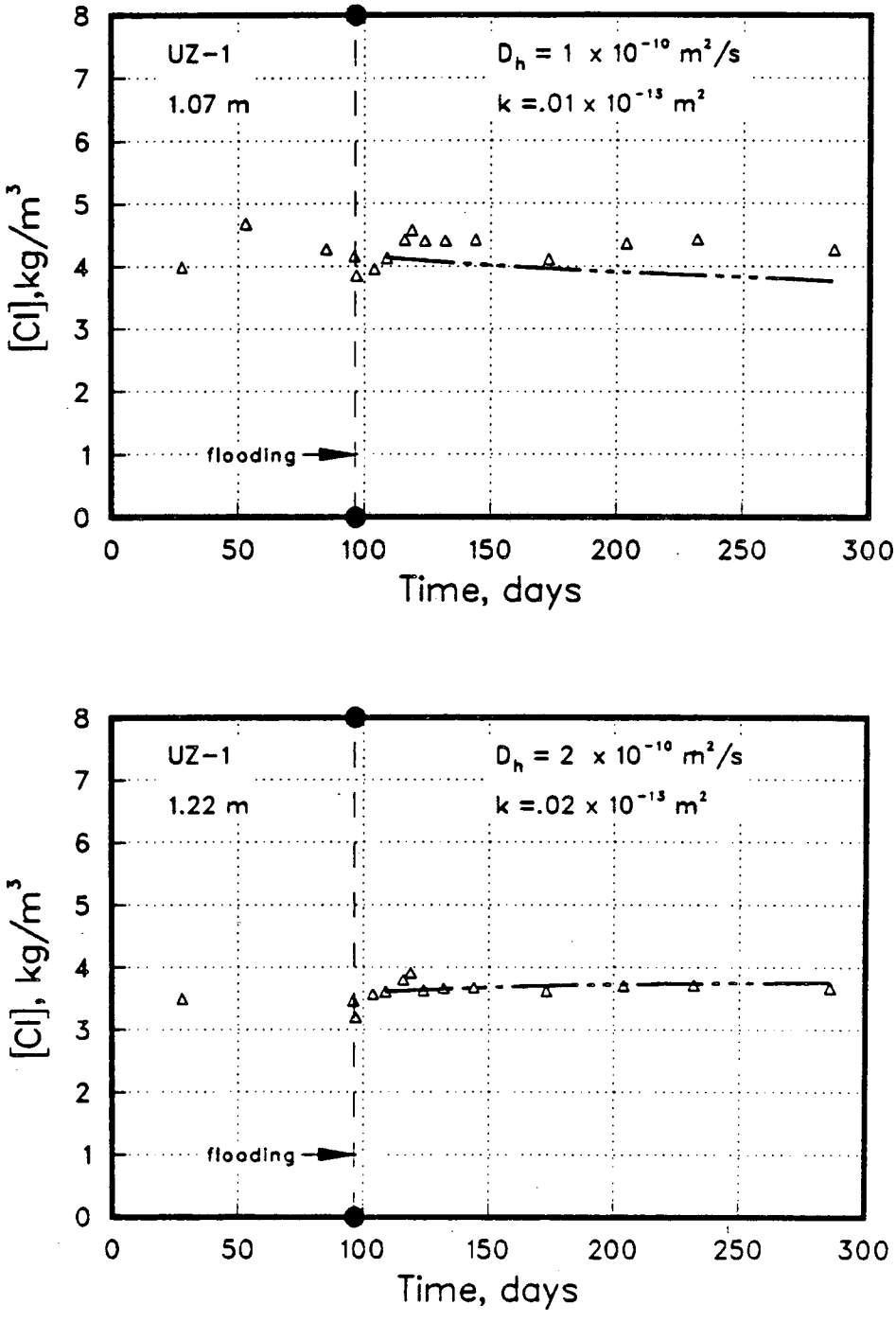

Figure 8.15 The results of the history-matching. Open triangles represent the observed data while the dashed line is model output.

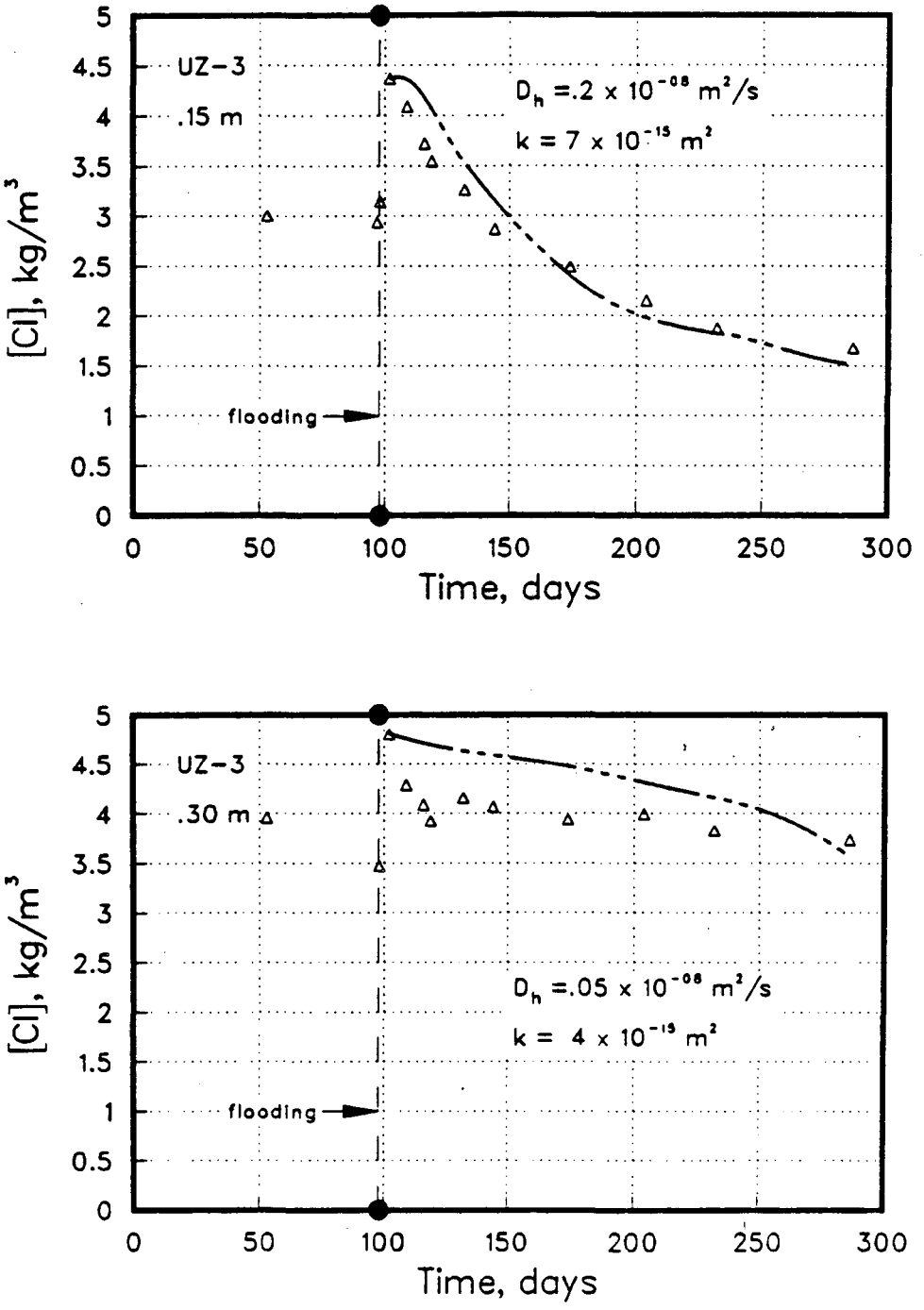

Figure 8.16 The results of the history-matching. Open triangles represent the observed data while the dashed line is model output.

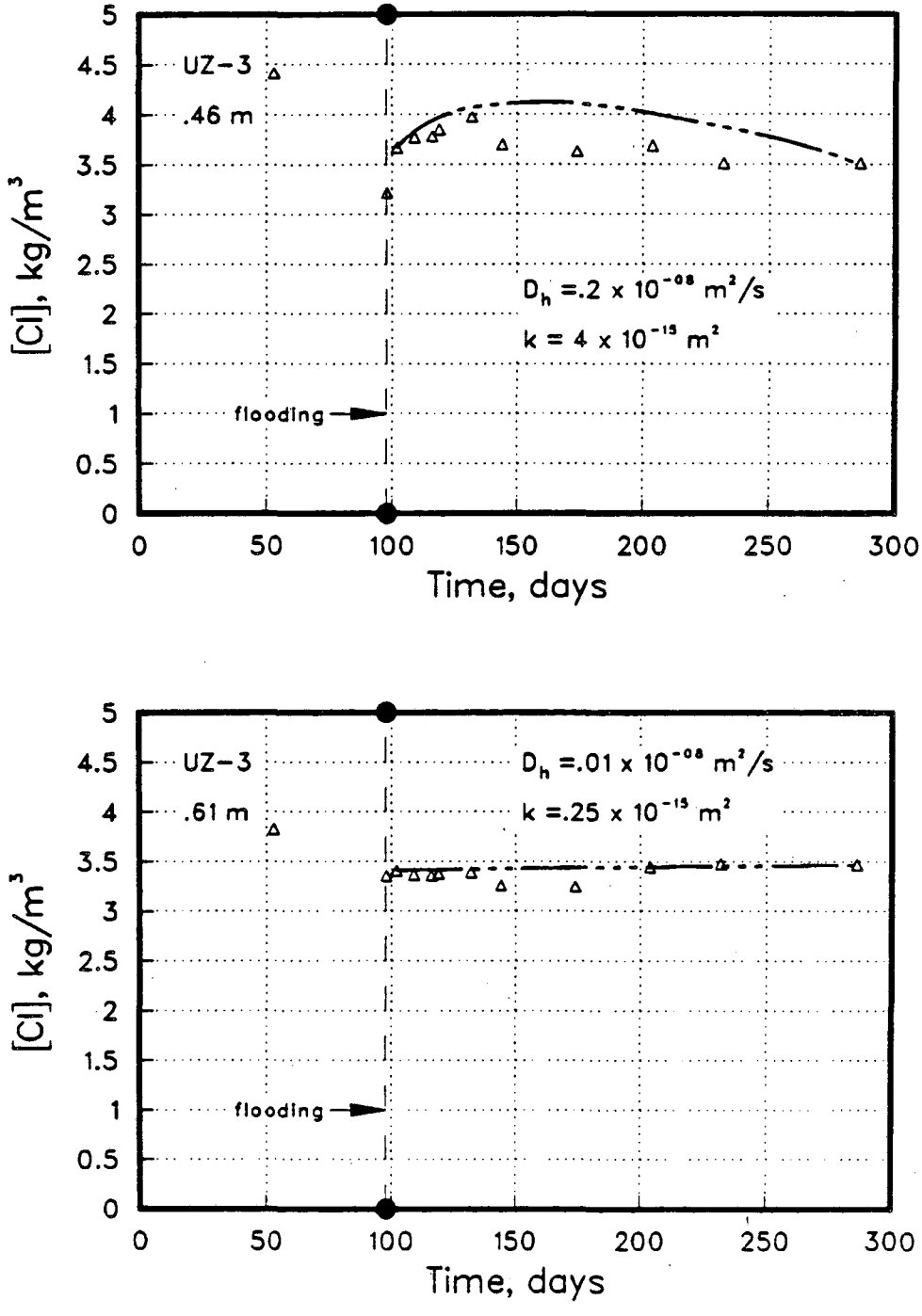

Figure 8.17 The results of the history-matching. Open triangles represent the observed data while the dashed line is model output.

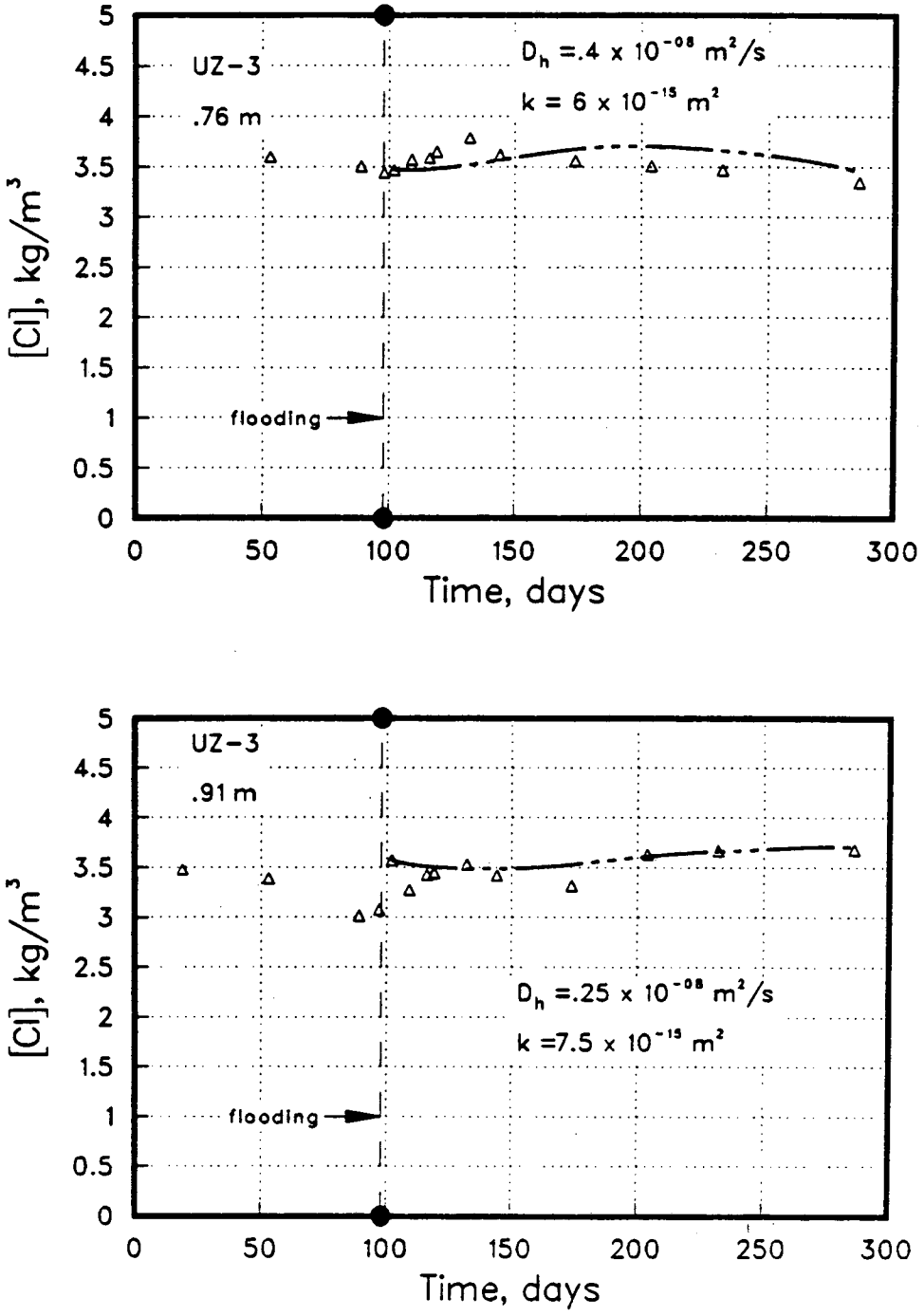

Figure 8.18 The results of the history-matching. Open triangles represent the observed data while the dashed line is model output.

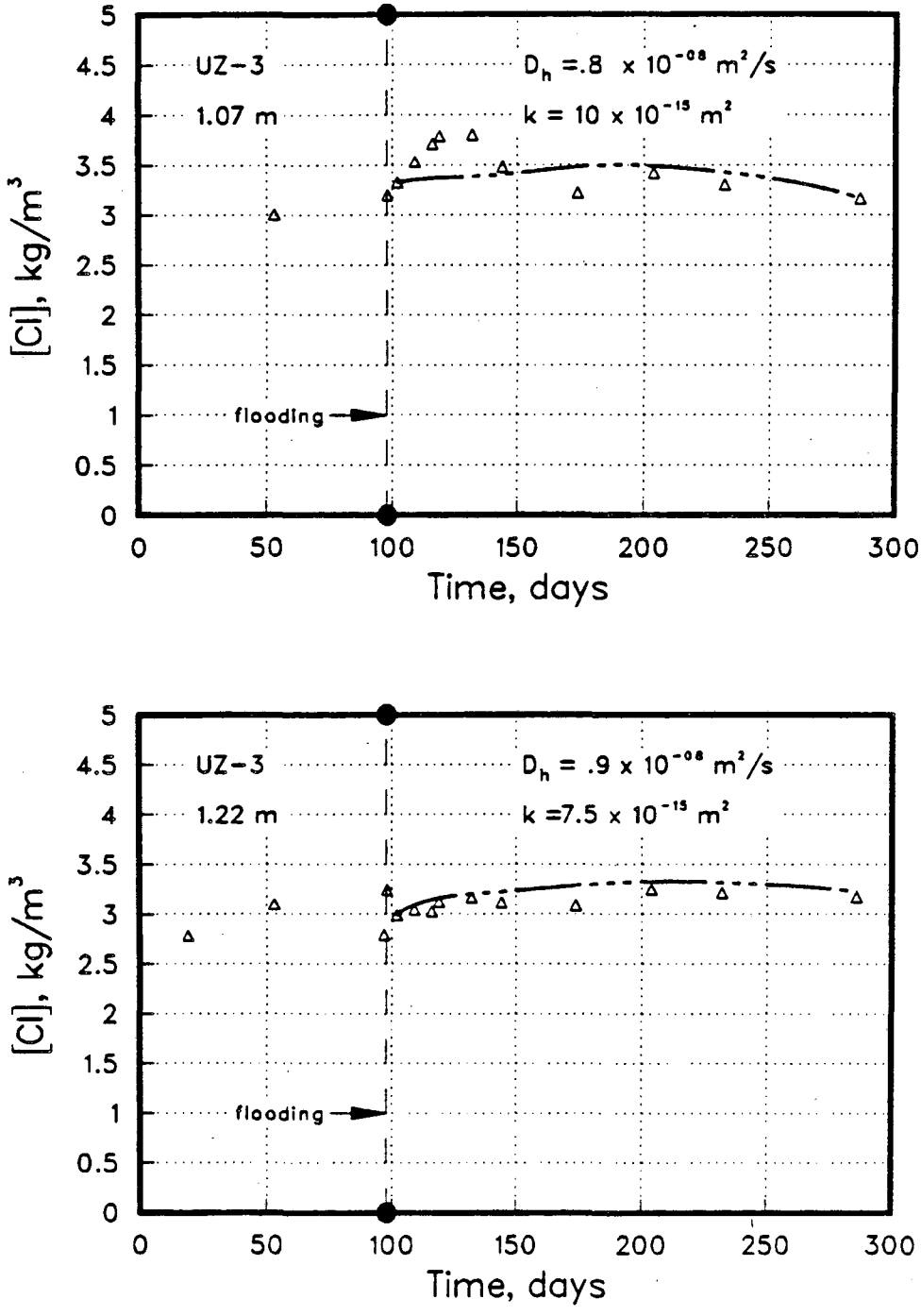

Figure 8.19 The results of the history-matching. Open triangles represent the observed data while the dashed line is model output.

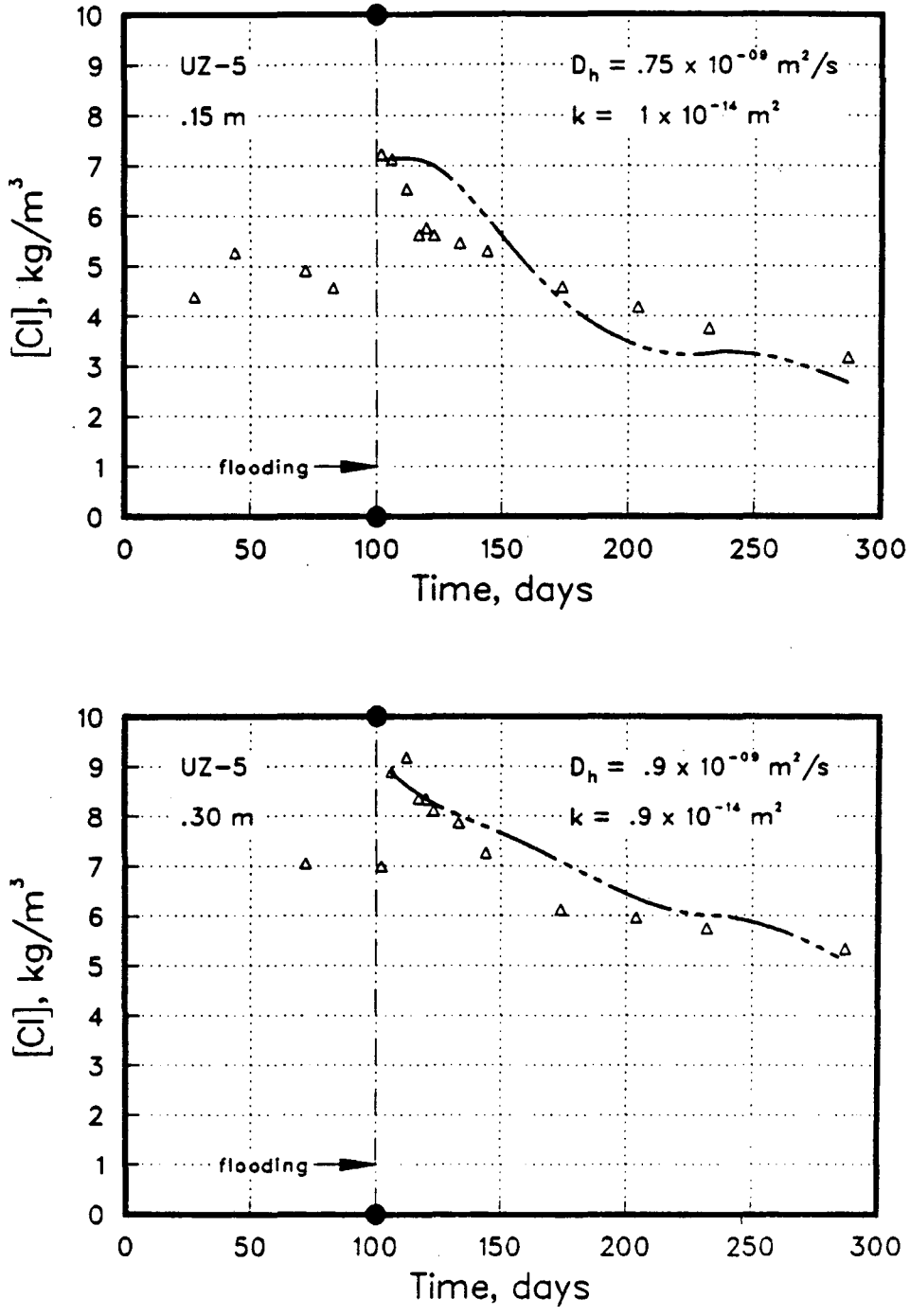

Figure 8.20 The results of the history-matching. Open triangles represent the observed data while the dashed line is model output.

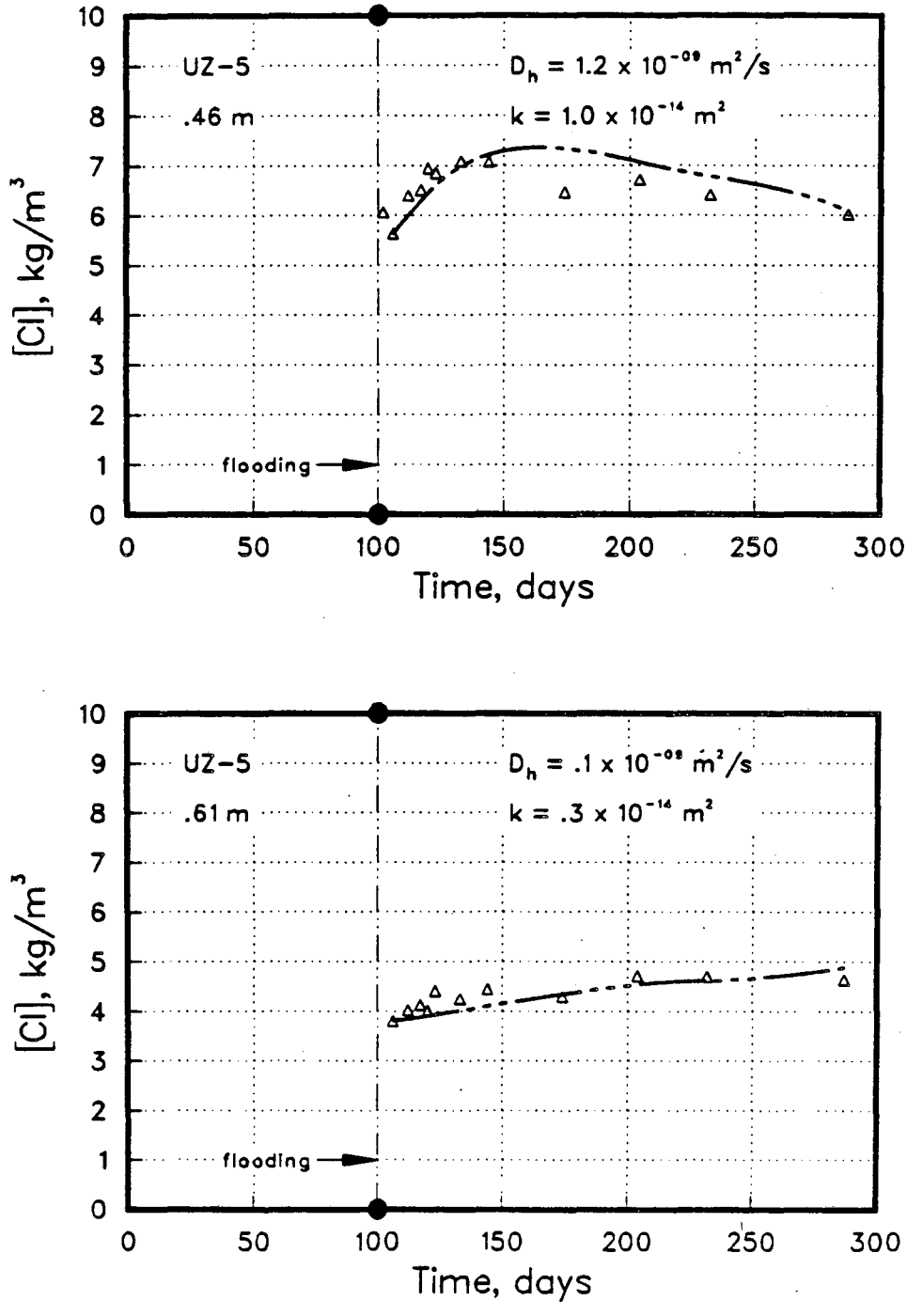

Figure 8.21 The results of the history-matching. Open triangles represent the observed data while the dashed line is model output.

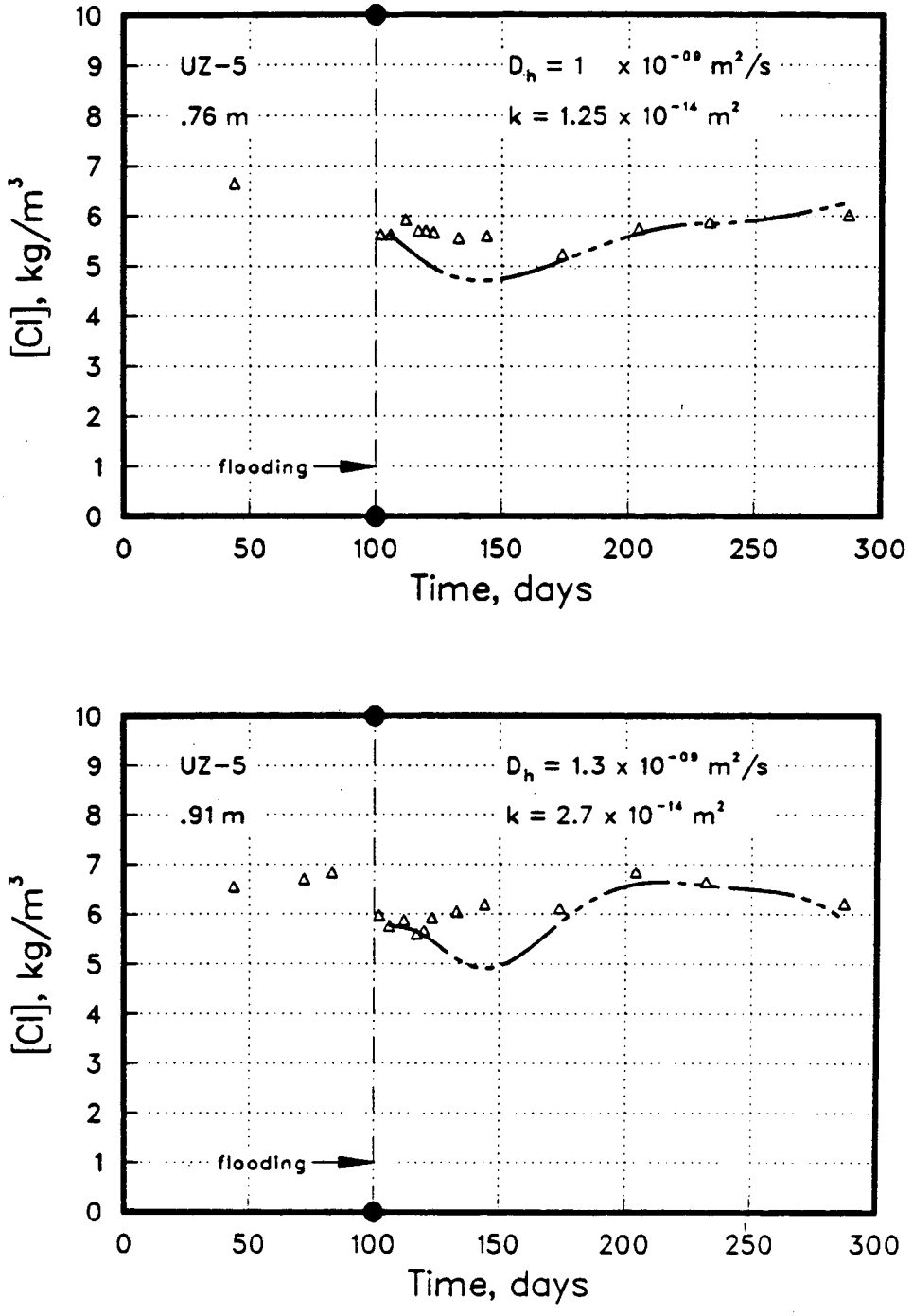

Figure 8.22 The results of the history-matching. Open triangles represent the observed data while the dashed line is model output.

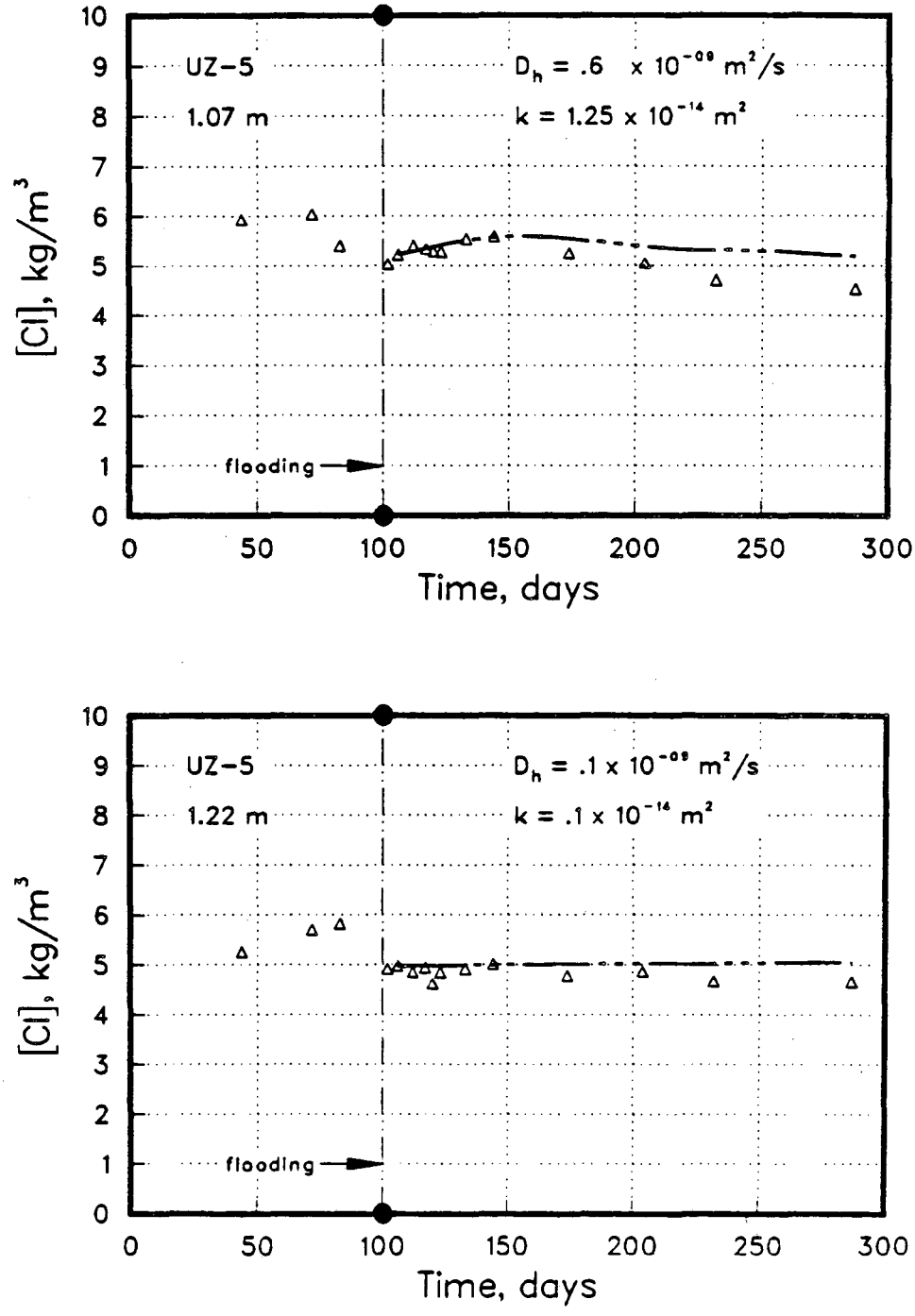

Figure 8.23 The results of the history-matching. Open triangles represent the observed data while the dashed line is model output.

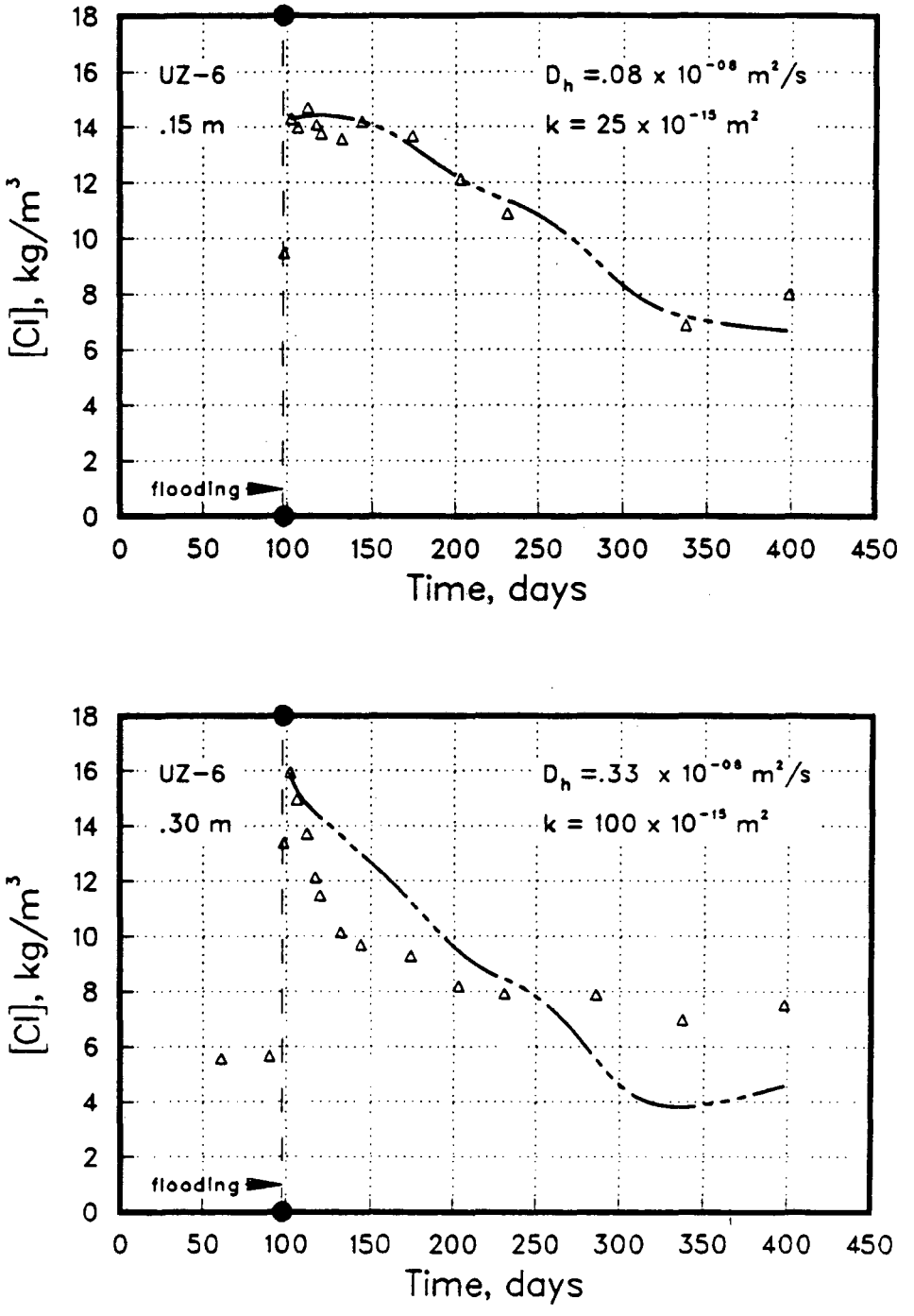

Figure 8.24 The results of the history-matching. Open triangles represent the observed data while the dashed line is model output.

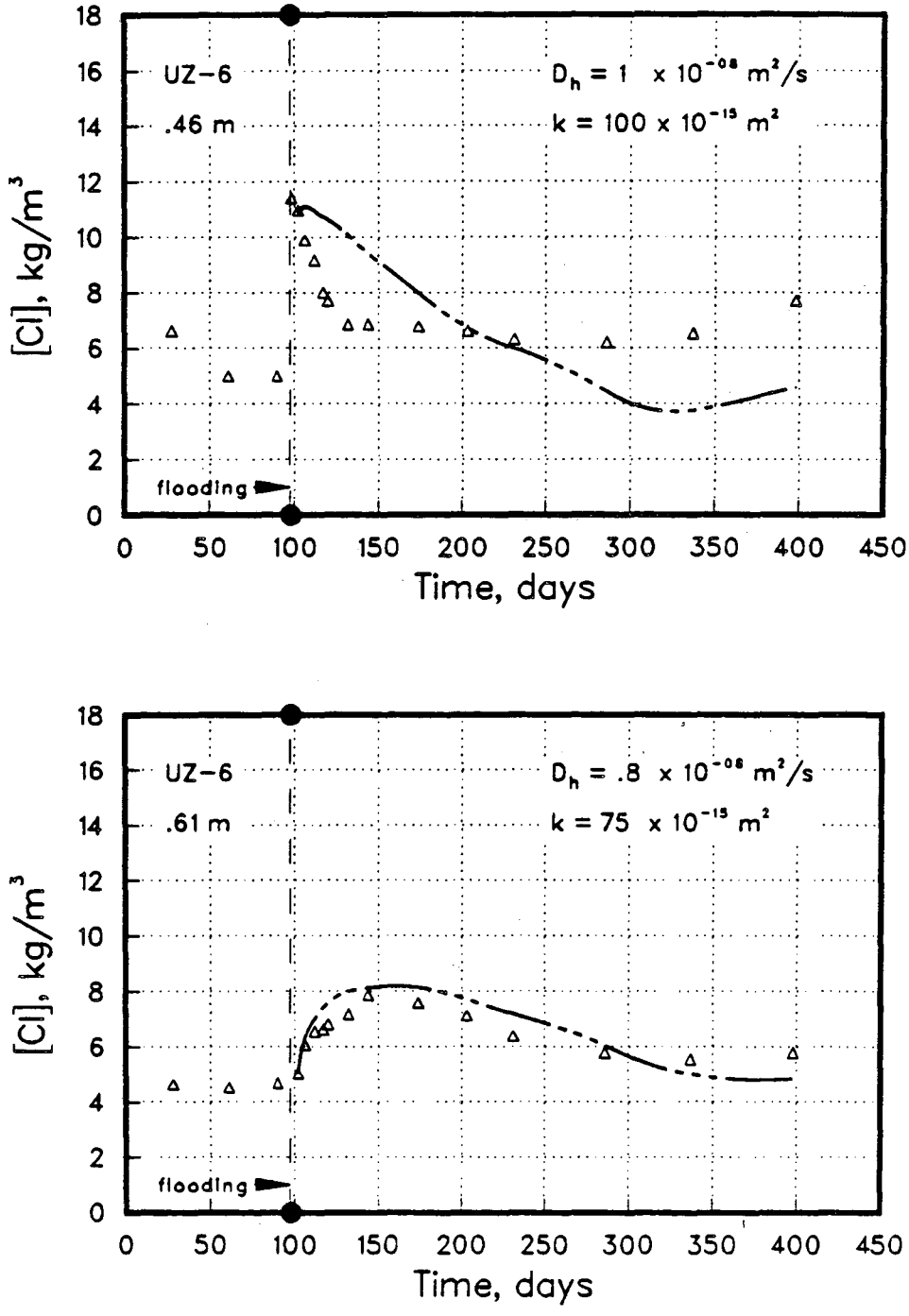

Figure 8.25 The results of the history-matching. Open triangles represent the observed data while the dashed line is model output.

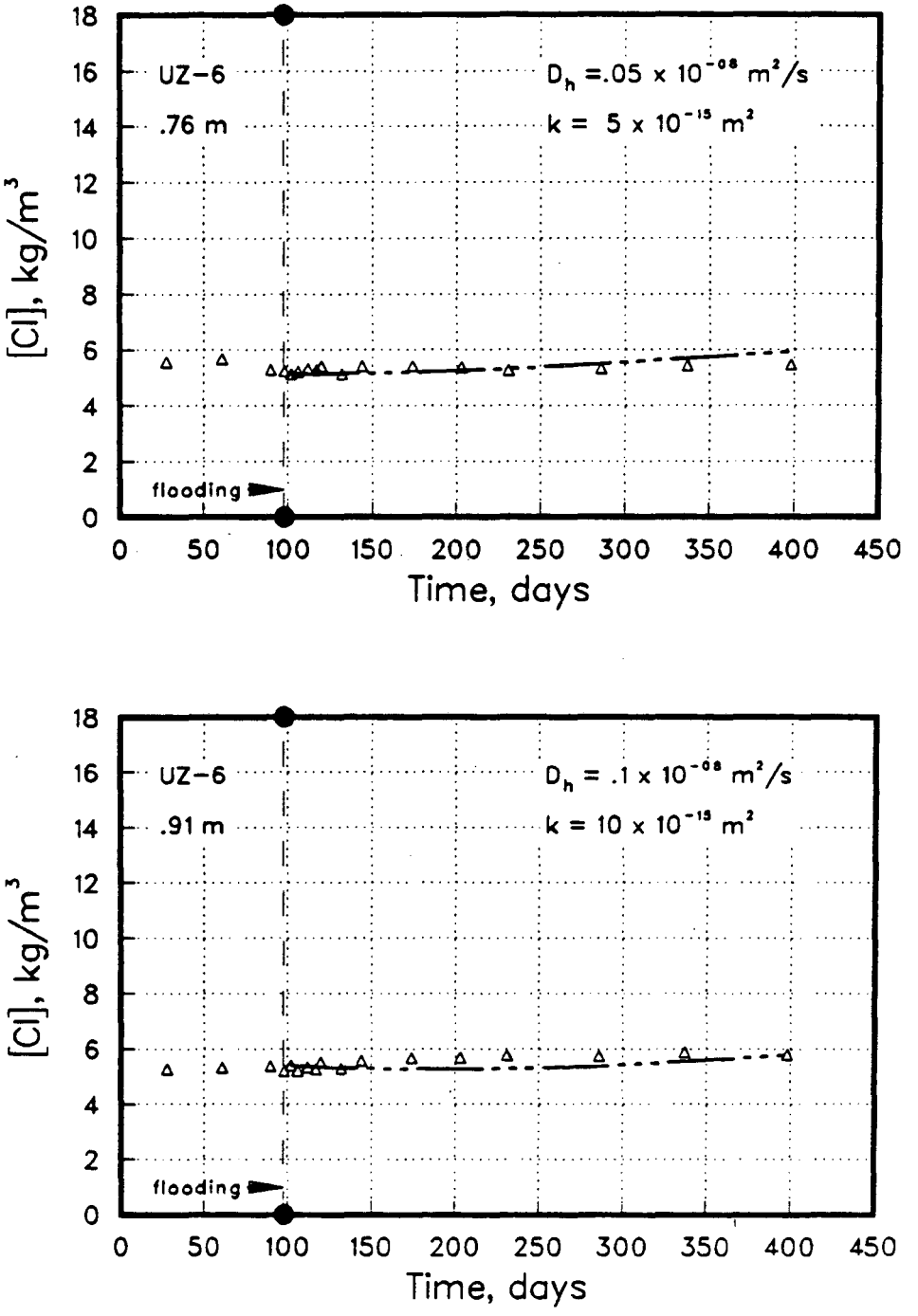

Figure 8.26 The results of the history-matching. Open triangles represent the observed data while the dashed line is model output.

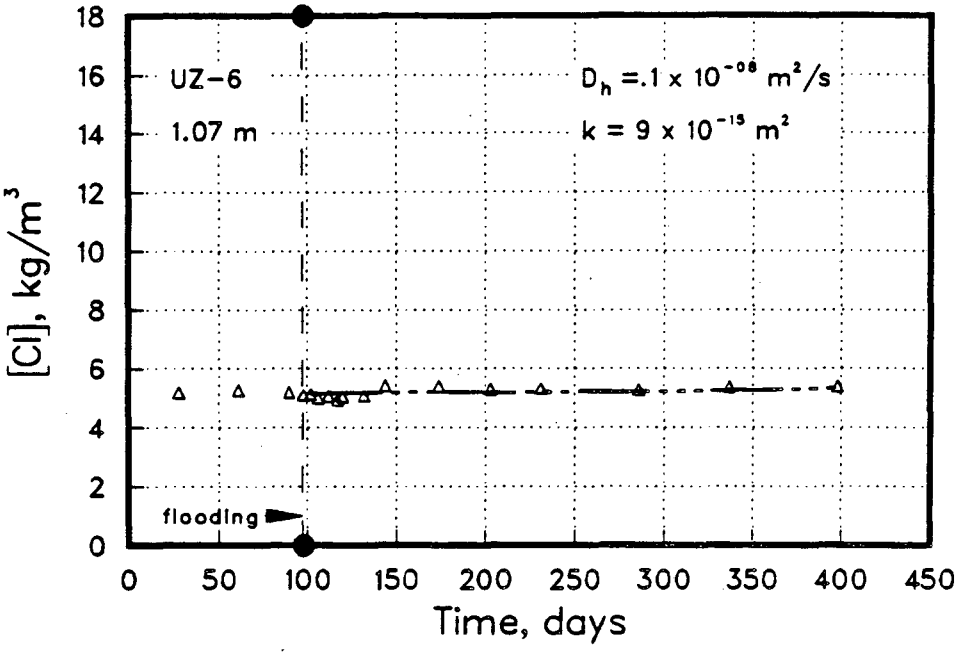

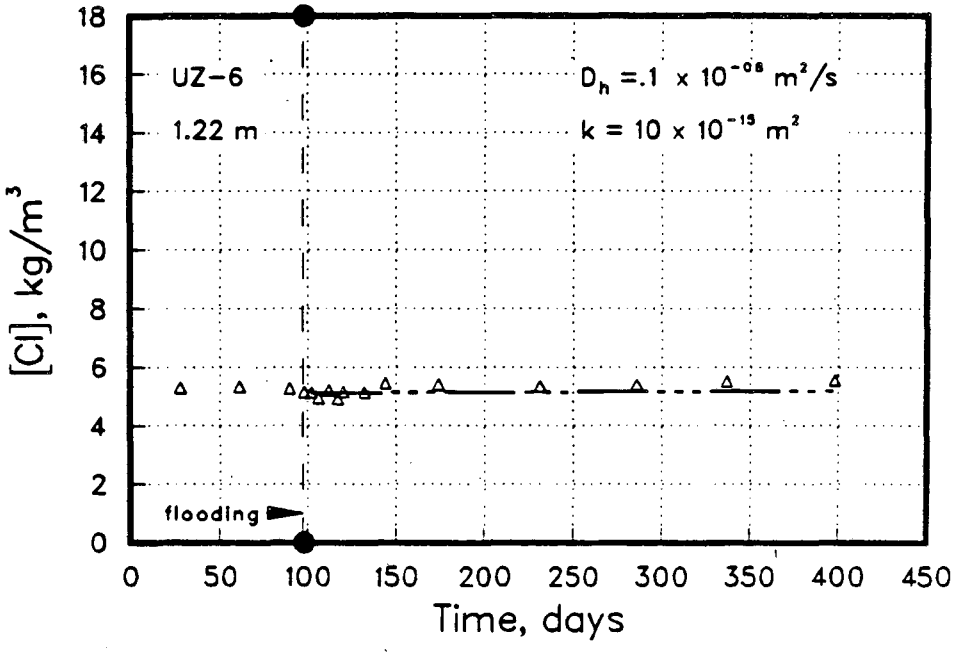

Figure 8.27 The results of the history-matching. Open triangles represent the observed data while the dashed line is model output.

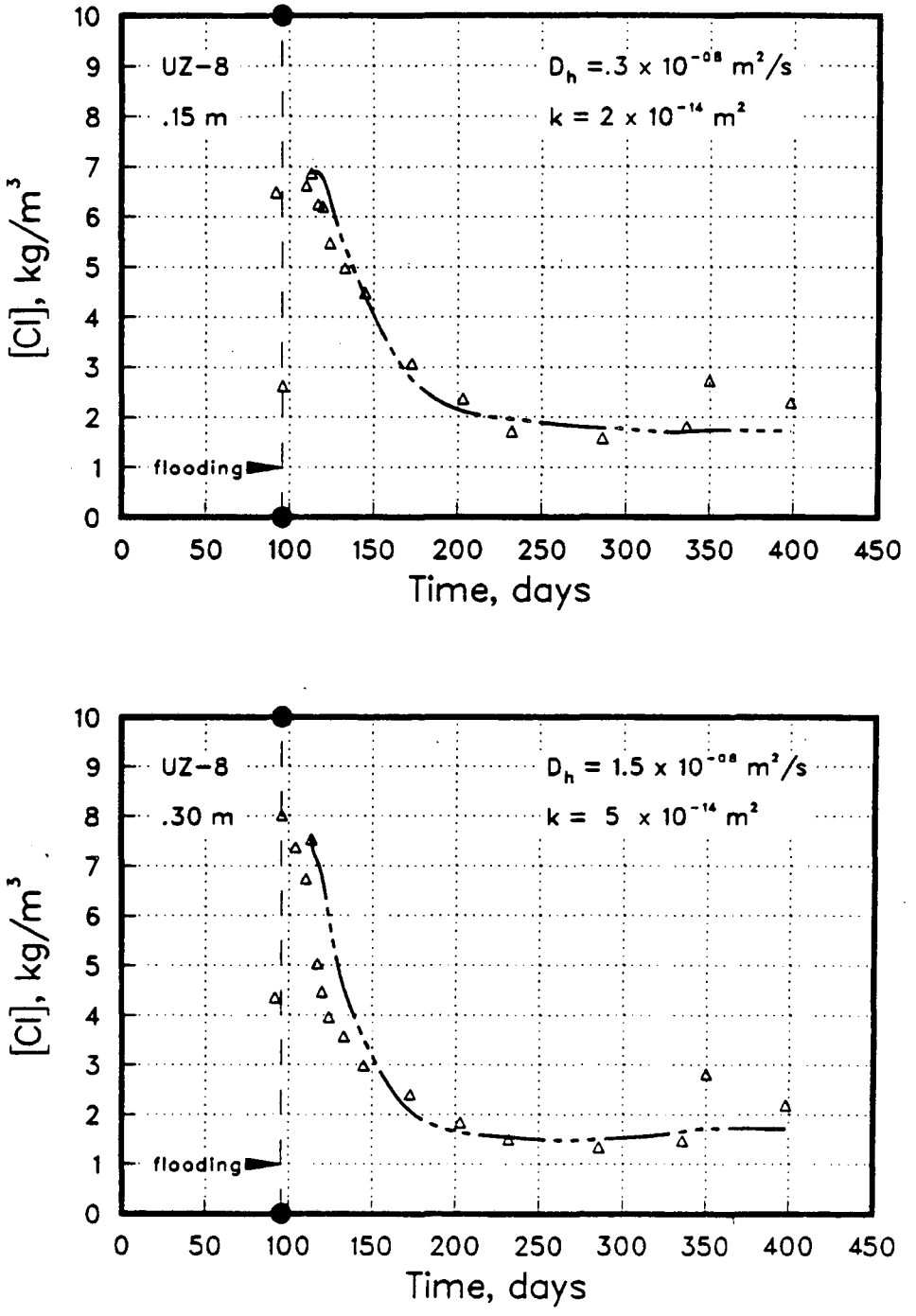

Figure 8.28 The results of the history-matching. Open triangles represent the observed data while the dashed line is model output.

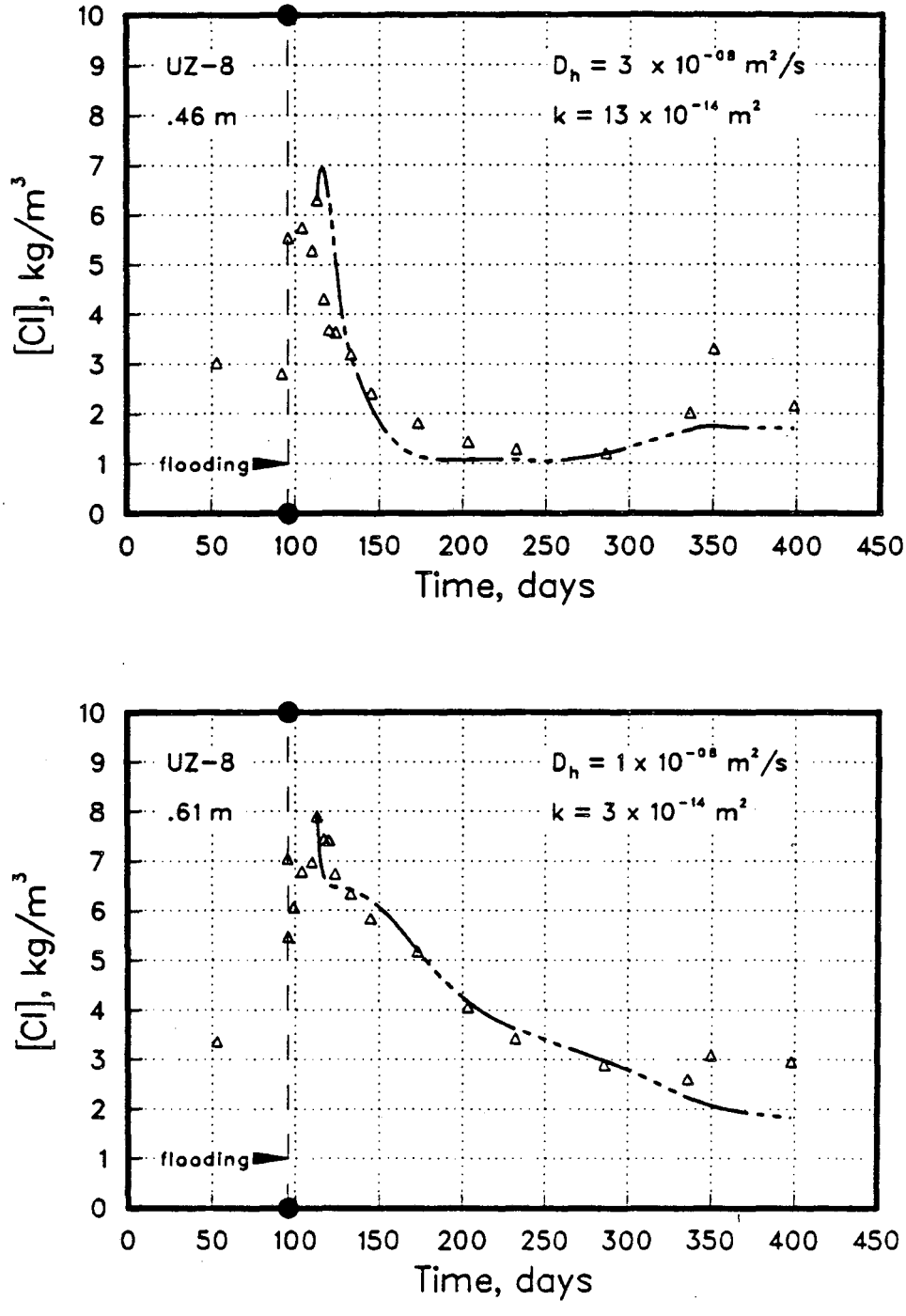

Figure 8.29 The results of the history-matching. Open triangles represent the observed data while the dashed line is model output.

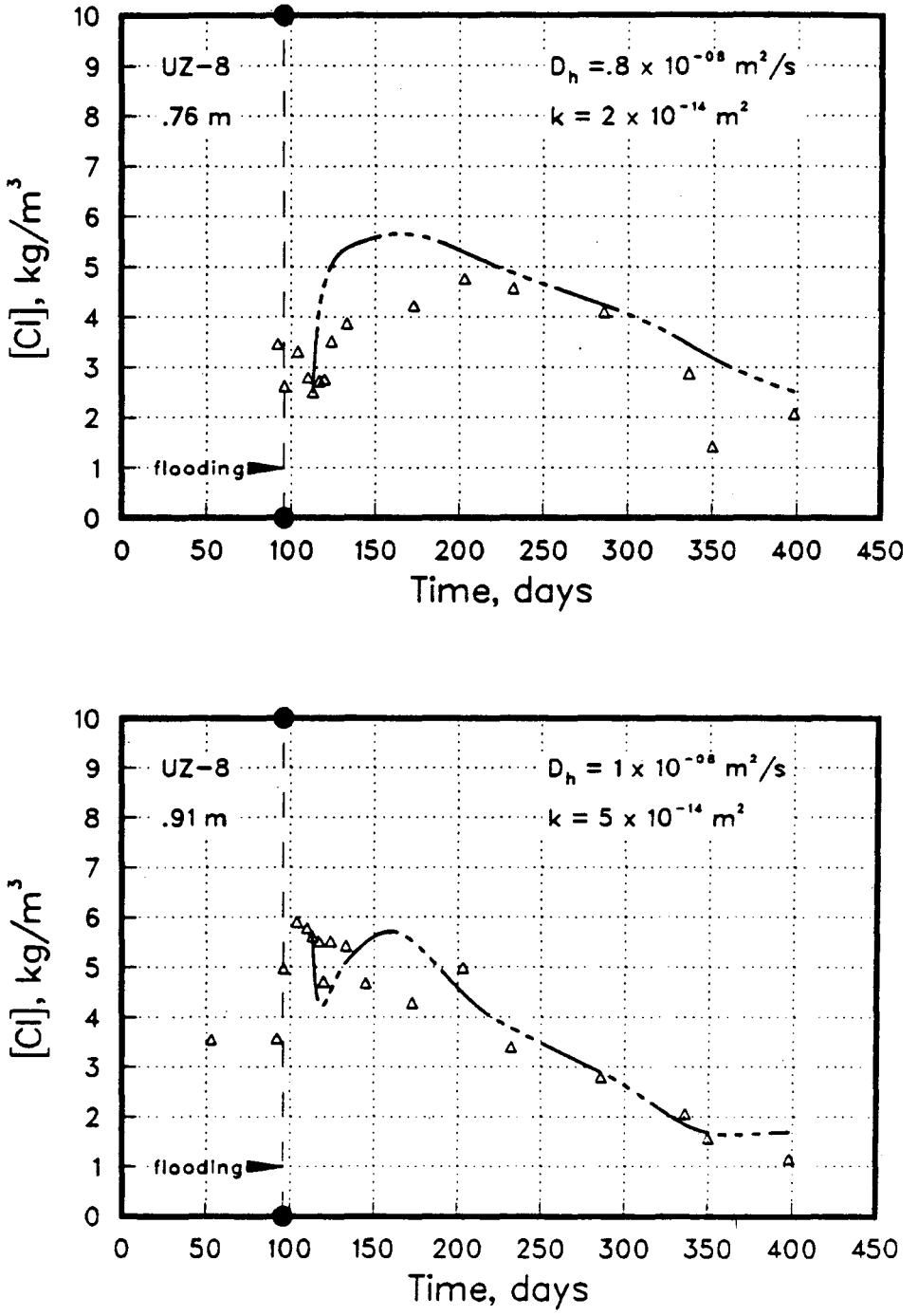

Figure 8.30 The results of the history-matching. Open triangles represent the observed data while the dashed line is model output.

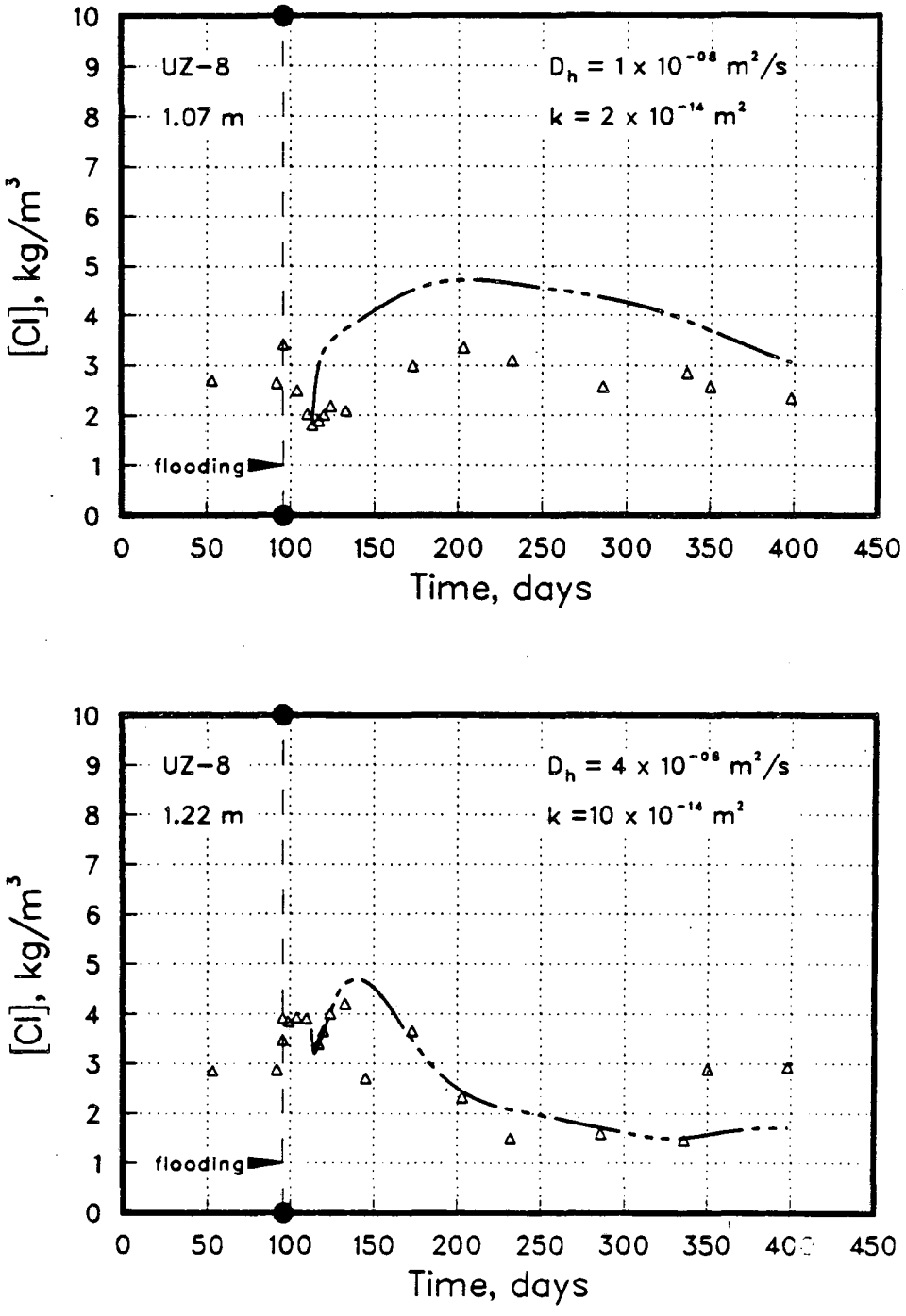

Figure 8.31 The results of the history-matching. Open triangles represent the observed data while the dashed line is model output.

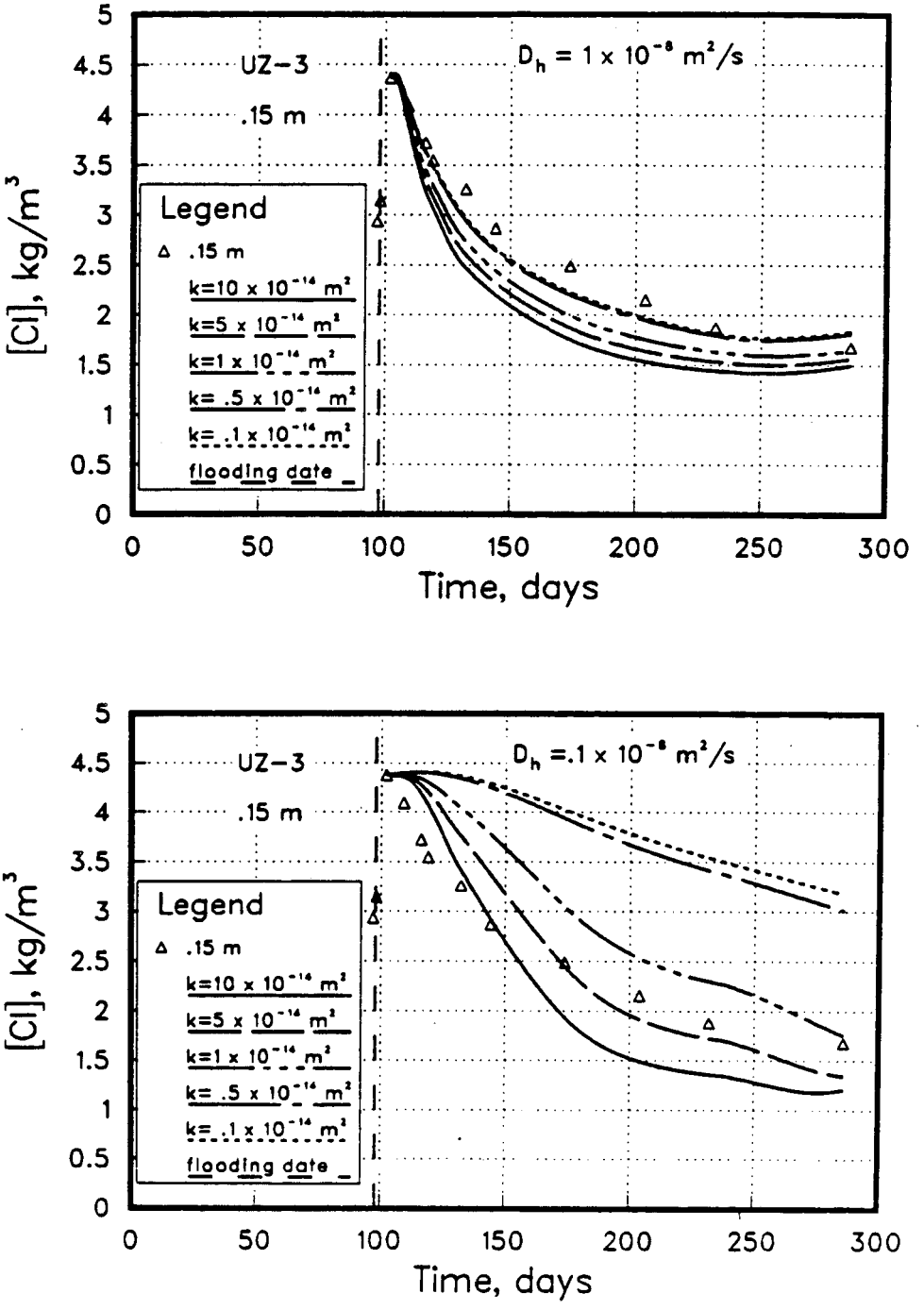

Figure 8.32 The relative effect of property variations in model output for the 0.15 m soil water sampler locations at UZ-3.

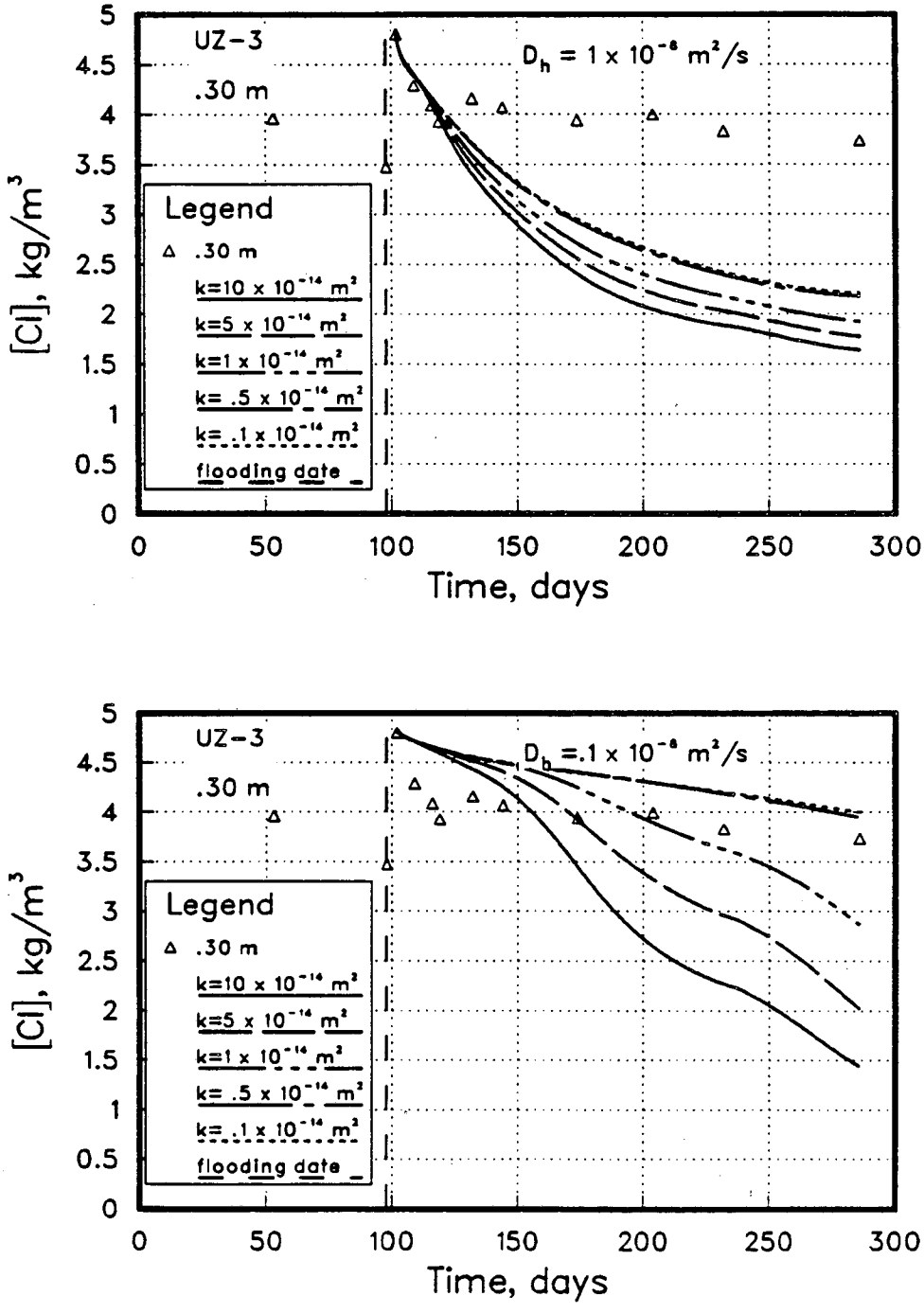

Figure 8.33 The relative effect of property variations in model output for the 0.30 m soil water sampler location at UZ-3.

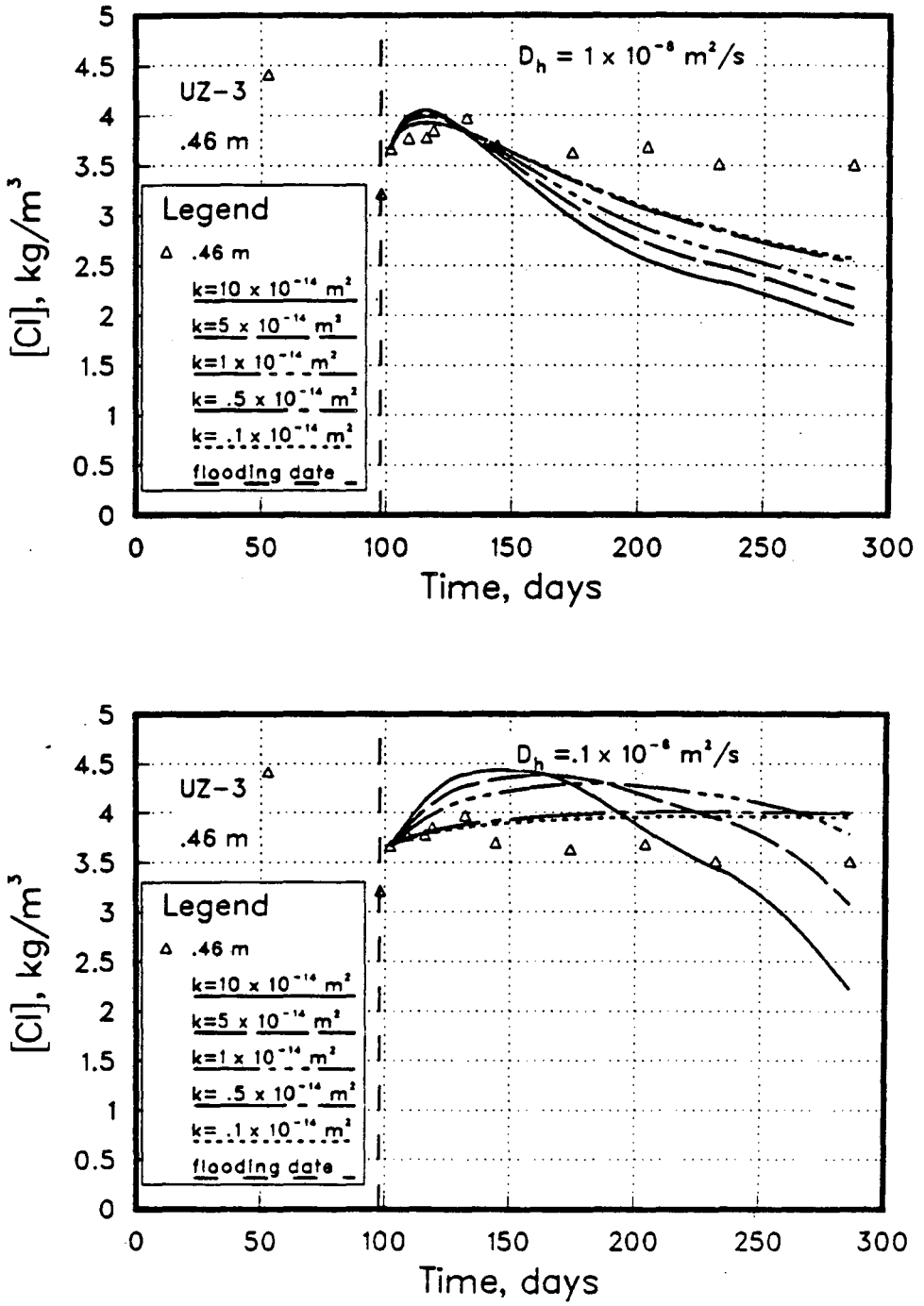

Figure 8.34 The relative effect of property variations in model output for the 0.46 m soil water sampler location at UZ-3.

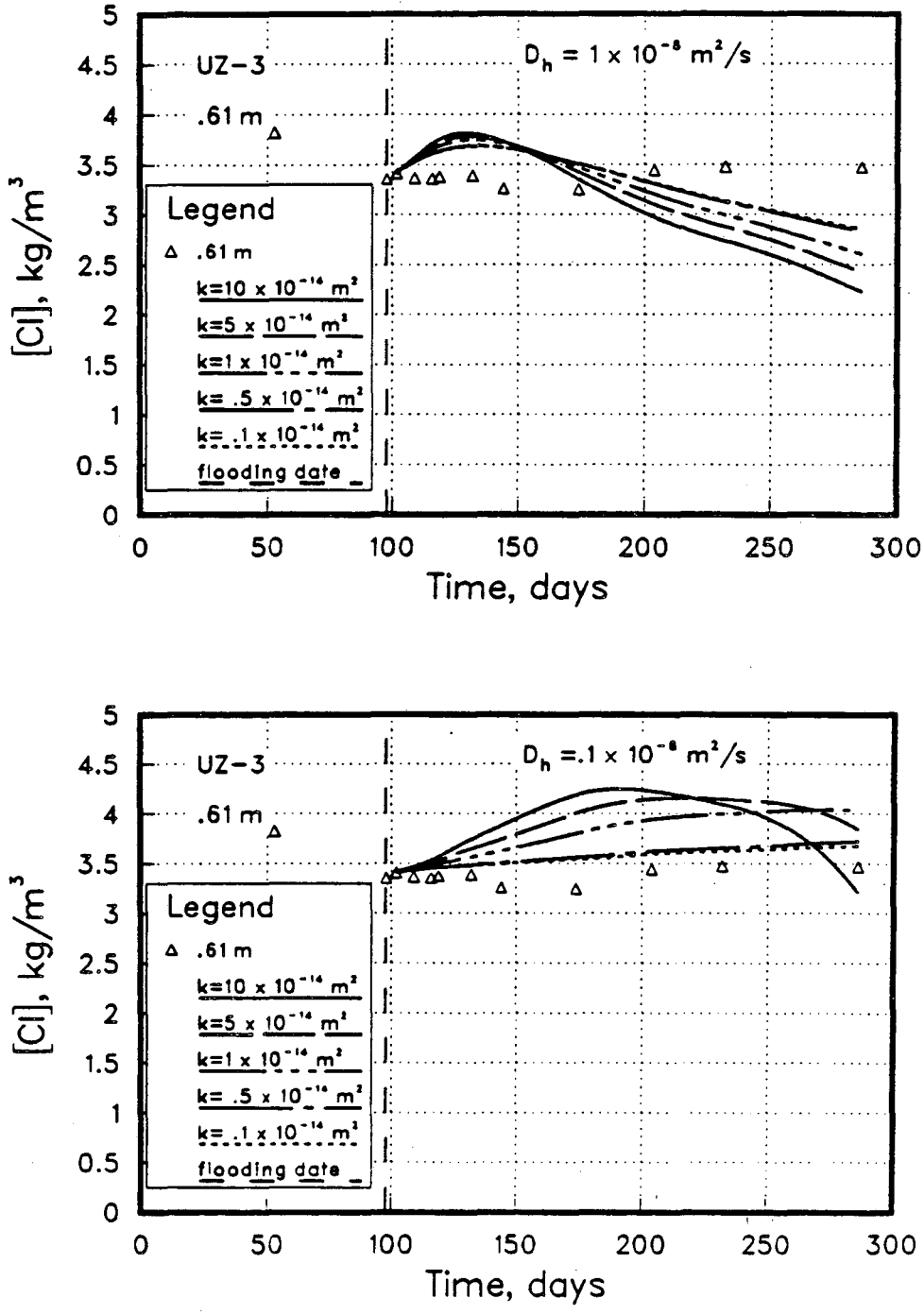

Figure 8.35 The relative effect of property variations in model output for the 0.61 m soil water sampler location at UZ-3.

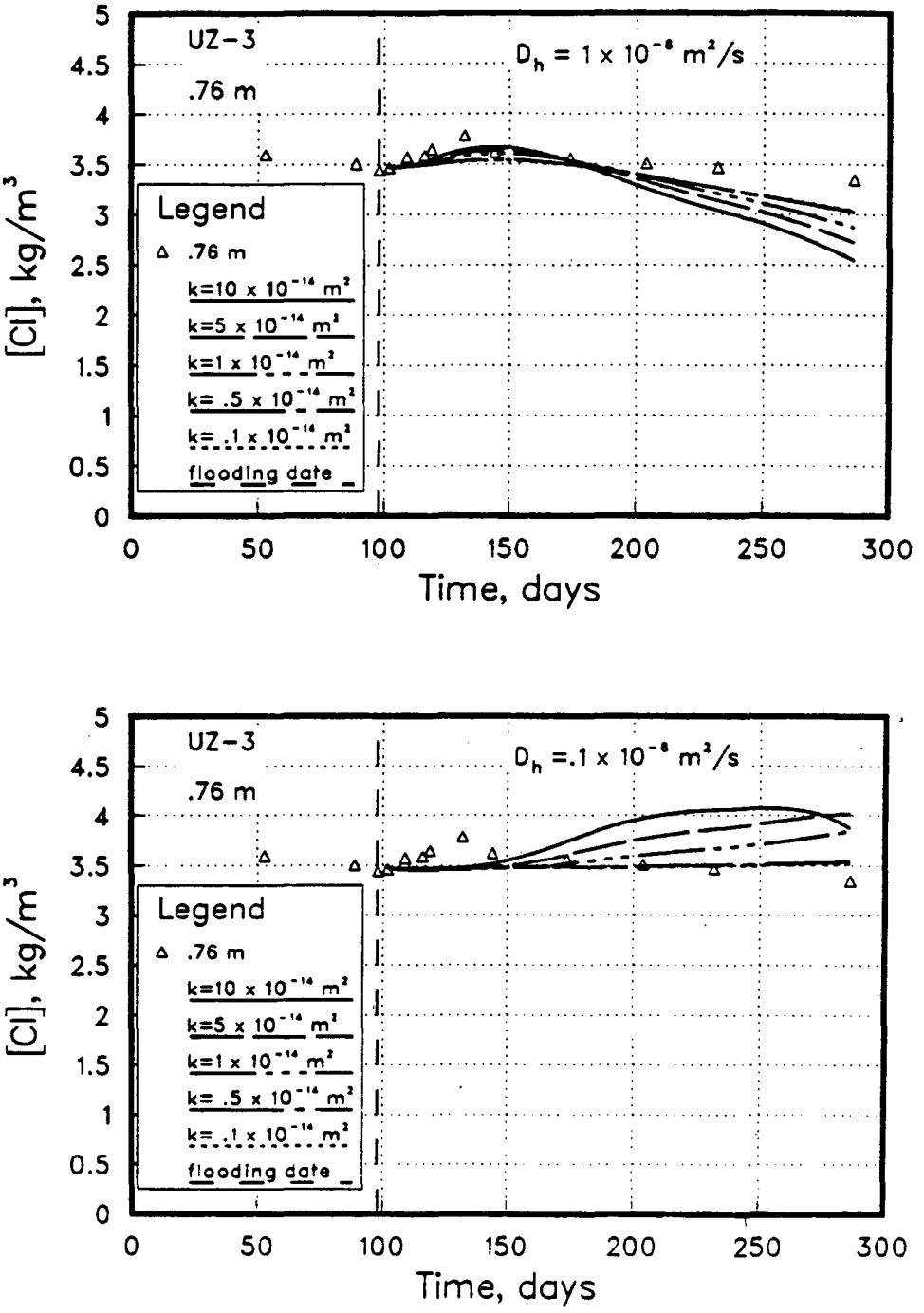

Figure 8.36 The relative effect of property variations in model output for the 0.76 m soil water sampler location at UZ-3.

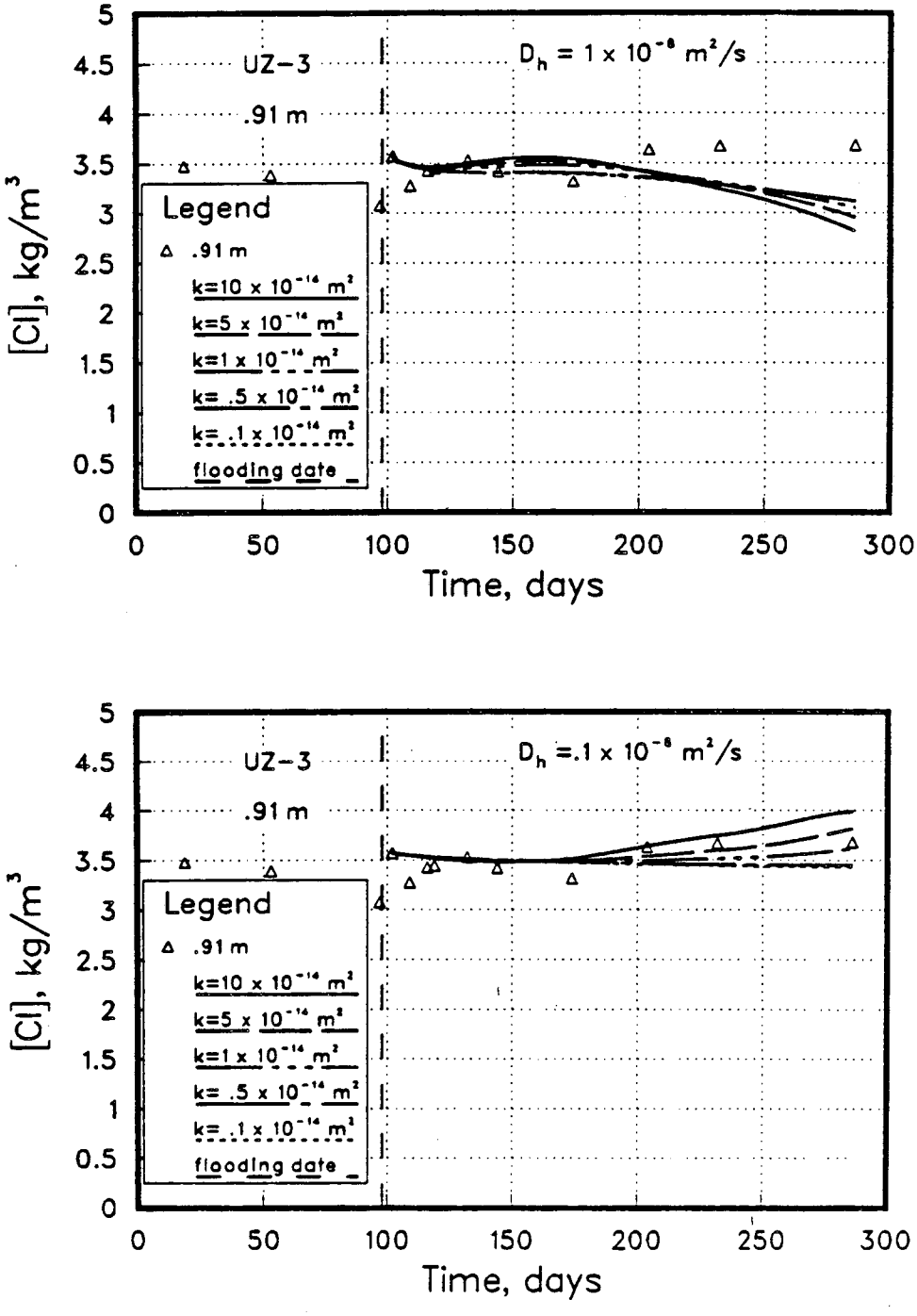

Figure 8.37 The relative effect of property variations in model output for the 0.91 m soil water sampler location at UZ-3.

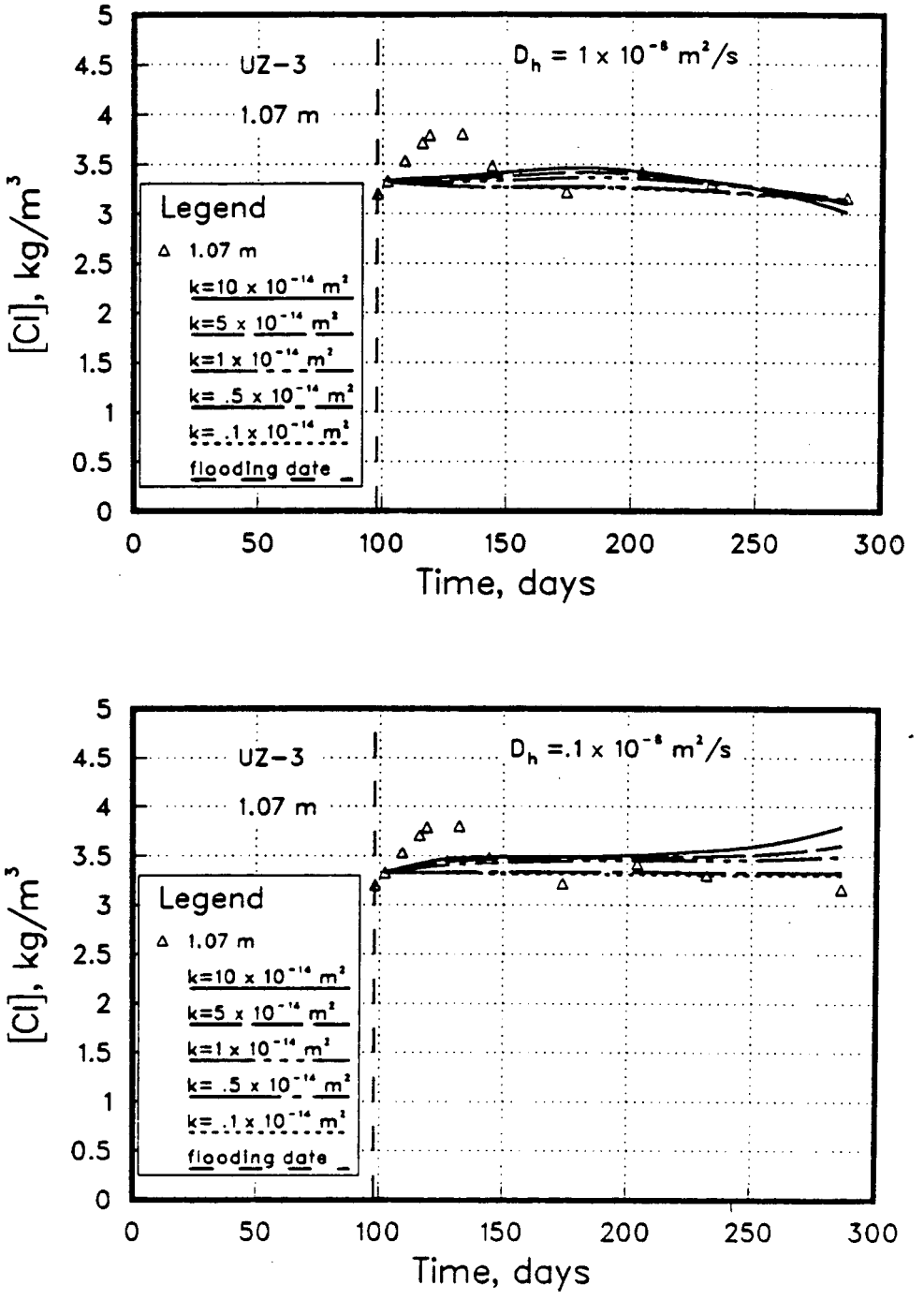

Figure 8.38 The relative effect of property variations in model output for the 1.07 m soil water sampler location at UZ-3.

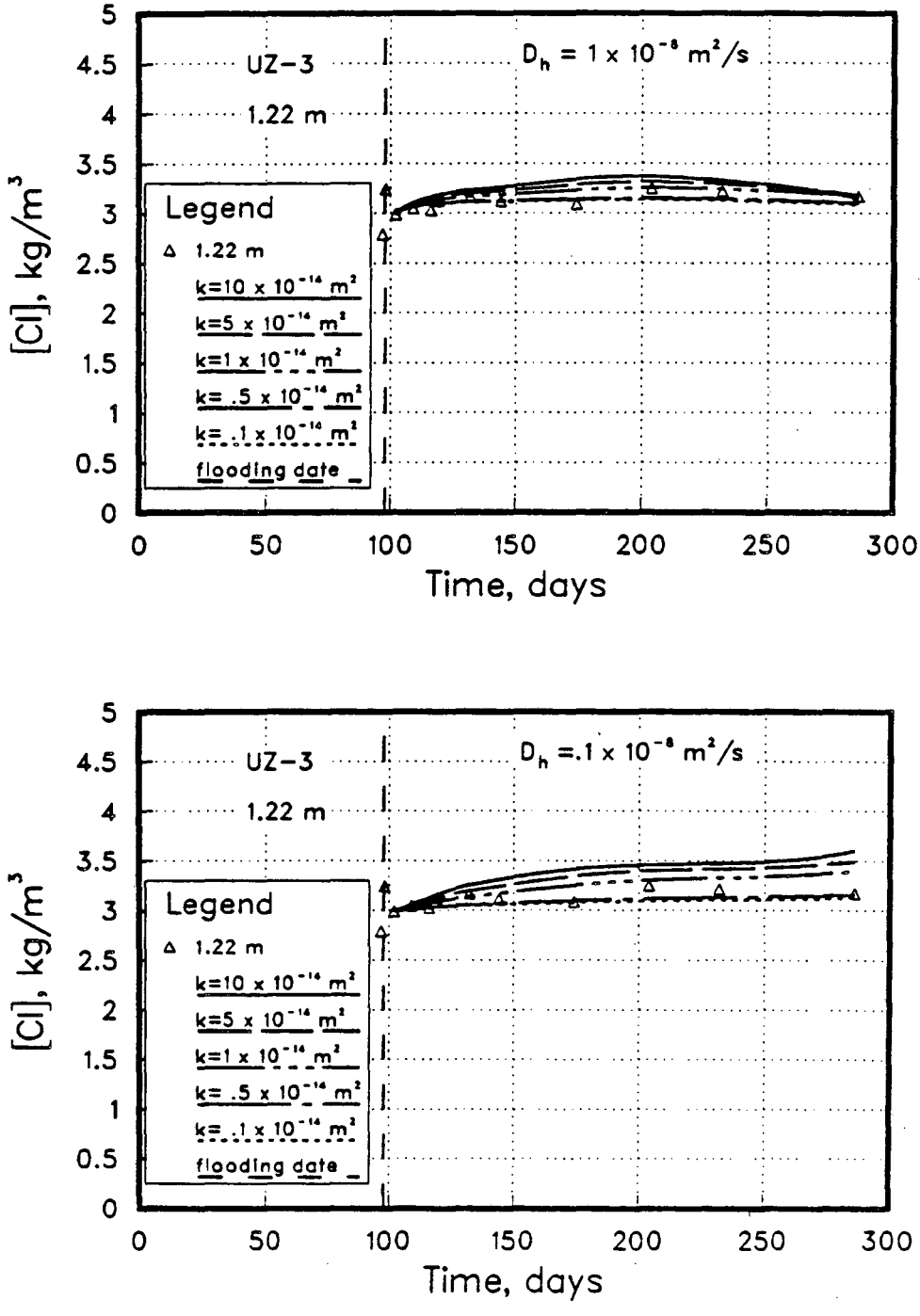

Figure 8.39 The relative effect of property variations in model output for the 1.22 m soil water sampler location at UZ-3.

the aid of *in situ* hydraulic conductivity measurements made at each site by Guelph permeameter. An attempt was made to minimize the magnitude of the dispersivity while maintaining the goodness-of-fit. This addition of judgement and utilization of existing data improved the uniqueness of the curve fits and allowed for results into which a much higher degree of confidence could be placed.

In the form that was available, CHAMP did not explicitly evaluate the dispersive fluxes separately from those due purely to molecular diffusion, but rather treated them together through one lumped parameter, the apparent dispersion coefficient, D_h. Therefore, dispersivities (α_l) were calculated assuming a linear relationship between D_h and v on the basis of the following expression, which is discussed in a later section:

$$\alpha_l = \frac{(D_h - D_e)}{\bar{v}} \tag{34}$$

where the effective coefficient of molecular diffusion was taken to be 1×10^{-11} m^2/s. This corresponds to $\tau = .01$. Since the average pore water velocity was not constant over the course of the experiment, due to the variable nature of the fluid potential boundary conditions, an effective average pore water velocity, $\bar{v}$, which represents an integrated average value over time of the linear pore velocity, was used in Eq. (34). This results in an approximation to the actual α_l. In Figure 8.40, measured gradients across the study zone are plotted vs time for each site. Since the gradient is linearly related to pore water velocity, this figure provides an indication of the degree to which pore water velocity may have varied throughout time. From the figure, it appears that the actual variation of pore water velocity was $\approx \pm 100\%$ of $\bar{v}$, at each site during the course of the experiment. D_h was treated as a constant, even though in reality it may have varied.

It should be noted that throughout this section, the parameter k or *intrinsic permeability* is used to describe the conductance property of the porous medium. k is a property only of the porous medium and has dimensions of L^2 while the more commonly used expression K or *hydraulic conductivity* ($L \cdot T^{-1}$) is a function of the fluid as well as the medium. In systems

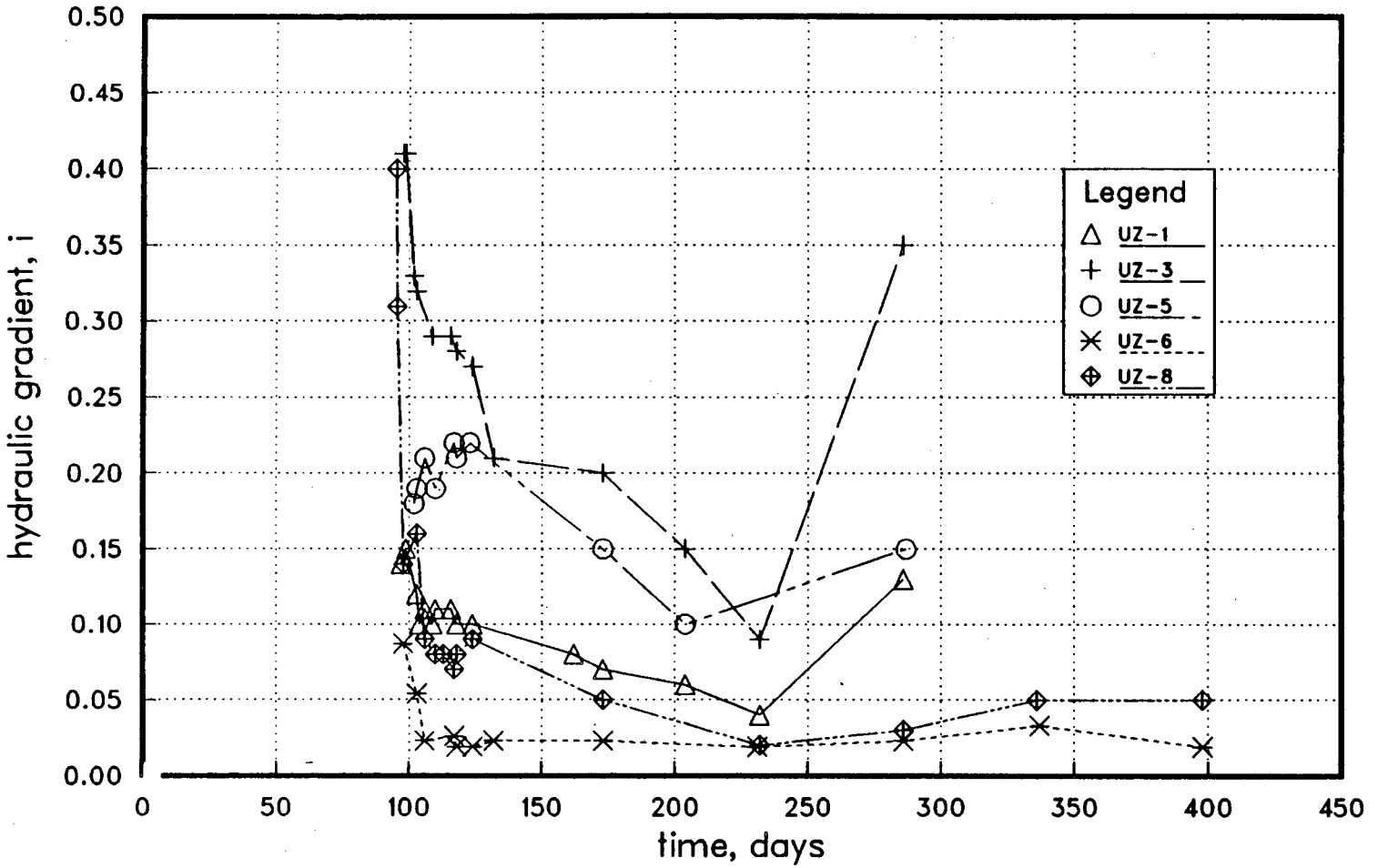

Figure 8.40 Fluid potential gradients measured at the five flooded sites throughout the period of ponding. Gradients were measured between the pond bottom surface and the shallow well located at each site.

where more than one fluid phase is present the use of k has obvious advantages, and it is widely used in the petroleum industry. In saturated systems the choice is purely arbitrary, and if we remember that

$$K = \frac{k\rho_f g}{\mu} \tag{35}$$

where ρ_f is the fluid density ($M \cdot L^{-3}$), g the acceleration of gravity ($L \cdot T^2$), and μ is the fluid viscosity ($M \cdot L^{-1} \cdot T^{-1}$), all of which can be taken as constants for practical purposes, then the conversion is easily made by K (m/s) $\approx 10^7 \cdot k$ (m^2).

9. RESULTS AND DISCUSSION

9.1. k and D_h

A summary of properties determined in the modeling effort is presented in Table 6 including values of k, D_h, v, and α_l. The arithmetic mean average pore water velocity of all 40 locations is 1.13 m/yr (3.7 ft/yr) varying from a low, based on plot averages of .3 m/yr (1 ft/yr) to 3.11 m/yr (10.2 ft/yr). For k an arithmetic mean value of 2.6 x 10^{-14} m^2 is calculated. This value of k corresponds to a saturated hydraulic conductivity of 8 m/yr (26 ft/yr). Average k values calculated in this manner at each site are within an order of magnitude, both above and below, of *in situ* k measurements made by Guelph permeameter prior to flooding *(Lawrence Berkeley Laboratory,* 1986c p. 32) and are within range of a series of ring infiltrometer measurements made by *Luthin* (1966).

Table 6. *Summary of Parameters Determined*

Site	Depth, m	pore water velocity, m/s	k, m^2	$\ln(k)$	D_h, m^2/s	$\ln(D_h)$	α_l, m	Pe_l
UZ-1	0.15	0.186×10^{-7}	1.1×10^{-14}	-32.14	0.50×10^{-9}	-21.42	0.03	0.93
	0.30	0.506×10^{-7}	3.0×10^{-14}	-31.14	2.50×10^{-9}	-21.42	0.05	0.51
	0.46	0.169×10^{-6}	10.0×10^{-14}	-29.93	1.00×10^{-9}	-20.72	0.01	4.23
	0.61	0.843×10^{-8}	0.5×10^{-14}	-32.93	0.50×10^{-9}	-21.42	0.06	0.42
	0.76	0.413×10^{-9}	0.025×10^{-14}	-35.93	0.01×10^{-9}	-25.33	0.001	1.03
	0.91	0.338×10^{-8}	0.2×10^{-14}	-33.85	0.20×10^{-9}	-22.33	0.06	0.42
	1.07	0.169×10^{-8}	0.1×10^{-14}	-34.54	0.10×10^{-9}	-23.03	0.05	0.42
	1.22	0.338×10^{-8}	0.2×10^{-14}	-34.54	0.20×10^{-9}	-21.42	0.06	0.42
UZ-3	0.15	0.241×10^{-7}	0.70×10^{-14}	-32.59	2.0×10^{-9}	-20.03	0.08	0.30
	0.30	0.138×10^{-7}	0.40×10^{-14}	-33.15	0.5×10^{-9}	-21.42	0.04	0.69
	0.46	0.138×10^{-7}	0.40×10^{-14}	-33.15	2.0×10^{-9}	-20.03	0.14	0.17
	0.61	0.863×10^{-9}	0.025×10^{-14}	-35.93	0.1×10^{-9}	-23.03	0.10	0.22
	0.76	0.207×10^{-7}	0.60×10^{-14}	-32.75	4.0×10^{-9}	-19.34	0.19	0.13
	0.91	0.259×10^{-7}	0.75×10^{-14}	-32.52	2.5×10^{-9}	-19.81	0.10	0.26
	1.07	0.345×10^{-7}	1.00×10^{-14}	-32.24	8.0×10^{-9}	-18.64	0.23	0.11
	1.22	0.259×10^{-7}	0.75×10^{-14}	-32.52	9.0×10^{-9}	-18.53	0.35	0.07
UZ-5	0.15	0.177×10^{-7}	1.00×10^{-14}	-32.24	0.75×10^{-9}	-21.01	0.04	0.59
	0.30	0.160×10^{-7}	0.90×10^{-14}	-32.34	0.90×10^{-9}	-20.83	0.06	0.44
	0.46	0.177×10^{-7}	1.00×10^{-14}	-32.24	1.20×10^{-9}	-20.54	0.07	0.37
	0.61	0.532×10^{-8}	0.30×10^{-14}	-33.44	0.10×10^{-9}	-23.03	0.02	1.33
	0.76	0.222×10^{-7}	1.25×10^{-14}	-32.01	1.00×10^{-9}	-20.72	0.05	0.55
	0.91	0.479×10^{-7}	2.70×10^{-14}	-31.24	1.30×10^{-9}	-20.46	0.03	0.92
	1.07	0.222×10^{-7}	1.25×10^{-14}	-32.01	0.60×10^{-9}	-21.23	0.03	0.92
	1.22	0.177×10^{-8}	0.10×10^{-14}	-34.54	0.10×10^{-9}	-23.03	0.05	0.44
UZ-6	0.15	0.561×10^{-8}	2.5×10^{-14}	-31.32	0.8×10^{-9}	-20.95	0.14	0.18
	0.30	0.225×10^{-7}	10.0×10^{-14}	-29.93	3.3×10^{-9}	-19.53	0.15	0.17
	0.46	0.224×10^{-7}	10.0×10^{-14}	-29.93	10.0×10^{-9}	-18.42	0.44	0.06
	0.61	0.168×10^{-7}	7.5×10^{-14}	-30.22	8.0×10^{-9}	-18.64	0.47	0.05
	0.76	0.112×10^{-8}	0.5×10^{-14}	-32.93	0.5×10^{-9}	-21.42	0.44	0.06
	0.91	0.225×10^{-8}	1.0×10^{-14}	-32.24	1.0×10^{-9}	-20.72	0.44	0.06
	1.07	0.202×10^{-8}	0.9×10^{-14}	-32.34	1.0×10^{-9}	-20.72	0.49	0.05
	1.22	0.225×10^{-8}	1.0×10^{-14}	-32.24	1.0×10^{-9}	-20.72	0.44	0.06
UZ-8	0.15	0.376×10^{-7}	$2. \times 10^{-14}$	-31.54	3.0×10^{-9}	-19.62	0.08	0.31
	0.30	0.940×10^{-7}	$5. \times 10^{-14}$	-30.63	15.0×10^{-9}	-18.01	0.16	0.16
	0.46	0.244×10^{-6}	$13. \times 10^{-14}$	-29.67	30.0×10^{-9}	-17.32	0.12	0.20
	0.61	0.564×10^{-7}	$3. \times 10^{-14}$	-31.14	10.0×10^{-9}	-18.42	0.18	0.14
	0.76	0.376×10^{-7}	$2. \times 10^{-14}$	-31.54	8.0×10^{-9}	-18.64	0.21	0.12
	0.91	0.940×10^{-7}	$5. \times 10^{-14}$	-30.63	10.0×10^{-9}	-18.42	0.11	0.23
	1.07	0.376×10^{-7}	$2. \times 10^{-14}$	-31.54	10.0×10^{-9}	-18.42	0.27	0.09
	1.22	0.188×10^{-6}	$10. \times 10^{-14}$	-29.93	40.0×10^{-9}	-17.03	0.21	0.12

A high degree of spatial variability is evident throughout the field. Permeabilities pond-wide vary by nearly 3 orders of magnitude from a high of 10×10^{-14} m^2 to a low of $.025 \times 10^{-14}$ m^2 while apparent dispersion coefficients fluctuate similarly. Within plots, heterogeneity is not as pronounced yet it is still exhibited to a significant extent. Values of k

determined at site UZ-1 suggest that pore water velocities at one location in the plot are 100 times the pore water velocities at locations positioned just a meter laterally away. At other sites as well, one to nearly two orders of magnitude is a typical range over which k and D_h are shown to vary. Because soil structure and pore geometry may exhibit a high degree of spatial variability, even at the local scale, it is not unlikely that other parameters, such as k and D_h, could also display such heterogeneity.

To determine the form of the population density function that best describes the distribution of k and D_h, the method as presented in *Warrick and Nielsen* (1980), has been applied to the data where fractile diagrams are generated based on the normal density function. The 40 values of k and D_h are listed in ascending order from $i = 1$ to $i = 40$ and the cumulative distribution function, P(x), is calculated as $i/40$. Corresponding values of the probability units, $(x - \mu)\sigma^{-1}$, where x represents the actual value of k and D_h, μ is the mean value of x, and σ is the standard deviation, are then obtained from tabular values of the cumulative normal distribution. This procedure is also performed in the same fashion using natural logarithms of x where μ and σ are now the mean and standard deviation of ln(x). The linearity of the ln(k) and ln(D_h) plots in Figure 9.1 demonstrates that a log-normal distribution best describes the variations of the two parameters.

In Figure 9.2 is shown the relative-frequency curves of ln(k) and ln(D_h) plotted with the theoretical distribution based on fitting the 40 values of ln(x) to the frequency density function for a normal distribution:

$$N(x;\mu;\sigma) = \frac{1}{\sigma\sqrt{2\pi}} e^{\frac{-(\ln(x)-\mu)^2}{2\sigma^2}} \qquad (36)$$

where μ and σ are based on the set of values ln(x). Data points plotted represent the number of observations of ln(x) that were observed to fall within a certain class width. In Figure 9.3 we see histograms of the observed values of k and D_h with the theoretical relative-frequency curve based on a log-normal distribution. The idealized distribution is an approximation and does not exactly match the observed values. A chi-square goodness-of-fit test has been

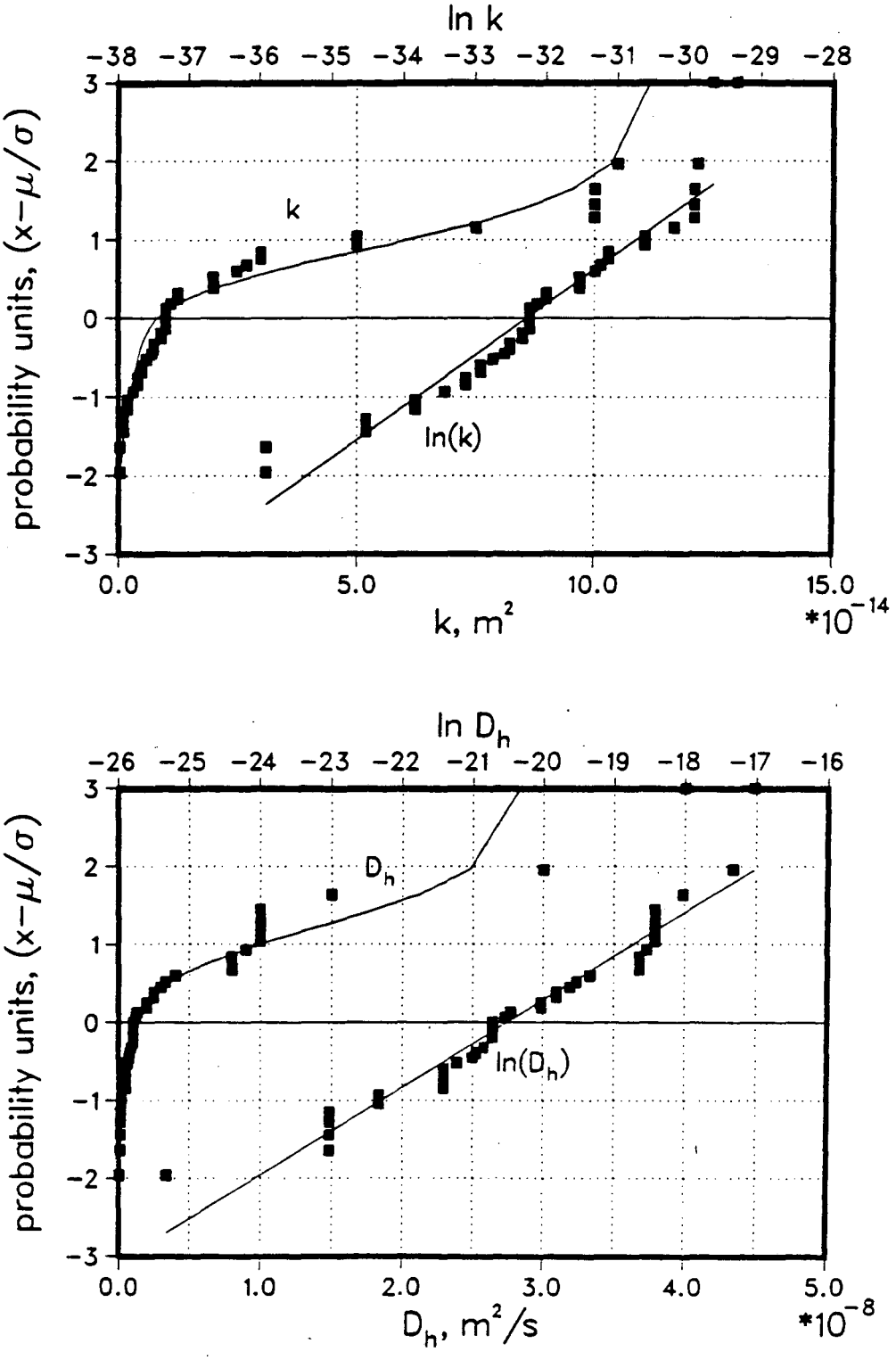

Figure 9.1 Fractile diagrams for permeability and apparent dispersion coefficient values determined in the history-matching. The linearity of the ln(k) and $\ln(D_h)$ suggests that the distribution of k and D_h is best described by a log-normal density. function.

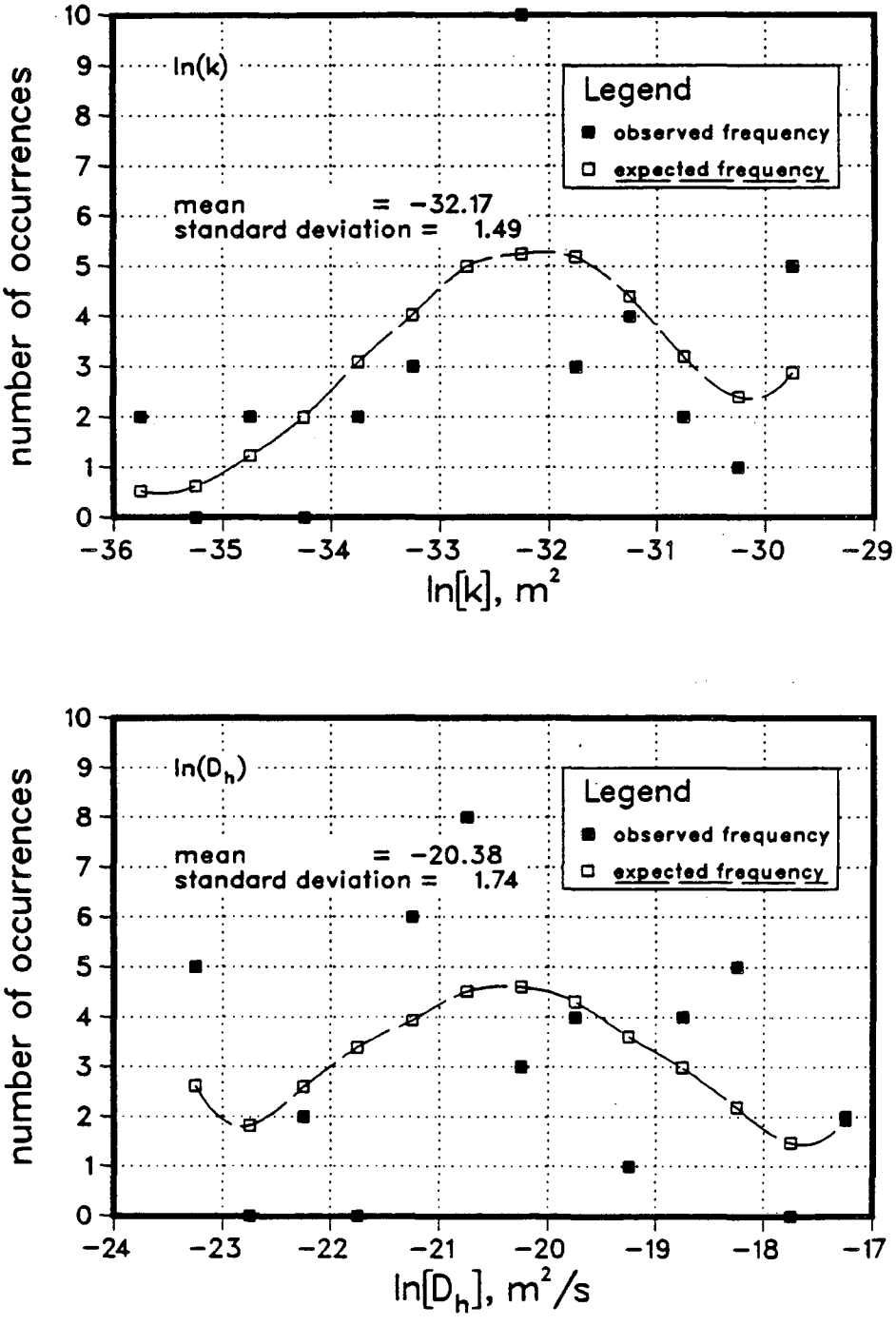

Figure 9.2 Frequency distributions of the observed values of permeability and apparent dispersion coefficient and the theoretical values based on the log-normal distribution.

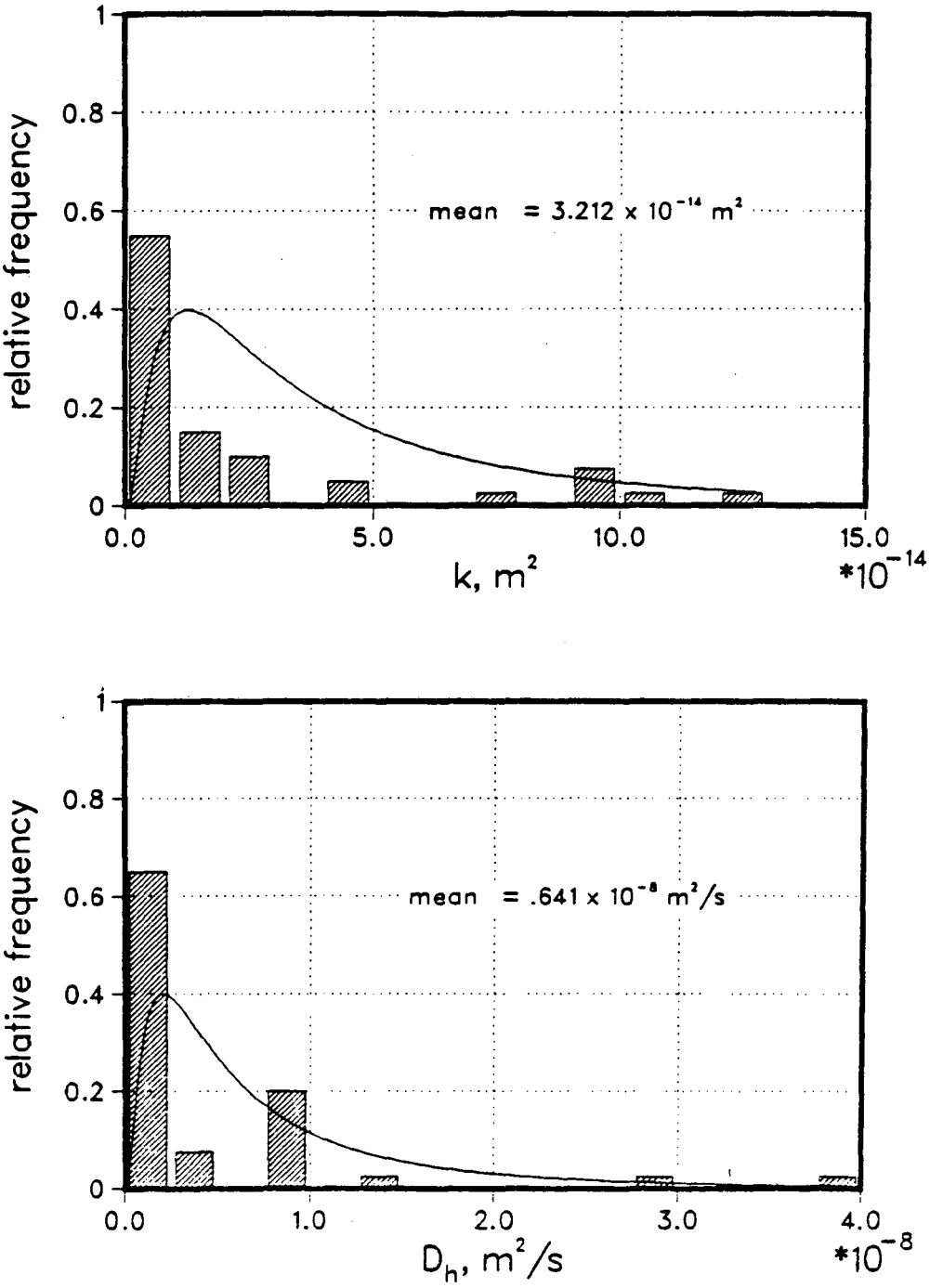

Figure 9.3 Histograms of the observed values of k and D_h with the theoretical log-normal distribution.

applied to both the k and D_h distributions to determine the agreement between the observed and the theoretical log-normal distribution. k and D_h both pass the test at the 5% significance level suggesting that, from the basis of this test, there is no reason to reject the hypothesis of a log-normally distributed population. It may be possible, however, to also consider other distributions i.e. the Gamma distribution.

In a log-normal distribution the mean is defined as $\mu_l = e^{(\mu+.5\sigma^2)}$, and the variance as $\sigma_l^2 = e^{(\sigma^2+2\mu)}(e^{\sigma^2}-1)$ where μ and σ are based on the set ln(x) *(Biggar and Nielsen,* 1976). For k, we have a mean value of 3.2×10^{-14} m^2 with a standard deviation of 9.14×10^{-14}. The arithmetic mean k calculated above is 20% lower than this value. For D_h, a mean value of 6.41×10^{-9} m^2/s is calculated with a standard deviation of 28.3×10^{-9}. The coefficient of variance (CV) is a parameter often used as a measure of relative variability and is defined as:

$$CV = \frac{\sigma_l}{\mu_l} \cdot 100\% \tag{37}$$

For k and D_h the CV values are both relatively high, 290% and 440% respectively, suggestive of a large degree of variability. For comparison, CV values for some soil parameters, i.e. bulk density, are often below 10% *(Warrick and Nielsen,* 1980).

In Figure 9.4, we see the effect of sample number on the measure of uncertainty by plotting number of samples vs the 95% confidence interval for k and D_h. This analysis assumes a measure of the sample mean and variance and can be calculated as,

$$-\mu_l - t_{\frac{\alpha}{2}(n-1)} \frac{\sigma_l}{\sqrt{n}} \leq \mu_l \leq \mu_l + t_{\frac{\alpha}{2}(n-1)} \frac{\sigma_l}{\sqrt{n}} \tag{38}$$

where μ_l and σ_l are calculated as above. The expression, $t_{\alpha/2(n-1)}$, refers to the t distribution with n-1 degrees of freedom at the $1-\alpha$ confidence interval. The figure indicates that to obtain an estimate of k within an order of magnitude of the true mean, 10 soil water samplers would be required, within ±100% 50 samplers would be needed; 150 measurements would estimate k within ±50% of its true value. A similar calculation performed on D_h indicates that 20 samplers would yield an estimate within an order of magnitude, 100 would be

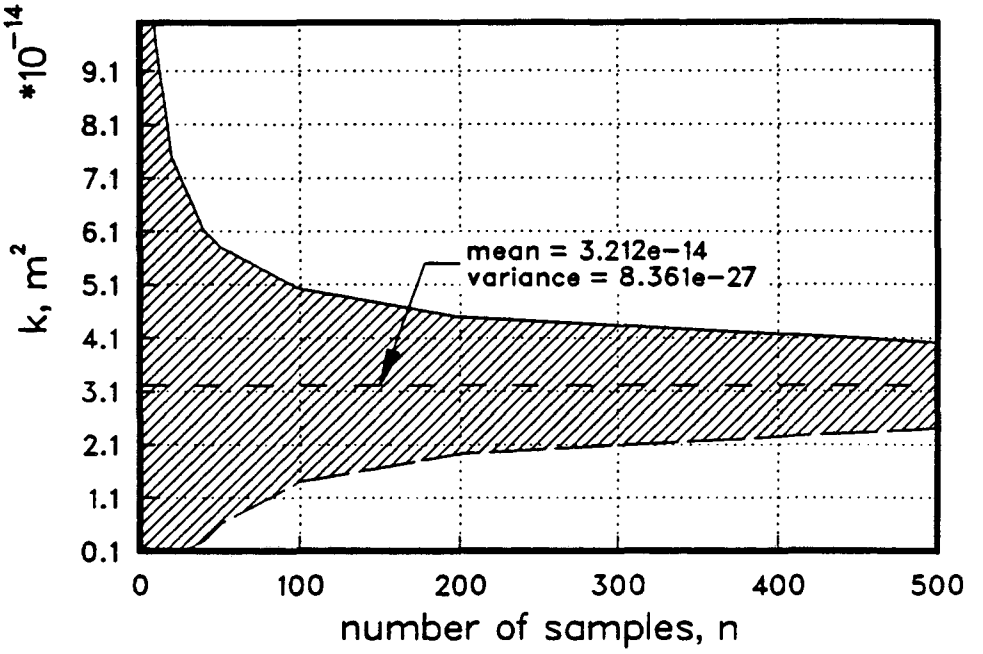

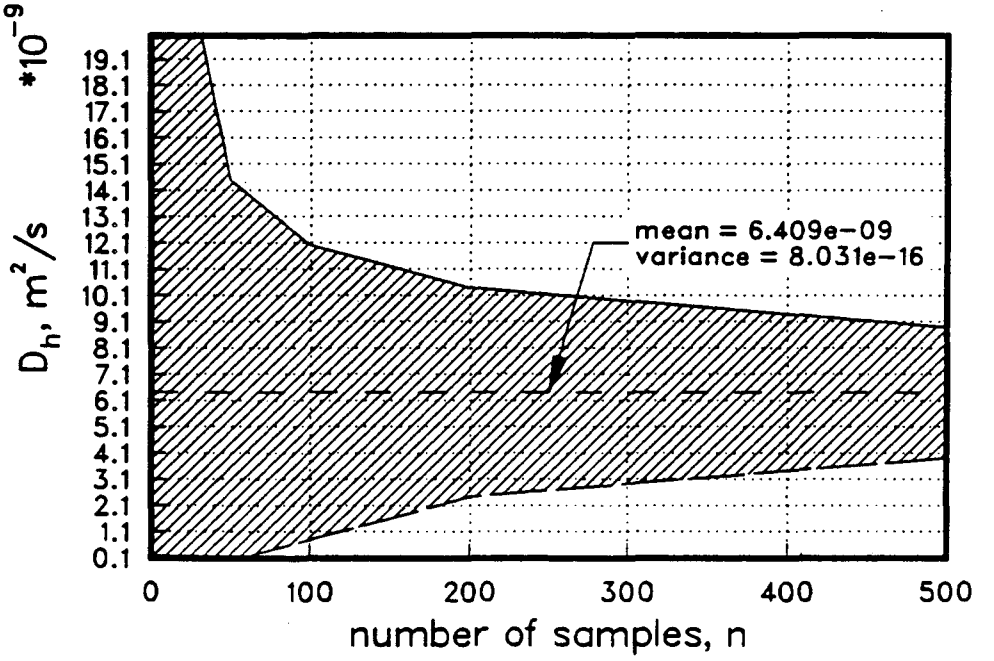

Figure 9.4 The effect of sample number on the accuracy of the mean k and D_h estimation.

required to be within ±100% and 350 samplers would produce an estimate within ±50% of the true mean.

The significance of variability cannot be overlooked in the prediction of solute fluxes at this and other sites. In the data presented we have seen that fluid velocities can vary by orders of magnitude within the confines of small field plots. The extent that this degree of heterogeneity extends deeper into the soil profile is not known, however, certainly an awareness must exist in data collection and analysis that the heterogeneous soil profile is a composite of numerous flow paths a large number of which have the ability to transmit solutes many times more rapidly than the mean fluid velocity.

9.2. Longitudinal Dispersivities

Longitudinal dispersivities determined through the use of CHAMP are presented in Table 6. They range from a low value of ≈ .1 cm to 49 cm. Dispersivity values obtained from laboratory column experiments on undisturbed cores of unconsolidated material generally fall in the range of .01 to 2 cm *(Freeze and Cherry,* 1979), considerably smaller than the values reported here. This tendency has been reported elsewhere *(Fried,* 1975; *Cherry et al.,* 1975; *Bredehoeft et al.,* 1976; *Anderson,* 1979 and *Biggar and Nielsen,* 1980) and can be attributed to several factors. Field-scale heterogeneity is often on a scale greater that that which can be conveniently included in a sample. Microscopic pore geometry variations, the type of heterogeneity that would be exhibited in a small sample, occur to such a completely random extent as to make only a minimal contribution to dispersion, however, large scale textural variability, layering, fingering, lateral discontinuities, and other types of major field structural heterogeneities often lead to fluid velocities which become highly spatially variable. The greater advective variability of the fluid stream in the field over that found in relatively small uniform laboratory samples will be exhibited in greater apparent dispersivity. Also, diffusion into immobile phases is not accounted for in deterministic treatments. This contribution to the apparent dispersion coefficient may be small in laboratory columns, but in the field it may account for the major portion of D_h *(Davidson et al.,* 1983).

In Figures 9.5 to 9.7, we see values of dispersivity plotted vs depth (travel distance) at the five monitoring sites. While the trend is not without exception, what is evident, is an increase in dispersivity with increasing scale of observation. At the shallower depths, dispersivities tend to be relatively smaller, while the largest values tend to be located at the deeper depths. Scale dependent dispersivity is a result of processes similar to those discussed above, i.e soil structural variability. As the scale of the observation is increased, the likelihood is greater that soil variability will be encountered. Also, greater travel distances allow for the effects of soil variability to act for longer periods of time on the solute distribution, thereby leading to a more dispersed solute plume. The trend towards increasing α_l with increased travel distance is consistent with other field observations *(Gelhar et al.,* 1985). No correlation was observed, however, between α_l, and D_h or v.

A functional relation between D_h and v, the average pore water velocity, has been investigated in the present study. Numerous investigators *(Harleman and Rumer,* 1962 and *Biggar and Nielsen,* 1976) have studied the relationship between apparent dispersion coefficient, D_h, average pore water velocity, v, molecular diffusion, D_o, and other characteristics of porous media and have suggested the following relationship

$$D_h = D_e + \alpha v^n \tag{39}$$

where alpha and n are constants to determined from data. Laboratory investigations indicate that for practical purposes n can be taken as unity, thereby reducing Eq. (39) to a linear equation

$$D_h = \tau D_o + \alpha_l v \tag{40}$$

where α_l is designated the longitudinal dispersivity (L).

In Figure 9.8, the 40 values of v are plotted vs D_h, and it appears that on the log-log axes the relation is approximately linear, with the equation

$$\ln(D_h) = 0.946 \cdot \ln(v) - 3.29 \tag{41}$$

describing the observed relationship with a correlation coefficient of .81. Converting this

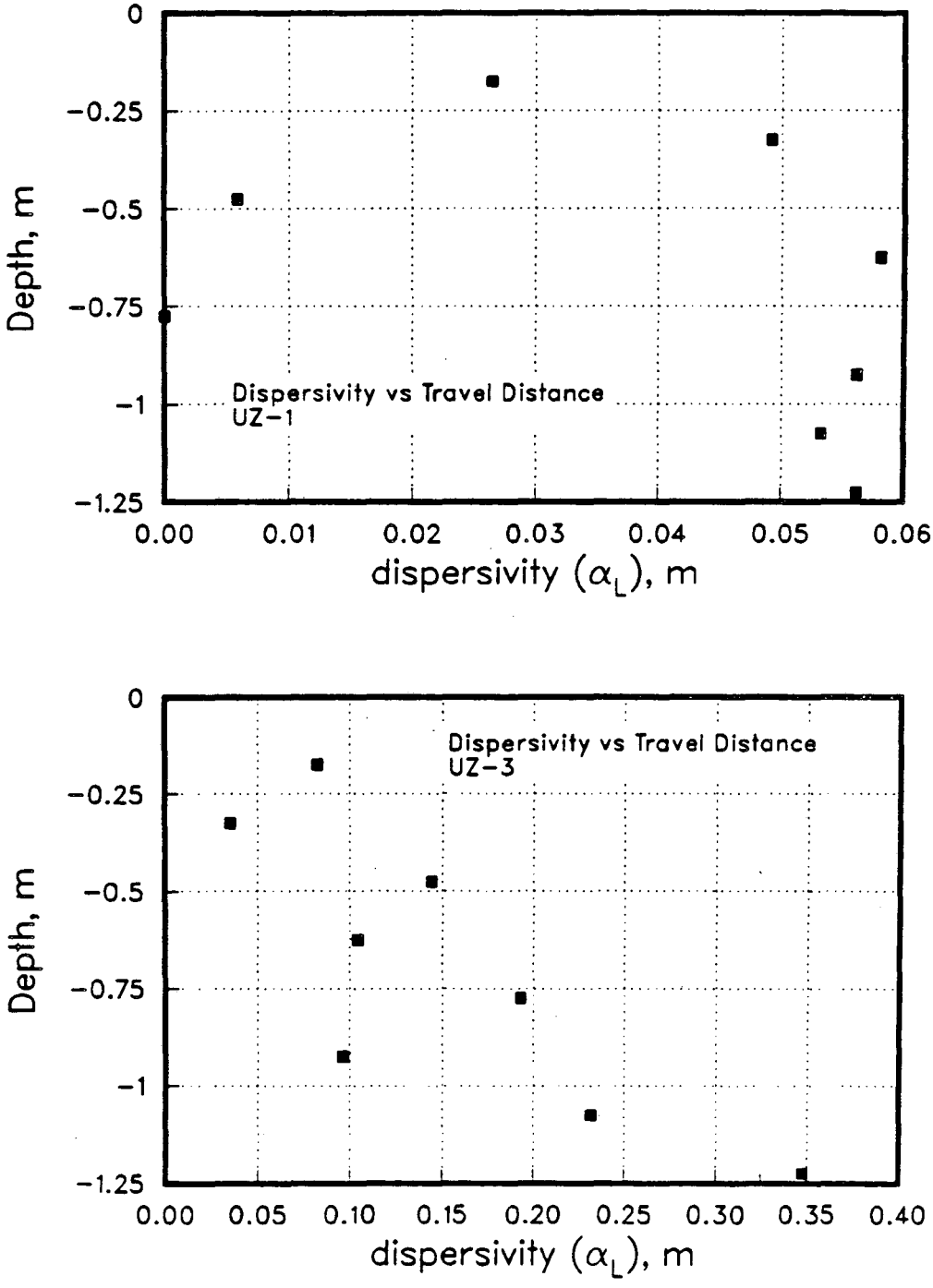

Figure 9.5 Values of dispersivity plotted versus depth (travel distance) at sites UZ-1 and UZ-3.

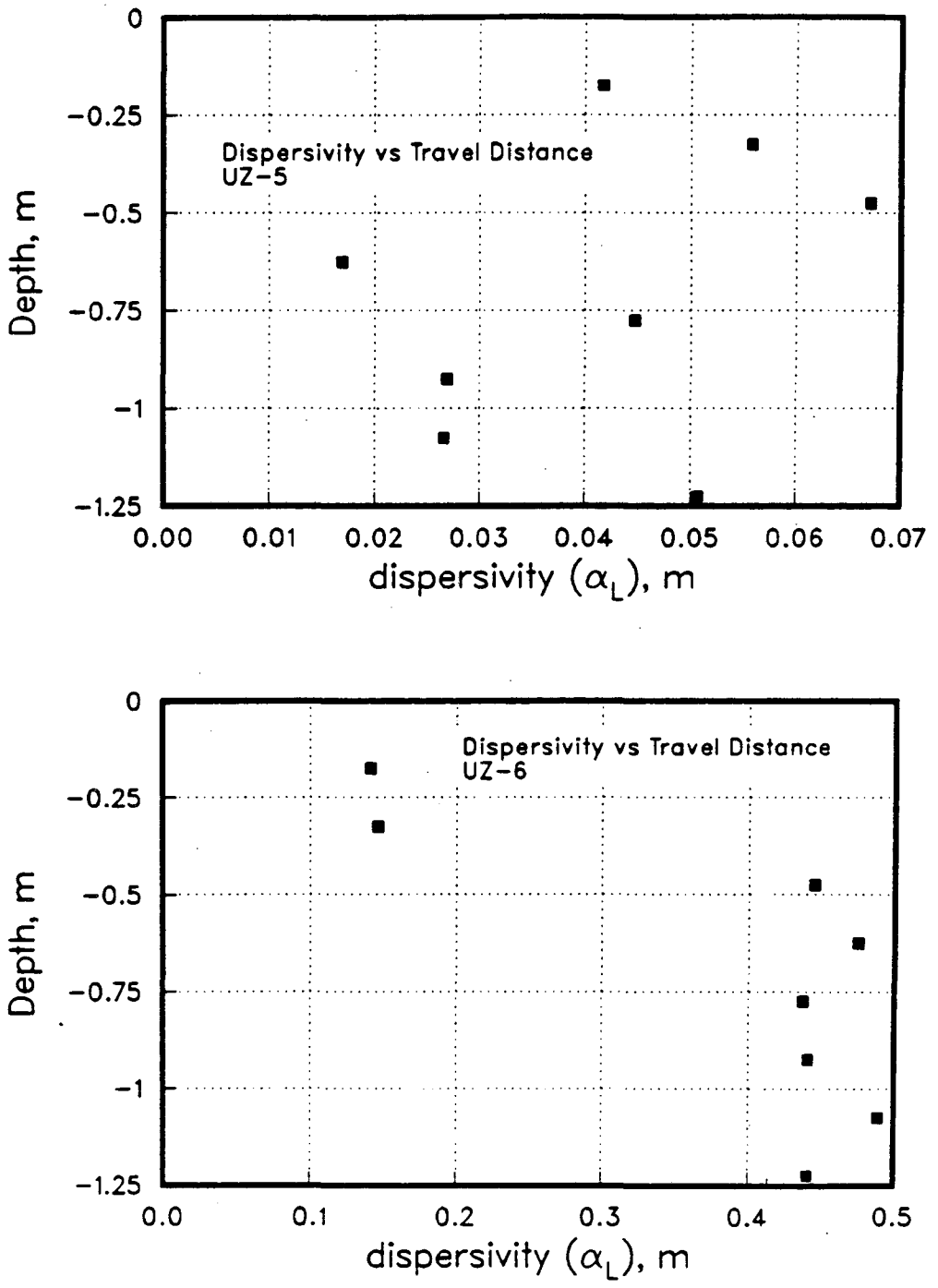

Figure 9.6 Values of dispersivity plotted versus depth (travel distance) at sites UZ-5 and UZ-6.

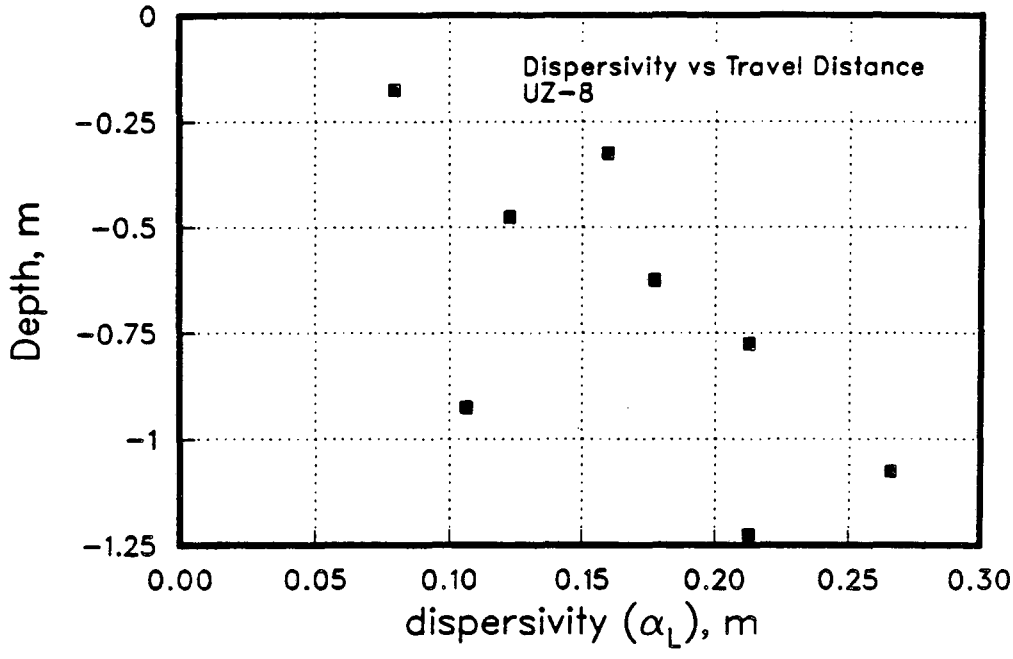

Figure 9.7 Values of dispersivity plotted versus depth (travel distance) at site UZ-8.

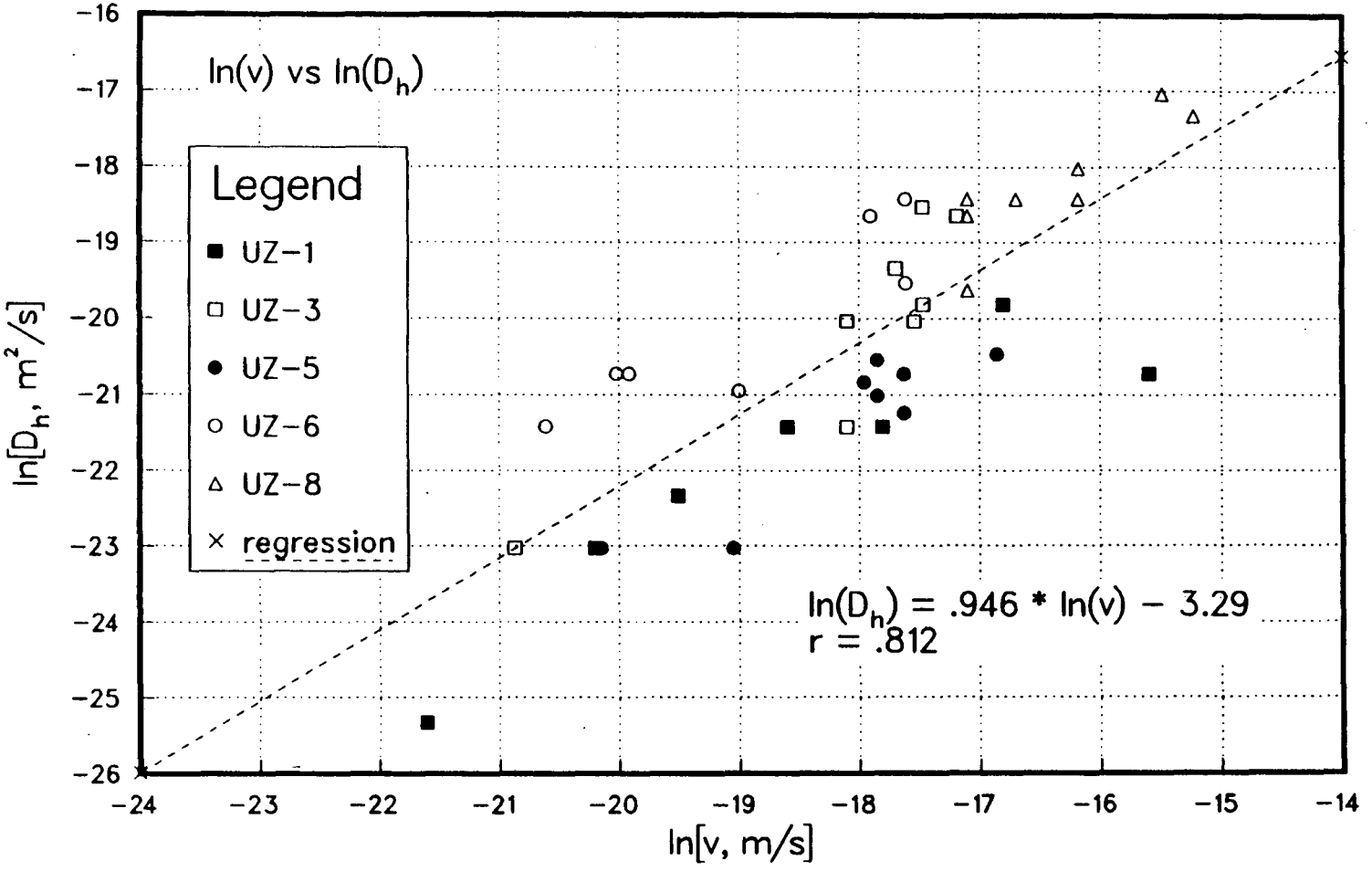

Figure 9.8 The demonstration of a functional relationship between apparent dispersion coefficient and average pore water velocity.

equation back to the actual values of v and D_h by applying the anti-log function to both sides, the following equation is obtained

$$D_h = .037 \cdot v^{.946} \tag{42}$$

suggesting that in this soil the parameter n of Eq. (39) may indeed be taken as unity. Eq. (34) is therefore a valid expression of the velocity dependence of the apparent dispersion coefficient. The above equation suggests that .037 m is an effective or composite dispersivity value for the Pond 1 soil based on the 40 values determined in the modeling effort. *Biggar and Nielsen* (1976) also demonstrated an approximately linear correlation between D_h and v, however, the fluid velocities were one to two orders of magnitude greater than those in this study. *Kirda et al.* (1973), in a study that involved chloride displacement through columns of sieved and packed sandy loam observed that at pore water velocities less than $\approx 1.7 \times 10^{-6}$ m/s the apparent dispersion coefficients were no longer velocity dependent and were essentially equal to the effective diffusion coefficient. Fluid velocities in the present study were significantly below this limit, and yet a similar functional relationship with velocity is still demonstrated. The greater degree of soil structural heterogeneity present in the field soil may help to explain this difference. It is also interesting to note that with only 40 samples in the present study (correlation coefficient of 0.81), the linear functional relationship appears to be demonstrated equally well as in *Biggar and Nielsen* (1976) with 359 samples (correlation coefficient of 0.79).

9.3. A Comparison of Part I and II Average Pore Water Velocities Determinations

The primary purpose in performing the numerical analysis of the chloride breakthrough data originally was to provide supporting evidence for the estimates of average pore water velocity that were made with the relatively simple chloride mass balance procedure used in Part I. In this section, average pore water velocities determined with the two methods are presented and compared. Calculations of selenium immobilization that were first performed in Section 5.2 have been repeated, based on a range of average pore water velocities that is suggested by the comparison, in order to examine the sensitivity of the selenium immobilization and discharge estimates to variations in fluid velocity.

Prior to presenting the velocity comparison, it should be stated that the measurements are not actually representative of identical sections of the soil profile. In the modeling procedure, 8 values of average pore water velocity were determined at each site. Each of these values represents an integrated average of actual velocity variations that occurred due to changing fluid potential boundary conditions. These 8 values must be combined in some manner into one site-specific average pore velocity before any comparisons can be made. The values of average pore water velocity determined at each soil water sampler location represent point measurements effective over the entire 2.75 m column. The velocities are not associated with a particular depth but rather with a particular areal position in a pond, a pond which is characterized by spatially varying soil hydraulic properties. If the velocities (permeabilities) were associated only with an individual layer, then the effective velocity would be calculated based on a harmonic mean of the individual permeabilities as in Eq. (1). However, since the velocities are associated with what more closely resembles a set of vertical, independent, non-interacting flow regions, a simple arithmetic average is more appropriate in choosing one site-specific fluid velocity. This manner of averaging ignores the indication of log-normally distributed flow and transport parameters obtained earlier, and it assumes that the eight velocity values are sufficient to adequately characterize the mean value of the entire study block, i.e. that each of the velocity estimates is suitably representative of the portion of study block volume that it is associated with.

In addition, the chloride mass balance calculation was performed only over the 1.22 m (4 ft) thick study block that corresponded to the depth over which soil water samplers were installed, and therefore the pore water velocity estimates apply only to that region. The modeling of chloride movement was performed over a section of the soil profile that extends deeper - to a depth of 2.75 m (9 ft). This depth was chosen because of the presence of a monitoring well that could be used as a lower fluid potential and concentration boundary condition in the history-matching effort. Therefore, with the awareness that the quantities compared are only approximately representative of the same vertical section of the soil profile, Table 7 presents average pore water velocities determined at each site by the two

methods.

Table 7. A Comparison of Average Pore Water Velocities Determined in Parts I and II.

Site	v Part II, m/year	v Part I, m/year	% Δv	± 50% v, m/year
UZ-1	1.01	1.9	-47	0.95-2.85
UZ-3	0.63	0.64	-1.6	0.32-0.96
UZ-5	0.59	0.44	+34	0.22-0.66
UZ-6	0.3	.76	-60.5	0.38-1.14
UZ-8	3.11	4.1	-24	2.05-6.15
average			≈ 33	

In the table above it is shown that the numerical code has independently resulted in average pore water velocity estimates that are reasonably similar to the estimates obtained in the chloride mass balance calculation. Site UZ-8 was shown in both estimates to clearly possess the largest pore water velocity, and site UZ-1 was determined in both methods to have the second highest. At UZ-3, the fluid velocities were nearly identical in the two procedures, and at UZ-5 the difference was only 34%. UZ-6 demonstrated the largest difference in the two methods on a percentage basis (60.5%), however, this difference still was less than 100%. This degree of agreement is considered quite close, and it is taken as an indicator of the validity of the fluid velocity estimates obtained in the chloride mass balance procedure in Part I.

In order to examine the effect on the selenium immobilization estimates of uncertainty in the fluid velocities, selenium immobilization calculations performed in Section 5.2 have been repeated using a range of average pore water velocities at each site. In Table 7 above, we see that the average difference between the two velocity estimates is approximately 33%. Therefore, a range of velocities of ± 50% of the average pore water velocity determined in Part I

has been chosen as an appropriate scale over which to examine the issue. In Table 8 is summarized the effect of this variation on the immobilization and discharge quantities. As previously presented in Table 4, the quantities have been normalized to the initial selenium inventories in the study blocks.

Table 8. The Effect of Average Pore Water Velocity Variations on Selenium Immobilization Quantities

Site	Immobilization/ Discharge v	Immobilization/ Discharge -50% v	Immobilization/ Discharge $+50\%$ v
UZ-1	75/33	83/16	72/49
UZ-3	91/5	94/2	89/7
UZ-5	94/1	94/.5	94.5/1.5
UZ-6	108/1.5	103/.7	113/2
UZ-8	66/47	79/24	57/71

The calculations shown in Table 8 indicate that the selenium immobilization estimates are fairly insensitive to choices in the average pore water velocity. The velocity range that was applied in this calculation represents a three-fold difference in velocity between the minimum and maximum values applied at each site. The difference was greatest at sites UZ-1 and UZ-8 where the selenium concentration of water exiting the study block (the concentration observed in the deepest soil water sampler) was appreciably different than that of water entering the study block (pond water). The greatest difference in immobilization quantities occurred at site UZ-8 where 57% and 79% of the initial selenium inventory was estimated to have been removed from solution based on the upper and lower velocity values, respectively. At site UZ-5, where the inflow and outflow concentrations were roughly equal, the variation in velocity had virtually no effect. Therefore, it can be concluded that regardless of whether

or not some degree of uncertainty exists in the pore water velocity estimates, an extensive quantity of selenium immobilization definitely took place in the shallow pond sediments during flooding.

10. CONCLUSIONS

Observations from the Pond 1 experiment indicate that selenium can be geochemically contained in pond bottom sediments at Kesterson Reservoir through the maintenance of permanently ponded conditions. Even though selenium concentrations in soil water of near-surface sediments were typically in the 1000's of ppb prior to and immediately after flooding, ponding with low-selenium water did not result in widespread adverse impacts on the quality of shallow groundwater sampled in the 1.83 to 12.2 m (6 to 40 ft) depth interval. Selenium concentrations in groundwater remained low ($\leq$ 20 ppb) at four of five monitored sites. A comparative analysis of the temporal variation of dissolved selenium and a conservative solute, chloride, indicated that roughly 60 to 80% of the initial inventory of soluble selenium was immobilized in the top 1.22 m (4 ft) of the soil profile within a month of pond flooding, and over the total monitoring period of approximately 7 to 10 months, depending on the site, immobilization ranged from 66 to 108% of the initial selenium inventory. Selenium levels in soil water sampled from the 1.22 m thick study block, after an initial increase after flooding, declined rapidly and continued to fall as long as the pond remained flooded. Selenium concentrations in soil water at the wet sites in Pond 1 were low in comparison to areas in the Reservoir where, in general, the water table was below the ground surface. Pond water concentrations approached target levels before the pond was allowed to dry. Drying of the pond soils, however, resulted in a 1 to 2 order of magnitude increase in selenium concentrations in near-surface soil water as levels returned to the pre-flooding conditions.

Numerical analysis of chloride breakthrough data, in general, confirmed the average pore water velocity determinations that were arrived at in the mass balance calculations and provided some indication as to the uncertainty level which could be associated with the velocity estimates. Sensitivity analysis of the effect of differences in velocity on the immobilization calculations, however, revealed that estimates of the quantity of immobilized selenium were fairly insensitive to even three-fold velocity variations.

Several investigators have examined the effects of ponding on the geochemical state in soils *(Takai,* 1956; *Ponnamperuma,* 1965; *Yamane and Sato,* 1968 and *Gunnison et al.,* 1985) and have concluded that soil reduction is the single most important and fundamental chemical change brought about by flooding. Rapid geochemical and biological changes in an initially well-aerated soil involve the depletion of oxygen in the soil by aerobic microorganisms and the subsequent establishment of an anaerobic and thereby reducing geochemical environment. Anaerobes utilize various electron receptors as alternates to oxygen (nitrate, manganese, ferric iron, sulfate, carbon dioxide, selenate?) in a thermodynamically determined step-wise manner for the oxidation of organic matter. The solubility dependence of selenium to oxidation-reduction potential has been examined by several investigators *(Lakin,* 1961; *Geering et al.,* 1968; *Weres et al.,* 1985 and *Elrashidi et al.,* 1987). An important result of these investigations has been the determination that under conditions of high redox, selenate is the dominant species in solution, whereas under conditions of moderate to low redox, more reduced species persist which have lower solubilities. These reduced forms include selenite, selenide, and elemental selenium. Eh measurements made in this study, while only qualitative in nature, indicate nonetheless that reduction of the shallow sediment region occurred quickly upon submergence with water. The Eh of the soil dropped by roughly 200 mV within several days of flooding. Measurements also indicated the Eh status of the soil to be highly spatially variable during the early days and weeks following flooding and that both oxidizing and reducing zones existed together. The measured Eh decline occurred over roughly the same length of time as the immobilization of selenium which was observed during a previous flooding episode. Data collected by others on the relationship between selenium occurrence and Eh suggest that the magnitude of the Eh decline may have been sufficient to result in selenium removal from solution. This conclusion, however, must remain essentially speculative and qualitative based on the nature of the Eh measurement and a lack of a more quantitative association between the two occurrences. Nonetheless, data presented here, indicating selenium immobilization and the reduction of the soil environment, are consistent with descriptions presented in the literature of the geochemical behavior of selenium and lend support to a system model whereby rapidly developing reducing

conditions in the newly flooded soils lead to the microbially mediated reduction of selenate to less soluble forms.

Various physical mechanisms have been identified by others that allow soluble selenium to migrate through the pond bottoms and into groundwater, including in general, the absence of a reducing environment and, more specifically, the presence of nitrate. This experiment has identified average pore water velocity as one parameter that can have a significant impact on the degree to which selenium undergoes chemical reactions that may cause its precipitation. A relationship has been observed between immobilization quantities and average pore velocity. Higher than average seepage rates have been shown to result in less selenium removal and to contribute to contamination of shallow groundwater underneath Pond 1. Also, the application of a first-order reaction to the observed migration of selenium through the study block has demonstrated that increases in the average pore water velocity are associated with decreases in the reaction rate. These facts suggests that the selenium removal mechanism is subject to kinetic restraints. Average pore water velocity effects selenium removal through variations in the residence time of infiltrating pore fluids as they pass through zones characterized by anaerobic bacterial activity and reducing conditions.

Redox measurements and rate estimates throughout the soil profile do not provide strong evidence for the existence of a thin (0 to 15 cm) surficial layer responsible for the majority of the observed selenium immobilization. The expectation that organic matter, the decomposition of which could lead to the depletion of available oxygen, would be found in greater quantities near the surface than at depth, might lead to speculation that the very shallowest sediments would be most important in promoting selenium removal. The presence of a more highly reducing region near the surface, however, was not definitely observed. The 1.22 m thick soil column seemed to be essentially without an Eh gradient between shallower and deeper portions of the soil profile. The estimation of reaction rates, as well, did not indicate that the ability of the soil to immobilize selenium was confined to the 0 to 15 cm layer. In fact, the 1.22 m thick soil column possessed an apparently equal capacity throughout for

effective selenium removal from solution. The accumulation of selenium near the surface is therefore analogous to a screening mechanism where the shallowest material is sufficiently effective to prevent significant quantities of selenium from migrating deeper into the soil profile. Selenium is able to penetrate deeper through macropore flow or the presence of high permeability material, however, it is still subject to immobilization through exposure to subsurface reducing environments.

The usefulness of a numerical model for solving the advection-dispersion equation has been demonstrated in the point estimation of soil hydraulic properties under transient flow conditions. Reasonable estimates of the soil properties were obtained without the use of an artificially introduced tracer or the manipulation of boundary and initial conditions. A high degree of spatial variability of water and solute transport parameters in a field soil has been exhibited, and the frequency distribution has been shown to be log-normal. There is some risk in not recognizing the appropriate sample distribution in mean parameter estimation, and in not considering the chance of extreme transport behavior. Dispersivities were calculated and presented in the spirit of supplementing the sparse existing database. α_l was shown to increase in a general sense with depth, but not to correlate with any other subsurface parameter. D_h and v were shown to be related in an approximately linear fashion, even though v was quite small.

Appendix I Sensitivity Studies

Initial Conditions

A potential problem in the numerical analysis of the chloride movement data and the subsequent determination of soil hydraulic properties lies in the manner in which the initial solute distributions have been chosen. History-matching was performed at soil water sampler locations that were distributed both vertically and areally in space. The eight locations were arranged on a grid and were separated from one another laterally by approximately one meter. The one solute distribution that was constructed from the observed chloride concentrations in the eight soil water sampler locations at T_o (the time from which history-matching began) was designated the initial chloride condition at each location. The actual distribution above and below each soil water sampler at this time may have been different. It may be reasonable to expect that the high degree of spatial variability that can often characterize soil hydraulic properties may also be demonstrated with regards to solute distributions. No serious attempt has been made in this experiment to evaluate this issue quantitatively, however, an understanding of its relative importance is certainly important. Therefore, in an attempt to assess the sensitivity of the results of the numerical modeling procedure to the choice of initial conditions, a series of calculations have been performed using CHAMP involving the application of different initial conditions to the data collected at one site. This sensitivity analysis, unfortunately, does not assist in the decision as to which set or form of initial conditions is the best or is the most correct, but it does illustrate the potential error and the risk involved in an incorrect choice.

In Figure 8.11 we see the initial chloride profile that was observed at site UZ-8 and that was applied at the eight soil water sampler locations at that site. In general, concentrations were highest near the surface, where evaporative fluxes prior to flooding concentrated solutes in a surficial salt crust, and were lower with depth, approaching levels measured in groundwater. The actual shape of the profile, however, because samples were collected from locations

separated from one another laterally, is not smooth but discontinuous, with local rises and declines in concentration, representing local variability in flow and transport. The overall trend of relatively high concentrations near the surface and lower ones at depth is what one would expect, and in fact is the form found at all five of the sites as well as various other unsaturated monitoring plots located in other ponds. It seems then that the initial condition chosen, whatever its exact form, should reflect this general trend. Since the total quantity of data regarding the initial solute distribution at this site is reflected in the nine points plotted, the simplest and most obvious assumption as to the choice of initial conditions is represented in a linear interpolation between those eight values. This was the form chosen in the history-matching procedure.

It is possible to fit the eight values to an exponentially declining curve of the form

$$C = C_1 + C_2 e^{-\alpha z} \tag{43}$$

where C_1 is the value approached asymptotically at depth and $C_1 + C_2$ is the concentration directly at the surface where $z = 0$. α is the constant of exponential decay. In Figure A1.1 we see eight curves shifted parallel to the main curve fit so that each intersects one of the values making up the initial chloride profile. Each of these curves was applied as the initial condition in sensitivity modeling performed at the appropriate site. The shape of the curves allows for the general trend of exponentially declining concentration that was observed, and the fact that each curve intersects the first observed concentration for the particular depth was necessary for the history-matching procedure. It is not being implied that these actually were the initial conditions or that they represent better choices. What is of interest is the degree to which the predicted chloride movement differs, at a particular depth, based on the new set of initial conditions, not whether the observed breakthrough curves are fitted more satisfactorily. The boundary conditions utilized in the main modeling effort were also used in these calculations, as well as the final fitted values of permeability, k, and apparent dispersion coefficient, D_h.

The results are included in Figures A1.2 to A1.5 where the predicted chloride movement

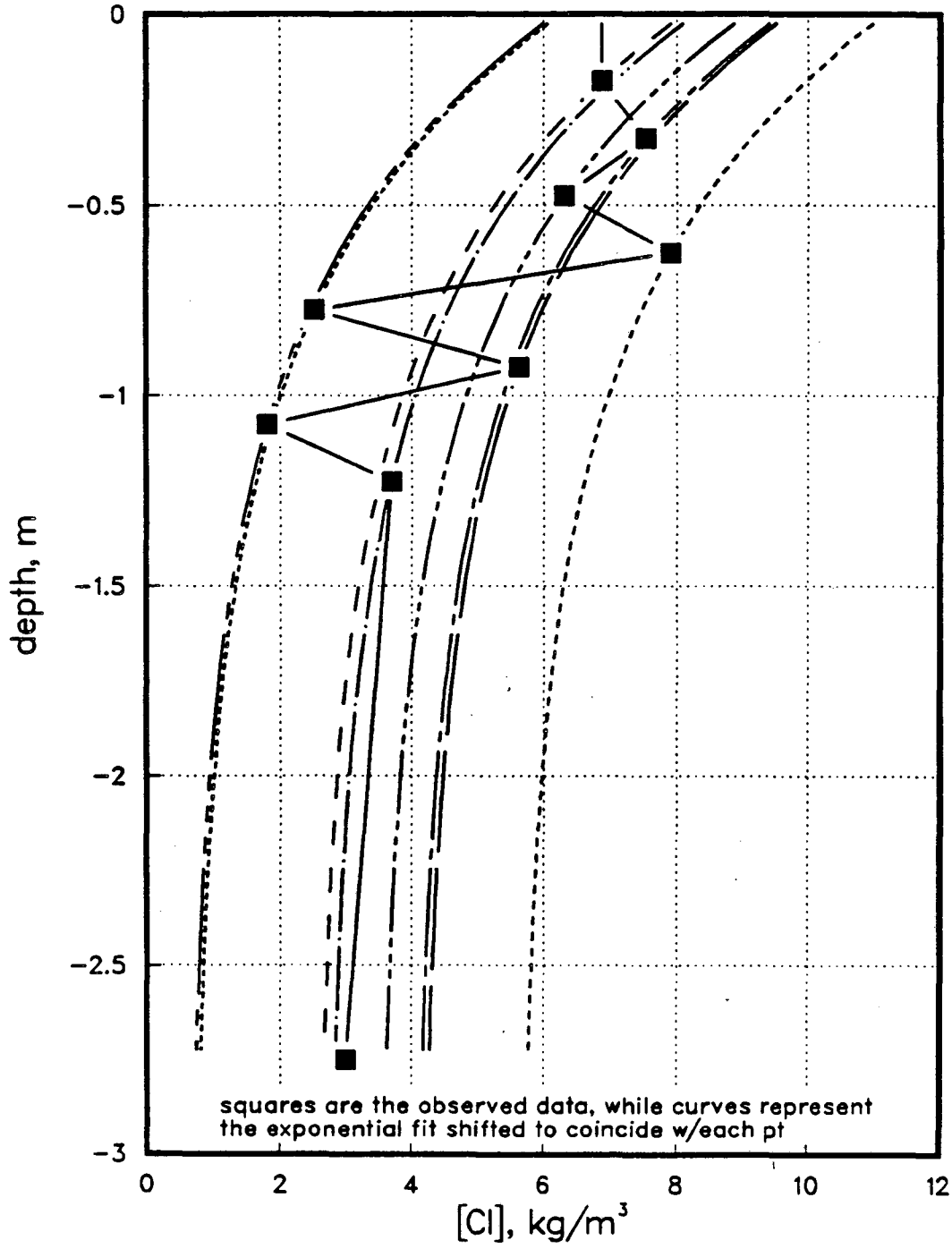

Figure A1.1 Variable initial conditions utilized in a study performed for site UZ-8 to determine the sensitivity of model output to variations in the chloride initial distribution.

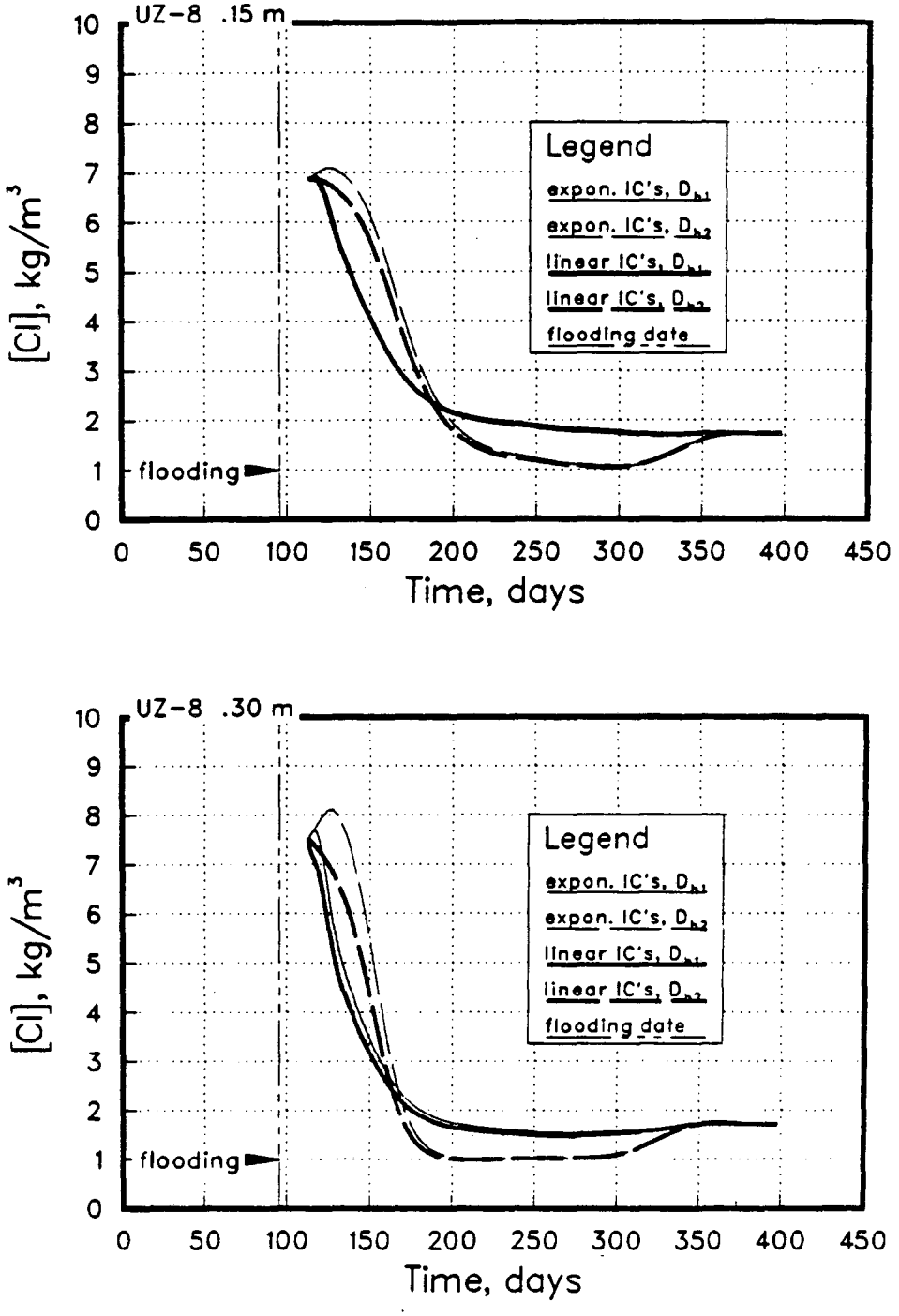

Figure A1.2 The effects of alternate initial conditions and apparent dispersion coefficient on model output at the 0.15 and 0.30 m deep soil water sampler locations at site UZ-8.

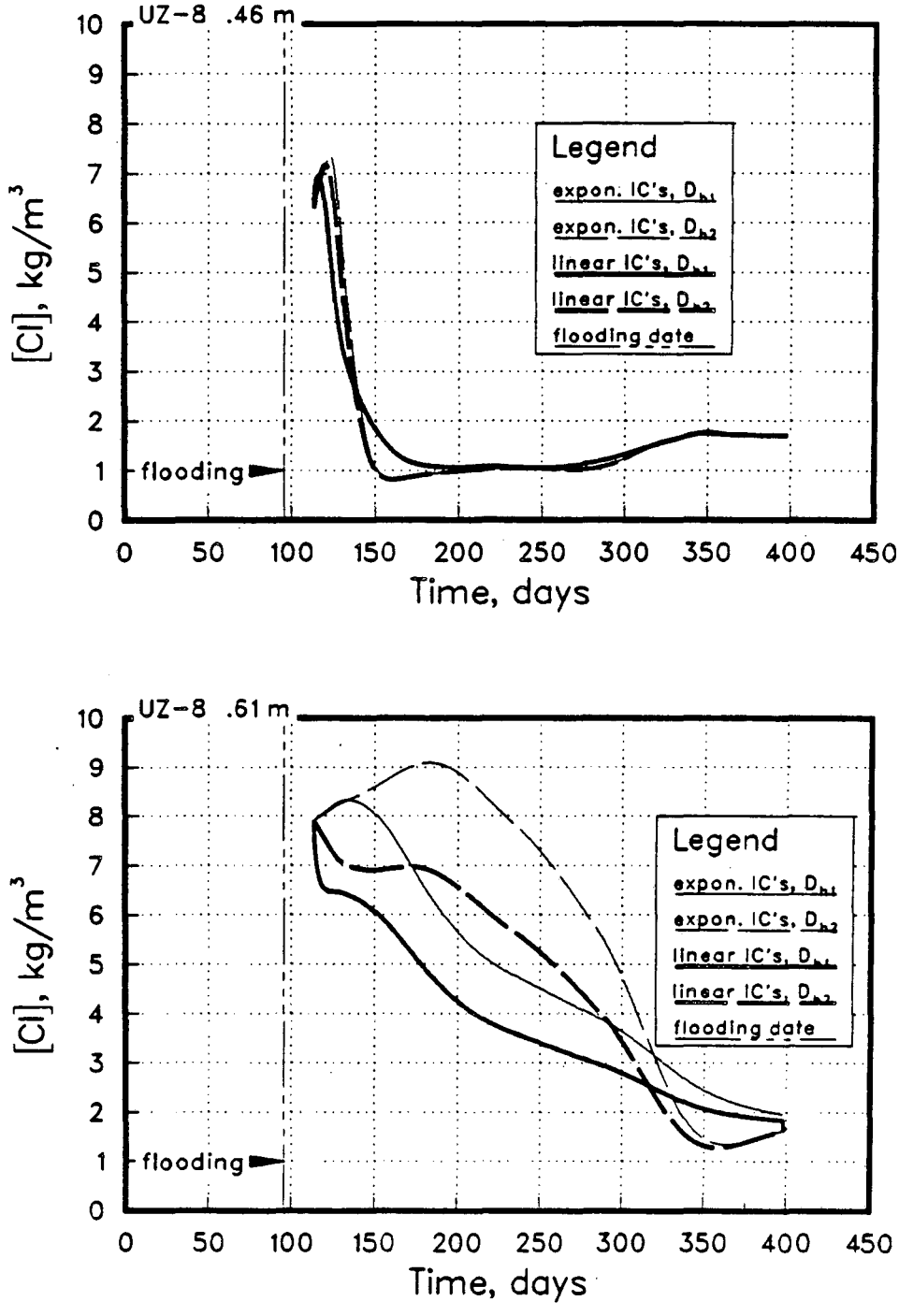

Figure A1.3 The effects of alternate initial conditions and apparent dispersion coefficient on model output at the 0.46 and 0.61 m deep soil water sampler locations at site UZ-8.

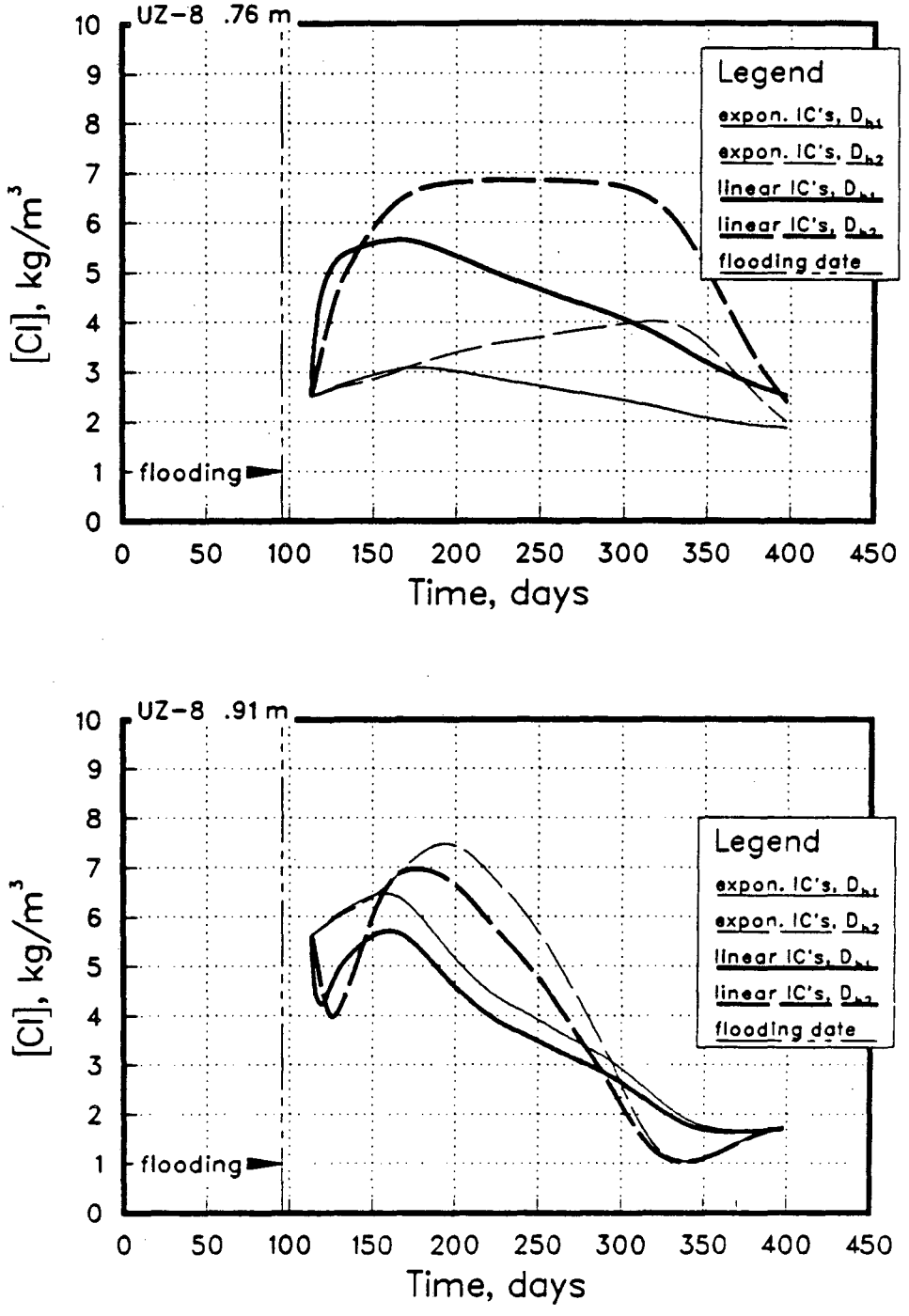

Figure A1.4 The effects of alternate initial conditions and apparent dispersion coefficient on model output at the 0.76 and 0.91 m deep soil water sampler locations at site UZ-8.

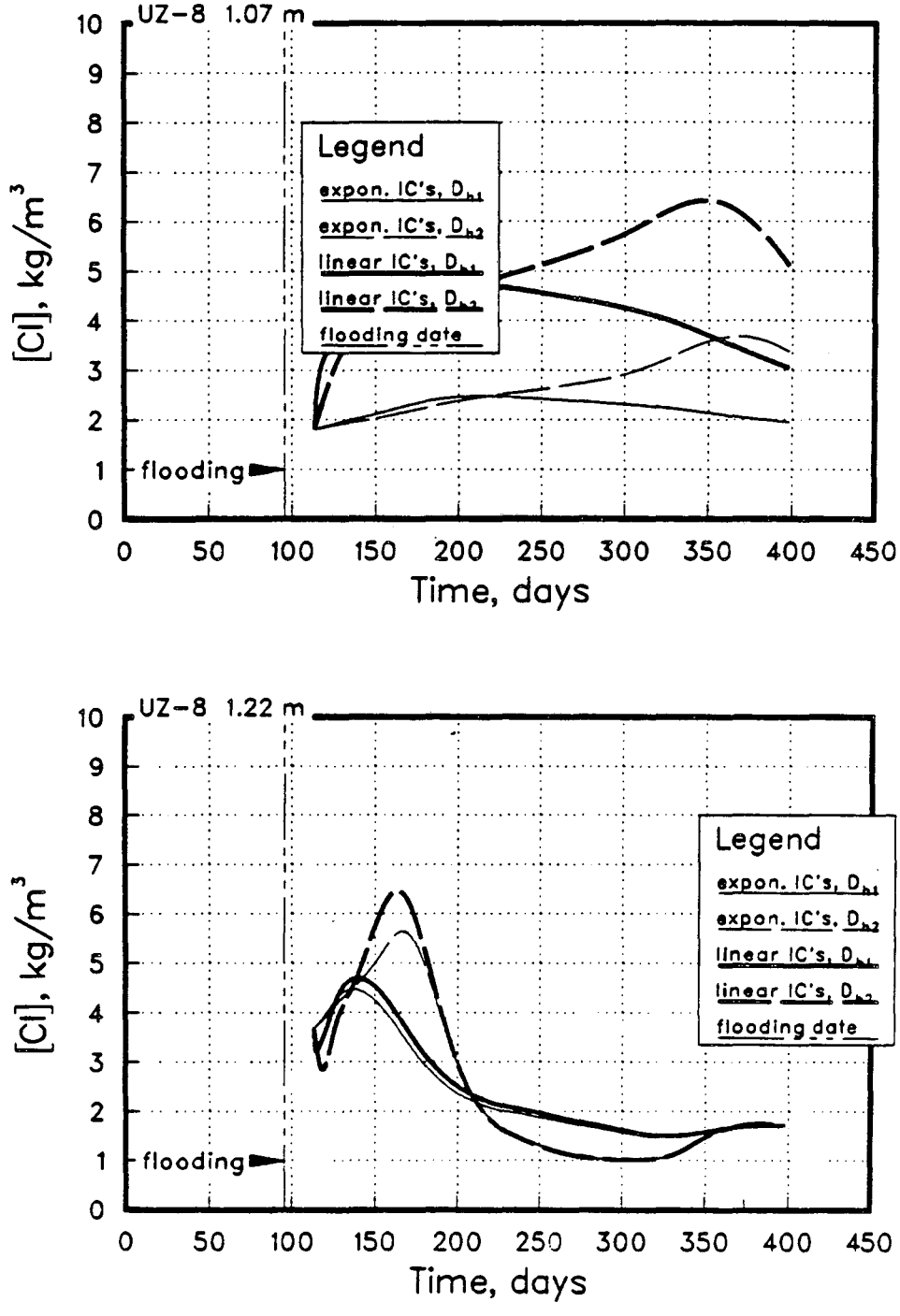

Figure A1.5 The effects of alternate initial conditions and apparent dispersion coefficient on model output at the 1.07 and 1.22 m deep soil water sampler locations at site UZ-8.

from the two sets of initial conditions are plotted together for each depth. Also included are results from an identical calculation performed with a value of apparent dispersion coefficient (D_h) one order of magnitude less than that determined in the history-matching procedure. This was done in an attempt to check if the difference induced by the differing initial conditions was a function of the dispersiveness of the system. What we see is that at two depths, .61 m and .76 m, a large difference is indicated in the predicted movement of the chloride resulting from the new initial condition, however, at the other depths the difference is shown to be small. The new initial conditions at the two depths differ from the observed distribution greatly, while at the other locations the exponential form at least falls within a range defined by observed values. In qualitative terms for this site, it appears that as long as the new initial condition approximates the observed profile in the sense that it is confined within its minimum and maximum values or that it represents some rough average, the smooth and the discontinuous profiles yield similar results. The system is sensitive to initial conditions in at least a gross sense, however, it does not appear that results may depend heavily on a detailed and highly accurate description of the initial solute distribution. Therefore, it seems that as long as the general form of the correct or actual distribution is obtained, and the values of the chosen distribution do not deviate greatly from the actual profile, meaningful and reliable estimates of the flow and transport parameters can be obtained with the history-matching procedure that has been applied in this study.

In addition, it appears that any error introduced due to invalid initial conditions will be smaller near the inlet of the flow region than at depth. This seems intuitively correct and is illustrated in Figures A1.2 and A1.3 for the upper three depths where there is essentially no difference in the predicted concentrations due to the two sets of initial conditions. The fluid velocities are such that the peak value of the initial solute concentration, located at the surface, passes through at an early time in the experiment, and that therefore the choice of initial conditions at these positions is much less important in history-matching than at depth.

We also see a slight relationship between the systems sensitivity to initial conditions and

dispersion. At relatively greater values of dispersion, one would expect greater smoothing of predicted concentrations and a dampening of the initial solute pulse as it moves through the soil column. We see especially in Figures A1.3 and A1.4 for the depths .61 and .76 m that the reduced dispersion coefficient, $D_{h,2}$, leads to a greater difference resulting from the different sets of initial conditions. Therefore, we can expect that in highly-dispersive systems, the choice of accurate initial conditions may be less critical than in systems with a lower degree of dispersion.

Therefore, we have seen at one site, in essentially only a qualitative sense, the degree to which reliable prediction of solute breakthrough may be dependent on the choice of good initial conditions. This says little, however, as to the acceptability of the initial conditions chosen in this study, only that the risk of a mistake in their choice may not be great. Certainly, this is not a detailed, exhaustive treatment of this issue, but it provides an appreciation for the degree of concern that needs to be directed towards this issue.

As an added thought, it may be possible to fashion a justifiably better scheme for designating the initial conditions with data similar to that collected in this study. Since we know through data collection at these and other plots throughout the Reservoir that solutes tend to be concentrated in the near surface region due to a strong evaporative tendency, we can claim with a fair degree of certainty that an appropriate initial condition should also take this general form. As long as the modeling is begun soon after the flooding event, it is very likely that the exponentially declining profile observed before flooding will still be exhibited to some degree. Measurements made areally, however, as in this experiment, will exhibit a certain degree of scatter, as we have seen, resulting from the spatially varying properties of flow and transport. If, however, we can claim at any particular location in a plot that the total inventory of chloride in the soil column prior to flooding is essentially a constant, we can adjust the shape of the initial condition profile so that it not only possesses the proper general trend but so that it also represents the mass inventory of solute when integrated over its depth. Therefore, a determination is required of the inventory of chloride present at a site. This

could be estimated from soil water samples collected prior to flooding. At each soil water sampler location, then, the initial condition chosen will intersect the observed value at that depth, will conform to some general exponentially declining trend, and when integrated over its total depth will yield the total mass of chloride determined to exist at the site. This manner of choosing initial conditions is an idea that, though only loosely outlined here, is logically based and results in a smooth initial profile. It does not force a concentration profile that may fluctuate widely with depth to apply at laterally dispersed sites. In a future experiment of this type, it may represent an improvement in the assignment of initial conditions over the method used in this study.

2-Dimensional Flow Effects

In view of the large spatial variability demonstrated with regards to soil hydraulic properties, it is reasonable to suggest that some potential may exist for 2- and 3-dimensional flow effects. All modeling performed in this study was done in 1-dimension in the vertical. A modeling effort involving more than one dimension was viewed as an impractical and unwarranted task, resulting in highly arbitrary conclusions. However, the extent to which the 1-dimensional treatment could be simplifying and misleading needs to be examined and discussed.

Calculations have been performed in an effort to gain insight into the degree to which flow and transport may deviate from the purely 1-dimensional treatment due to the presence of some simple types of soil heterogeneity. Two types of soil structural heterogeneity are examined: vertical heterogeneity and layering. Vertical heterogeneities could be large pores, channels, shrinkage cracks, animal holes, and subtle textural variations. Remnants of shrinkage cracks resulting from long-term dessication cracking may persist as natural fissures in swelling clay soil. Macropores can provide paths for rapid transport of solutes to depth, solutes which are then able to diffuse into the surrounding soil matrix. Layering, if it is discontinuous, could conceivably result in circuitous flow paths. Continuous layering would only result

in a reduction of a 1-dimensional fluid velocity to that allowed by a harmonic mean permeability of the permeabilities of the individual layers.

Whether or not these types of variability are significant in altering the 1-D flow field is evaluated in two sets of calculations involving simple arrangements within a matrix material of vertical and horizontal layers producing permeability contrasts with the matrix. For the case of vertical heterogeneity, a single, narrow, high-permeability, vertical "layer" has been used in a 2-D grid. Solute breakthrough resulting from different ratios of matrix permeability to macropore permeability and to different ratios of longitudinal to transverse dispersion coefficient is monitored in various nodes of the grid. For the case of horizontal layering, a single, discontinuous, low-permeability layer is utilized, and solute breakthrough is monitored at positions located laterally some distance from the layer. Different ratios of matrix to layer permeability are applied.

Vertical Heterogeneity

A 2 m deep by .26 m wide flow region has been discretized into 175 volume elements, with a 1 cm wide vertical column used to represent the high permeability zone, i.e. a crack or some type of soil macropore that allows water and solutes to flow downward more rapidly than the matrix will allow. The high permeability zone fully extends through the grid space. The analysis involves fully-saturated steady flow with a step input concentration of $C_o = 1$ at the surface at time t=0. At the bottom boundary, the concentration of solute is set equal to zero. Initially throughout the soil column, the solute concentration is $C_i = 0$ everywhere. A gradient of .4 is applied across the flow region. The calculation is performed for a one year period. Two values of k_m, the matrix permeability, are chosen: 2×10^{-16} and 2×10^{-15} m^2. Two values of $D_{h,l}$, the longitudinal component of the apparent dispersion coefficient, are used: 6×10^{-9} and 6×10^{-10} m^2/s. The transverse component of the apparent dispersion coefficient, $D_{h,t}$, is set to one-tenth and one-hundreth of the $D_{h,l}$. For each of these cases, ratios of macropore permeability, k_h, to the matrix permeability, k_m, of 1, 2, 10, 50 and 100

are applied. Analytical solutions are also included using Eq. (31) for the ratio $k_h/k_m = 1$ (with k_m set equal to either of the two values mentioned above) which reduces the 2-D problem to one dimension. Table 9 provides a summary of the cases run and the parameters chosen for each.

Table 9. *Vertical Heterogeneity Sensitivity Analysis*

Case	k_m ,m^2	$D_{h,l}$ m^2/s	$D_{h,l}/D_{h,t}$	Comments
A	2×10^{-16}	6×10^{-9}	10	
B	2×10^{-15}	6×10^{-9}	10	
C	2×10^{-15}	6×10^{-9}	100	
D	2×10^{-15}	6×10^{-10}	10	
E	2×10^{-15}	6×10^{-9}	10	Lateral Flow vs No Lateral Flow

Solute breakthrough is monitored at two nodal positions, .075 m laterally from the vertical "layer" and at a distance of .225 m away laterally. Both nodes are located .475 m below the soil surface. In Figures A1.6 to A1.10 we see the results of the calculations for the 5 cases. The point of greatest interest here is to what degree does the presence of the high permeability zone lead to results which differ from purely a 1-D case, i.e. to what extent are lateral solute fluxes contributing to the observed breakthrough curve and how much are the lateral fluxes a function of distance from the macropore, matrix permeability, macropore permeability, and the longitudinal and transverse dispersion coefficients.

A The analytical solution Eq. (31) has been plotted for the one-dimensional situation of A, and we see that it matches the numerical result when $k_h/k_m = 1$. This same result is obtained for all cases A through D. The value of k_m applied in this instance,

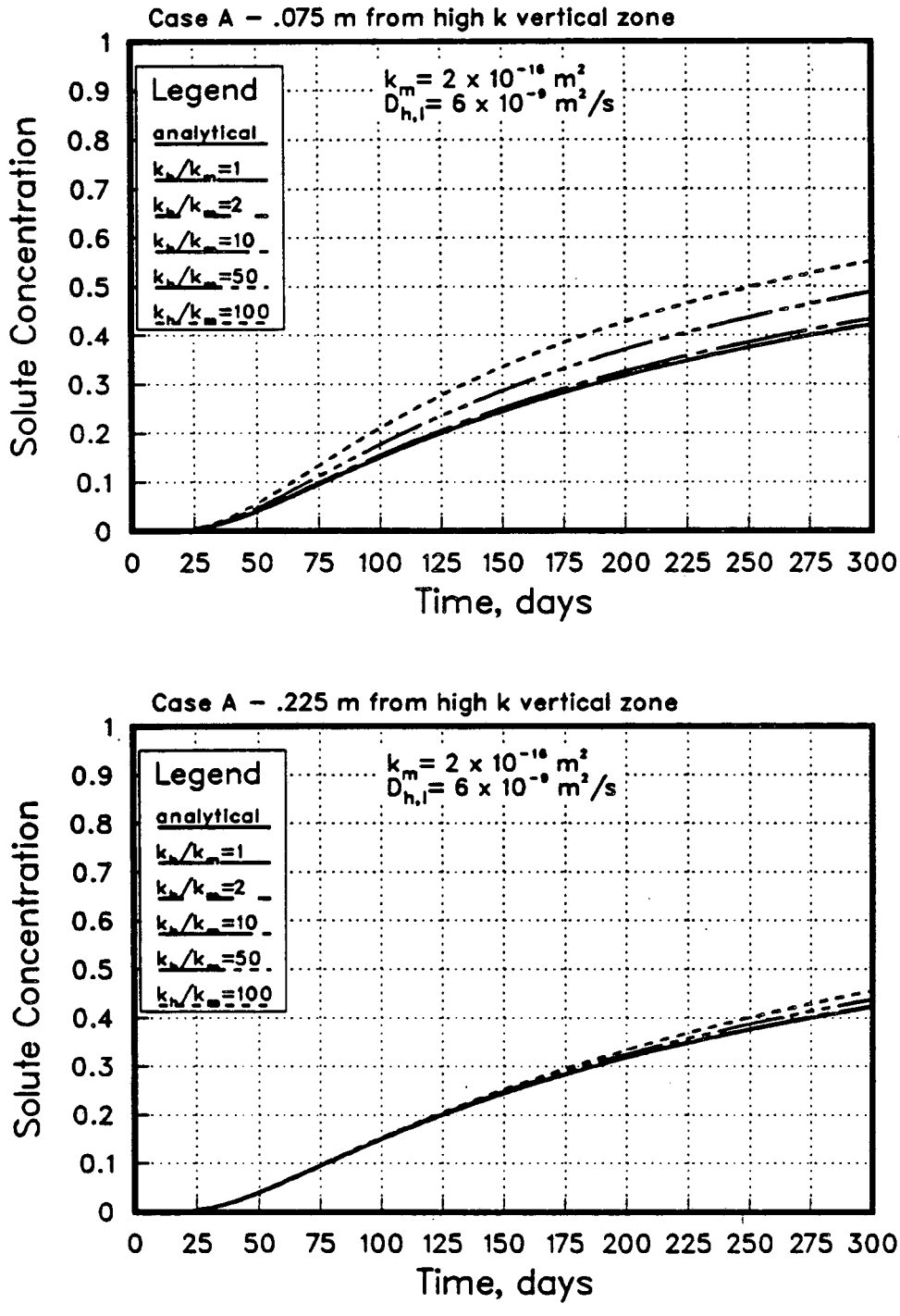

Figure A1.6 The results of a sensitivity study examining the potential deviation from purely vertical 1-dimensional solute transport - Case A.

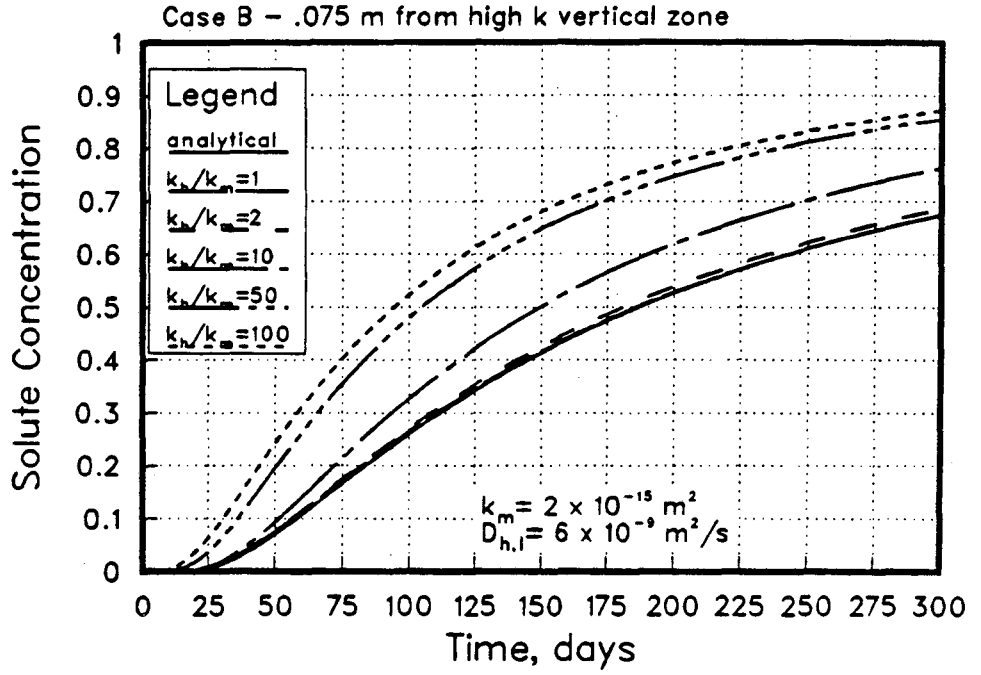

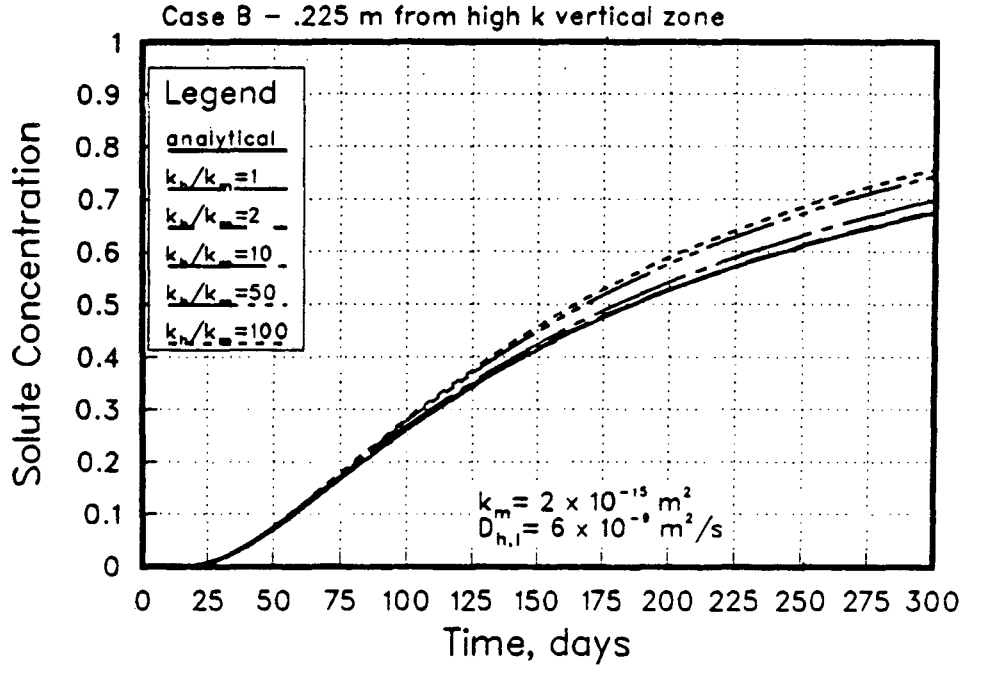

Figure A1.7 The results of a sensitivity study examining the potential deviation from purely vertical 1-dimensional solute transport - Case B.

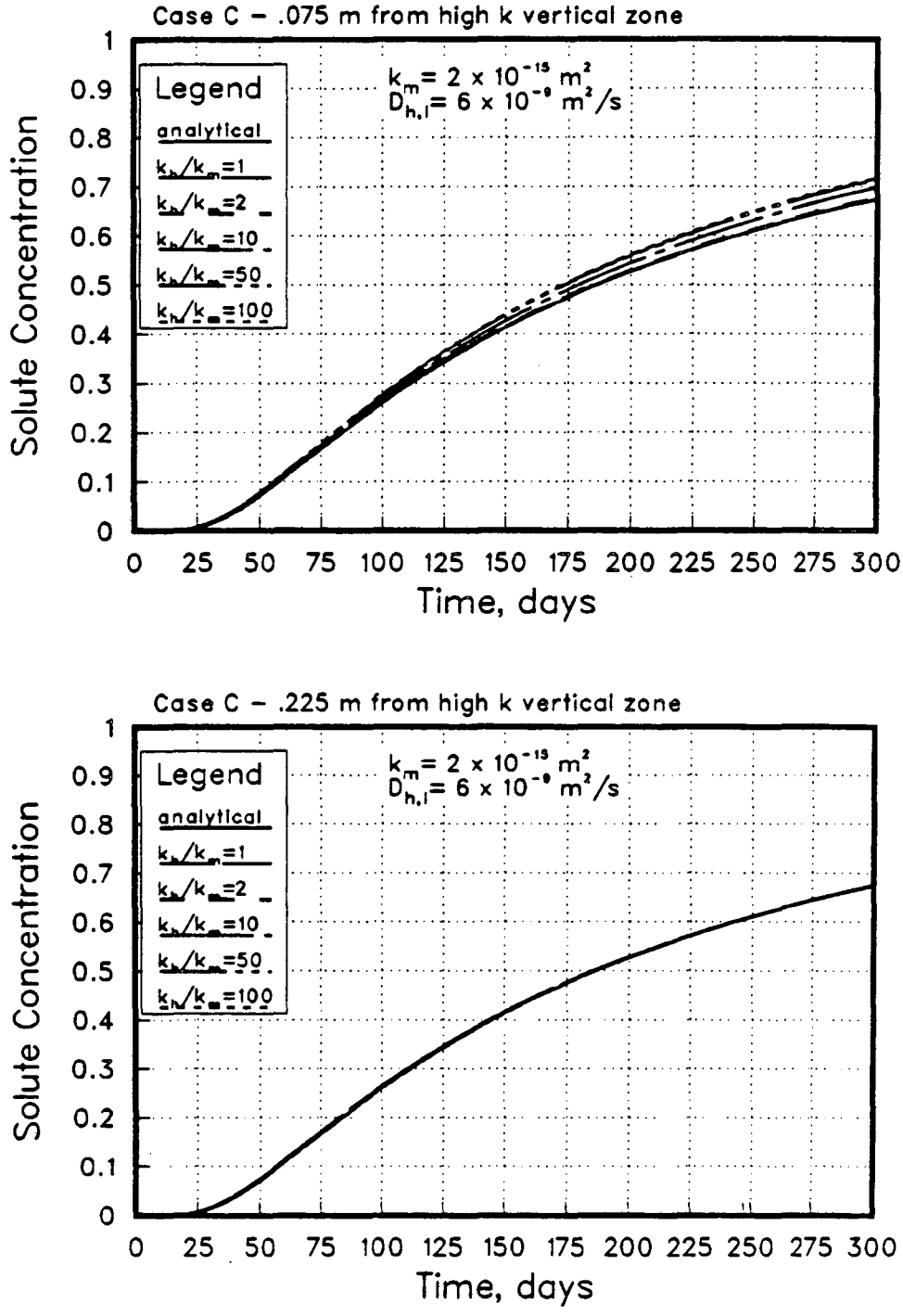

Figure A1.8 The results of a sensitivity study examining the potential deviation from purely vertical 1-dimensional solute transport - Case C.

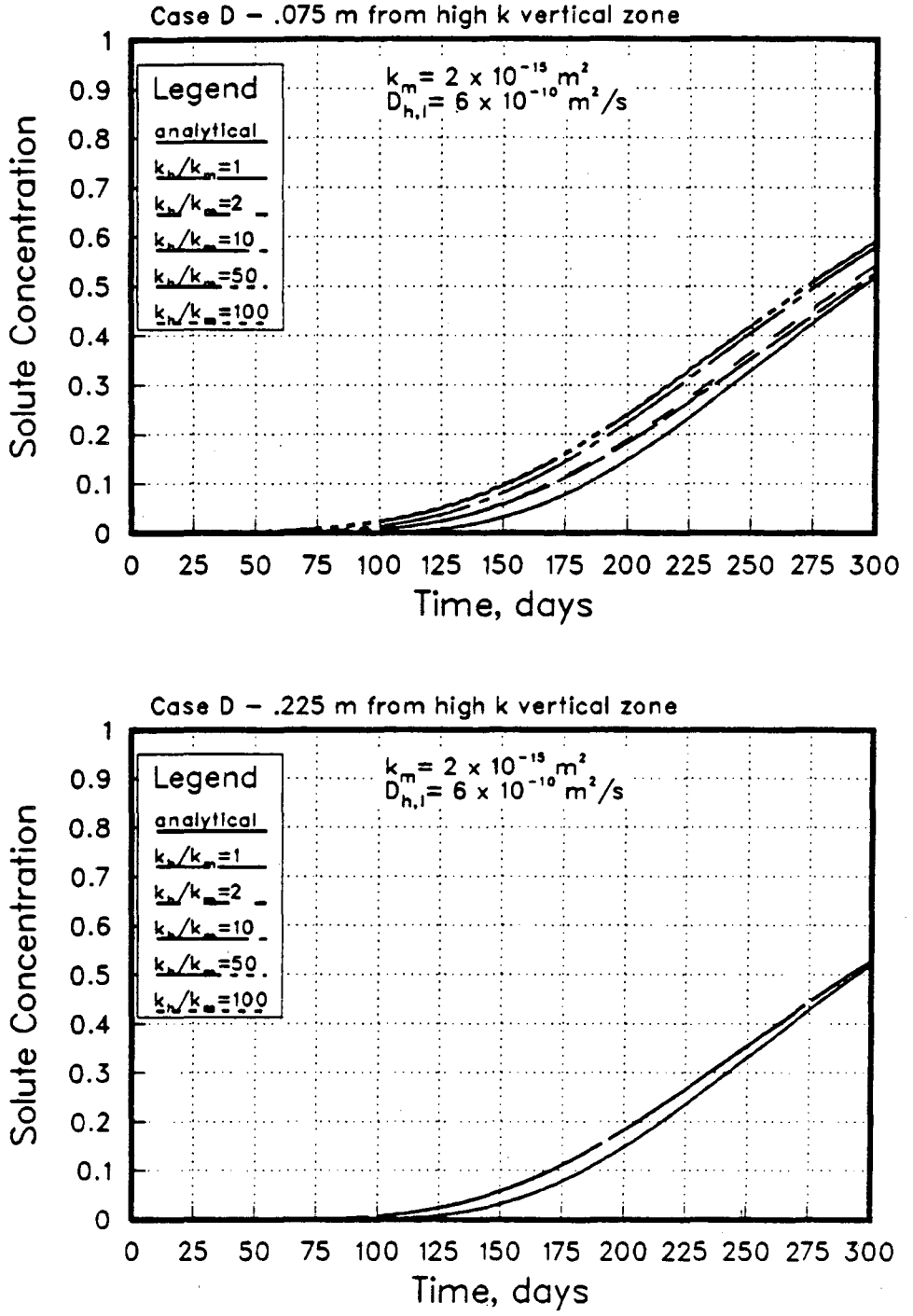

Figure A1.9 The results of a sensitivity study examining the potential deviation from purely vertical 1-dimensional solute transport - Case D.

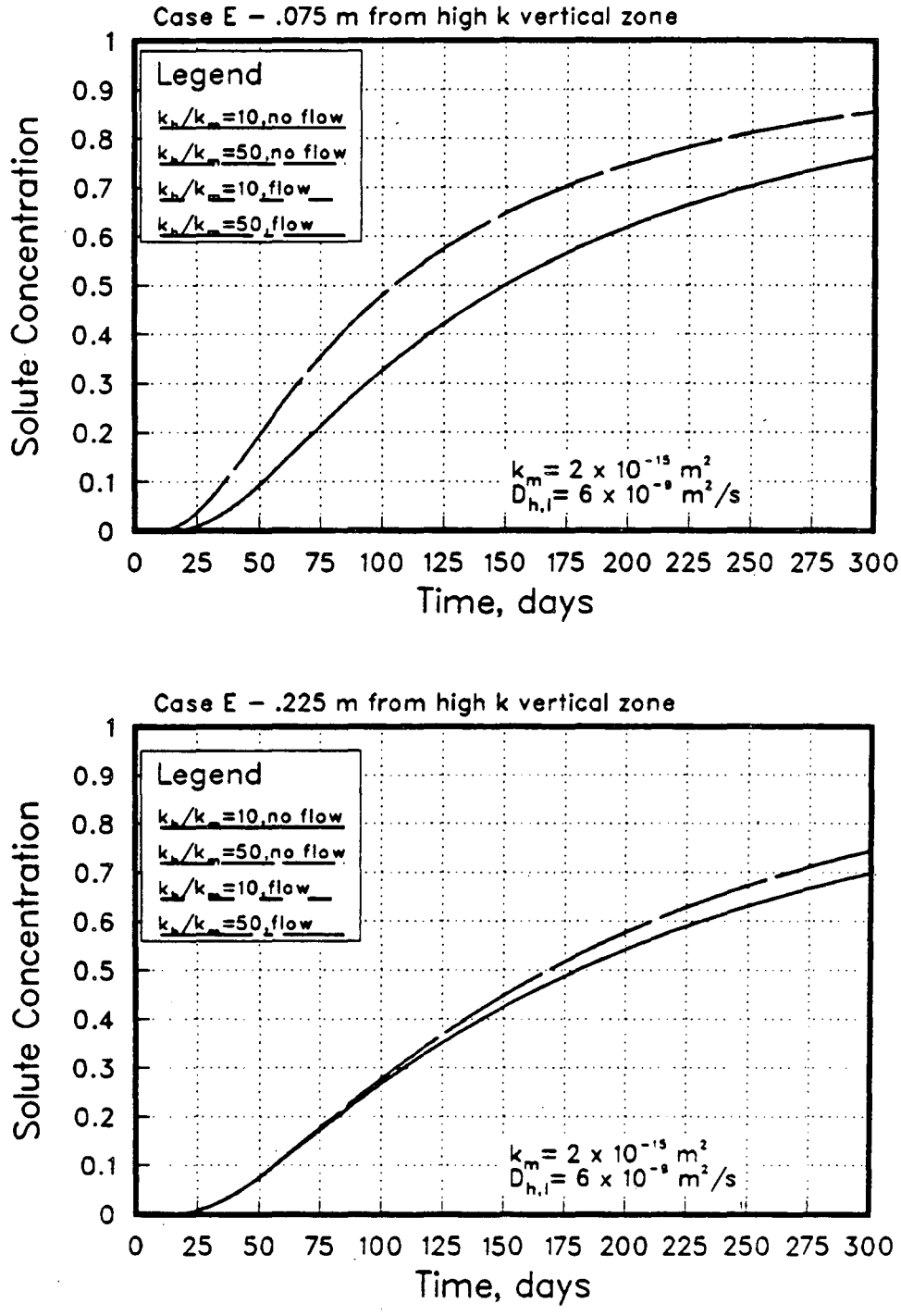

Figure A1.10 The results of a sensitivity study examining the potential deviation from purely vertical 1-dimensional solute transport - Case E.

2×10^{-16} m^2, can be considered a low range value for the Kesterson pond soils. It essentially represents the lowest value determined in the history-matching effort (Table 6), although it should be remembered that the modeling results theoretically represent a composite value of matrix and macropore permeability. This value is also lower by an amount less than one order of magnitude than any determined by Guelph permeameter in the Pond 1 soils *(Lawrence Berkeley Laboratory*, 1986c p. 32), although this type of measurement also theoretically incorporates macropore flow contributions. In Figure A1.6 we see that very little effect is evident in the system from the presence of the macropore until a permeability contrast of 100 is reached and only at the nearer of the two nodes. These results reflect a value of the apparent dispersion coefficient of 6×10^{-9} m^2/s, the mean value of dispersion coefficients determined in the history-matching. Other values of the longitudinal dispersion coefficient or of the ratio between the longitudinal and transverse coefficients were not investigated with this permeability since the combination of parameters reported here produced the highest amount of lateral flux and therefore represent the worst case. It should be mentioned that a variation in k as high as two orders of magnitude was not observed within any of the 5 monitoring plots.

B Here we see that the node positioned .075 m from the macropore is affected greatly by permeability contrasts of 10 or greater, an amount of variability that has been observed in the data determined in the history-matching. The matrix permeability applied in this case is 2×10^{-15} m^2, a value which can be considered more representative of actual conditions in the pond soils than the the value used in A. Identical longitudinal and transverse apparent dispersion coefficients were used as in A. In the more distant node, a much smaller effect is observed.

C Case C represents the situation as in B, however, the transverse dispersion coefficient is set to one-hundreth of the longitudinal value rather than one-tenth. In neither nodal position does the predicted breakthrough deviate greatly from the case of $k_h/k_m = 1$.

D Here the longitudinal value has been set to 6×10^{-10} m^2/s and the transverse value to one-tenth of the longitudinal. This case demonstrates the effect of lower dispersion

overall in the system. Permeability is as in B and C. Little deviation is observed from the homogeneous case.

E Case E is a check to insure that the only solute fluxes occurring laterally are those due to dispersion. The parameters found in case B are applied for two situations. In the first, a change was made in CHAMP to set lateral flow of water, if any, between adjacent nodes to 0. The results were then compared to results where lateral flow was allowed to occur. The results from the two runs are identical, providing assurance that the only 2-D solute transport contribution is from dispersive fluxes. This result is expected and obvious considering that in the steady flow situation, with the macropore fully extending through the grid, the fluid potential varies linearly between the two boundaries and is not a function of distance from the macropore. This result only confirms the internal functioning of the code. The results it provides though can only be as good as the problem description as reflected in initial/boundary conditions and the geometric description of the problem. A transient flow situation or one with only a partially penetrating macropore would demonstrate lateral gradients and would therefore exhibit lateral advection to some degree.

Therefore, a series of calculations have been performed involving various values of critical flow and transport parameters varied over ranges that are considered reasonable for the particular field situation. The results suggest that within these ranges when matrix permeabilities are on the order of 2×10^{-16} m^2 lateral transport is essentially negligible regardless of the value of the dispersion coefficients, macropore permeability or the crack spacing. When the matrix permeability is increased an order of magnitude, the mean value of longitudinal dispersion is used, and a ratio of 10 is assumed for the longitudinal to transverse dispersion coefficient, significant lateral dispersive fluxes can occur at nodal points within 10 cm of a macropore with a permeability contrast of 10 or more. If the longitudinal dispersion coefficient is reduced an order of magnitude or the ratio is increased to 100 between the longitudinal and transverse components, the lateral effects become small again.

Calculations have been performed here in an attempt to provide a qualitative feel for the issue of 2-D transport resulting from vertical heterogeneity and to gain an understanding of the relative importance of the magnitude of flow and transport properties on the issue. Combinations of parameters have been identified that conceivably can result in considerable deviations from purely 1-D transport during infiltration. Whether or not these combinations exist in the soils of this experiment is unclear, however. As discussed elsewhere, variations in k and D_h of 1 to nearly 2 orders of magnitude have been determined within plots in this experiment. Little detailed information was collected as to the spacing of zones of high permeability such as soil cracks. We do know that on the scale of 3 m, however, what sort of variability is possible. Facts which are reassuring are that on the basis of the analysis presented here, the soil water sampler would have to have been positioned within 10 cm approximately of the macropore to be influenced by it. Also, it took permeability variations of at least 10, towards the upper end of the observed variation, to see an effect. In addition, knowledge as to the correct ratio of longitudinal to transverse dispersion in this system is not available. If the ratio is greater than 10, the 1-D evaluation is in all likelihood, an appropriate estimate. A new appreciation of the significance of each parameter, its magnitude and effect has been gained, however, in the end, a definitive conclusion regarding potential 2-D solute transport in this system and to possible implications towards results obtained from the 1-D treatment, has to be left unresolved.

Discontinuous Layering

A 2.05 m deep by .8 m wide region was discretized into 216 elements. At a depth of .34 m from the surface, a .02 m thick material was placed extending half-way (.4 m) across the grid. Of interest here is a study of the effect of low permeability in this discontinuous soil horizon on the movement of solutes in the flow region. If the layer was continuous, fluid flow paths would be strictly vertical and velocities would be reduced to some value based on the effective vertical permeability of the medium. History-matching of this type of situation would correctly yield the effective vertical permeability. However, if the layer is

discontinuous, flow paths may acquire a horizontal component, as water "piles up" above the low permeability layer and passes around it to the higher permeability material. A matrix material permeability, k_m, of 1 x 10^{-14} m^2 has been chosen. This is approximately the mean permeability value of the pond soil determined from the history-matching procedure. The mean apparent dispersion coefficient of 6 x 10^{-9} m^2/s has also been used for the longitudinal component with a ratio of 10 between the longitudinal and transverse components. Solute breakthrough was monitored at three locations within the grid. The first position was at the same vertical level as the layer, positioned 5 cm laterally away from the layers edge. The second position was also at the same depth, but 25 cm laterally away. The third node was located 33 cm directly underneath the first node. The first node was located to be in the zone of maximum lateral flow; the second would indicate how far away from the layer the disturbance might extend; and the third would demonstrate if the disturbance could extend to some depth below the layer. Permeabilities of the heterogeneous layer material, k_h, were set to 1, .5, .1 and .01 times the matrix permeability. The initial condition throughout the column was $C_i = 0$. A step input concentration $C_o = 0$ was applied at the surface. The calculation was performed for a one year time period. No restrictions were made in the code preventing lateral advection.

In Figure A1.11 are plotted breakthrough curves for the three nodes considering the different layer permeabilities. An analytical solution Eq. (31) is also included for the 1-D situation, and it matches the numerical solution for the case of $k_h/k_m = 1$ (k_m = 1 x 10^{-14} m^2). It appears that based on these figures, it can be concluded that the contribution of lateral transport to the calculated breakthrough curves are small in this system. No further combinations of matrix permeability, or longitudinal and transverse apparent dispersion coefficient were examined since it appears that overall the effect is rather minimal. If a heterogeneous soil profile like the one examined here existed in one of the experimental monitoring plots, and a soil water sampler located adjacent to the discontinuous layer yielded a breakthrough curve affected to the degree indicated here, the error made in one-dimensional history-matching would not be great.

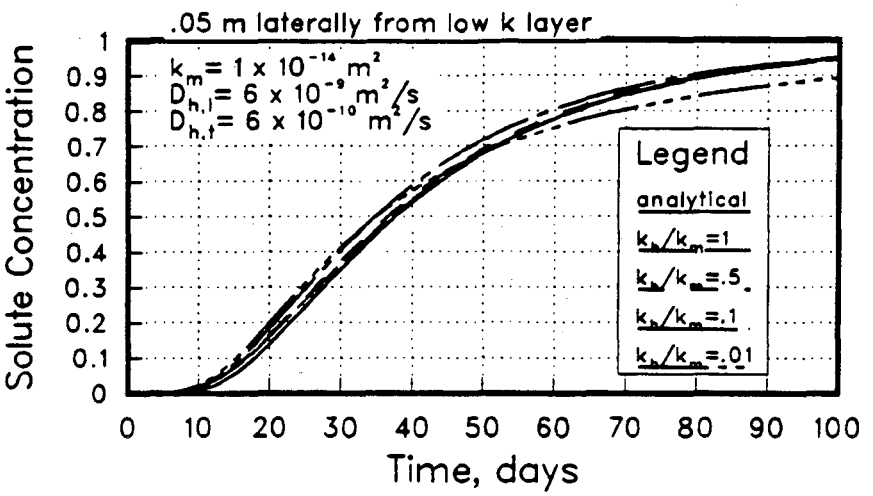

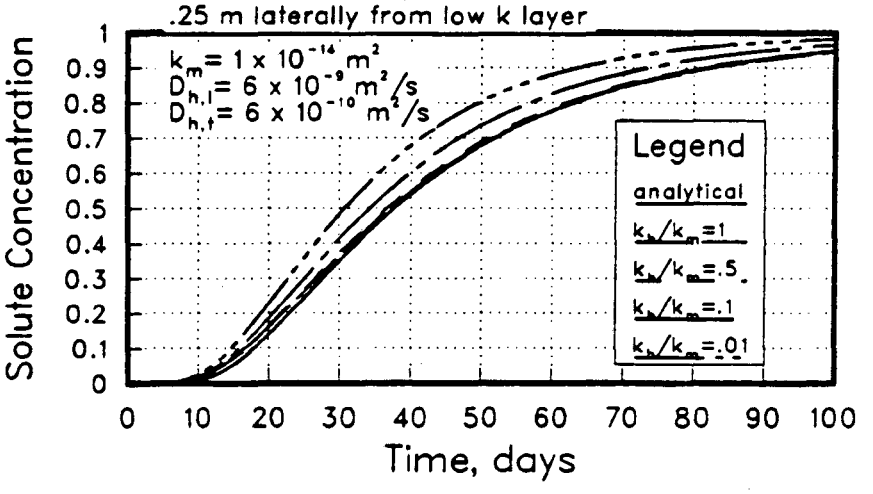

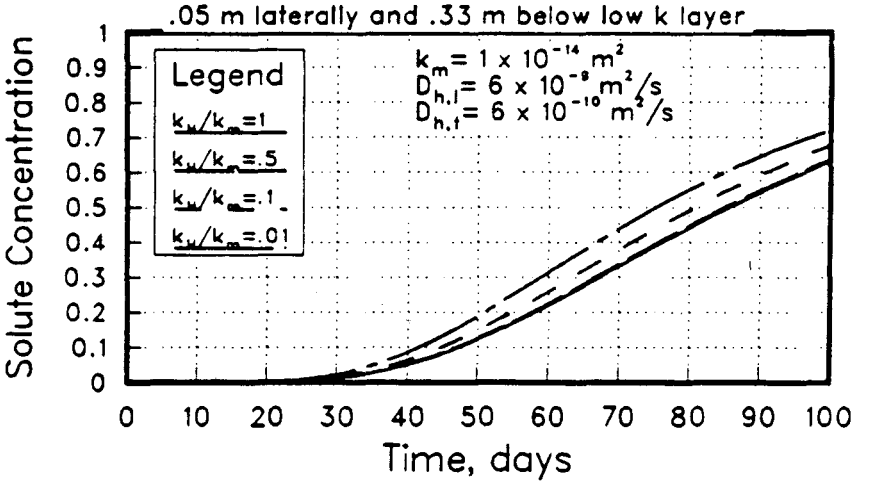

Figure A1.11 The results of a sensitivity study examining the potential deviation from purely vertical 1-dimensional solute transport that might exist under different scenarios of layered heterogeneity.

APPENDIX 2

Pond 1 Resaturation Monitoring Chemical Data TOTAL SELENIUM CONCENTRATION, ppb VS. DEPTH, m uz-1

The AVERAGE represents average of non-zero concentrations.
Zero values represent no sample recovery at that depth.

pond	0.15	0.30	0.46	0.61	0.76	0.91	1.07	1.22	AVERAGE	DAY	NO. OF SAMPLES
0.00	0.00	165.40	0.00	105.88	0.00	58.48	0.00	0.00	109.92	19.00	3
0.00	1032.80	180.00	490.60	0.00	290.20	31.72	40.62	23.04	298.43	28.00	7
0.00	2068.00	0.00	212.60	76.56	210.60	36.60	54.58	0.00	443.16	53.00	6
0.00	3804.00	0.00	272.20	0.00	0.00	55.02	64.92	0.00	1049.03	84.00	4
0.00	0.00	284.40	367.60	76.82	151.60	72.42	102.04	60.94	159.40	96.00	7
0.00	3010.00	2624.00	455.00	3032.00	393.60	603.00	170.20	143.84	1303.95	97.00	8
0.00	120.20	2110.00	60.28	249.20	778.80	135.80	298.80	308.60	507.71	104.00	8
34.08	25.12	1192.00	27.10	28.16	1066.00	98.40	590.40	504.80	441.50	109.00	8
29.12	19.58	192.40	20.64	46.30	940.80	70.68	643.60	547.40	310.18	116.00	8
0.00	18.28	60.96	16.96	16.60	1052.40	77.72	855.20	656.20	344.29	119.00	8
17.56	19.22	54.48	19.24	11.96	814.00	82.80	884.00	582.40	308.51	124.00	8
23.72	27.36	68.14	21.60	16.20	896.40	121.20	1010.40	687.20	356.06	132.00	8
22.84	24.54	56.32	31.04	26.94	1144.00	130.80	1168.00	640.20	402.73	144.00	8
18.00	19.06	28.56	22.12	78.08	581.40	121.80	914.40	540.20	288.20	173.00	8
15.14	9.16	13.80	12.88	65.68	186.40	120.20	832.00	510.20	218.79	204.00	8
17.04	11.10	14.28	12.58	7.72	160.60	145.80	678.80	489.40	189.79	232.00	8
15.02	6.34	14.08	8.00	16.86	103.40	108.00	350.00	395.40	125.26	286.00	8
22.26	94.72	48.72	44.88	49.80	17.86	110.60	21.90	168.20	69.33	337.00	8
21.88	18.02	17.74	20.66	27.46	16.26	74.58	21.00	106.40	37.77	341.00	8
18.94	13.22	14.26	14.72	13.16	10.74	59.38	16.54	94.20	29.53	344.00	8
8.60	8.22	12.66	6.58	22.42	12.14	41.44	11.54	111.20	28.27	398.00	8
0.00	5.58	9.44	6.04	15.84	8.72	19.04	4.40	19.98	11.13	420.00	8
0.00	0.00	0.00	15.70	0.00	0.00	22.70	17.92	25.62	20.49	448.00	4
0.00	219.40	595.20	133.40	138.00	69.42	19.36	25.60	38.28	154.83	451.00	8
0.00	613.00	171.80	191.20	211.20	69.48	27.20	60.98	55.90	175.09	476.00	8
459.20	1028.00	490.00	265.00	684.00	113.60	44.12	112.20	88.40	352.92	478.40	8
156.40	1562.00	2170.00	378.60	1440.00	131.00	48.90	134.60	106.20	746.41	478.71	8
110.60	2446.00	1542.00	488.00	2294.00	120.60	48.48	125.20	115.00	897.41	479.69	8
0.00	1670.00	2344.00	880.00	2044.00	121.60	47.90	126.80	123.60	919.74	481.79	8
0.00	1442.00	2068.00	1136.00	1530.00	125.40	46.98	115.20	134.40	824.75	482.55	8
40.50	1612.00	1308.00	1176.00	894.00	108.20	47.54	118.20	149.20	676.64	483.71	8
64.16	1166.00	1344.00	1408.00	694.20	128.80	49.96	180.40	138.40	638.72	484.55	8
0.00	1248.00	704.60	1470.00	422.60	124.00	46.12	127.20	179.00	540.19	487.00	8
30.18	499.80	208.40	545.40	201.00	115.20	49.38	130.00	180.00	241.15	495.00	8
22.22	112.80	69.66	104.00	145.80	112.60	55.64	126.20	189.00	114.46	502.00	8
21.40	30.02	29.92	20.58	128.00	93.80	55.98	118.60	201.80	84.84	509.00	8
15.68	18.72	15.16	12.68	99.40	60.70	54.48	107.80	182.60	68.94	539.00	8
12.88	17.74	11.82	10.94	32.98	70.76	64.62	64.62	183.00	57.08	572.00	8
0.00	0.00	0.00	0.00	25.70	24.88	11.62	15.94	93.20	34.27	621.00	5
0.00	0.00	0.00	8.40	41.12	11.18	8.86	4.54	8.12	13.70	648.00	6

Pond 1 Resaturation Monitoring Chemical Data TOTAL SELENIUM CONCENTRATION, ppb VS. DEPTH, m uz-2

The AVERAGE represents average of non-zero concentrations.
Zero values represent no sample recovery at that depth.

pond	0.15	0.30	0.46	0.56	0.71	AVERAGE	DAY	NO. OF SAMPLES
0.00	81.74	24.36	12.16	7.08	4.60	25.99	72.00	5
0.00	74.60	15.06	5.12	4.62	3.82	20.84	94.00	5
0.00	48.12	7.40	1.82	1.40	4.60	12.67	113.00	5
0.00	54.84	7.54	8.18	3.50	3.44	15.50	120.00	5
0.00	53.62	8.24	0.82	0.62	2.34	12.73	133.00	5
0.00	82.24	44.22	5.10	5.24	6.12	28.58	145.00	5
0.00	100.20	24.60	4.50	7.66	4.80	28.35	148.00	5
204.80	534.80	193.00	3.56	3.02	6.74	148.22	155.00	5
99.24	1254.00	583.40	6.02	5.08	5.30	370.76	173.00	5
162.20	574.40	0.00	3.42	2.90	3.44	146.04	204.00	4
69.16	170.60	274.80	7.00	3.60	4.16	92.03	231.00	5
0.00	0.00	16.62	3.14	3.74	4.56	7.01	286.00	4
0.00	84.34	20.70	2.92	2.78	3.38	22.82	336.00	5
0.00	0.00	21.44	4.24	3.24	3.70	8.15	397.00	4
0.00	327.60	25.50	4.20	3.60	0.00	90.23	478.00	4
0.00	349.00	5.48	4.20	4.24	21.34	76.85	649.00	5

Pond 1 Resaturation Monitoring Chemical Data TOTAL SELENIUM CONCENTRATION, ppb VS. DEPTH, m uz-3

The AVERAGE represents average of non-zero concentrations.
Zero values represent no sample recovery at that depth.

pond	0.15	0.30	0.46	0.61	0.76	0.91	1.07	1.22	AVERAGE	DAY	NO. OF SAMPLES
0.00	0.00	0.00	0.00	0.00	356.20	591.00	30.72	100.76	269.67	19.00	4
0.00	4000.00	1111.60	30.30	51.94	380.00	409.40	22.22	157.80	770.41	53.00	8
0.00	0.00	0.00	0.00	0.00	466.00	376.00	0.00	0.00	421.00	89.00	2
0.00	3776.00	0.00	0.00	0.00	0.00	0.00	0.00	197.60	1986.80	97.00	2
0.00	4272.00	2836.00	2286.00	1064.00	1270.00	500.00	514.80	842.00	1698.10	98.00	8
0.00	3516.00	2428.00	733.80	112.80	1480.00	404.00	181.80	1336.00	1274.05	102.00	8
0.00	1572.00	1354.00	274.00	49.90	1358.00	312.00	55.30	1042.80	752.25	109.00	8
32.20	976.80	997.60	197.20	29.40	1307.60	1325.60	137.00	671.40	705.33	116.00	8
22.98	769.40	755.60	168.60	15.58	1194.00	84.98	47.36	535.20	446.34	119.00	8
26.94	594.00	605.40	226.20	12.24	1210.40	75.06	113.40	412.40	406.14	132.00	8
23.86	275.60	286.60	192.20	10.72	1018.00	64.40	97.40	251.20	274.52	144.00	8
18.50	205.80	181.20	158.80	9.40	437.80	53.76	73.90	173.80	161.81	174.00	8
15.58	178.40	141.60	113.40	7.88	152.20	42.82	72.08	139.60	108.00	204.00	8
14.68	193.00	171.60	128.20	10.18	100.38	45.68	82.70	164.60	112.04	232.00	8
15.20	126.60	113.20	101.20	7.66	80.86	36.86	71.68	145.20	85.41	286.00	8
0.00	0.00	0.00	67.96	0.00	0.00	37.76	55.18	125.00	71.48	336.00	4
0.00	0.00	0.00	0.00	0.00	338.60	0.00	63.18	137.20	179.66	341.00	3
0.00	0.00	0.00	412.60	34.18	418.80	81.24	54.34	226.40	204.59	344.00	6
0.00	1328.00	625.00	397.00	107.00	285.80	75.80	65.72	211.40	384.46	350.00	8
0.00	884.00	522.60	183.20	33.86	239.00	82.16	100.00	85.20	266.25	397.00	8
0.00	0.00	0.00	171.60	17.32	76.16	73.34	159.00	45.82	90.54	420.00	6
0.00	1126.00	1322.00	0.00	40.48	698.60	224.80	226.00	200.00	548.27	468.00	7
0.00	0.00	1500.00	162.40	45.50	731.80	240.00	0.00	188.40	478.02	475.00	6
0.00	2192.00	2080.00	1118.00	82.00	600.40	211.20	1136.00	189.40	951.13	482.46	8
0.00	1902.00	2332.00	1486.00	254.60	732.80	170.20	649.00	174.20	962.60	482.67	8
162.20	1958.00	2492.00	1704.00	255.40	883.80	199.80	2086.00	207.40	1218.30	483.51	8
174.60	2118.00	5116.00	3334.00	446.40	1078.00	216.80	2162.00	282.40	1844.20	484.54	8
0.00	2106.00	4720.00	3002.00	228.20	1578.00	236.40	2112.00	677.20	1832.48	487.00	8
72.20	2096.00	4248.00	2858.00	121.40	1770.00	245.20	1960.00	811.00	1762.45	488.00	8
38.34	1342.00	3292.00	2308.00	104.60	1894.00	268.40	1542.00	1196.00	1493.38	495.00	8
20.68	0.00	2018.00	1560.00	68.66	1498.00	246.80	884.00	952.00	1032.49	502.00	7
20.72	245.00	1324.00	976.00	62.04	1244.00	0.00	732.00	748.00	761.58	509.00	7
15.08	98.40	481.60	232.80	49.50	490.80	307.40	393.80	531.40	322.98	539.00	8
0.00	63.34	170.80	131.00	41.32	62.68	303.20	303.60	397.60	184.19	572.00	8
0.00	0.00	0.00	0.00	0.00	37.10	203.20	171.20	258.00	167.38	621.00	4
0.00	1576.00	1324.00	319.80	27.18	106.80	158.20	147.80	202.20	482.75	648.00	8

Pond 1 Resaturation Monitoring Chemical Data TOTAL SELENIUM CONCENTRATION, ppb VS. DEPTH, m uz-4

The AVERAGE represents average of non-zero concentrations.
Zero values represent no sample recovery at that depth.

pond	0.15	0.30	0.46	0.61	0.76	0.91	1.07	1.22	AVERAGE	DAY	NO. OF SAMPLES
0.00	0.00	0.00	660.20	0.00	275.80	259.40	41.30	13.42	250.02	19.00	5
0.00	0.00	2366.00	226.00	2096.00	194.00	255.60	9.18	6.06	736.12	44.00	7
0.00	0.00	2734.00	1088.00	771.80	0.00	0.00	14.06	10.52	923.68	61.00	5
0.00	0.00	818.80	762.80	323.20	433.20	51.08	52.86	4.72	349.52	112.00	7
0.00	0.00	364.40	688.00	249.60	429.80	32.18	24.48	5.64	256.30	133.00	7
0.00	0.00	325.00	654.40	447.60	535.20	330.20	188.00	489.00	424.20	145.00	7
160.60	3336.00	205.00	122.00	1234.00	3196.00	1842.00	988.00	3268.00	1773.88	148.00	8
110.40	1066.00	70.50	70.12	148.60	3184.00	196.60	228.00	465.20	678.63	155.00	8
77.90	123.40	49.08	56.56	70.92	1252.00	73.62	59.46	71.88	219.62	174.00	8
65.76	30.86	0.00	39.00	41.48	56.80	42.48	31.92	37.14	39.95	203.00	7
80.22	32.84	45.48	36.88	42.72	61.54	42.64	38.54	39.24	42.49	231.00	8
0.00	12.34	22.52	12.46	33.48	28.32	37.96	26.80	33.26	25.89	286.00	8
0.00	0.00	0.00	0.00	0.00	0.00	0.00	0.00	27.04	27.04	336.00	1
0.00	0.00	0.00	0.00	0.00	0.00	0.00	149.00	38.74	93.87	341.00	2
0.00	0.00	0.00	0.00	673.80	0.00	425.00	144.60	53.96	324.34	344.00	4
0.00	0.00	0.00	0.00	876.00	0.00	342.20	127.60	80.80	356.65	350.00	4
0.00	0.00	0.00	0.00	0.00	906.00	105.20	64.32	80.86	289.10	397.00	4
0.00	0.00	0.00	0.00	1726.00	1040.00	85.20	24.16	62.38	587.55	420.00	5
0.00	0.00	0.00	0.00	1542.00	733.80	63.08	0.00	42.96	595.46	451.00	4
0.00	0.00	936.00	1204.00	807.00	268.00	54.50	19.82	43.64	447.57	472.00	7
0.00	0.00	729.20	984.00	460.20	162.80	104.60	18.08	58.10	359.57	478.00	7
75.40	3606.00	509.20	711.60	483.60	247.60	220.20	136.20	319.00	779.18	502.00	8
33.68	1508.00	500.20	52.50	63.32	64.54	41.70	78.48	663.80	371.57	509.00	8
45.40	48.42	34.20	21.30	25.52	27.80	19.74	22.56	36.82	29.56	539.00	8
0.00	0.00	0.00	0.00	0.00	0.00	0.00	0.00	18.96	18.96	621.00	1
0.00	0.00	1878.00	1912.00	1466.00	294.20	0.00	35.96	73.32	943.25	649.00	6

Pond 1 Resaturation Monitoring Chemical Data TOTAL SELENIUM CONCENTRATION, ppb VS. DEPTH, m uz-5

The AVERAGE represents average of non-zero concentrations.
Zero values represent no sample recovery at that depth.

pond	0.15	0.30	0.46	0.61	0.76	0.91	1.07	1.22	AVERAGE	DAY	NO. OF SAMPLES
0.00	430.20	0.00	0.00	0.00	0.00	0.00	0.00	0.00	430.20	28.00	1
0.00	4.12	0.00	0.00	0.00	28.20	14.94	4.90	4.16	11.26	44.00	5
0.00	416.40	268.80	0.00	0.00	0.00	9.82	4.56	4.12	140.54	72.00	5
0.00	378.60	0.00	76.08	0.00	0.00	25.82	6.10	8.82	98.88	83.00	5
0.00	864.00	545.20	598.40	0.00	254.00	28.08	7.92	5.22	298.97	102.00	7
0.00	224.40	471.80	108.40	52.36	412.60	23.86	6.50	4.52	163.06	106.00	8
46.58	156.00	76.00	36.72	44.64	460.40	17.26	6.88	5.56	100.18	112.00	8
47.52	137.20	60.00	34.00	43.54	419.60	20.96	6.10	8.72	91.26	117.00	8
0.00	104.00	44.20	28.60	36.14	357.40	19.12	7.94	8.92	75.79	120.00	8
26.36	116.00	41.18	23.04	11.54	270.00	15.52	4.80	9.18	61.28	123.00	8
29.62	108.36	54.56	33.66	22.84	202.60	20.74	6.58	18.48	58.48	133.00	8
27.18	101.40	51.14	30.48	20.62	132.20	21.86	8.02	26.84	48.94	144.00	8
24.82	53.54	42.34	22.70	16.80	60.44	22.86	7.46	22.48	31.08	174.00	8
21.24	24.90	37.26	19.66	13.04	43.40	24.68	8.18	21.98	24.14	204.00	8
17.78	22.22	38.78	20.76	18.52	40.62	31.76	10.14	10.34	24.14	232.00	8
14.32	30.12	29.92	14.32	17.48	31.82	24.38	6.22	4.52	19.85	287.00	8
7.02	49.62	19.72	13.80	20.68	15.66	19.32	3.98	3.22	18.25	336.00	8
0.00	64.58	15.84	13.18	17.72	15.50	19.80	4.00	3.26	19.24	337.00	8
0.00	65.54	19.56	16.50	0.00	17.36	24.74	4.08	4.28	21.72	341.00	7
0.00	131.20	23.68	18.18	0.00	18.78	27.42	4.36	3.34	32.42	344.00	7
0.00	104.20	39.34	42.72	0.00	14.54	21.72	2.90	2.40	32.55	350.00	7
0.00	0.00	0.00	0.00	0.00	0.00	0.00	3.68	3.00	3.34	397.00	2
0.00	0.00	0.00	0.00	0.00	0.00	0.00	5.26	0.00	5.26	405.00	1
0.00	0.00	0.00	0.00	0.00	0.00	0.00	7.58	3.38	5.48	420.00	2
0.00	0.00	0.00	0.00	0.00	0.00	0.00	5.98	3.50	4.74	448.00	2
0.00	0.00	381.00	748.20	222.80	140.60	0.00	5.76	3.14	250.25	451.00	6
0.00	607.60	428.00	582.00	88.60	137.20	31.00	6.14	4.12	235.58	472.00	8
0.00	0.00	426.80	551.80	60.56	99.60	26.38	3.98	2.94	167.44	476.00	7
0.00	3.06	1454.00	1780.00	1174.00	194.20	17.22	4.64	3.88	578.88	487.00	8
106.60	10.82	5.84	1258.00	730.40	194.40	15.88	3.78	2.32	277.68	488.00	8
43.58	7.22	3.88	2210.00	451.80	394.80	15.36	4.66	7.92	386.96	495.00	8
33.32	6.04	2.76	67.38	96.20	385.40	18.38	5.58	9.58	73.92	509.00	8
23.02	10.46	1.30	1.40	100.00	270.40	26.94	8.96	16.70	54.52	539.00	8
0.00	97.40	64.08	62.78	63.24	122.20	55.36	18.28	49.96	66.66	572.00	8
2.74	58.42	60.06	40.08	55.22	28.10	58.72	18.12	24.36	42.89	621.00	8
3.52	63.72	49.58	44.20	50.64	28.42	112.80	16.48	13.16	47.38	649.00	8

Pond 1 Resaturation Monitoring Chemical Data TOTAL SELENIUM CONCENTRATION, ppb VS. DEPTH, m uz-6

The AVERAGE represents average of non-zero concentrations.
Zero values represent no sample recovery at that depth.

pond	0.15	0.30	0.46	0.61	0.76	0.91	1.07	1.22	AVERAGE	DAY	NO. OF SAMPLES
0.00	0.00	0.00	40.16	25.46	10.32	9.08	5.58	4.56	15.86	28.00	6
0.00	0.00	20.78	15.34	13.30	4.30	5.40	3.96	3.20	9.47	61.00	7
0.00	0.00	51.94	23.54	18.52	5.34	5.56	4.04	3.34	16.04	90.00	7
0.00	254.60	179.20	173.20	0.00	10.56	5.76	4.38	4.64	90.33	98.00	7
0.00	196.20	171.60	168.00	196.80	8.56	5.96	4.24	5.48	94.33	102.00	8
0.00	53.24	132.00	145.20	107.60	4.68	4.92	2.30	2.08	56.50	106.00	8
30.40	32.84	72.40	75.80	19.94	3.86	5.12	2.28	2.14	26.80	112.00	8
63.08	42.70	92.16	81.64	20.40	5.46	8.86	6.64	6.24	33.01	117.00	8
0.00	52.58	66.32	60.82	14.00	3.36	7.90	2.26	1.84	26.13	120.00	8
34.72	80.56	73.66	67.30	13.92	0.00	8.68	2.06	1.04	35.32	132.00	7
28.40	103.00	58.68	66.84	18.02	6.50	13.18	4.86	5.00	34.51	144.00	8
22.44	75.58	49.60	59.94	15.54	5.44	14.78	4.72	3.66	28.66	174.00	8
20.58	52.64	38.56	49.34	13.50	4.50	11.80	4.02	2.20	22.07	203.00	8
19.72	22.02	39.16	55.62	15.28	5.44	16.42	4.96	3.22	20.27	231.00	8
14.54	0.00	17.84	39.70	10.96	3.64	12.14	3.36	2.46	12.87	286.00	7
24.04	12.12	6.80	8.82	12.16	3.22	7.70	2.86	2.64	7.04	337.00	8
19.88	11.98	8.30	7.96	11.68	1.84	3.64	2.50	2.34	6.28	398.00	8
0.00	0.00	0.00	0.00	0.00	3.88	5.50	4.08	3.48	4.24	468.00	4
0.00	237.40	46.84	0.00	158.20	2.50	3.60	2.80	2.74	64.87	472.00	7
0.00	146.20	36.84	38.36	62.00	2.20	3.68	2.82	2.68	36.85	476.00	8
127.00	180.80	193.20	208.00	137.80	3.06	3.82	2.62	3.16	91.56	483.47	8
107.40	116.00	132.00	179.00	164.60	2.83	3.72	2.04	2.38	75.32	484.46	8
0.00	53.80	64.82	117.00	59.02	2.28	3.28	2.34	2.26	38.10	487.00	8
24.64	40.60	52.28	128.00	33.78	1.98	3.56	2.66	2.50	33.17	488.00	8
29.26	30.02	22.72	117.20	15.18	2.42	3.40	2.70	2.62	24.53	495.00	8
35.24	22.36	13.46	50.90	10.22	2.60	3.92	2.56	2.34	13.54	509.00	8
20.56	20.46	11.68	32.58	12.02	3.36	4.64	2.90	2.28	11.24	539.00	8
0.00	21.24	12.04	31.40	13.04	4.60	5.52	4.10	3.16	11.89	572.00	8
20.34	12.10	8.16	10.92	8.60	3.16	4.38	3.54	2.12	8.82	621.00	8
46.98	11.06	8.10	15.86	8.00	2.42	3.18	2.50	1.94	8.63	649.00	8

Pond 1 Resaturation Monitoring Chemical Data TOTAL SELENIUM CONCENTRATION, ppb VS. DEPTH, m uz-7

The AVERAGE represents average of non-zero concentrations.
Zero values represent no sample recovery at that depth.

pond	0.15	0.30	0.46	0.61	0.76	0.91	1.07	1.22	AVERAGE	DAY	NO. OF SAMPLES
0.00	0.00	0.00	0.00	0.00	0.00	0.00	67.02	29.10	48.06	44.00	2
0.00	0.00	0.00	0.00	353.00	570.80	80.08	65.54	35.64	221.01	61.00	5
0.00	1606.40	0.00	0.00	374.00	615.20	88.40	0.00	0.00	671.00	84.00	4
0.00	0.00	0.00	0.00	0.00	171.60	36.66	53.32	37.68	74.82	113.00	4
0.00	0.00	0.00	206.00	0.00	125.40	63.88	71.36	52.90	103.91	120.00	5
0.00	0.00	0.00	157.40	56.56	143.80	94.40	105.20	67.84	104.20	145.00	6
0.00	0.00	0.00	145.40	37.40	45.00	93.20	90.80	126.00	89.63	203.00	6
0.00	0.00	6.34	76.90	19.22	22.86	67.98	140.20	15.02	49.79	231.00	7
0.00	0.00	0.00	13.58	11.58	11.10	13.60	15.06	7.48	12.07	287.00	6
0.00	0.00	132.40	50.40	0.00	9.54	0.00	11.28	7.74	42.27	337.00	5
0.00	0.00	0.00	0.00	0.00	71.56	0.00	18.24	0.00	44.90	398.00	2
0.00	0.00	0.00	0.00	0.00	157.60	0.00	71.94	0.00	114.77	478.00	2
0.00	0.00	165.40	173.80	0.00	46.52	0.00	203.60	60.06	129.88	649.00	5

Pond 1 Resaturation Monitoring Chemical Data TOTAL SELENIUM CONCENTRATION, ppb VS. DEPTH, m uz-8

The AVERAGE represents average of non-zero concentrations.
Zero values represent no sample recovery at that depth.

pond	0.15	0.30	0.46	0.61	0.76	0.91	1.07	1.22	AVERAGE	DAY	NO. OF SAMPLES
0.00	0.00	0.00	320.80	182.40	0.00	194.40	138.60	15.96	170.43	53.00	5
0.00	2424.00	662.80	256.40	0.00	299.80	199.60	134.20	16.90	570.53	92.00	7
0.00	1772.00	2822.00	2516.00	3024.00	1860.00	694.60	2036.00	0.00	2103.51	95.38	7
119.60	1104.00	2810.00	2810.00	2602.00	769.20	806.80	1344.00	625.60	1608.95	95.75	8
0.00	1430.00	2100.00	2014.00	1888.00	640.20	884.00	898.00	574.60	1303.60	99.00	8
0.00	1578.00	1842.00	1472.00	1940.00	391.80	1172.00	485.60	799.20	1210.07	104.00	8
0.00	1184.00	1140.00	1038.00	1622.00	118.80	1099.20	279.00	792.20	909.15	110.00	8
18.78	954.00	726.60	933.20	2046.00	55.64	1040.00	135.80	0.00	841.61	113.00	7
22.70	334.00	213.40	521.40	1670.40	67.10	935.60	68.20	136.40	493.31	117.00	8
0.00	193.60	137.80	359.60	1660.00	184.60	855.60	157.40	770.60	539.90	120.00	8
12.28	161.60	90.00	204.60	1240.00	236.80	711.60	154.80	695.40	436.85	124.00	8
16.88	121.00	127.12	118.40	1305.20	354.00	824.20	142.84	842.40	479.40	133.00	8
18.70	103.00	98.80	22.07	1076.00	468.60	687.00	164.60	779.60	424.98	145.00	8
14.98	66.92	56.28	32.52	574.20	428.00	439.40	163.20	710.40	308.87	173.00	8
18.46	35.40	23.40	24.46	171.80	432.60	323.60	187.80	265.60	183.08	203.00	8
17.62	28.28	15.90	27.00	72.94	379.20	261.00	145.40	97.88	128.45	232.00	8
6.46	18.28	9.76	14.38	64.72	218.80	108.80	37.28	96.40	71.05	286.00	8
11.44	15.88	8.06	12.76	35.50	68.96	49.28	17.68	44.10	31.53	336.00	8
6.24	12.24	6.14	12.02	18.26	26.92	9.80	10.16	4.76	12.54	350.00	8
3.44	10.98	5.78	8.24	17.66	28.22	7.70	9.24	4.90	11.59	398.00	8
0.00	0.00	0.00	0.00	17.32	22.88	8.10	6.96	5.68	12.19	448.00	5
0.00	317.60	0.00	0.00	20.20	12.82	8.72	5.90	7.36	62.10	468.00	6
0.00	422.60	91.60	74.36	16.16	10.92	7.36	5.78	5.30	79.26	472.00	8
0.00	438.20	59.74	48.02	15.06	10.06	7.72	6.46	5.76	73.88	475.00	8
0.00	781.60	70.14	36.54	15.50	9.30	7.24	0.00	4.88	132.17	476.75	7
90.00	492.40	154.00	243.00	130.20	10.86	6.46	86.60	4.34	140.98	477.38	8
76.52	362.20	212.60	546.60	769.40	9.00	6.48	242.40	4.82	269.19	477.52	8
0.00	0.00	241.40	626.60	908.00	9.44	7.04	261.40	4.90	294.11	477.73	7
32.08	366.20	234.20	691.20	819.80	9.74	7.04	249.20	5.46	297.86	478.38	8
25.56	243.00	217.00	674.20	746.80	8.90	5.66	190.80	4.84	261.40	478.60	8
15.32	308.00	144.00	511.20	476.60	9.20	5.76	79.54	5.02	192.42	479.46	8
0.00	233.00	69.84	399.40	323.80	9.04	5.60	17.32	4.52	132.82	481.67	8
0.00	145.40	50.42	246.80	189.20	8.52	5.50	12.88	5.68	83.05	482.63	8
6.50	115.80	29.48	146.80	105.60	7.72	4.16	9.12	3.84	52.82	483.67	8
12.10	92.20	24.00	89.40	75.12	7.60	4.06	8.20	3.50	38.01	484.50	8
0.00	63.10	16.66	46.38	41.40	8.86	5.50	9.36	4.84	24.51	487.00	8
4.86	34.78	13.16	25.68	24.16	11.58	5.24	7.52	5.10	15.90	495.00	8
8.40	23.26	13.80	9.44	18.40	15.14	6.38	7.72	6.16	12.54	509.00	8
9.02	11.66	6.82	9.56	13.18	20.12	7.62	7.20	6.04	10.28	539.00	8
0.00	11.72	5.98	8.56	13.38	28.96	11.68	9.40	7.14	12.10	572.00	8
14.64	15.84	8.22	31.12	11.86	16.60	7.66	7.80	6.58	13.21	621.00	8
26.62	17.12	9.98	28.20	13.56	14.84	6.10	6.98	6.10	12.86	648.00	8

Pond 1 Resaturation Monitoring Chemical Data TOTAL SELENIUM CONCENTRATION, ppb VS. DEPTH, m uz-9

The AVERAGE represents average of non-zero concentrations.
Zero values represent no sample recovery at that depth.

pond	0.15	0.30	0.46	0.61	0.76	0.91	1.07	1.22	AVERAGE	DAY	NO. OF SAMPLES
0.00	0.00	0.00	1004.00	0.00	0.00	221.40	0.00	0.00	612.70	61.00	2
0.00	4656.00	0.00	1664.00	0.00	353.60	69.42	7.16	10.32	1126.75	79.00	6
0.00	2328.00	2468.00	848.80	181.60	72.78	16.64	4.54	10.70	741.38	104.00	8
0.00	0.00	2122.00	656.40	98.00	28.74	5.66	3.66	3.86	416.90	113.00	7
0.00	0.00	1916.00	646.00	30.66	13.18	4.04	3.78	4.46	374.02	133.00	7
0.00	0.00	1386.00	302.80	16.00	7.72	4.92	3.84	5.40	246.67	145.00	7
0.00	0.00	945.60	205.40	159.20	10.50	22.00	29.06	5.02	196.68	173.00	7
0.00	0.00	0.00	102.00	147.20	9.86	4.52	54.88	4.06	53.75	204.00	6
0.00	3752.00	2398.00	1004.00	1984.00	147.20	48.94	1011.20	801.00	1368.29	231.00	8
0.00	790.00	108.60	22.58	179.60	81.40	6.18	74.88	16.00	159.91	286.00	8
0.00	0.00	0.00	0.00	0.00	0.00	0.00	0.00	5.66	5.66	336.00	1
0.00	0.00	2642.00	824.80	184.00	28.12	13.14	12.76	4.88	529.96	341.00	7
0.00	0.00	2494.00	784.00	162.60	26.34	9.36	6.62	3.04	497.99	350.00	7
0.00	0.00	2614.00	823.20	231.20	39.54	13.20	14.06	3.42	519.80	397.00	7
0.00	0.00	2074.00	560.80	363.40	48.90	14.60	16.36	4.66	440.39	468.00	7
0.00	0.00	1478.00	353.20	152.20	18.66	5.76	105.00	5.10	302.56	478.00	7
0.00	0.00	1096.00	352.20	219.20	21.40	4.14	14.48	7.52	244.99	649.00	7

Pond 1 Resaturation Monitoring Chemical Data SELENITE CONCENTRATION, ppb VS. DEPTH, m uz-1

The AVERAGE represents average of non-zero concentrations.
Zero values represent no sample recovery at that depth.

pond	0.15	0.30	0.46	0.61	0.76	0.91	1.07	1.22	AVERAGE	DAY	NO. OF SAMPLES
0.00	0.00	31.03	0.00	3.04	0.00	15.38	0.00	0.00	16.48	19.00	3
0.00	11.54	26.48	6.36	0.00	2.36	4.37	3.30	3.82	8.32	28.00	7
0.00	13.21	0.00	5.46	3.77	11.18	9.04	5.90	0.00	8.09	53.00	6
0.00	9.95	0.00	4.71	0.00	0.00	9.17	5.48	0.00	7.33	84.00	4
0.00	0.00	9.34	3.14	3.95	7.11	8.95	3.77	4.26	5.79	96.00	7
29.26	30.07	176.90	23.49	105.40	7.66	91.50	5.18	5.53	55.72	97.00	8
21.84	172.70	27.17	25.81	18.56	10.38	37.22	6.07	6.85	38.10	104.00	8
17.26	12.17	122.90	13.61	13.44	8.86	27.94	5.65	5.99	26.32	109.00	8
14.77	9.40	45.00	9.31	7.65	10.76	21.57	5.90	6.86	14.56	116.00	8
8.59	1.14	3.89	0.79	0.67	8.91	21.40	5.75	5.98	6.07	119.00	8
10.88	11.19	20.28	6.37	6.06	7.56	5.45	26.29	6.50	11.21	124.00	8
10.69	12.36	13.39	6.61	7.21	9.82	27.58	5.80	6.86	11.20	132.00	8
8.56	7.02	27.79	9.05	9.35	9.52	23.18	5.94	8.26	12.51	144.00	8
8.24	8.47	16.92	11.70	22.07	8.42	11.63	6.00	6.01	11.40	173.00	8
7.01	3.08	6.96	5.97	38.14	10.82	12.70	4.90	5.72	11.04	204.00	8
3.81	2.54	4.17	3.17	2.30	12.01	9.46	4.92	5.57	5.52	232.00	8
9.58	2.91	6.68	2.96	10.57	11.23	7.70	4.49	2.60	6.14	286.00	8
13.77	16.52	22.04	13.14	28.72	10.33	10.99	6.38	5.92	14.25	337.00	8
13.24	10.38	8.45	11.93	16.55	10.27	10.39	2.42	5.62	9.50	341.00	8
9.80	5.95	5.01	6.67	6.56	6.08	9.90	6.84	6.32	6.67	344.00	8
4.31	3.89	5.50	2.57	14.01	6.78	8.25	5.97	5.27	6.53	398.00	8
0.00	3.27	4.32	2.90	10.07	6.04	7.02	3.15	7.19	5.50	420.00	8
0.00	0.00	0.00	3.85	0.00	0.00	6.22	6.30	5.65	5.51	448.00	4
0.00	38.92	14.98	6.62	17.12	6.89	5.09	5.36	5.50	12.56	451.00	8
0.00	13.28	23.91	6.11	14.85	6.67	4.02	4.40	3.87	9.64	476.00	8
29.96	15.73	26.36	7.05	24.37	6.72	4.65	4.13	4.79	11.72	478.40	8
24.66	0.00	32.59	7.13	29.34	6.48	4.75	4.10	4.72	12.73	478.71	7
18.05	36.78	20.22	5.83	4.00	6.55	4.57	4.18	4.79	10.87	479.69	8
0.00	19.09	48.80	6.35	38.32	6.17	2.51	3.84	4.09	16.15	481.79	8
0.00	18.51	53.50	6.37	36.78	6.23	1.77	3.36	2.86	16.17	482.55	8
5.42	60.90	16.32	6.47	37.72	6.05	2.45	3.30	3.20	17.05	483.71	8
6.91	69.50	14.85	5.36	35.30	6.09	2.63	3.59	3.63	17.62	484.55	8
0.00	14.58	70.00	6.46	51.80	7.03	3.38	4.01	3.54	20.10	487.00	8
2.99	19.20	62.80	9.98	40.61	6.48	3.04	3.18	3.30	18.57	495.00	8
3.51	22.89	32.45	10.18	29.10	6.73	3.42	4.07	4.23	14.13	502.00	8
6.83	19.15	19.26	10.41	23.94	7.22	3.92	4.65	4.48	11.63	509.00	8
5.58	13.16	9.61	7.95	33.16	7.14	4.05	4.74	4.09	10.49	539.00	8
2.36	10.19	4.92	6.30	13.34	6.56	3.79	3.77	3.15	6.50	572.00	8
0.00	0.00	0.00	0.00	19.07	8.23	3.61	3.87	2.79	7.51	621.00	5
0.00	0.00	0.00	4.33	20.59	5.35	3.10	3.19	2.98	6.59	648.00	6

Pond 1 Resaturation Monitoring Chemical Data SELENITE CONCENTRATION, ppb VS. DEPTH, m uz-2

The AVERAGE represents average of non-zero concentrations.
Zero values represent no sample recovery at that depth.

pond	0.15	0.30	0.46	0.56	0.71	AVERAGE	DAY	NO. OF SAMPLES
0.00	22.88	10.19	2.40	2.50	2.23	8.04	72.00	5
0.00	18.23	5.80	1.73	1.20	1.20	5.63	94.00	5
0.00	12.66	4.06	1.49	1.32	1.29	4.16	113.00	5
0.00	15.46	3.97	1.25	0.83	1.16	4.53	120.00	5
0.00	15.54	4.22	1.43	1.34	1.82	4.87	133.00	5
0.00	18.37	6.43	2.14	2.30	2.28	6.30	145.00	5
0.00	0.00	0.00	0.00	0.00	0.00	0.00	148.00	0
0.00	40.70	39.71	0.76	0.67	0.87	16.54	155.00	5
44.60	62.00	67.70	2.15	1.57	1.69	27.02	173.00	5
37.20	73.70	0.00	1.63	1.98	1.89	19.80	204.00	4
15.60	63.30	86.30	1.44	1.63	1.63	30.86	231.00	5
0.00	0.00	6.63	0.96	1.17	1.53	2.57	288.00	4
0.00	29.70	12.53	1.79	1.80	1.94	9.55	336.00	5
0.00	0.00	13.47	1.81	1.53	1.64	4.61	397.00	4
0.00	37.17	13.71	2.13	2.98	0.00	14.00	478.00	4
0.00	35.60	2.94	1.73	2.07	10.07	10.48	649.00	5

Pond 1 Resaturation Monitoring Chemical Data SELENITE CONCENTRATION, ppb VS. DEPTH, m uz-3

The AVERAGE represents average of non-zero concentrations.
Zero values represent no sample recovery at that depth.

pond	0.15	0.30	0.46	0.61	0.76	0.91	1.07	1.22	AVERAGE	DAY	NO. OF SAMPLES
0.00	0.00	0.00	0.00	0.00	75.40	30.95	4.50	5.22	29.02	19.00	4
0.00	196.30	62.90	9.10	25.68	53.80	53.30	8.18	9.39	52.33	53.00	8
0.00	0.00	0.00	0.00	0.00	34.41	46.10	0.00	0.00	40.26	89.00	2
0.00	70.10	0.00	0.00	0.00	0.00	0.00	0.00	23.53	46.81	97.00	2
0.00	78.00	50.50	36.11	34.00	26.72	7.67	7.35	9.26	31.20	98.00	8
19.83	167.50	124.40	143.40	67.70	87.10	76.00	34.10	38.11	92.29	102.00	8
17.48	83.70	127.90	182.60	39.68	118.70	90.20	31.41	116.80	98.87	109.00	8
14.19	81.60	125.30	144.90	21.09	116.20	76.00	26.41	105.00	87.06	116.00	8
6.91	98.90	95.50	114.00	5.49	92.30	48.20	22.22	95.10	71.46	119.00	8
10.50	146.10	107.70	116.70	3.14	106.50	44.60	40.30	94.50	82.44	132.00	8
5.80	155.70	105.30	109.40	3.06	121.80	37.25	35.31	59.30	78.39	144.00	8
8.53	127.10	99.90	94.70	3.93	107.80	37.90	33.60	63.70	71.08	174.00	8
6.58	127.10	82.90	84.70	3.98	86.60	30.95	31.96	58.80	63.37	204.00	8
0.71	122.30	97.20	85.10	4.11	71.20	28.56	38.20	50.80	62.18	232.00	8
0.00	71.10	46.00	67.30	1.47	50.80	24.81	31.16	41.40	41.76	286.00	8
0.00	0.00	0.00	36.58	0.00	0.00	28.44	34.06	4.91	26.00	336.00	4
0.00	0.00	0.00	0.00	0.00	67.20	0.00	24.87	41.30	44.46	341.00	3
0.00	0.00	0.00	58.60	19.16	82.00	28.38	28.16	41.50	42.97	344.00	6
0.00	131.70	100.40	78.00	28.12	80.10	36.41	36.16	38.00	66.11	350.00	8
0.00	129.60	78.30	59.30	20.08	73.50	39.83	40.80	27.51	58.62	397.00	8
0.00	0.00	0.00	80.50	8.82	35.76	41.44	81.30	14.60	43.74	420.00	6
0.00	110.20	90.40	0.00	18.46	60.80	31.19	60.50	40.11	58.81	468.00	7
0.00	0.00	0.00	48.90	18.65	45.50	31.18	0.00	32.25	35.30	475.00	5
0.00	105.20	56.40	49.70	20.15	75.10	31.85	70.20	37.10	55.71	482.46	8
0.00	96.90	54.10	41.80	27.15	43.60	25.17	57.70	30.70	47.14	482.67	8
17.84	93.40	76.50	47.40	35.84	44.07	24.45	58.80	32.17	51.58	483.51	8
20.50	109.80	117.50	37.70	66.40	43.60	25.03	57.70	32.35	61.26	484.54	8
0.00	133.50	127.30	43.10	93.00	55.00	27.08	60.30	36.87	72.02	487.00	8
5.44	170.60	178.00	51.40	76.20	64.20	26.73	69.30	40.05	84.56	488.00	8
3.50	207.20	165.40	80.20	76.90	69.50	29.53	82.20	49.80	95.09	495.00	8
2.30	0.00	160.30	90.40	52.80	65.70	29.18	92.50	55.40	78.04	502.00	7
6.74	145.30	177.60	98.30	44.50	82.70	0.00	93.00	59.00	100.06	509.00	7
6.01	52.50	138.20	92.10	32.13	86.20	29.71	72.10	58.30	70.15	539.00	8
0.00	28.62	95.70	87.90	23.35	26.30	27.39	27.58	55.10	46.49	572.00	8
0.00	0.00	0.00	0.00	0.00	13.63	27.24	74.80	54.10	42.44	621.00	4
0.00	70.90	72.00	51.40	14.47	46.70	29.08	0.00	49.00	47.65	648.00	7

Pond 1 Resaturation Monitoring Chemical Data SELENITE CONCENTRATION, ppb VS. DEPTH, m uz-4

The AVERAGE represents average of non-zero concentrations.
Zero values represent no sample recovery at that depth.

pond	0.15	0.30	0.46	0.61	0.76	0.91	1.07	1.22	AVERAGE	DAY	NO. OF SAMPLES
0.00	0.00	0.00	5.90	0.00	3.92	2.89	2.72	1.59	3.40	19.00	5
0.00	0.00	18.53	13.88	15.77	3.72	2.95	2.46	1.88	8.46	44.00	7
0.00	0.00	28.40	15.27	10.13	0.00	0.00	2.78	2.28	11.77	61.00	5
0.00	0.00	9.02	16.31	7.24	1.65	1.98	3.82	1.08	5.87	112.00	7
0.00	0.00	20.68	14.97	7.12	2.66	2.24	7.19	1.76	8.09	133.00	7
0.00	0.00	13.11	10.39	7.52	2.58	3.36	6.57	3.64	6.74	145.00	7
104.90	52.70	75.30	41.30	131.61	28.05	113.90	54.90	139.20	79.62	148.00	8
44.50	73.80	30.10	34.16	35.96	42.20	65.90	47.70	102.00	53.98	155.00	8
34.70	36.30	18.27	22.95	28.74	119.80	29.00	24.22	30.26	38.69	174.00	8
25.35	4.09	0.00	6.72	8.59	13.71	10.38	6.14	7.24	8.12	203.00	7
27.94	6.52	10.87	5.68	8.10	25.11	10.87	6.16	8.76	10.26	231.00	8
0.00	2.25	6.62	1.86	9.46	5.88	8.66	6.85	9.25	6.35	286.00	8
0.00	0.00	0.00	0.00	0.00	0.00	0.00	0.00	10.98	10.98	336.00	1
0.00	0.00	0.00	0.00	0.00	0.00	0.00	37.57	14.95	26.26	341.00	2
0.00	0.00	0.00	0.00	30.21	0.00	72.30	26.27	24.50	38.32	344.00	4
0.00	0.00	0.00	0.00	58.50	0.00	45.80	28.48	28.11	40.22	350.00	4
0.00	0.00	0.00	0.00	0.00	115.90	53.00	31.13	43.40	60.86	397.00	4
0.00	0.00	0.00	0.00	295.60	82.00	41.07	13.16	35.87	93.54	420.00	5
0.00	0.00	0.00	0.00	70.30	50.10	24.46	0.00	16.07	40.23	451.00	4
0.00	0.00	29.61	48.10	34.53	30.34	20.88	9.07	15.16	26.81	472.00	7
0.00	0.00	26.49	33.23	19.14	22.89	20.98	9.27	19.89	21.70	478.00	7
24.07	30.20	21.81	29.32	32.03	23.32	23.90	9.65	26.13	24.55	502.00	8
11.98	59.30	22.64	13.58	25.80	28.29	14.57	21.33	92.70	34.78	509.00	8
11.60	4.24	6.70	6.05	8.55	11.81	5.97	7.57	11.35	7.78	539.00	8
0.00	0.00	0.00	0.00	0.00	0.00	0.00	0.00	8.17	8.17	621.00	1
0.00	0.00	50.00	30.64	75.10	24.75	0.00	17.33	47.70	40.92	649.00	6

Pond 1 Resaturation Monitoring Chemical Data SELENITE CONCENTRATION, ppb VS. DEPTH, m uz-5

The AVERAGE represents average of non-zero concentrations.
Zero values represent no sample recovery at that depth.

pond	0.15	0.30	0.46	0.61	0.76	0.91	1.07	1.22	AVERAGE	DAY	NO. OF SAMPLES
0.00	24.89	0.00	0.00	0.00	0.00	0.00	0.00	0.00	24.89	28.00	1
0.00	16.22	0.00	0.00	0.00	6.88	4.32	1.63	1.64	6.14	44.00	5
0.00	31.40	9.78	0.00	0.00	0.00	4.19	2.51	2.27	10.03	72.00	5
0.00	23.35	0.00	11.61	0.00	0.00	7.25	2.95	2.12	9.46	83.00	5
32.26	297.50	80.10	165.70	0.00	10.59	6.20	2.85	1.74	80.67	102.00	7
30.45	41.80	139.70	45.00	8.68	15.21	6.59	3.15	2.35	32.81	106.00	8
22.18	4.70	21.66	2.92	14.44	15.57	5.96	2.84	1.54	8.70	112.00	8
17.34	36.50	20.00	14.67	16.44	19.00	5.01	1.88	1.01	14.31	117.00	8
0.00	4.71	0.60	1.48	14.31	12.27	3.76	0.63	0.37	4.77	120.00	8
13.36	0.00	0.00	0.00	4.71	13.08	3.95	1.77	1.02	4.91	123.00	5
9.86	2.38	9.01	16.30	9.84	16.27	4.27	2.02	1.52	7.70	133.00	8
6.58	4.84	7.05	27.30	8.87	11.14	4.20	2.66	2.12	8.52	144.00	8
10.04	4.59	11.65	7.10	5.77	11.58	3.66	1.44	1.75	5.94	174.00	8
7.54	5.17	8.47	7.70	3.70	11.01	4.21	2.04	2.01	5.54	204.00	8
1.32	7.23	7.61	5.12	4.70	14.44	5.93	2.55	1.94	6.19	232.00	8
0.00	15.97	10.76	5.22	2.06	13.59	3.59	1.80	1.42	6.80	287.00	8
5.91	13.00	7.87	4.80	2.84	9.68	5.68	1.58	1.63	5.89	336.00	8
0.00	34.10	4.74	3.30	4.03	3.56	5.35	1.55	1.65	7.28	337.00	8
0.00	23.90	6.19	4.20	0.00	5.85	6.24	1.65	1.60	7.09	341.00	7
0.00	96.10	8.54	6.85	0.00	9.22	8.88	2.28	2.12	19.14	344.00	7
0.00	46.10	15.43	22.44	0.00	5.06	8.04	1.63	1.59	14.33	350.00	7
0.00	0.00	0.00	0.00	0.00	0.00	0.00	2.09	1.68	1.88	397.00	2
0.00	0.00	0.00	0.00	0.00	0.00	0.00	1.78	0.00	1.78	405.00	1
0.00	0.00	0.00	0.00	0.00	0.00	0.00	2.93	2.87	2.90	420.00	2
0.00	0.00	0.00	0.00	0.00	0.00	0.00	2.10	2.37	2.23	448.00	2
0.00	0.00	82.30	55.50	44.10	24.54	0.00	2.81	2.39	35.27	451.00	6
0.00	0.00	81.30	37.79	25.99	18.66	10.92	2.66	2.28	25.66	472.00	7
0.00	0.00	80.40	27.04	19.05	13.36	8.74	2.31	2.15	21.86	476.00	7
0.00	154.40	187.90	198.90	1036.00	15.80	5.72	1.48	1.73	200.24	487.00	8
28.69	307.00	247.30	76.00	165.40	12.52	4.42	0.84	0.88	101.80	488.00	8
5.87	41.40	96.90	388.50	87.50	18.20	4.22	1.19	1.58	79.94	495.00	8
13.80	29.40	77.90	285.70	14.96	23.95	4.37	1.53	1.22	54.88	509.00	8
7.48	16.90	11.00	39.40	51.60	18.39	4.19	1.71	1.29	18.06	539.00	8
0.00	26.10	17.32	21.29	33.13	21.03	5.05	3.00	3.17	16.26	572.00	8
96.70	22.54	32.16	14.25	26.10	18.69	5.30	2.60	2.73	15.55	621.00	8
20.50	25.50	16.34	16.39	23.20	18.33	8.09	3.57	3.63	14.38	649.00	8

Pond 1 Resaturation Monitoring Chemical Data SELENITE CONCENTRATION, ppb VS. DEPTH, m uz-6

The AVERAGE represents average of non-zero concentrations.
Zero values represent no sample recovery at that depth.

pond	0.15	0.30	0.46	0.61	0.76	0.91	1.07	1.22	AVERAGE	DAY	NO. OF SAMPLES
0.00	0.00	0.00	3.01	3.52	3.21	3.41	3.24	3.39	3.30	28.00	6
0.00	0.00	2.75	3.01	4.75	3.11	3.24	2.61	3.08	3.22	61.00	7
0.00	0.00	3.77	3.42	4.35	3.35	3.22	3.17	3.29	3.51	90.00	7
0.00	26.68	6.00	6.36	0.00	2.00	2.25	2.09	1.96	6.76	98.00	7
17.82	69.00	14.13	12.31	39.86	2.34	2.13	1.97	2.95	18.09	102.00	8
22.14	11.10	21.98	16.60	45.42	2.62	2.64	2.19	2.12	13.08	106.00	8
19.04	7.55	20.06	15.03	9.78	1.85	1.81	1.57	1.47	7.39	112.00	8
17.91	3.11	5.16	6.26	6.31	1.63	1.53	1.57	1.43	3.38	117.00	8
0.00	19.30	12.43	10.07	2.58	1.60	1.68	1.12	1.42	6.27	120.00	8
12.53	31.67	37.38	11.60	6.20	0.00	2.22	1.84	1.91	13.26	132.00	7
6.87	34.02	12.38	12.06	5.30	2.31	2.59	2.45	2.54	9.21	144.00	8
4.44	36.12	12.28	10.31	4.88	1.73	2.03	1.94	1.91	8.90	174.00	8
5.53	24.74	10.15	7.90	4.00	1.85	1.71	1.91	1.74	6.75	203.00	8
2.34	11.49	13.63	11.05	5.28	2.71	3.08	3.12	2.64	6.63	231.00	8
0.00	0.00	8.32	10.43	4.57	2.60	2.54	2.72	2.60	4.83	286.00	7
13.56	6.05	3.60	7.02	8.14	2.63	2.88	2.27	2.49	4.39	337.00	8
11.04	5.58	4.23	5.66	6.99	2.39	3.09	2.53	2.69	4.14	398.00	8
0.00	0.00	0.00	0.00	0.00	2.83	3.36	2.85	3.26	3.08	468.00	4
0.00	28.23	5.97	0.00	10.46	2.84	3.37	2.99	3.02	8.13	472.00	7
0.00	20.13	5.46	7.01	9.92	2.72	3.26	2.97	3.00	6.81	476.00	8
18.94	11.47	9.06	7.08	12.03	2.05	2.49	2.29	2.34	6.10	483.47	8
8.82	24.18	9.97	8.72	13.94	1.98	2.28	2.30	2.41	8.22	484.46	8
0.00	19.36	15.46	12.03	19.40	1.90	2.35	2.27	2.43	9.40	487.00	8
4.33	15.03	20.03	13.23	17.44	1.91	2.35	2.36	2.27	9.33	488.00	8
4.37	12.41	11.00	14.80	6.14	2.06	2.41	2.35	2.29	6.68	495.00	8
17.00	8.74	5.44	14.93	2.93	2.46	2.93	2.82	2.75	5.38	509.00	8
2.29	7.71	4.35	1.99	4.66	1.82	2.30	2.68	2.21	3.47	539.00	8
0.00	7.79	5.12	19.08	6.38	3.28	3.31	4.11	3.25	6.54	572.00	8
11.30	4.01	2.28	4.99	2.88	2.21	2.19	2.50	1.92	2.87	621.00	8
47.60	4.18	3.20	10.61	4.04	2.84	3.03	3.00	2.62	4.19	649.00	8

Pond 1 Resaturation Monitoring Chemical Data SELENITE CONCENTRATION, ppb VS. DEPTH, m uz-7

The AVERAGE represents average of non-zero concentrations.
Zero values represent no sample recovery at that depth.

pond	0.15	0.30	0.46	0.61	0.76	0.91	1.07	1.22	AVERAGE	DAY	NO. OF SAMPLES
0.00	0.00	0.00	0.00	0.00	0.00	0.00	5.74	5.34	5.54	44.00	2
0.00	0.00	0.00	0.00	15.69	11.50	5.20	5.24	5.23	8.57	61.00	5
0.00	13.05	0.00	0.00	9.60	8.70	6.24	0.00	0.00	9.40	84.00	4
0.00	0.00	0.00	0.00	0.00	7.95	2.92	2.16	1.75	3.69	113.00	4
0.00	0.00	0.00	6.59	0.00	5.83	3.82	2.54	2.46	4.25	120.00	5
0.00	0.00	0.00	4.80	11.56	7.06	5.20	4.01	3.99	6.10	145.00	6
0.00	0.00	0.00	50.70	8.30	9.66	6.59	4.19	9.76	14.87	203.00	6
0.00	0.00	4.88	26.38	12.40	6.40	23.10	26.20	6.84	15.17	231.00	7
0.00	0.00	0.00	7.63	8.05	6.46	8.76	10.03	4.68	7.60	287.00	6
0.00	0.00	26.30	21.20	0.00	7.40	0.00	8.85	5.75	13.90	337.00	5
0.00	0.00	0.00	0.00	0.00	13.47	0.00	13.35	0.00	13.41	398.00	2
0.00	0.00	0.00	0.00	0.00	10.70	0.00	22.80	0.00	16.75	478.00	2
0.00	0.00	21.70	30.20	0.00	28.90	0.00	13.30	38.07	26.43	649.00	5

Pond 1 Resaturation Monitoring Chemical Data SELENITE CONCENTRATION, ppb VS. DEPTH, m uz-8

The AVERAGE represents average of non-zero concentrations.
Zero values represent no sample recovery at that depth.

pond	0.15	0.30	0.46	0.61	0.76	0.91	1.07	1.22	AVERAGE	DAY	NO. OF SAMPLES
0.00	0.00	0.00	37.00	13.87	0.00	11.98	10.58	5.12	15.71	53.00	5
0.00	81.80	53.00	18.78	0.00	9.41	11.89	5.66	3.81	26.34	92.00	7
0.00	163.90	96.10	69.20	84.30	115.90	10.95	70.60	0.00	87.28	95.38	7
25.98	120.40	97.70	137.40	116.50	82.70	11.63	106.60	10.25	85.40	95.75	8
9.29	168.40	116.10	161.70	130.20	98.80	13.20	115.60	11.90	101.74	99.00	8
11.97	245.50	164.30	206.10	139.50	128.50	19.03	125.80	11.35	130.01	104.00	8
9.21	274.10	199.20	184.20	117.50	67.20	15.57	82.60	10.02	118.80	110.00	8
11.02	289.80	194.00	151.50	113.40	26.43	11.09	56.30	0.00	120.36	113.00	7
12.06	258.80	114.60	134.90	136.90	24.63	23.94	60.44	11.30	95.69	117.00	8
0.00	115.10	40.20	119.50	99.70	34.45	18.42	57.40	9.20	61.75	120.00	8
7.37	60.50	22.02	90.20	61.60	44.33	14.70	54.10	6.93	44.30	124.00	8
8.44	56.24	30.07	50.62	73.30	67.40	23.99	57.20	8.09	45.86	133.00	8
8.03	35.65	19.23	18.58	84.40	82.30	17.69	58.70	8.61	40.65	145.00	8
7.49	33.92	17.90	13.88	59.20	85.50	13.47	63.50	8.59	37.00	173.00	8
5.89	17.02	9.44	11.93	76.30	92.00	9.68	73.50	8.20	37.26	203.00	8
2.53	11.73	5.50	15.15	36.42	121.42	13.67	90.30	9.14	37.92	232.00	8
0.00	9.16	4.09	8.24	43.50	103.60	13.42	24.56	8.55	26.89	286.00	8
7.53	8.07	4.02	5.82	22.45	51.00	11.35	9.75	9.63	15.28	336.00	8
4.47	5.33	2.24	4.60	9.57	17.97	5.38	4.40	0.56	6.26	350.00	8
1.44	5.91	3.40	5.93	10.80	12.79	5.12	5.14	2.42	6.44	398.00	8
0.00	0.00	0.00	0.00	12.91	10.91	4.82	4.08	2.76	7.10	448.00	5
0.00	32.87	0.00	0.00	13.79	7.63	4.23	2.98	4.08	10.93	468.00	6
0.00	34.89	19.62	33.86	10.57	6.44	4.03	2.64	3.00	14.38	472.00	8
0.00	33.87	19.59	32.78	9.72	6.60	4.69	3.17	3.42	14.23	475.00	8
0.00	37.02	18.55	26.87	8.61	5.79	4.19	0.00	3.53	14.94	476.75	7
25.16	39.22	17.95	28.80	11.70	7.83	4.36	3.66	3.27	14.60	477.38	8
20.29	53.20	19.71	28.73	40.40	6.28	4.04	4.13	3.22	19.96	477.52	8
0.00	0.00	20.54	29.14	33.50	5.87	4.02	4.12	2.97	14.31	477.73	7
8.97	44.00	16.97	27.02	32.90	5.82	3.85	5.64	2.88	17.39	478.38	8
8.57	0.00	15.28	31.35	47.80	5.78	3.84	0.00	2.84	17.81	478.60	6
2.69	44.60	19.17	32.18	76.30	5.78	3.59	10.85	2.68	24.39	479.46	8
0.00	48.50	26.27	40.95	94.50	6.64	4.01	9.62	2.86	29.17	481.67	8
0.00	0.00	28.76	53.70	89.60	5.64	3.22	7.11	2.46	27.21	482.63	7
2.63	35.80	19.45	64.20	81.50	6.37	3.06	5.77	2.27	27.30	483.67	8
4.77	42.79	18.51	59.30	59.90	5.91	2.99	4.88	2.42	24.59	484.50	8
0.00	32.53	13.39	38.31	30.40	6.98	3.42	5.21	2.98	16.65	487.00	8
2.44	22.93	9.58	18.84	12.12	7.47	3.00	3.61	3.16	10.09	495.00	8
4.10	15.26	6.36	8.29	6.73	7.98	3.08	3.29	3.50	6.81	509.00	8
0.73	6.50	3.11	5.14	4.22	8.79	2.58	3.47	2.88	4.58	539.00	8
0.00	7.25	3.98	5.37	5.70	9.17	3.58	3.19	3.55	5.22	572.00	8
8.85	9.58	4.50	17.76	4.43	4.93	2.91	3.90	3.20	6.40	621.00	8
19.91	11.58	5.80	20.36	6.64	5.71	3.14	3.59	2.94	7.47	648.00	8

Pond 1 Resaturation Monitoring Chemical Data SELENITE CONCENTRATION, ppb VS. DEPTH, m uz-9

The AVERAGE represents average of non-zero concentrations.
Zero values represent no sample recovery at that depth.

pond	0.15	0.30	0.46	0.61	0.76	0.91	1.07	1.22	AVERAGE	DAY	NO. OF SAMPLES
0.00	0.00	0.00	22.37	0.00	0.00	8.04	0.00	0.00	15.21	61.00	2
0.00	66.30	0.00	50.80	0.00	10.48	5.68	3.14	4.48	23.48	79.00	6
0.00	0.00	77.00	27.93	7.33	9.03	4.48	2.21	2.95	18.70	104.00	7
0.00	0.00	88.40	20.57	5.43	7.25	2.06	1.26	1.82	18.11	113.00	7
0.00	0.00	94.60	23.75	6.44	5.78	1.36	0.67	1.24	19.12	133.00	7
0.00	0.00	77.90	29.09	6.41	4.00	1.68	1.52	1.82	17.49	145.00	7
0.00	0.00	63.40	18.40	7.11	3.73	1.87	0.73	0.89	13.73	173.00	7
0.00	0.00	0.00	63.40	56.30	5.05	2.25	14.66	1.71	23.90	204.00	6
0.00	112.10	389.30	145.30	231.90	33.41	12.72	135.20	74.50	141.80	231.00	8
0.00	124.20	66.70	12.39	103.30	44.10	3.83	49.30	10.92	51.84	286.00	8
0.00	0.00	0.00	0.00	0.00	0.00	0.00	0.00	3.27	3.27	336.00	1
0.00	0.00	630.00	158.20	90.60	15.20	8.65	8.30	2.33	130.47	341.00	7
0.00	0.00	72.40	151.30	100.70	16.67	7.45	5.24	1.09	50.69	350.00	7
0.00	0.00	641.00	155.30	109.30	22.08	9.13	10.45	1.79	135.58	397.00	7
0.00	0.00	370.00	91.10	108.40	27.51	11.66	13.78	2.93	89.05	468.00	7
0.00	0.00	279.00	56.60	57.60	11.67	3.00	53.30	2.51	66.24	478.00	7
0.00	0.00	228.50	148.00	132.80	11.94	1.93	8.01	5.28	76.64	649.00	7

Pond 1 Resaturation Monitoring Chemical Data CHLORIDE CONCENTRATION, ppm VS. DEPTH, m uz-1

The AVERAGE represents average of non-zero concentrations.
Zero values represent no sample recovery at that depth.

pond	0.15	0.30	0.46	0.61	0.76	0.91	1.07	1.22	AVERAGE	DAY	NO. OF SAMPLES
0.00	0.00	3803.00	0.00	3025.00	0.00	3771.00	0.00	0.00	3533.00	19.00	3
0.00	4180.00	4118.00	0.00	0.00	3435.00	3508.00	3992.00	3498.00	3785.17	28.00	6
0.00	4527.00	0.00	2763.00	3048.00	4475.00	3918.00	4685.00	0.00	3902.33	53.00	6
0.00	7542.00	0.00	3267.00	0.00	0.00	3498.00	4275.00	0.00	4645.50	84.00	4
0.00	0.00	4433.00	3351.00	3162.00	3878.00	3340.00	4160.00	3466.00	3684.00	98.00	7
1282.00	4958.00	5903.00	1555.00	6576.00	3960.00	1765.00	3855.00	3204.00	3972.00	97.00	8
1197.00	1178.00	7363.00	1178.00	2269.00	4202.00	2674.00	3960.00	3571.00	3286.38	104.00	8
1303.00	1313.00	7384.00	1368.00	2038.00	4443.00	2668.00	4139.00	3613.00	3370.50	109.00	8
1282.00	1378.00	5819.00	1513.00	2321.00	4391.00	2952.00	4422.00	3803.00	3324.63	116.00	8
0.00	1492.00	4412.00	1618.00	2363.00	4538.00	2983.00	4580.00	3908.00	3236.75	119.00	8
1303.00	1388.00	3258.00	1471.00	2237.00	4286.00	2847.00	4412.00	3634.00	2913.63	124.00	8
1040.00	1124.00	1859.00	1355.00	2290.00	4139.00	2658.00	4412.00	3666.00	2687.88	132.00	8
1029.00	1408.00	2090.00	1239.00	2647.00	4317.00	2910.00	4422.00	3676.00	2838.63	144.00	8
1008.00	1124.00	1460.00	1239.00	2290.00	3918.00	2815.00	4118.00	3624.00	2573.50	173.00	8
1011.20	1112.49	1322.07	1222.52	2107.97	4154.81	3126.15	4367.88	3711.21	2640.64	204.00	8
960.55	1082.80	1274.91	1550.85	2532.36	4184.50	3248.40	4432.50	3719.95	2753.28	232.00	8
1540.98	1091.67	1214.53	2225.47	3001.22	4229.79	3264.48	4268.40	3671.67	2870.90	286.00	8
0.00	0.00	0.00	0.00	0.00	0.00	0.00	0.00	0.00	0.00	337.00	0
0.00	0.00	0.00	0.00	0.00	0.00	0.00	0.00	0.00	0.00	341.00	0
0.00	0.00	0.00	0.00	0.00	0.00	0.00	0.00	0.00	0.00	344.00	0
0.00	0.00	0.00	0.00	0.00	0.00	0.00	0.00	0.00	0.00	398.00	0
0.00	0.00	0.00	0.00	0.00	0.00	0.00	0.00	0.00	0.00	420.00	0
0.00	0.00	0.00	0.00	0.00	0.00	0.00	0.00	0.00	0.00	448.00	0
0.00	0.00	0.00	0.00	0.00	0.00	0.00	0.00	0.00	0.00	451.00	0
0.00	0.00	0.00	0.00	0.00	0.00	0.00	0.00	0.00	0.00	476.00	0
0.00	0.00	0.00	0.00	0.00	0.00	0.00	0.00	0.00	0.00	478.40	0
0.00	0.00	0.00	0.00	0.00	0.00	0.00	0.00	0.00	0.00	478.71	0
0.00	0.00	0.00	0.00	0.00	0.00	0.00	0.00	0.00	0.00	479.69	0
0.00	0.00	0.00	0.00	0.00	0.00	0.00	0.00	0.00	0.00	481.79	0
0.00	0.00	0.00	0.00	0.00	0.00	0.00	0.00	0.00	0.00	482.55	0
0.00	0.00	0.00	0.00	0.00	0.00	0.00	0.00	0.00	0.00	483.71	0
0.00	0.00	0.00	0.00	0.00	0.00	0.00	0.00	0.00	0.00	484.55	0
0.00	0.00	0.00	0.00	0.00	0.00	0.00	0.00	0.00	0.00	487.00	0
0.00	0.00	0.00	0.00	0.00	0.00	0.00	0.00	0.00	0.00	495.00	0
0.00	0.00	0.00	0.00	0.00	0.00	0.00	0.00	0.00	0.00	502.00	0
0.00	0.00	0.00	0.00	0.00	0.00	0.00	0.00	0.00	0.00	509.00	0
0.00	0.00	0.00	0.00	0.00	0.00	0.00	0.00	0.00	0.00	539.00	0
0.00	0.00	0.00	0.00	0.00	0.00	0.00	0.00	0.00	0.00	572.00	0
0.00	0.00	0.00	0.00	0.00	0.00	0.00	0.00	0.00	0.00	621.00	0
0.00	0.00	0.00	0.00	0.00	0.00	0.00	0.00	0.00	0.00	648.00	0

Pond 1 Resaturation Monitoring Chemical Data CHLORIDE CONCENTRATION, ppm VS. DEPTH, m uz-3

The AVERAGE represents average of non-zero concentrations.
Zero values represent no sample recovery at that depth.

pond	0.15	0.30	0.46	0.61	0.76	0.91	1.07	1.22	AVERAGE	DAY	NO. OF SAMPLES
0.00	0.00	0.00	0.00	0.00	0.00	3477.49	0.00	2781.99	3129.74	19.00	2
0.00	3006.29	3980.86	4416.41	3825.24	3597.48	3390.55	3009.77	3096.70	3537.91	53.00	8
0.00	0.00	0.00	0.00	0.00	3503.57	3016.72	0.00	0.00	3260.15	89.00	2
0.00	2938.48	0.00	0.00	0.00	0.00	3077.58	0.00	2790.68	2935.58	97.00	3
0.00	3147.13	3474.01	3216.68	3355.78	3442.71	0.00	3202.77	3244.49	3297.65	98.00	7
1311.01	4369.46	4805.26	3667.01	3411.42	3465.32	3571.38	3331.12	2991.88	3701.61	102.00	8
1340.81	4093.81	4288.84	3769.93	3365.95	3571.42	3275.40	3533.11	3047.29	3618.22	109.00	8
1741.31	3722.91	4088.59	3780.38	3358.98	3587.09	3428.89	3708.98	3029.87	3587.96	116.00	8
1223.12	3547.05	3926.21	3851.08	3377.56	3650.14	3447.45	3789.92	3124.20	3589.20	119.00	8
1204.46	3260.77	4158.00	3974.72	3389.94	3786.19	3531.33	3803.65	3164.76	3633.67	132.00	8
1060.00	2870.00	4070.00	3700.00	3260.00	3620.00	3420.00	3480.00	3120.00	3442.50	144.00	8
960.00	2490.00	3940.00	3630.00	3250.00	3560.00	3320.00	3220.00	3090.00	3312.50	174.00	8
1010.71	2155.36	3997.60	3686.21	3444.40	3512.25	3634.02	3418.31	3249.57	3387.22	204.00	8
978.01	1879.18	3831.72	3510.37	3475.44	3468.46	3671.04	3304.29	3216.97	3294.68	232.00	8
1542.96	1679.72	3738.17	3510.23	3471.66	3348.92	3682.06	3166.57	3173.59	3221.36	286.00	8
0.00	0.00	0.00	0.00	0.00	0.00	0.00	0.00	0.00	0.00	336.00	0
0.00	0.00	0.00	0.00	0.00	0.00	0.00	0.00	0.00	0.00	341.00	0
0.00	0.00	0.00	0.00	0.00	0.00	0.00	0.00	0.00	0.00	344.00	0
0.00	0.00	0.00	0.00	0.00	0.00	0.00	0.00	0.00	0.00	350.00	0
0.00	0.00	0.00	0.00	0.00	0.00	0.00	0.00	0.00	0.00	397.00	0
0.00	0.00	0.00	0.00	0.00	0.00	0.00	0.00	0.00	0.00	420.00	0
0.00	0.00	0.00	0.00	0.00	0.00	0.00	0.00	0.00	0.00	468.00	0
0.00	0.00	0.00	0.00	0.00	0.00	0.00	0.00	0.00	0.00	475.00	0
0.00	0.00	0.00	0.00	0.00	0.00	0.00	0.00	0.00	0.00	482.46	0
0.00	0.00	0.00	0.00	0.00	0.00	0.00	0.00	0.00	0.00	482.67	0
0.00	0.00	0.00	0.00	0.00	0.00	0.00	0.00	0.00	0.00	483.51	0
0.00	0.00	0.00	0.00	0.00	0.00	0.00	0.00	0.00	0.00	484.54	0
0.00	0.00	0.00	0.00	0.00	0.00	0.00	0.00	0.00	0.00	487.00	0
0.00	0.00	0.00	0.00	0.00	0.00	0.00	0.00	0.00	0.00	488.00	0
0.00	0.00	0.00	0.00	0.00	0.00	0.00	0.00	0.00	0.00	495.00	0
0.00	0.00	0.00	0.00	0.00	0.00	0.00	0.00	0.00	0.00	502.00	0
0.00	0.00	0.00	0.00	0.00	0.00	0.00	0.00	0.00	0.00	509.00	0
0.00	0.00	0.00	0.00	0.00	0.00	0.00	0.00	0.00	0.00	539.00	0
0.00	0.00	0.00	0.00	0.00	0.00	0.00	0.00	0.00	0.00	572.00	0
0.00	0.00	0.00	0.00	0.00	0.00	0.00	0.00	0.00	0.00	621.00	0
0.00	0.00	0.00	0.00	0.00	0.00	0.00	0.00	0.00	0.00	648.00	0

Pond 1 Resaturation Monitoring Chemical Data CHLORIDE CONCENTRATION, ppm VS. DEPTH, m uz-5

The AVERAGE represents average of non-zero concentrations.
Zero values represent no sample recovery at that depth.

pond	0.15	0.30	0.46	0.61	0.76	0.91	1.07	1.22	AVERAGE	DAY	NO. OF SAMPLES
0.00	4389.00	0.00	0.00	0.00	0.00	0.00	0.00	0.00	4389.00	28.00	1
0.00	5271.00	0.00	0.00	0.00	6663.00	6557.00	5940.00	5260.00	5938.20	44.00	5
0.00	4910.00	7056.00	0.00	0.00	0.00	6706.00	6036.00	5707.00	6083.00	72.00	5
0.00	4570.00	0.00	0.00	0.00	0.00	6844.00	5409.00	5824.00	5661.75	83.00	4
1573.00	7226.00	6993.00	6057.00	0.00	5632.00	5983.00	5037.00	4910.00	5976.86	102.00	7
1711.00	7131.00	8884.00	5632.00	3804.00	5632.00	5770.00	5228.00	4973.00	5881.75	106.00	8
1743.00	8536.00	9182.00	6397.00	4017.00	5930.00	5887.00	5409.00	4857.00	6026.88	112.00	8
1868.00	5822.00	8353.00	6514.00	4123.00	5717.00	5600.00	5345.00	4942.00	5777.00	117.00	8
0.00	5760.00	8342.00	6950.00	4006.00	5717.00	5675.00	5303.00	4823.00	5797.00	120.00	8
1626.00	5822.00	8130.00	6854.00	4410.00	5675.00	5930.00	5292.00	4846.00	5844.88	123.00	8
1700.00	5462.00	7864.00	7088.00	4251.00	5569.00	6057.00	5547.00	4920.00	5844.75	133.00	8
1637.00	5303.00	7269.00	7078.00	4442.00	5811.00	6206.00	5590.00	5016.00	5814.38	144.00	8
1424.00	4591.00	6132.00	6461.00	4293.00	5239.00	6121.00	5260.00	4782.00	5359.88	174.00	8
1374.28	4192.43	5972.04	6711.37	4712.57	5747.63	6848.80	5053.53	4862.18	5512.57	204.00	8
1362.23	3765.35	5752.82	6409.48	4715.42	5875.07	6653.99	4708.44	4666.52	5318.39	232.00	8
2039.86	3184.11	5344.25	6024.56	4638.58	6025.26	6224.36	4540.78	4664.78	5080.84	287.00	8
0.00	0.00	0.00	0.00	0.00	0.00	0.00	0.00	0.00	0.00	336.00	0
0.00	0.00	0.00	0.00	0.00	0.00	0.00	0.00	0.00	0.00	337.00	0
0.00	0.00	0.00	0.00	0.00	0.00	0.00	0.00	0.00	0.00	341.00	0
0.00	0.00	0.00	0.00	0.00	0.00	0.00	0.00	0.00	0.00	344.00	0
0.00	0.00	0.00	0.00	0.00	0.00	0.00	0.00	0.00	0.00	350.00	0
0.00	0.00	0.00	0.00	0.00	0.00	0.00	0.00	0.00	0.00	397.00	0
0.00	0.00	0.00	0.00	0.00	0.00	0.00	0.00	0.00	0.00	405.00	0
0.00	0.00	0.00	0.00	0.00	0.00	0.00	0.00	0.00	0.00	420.00	0
0.00	0.00	0.00	0.00	0.00	0.00	0.00	0.00	0.00	0.00	448.00	0
0.00	0.00	0.00	0.00	0.00	0.00	0.00	0.00	0.00	0.00	451.00	0
0.00	0.00	0.00	0.00	0.00	0.00	0.00	0.00	0.00	0.00	472.00	0
0.00	0.00	0.00	0.00	0.00	0.00	0.00	0.00	0.00	0.00	476.00	0
0.00	0.00	0.00	0.00	0.00	0.00	0.00	0.00	0.00	0.00	487.00	0
0.00	0.00	0.00	0.00	0.00	0.00	0.00	0.00	0.00	0.00	488.00	0
0.00	0.00	0.00	0.00	0.00	0.00	0.00	0.00	0.00	0.00	495.00	0
0.00	0.00	0.00	0.00	0.00	0.00	0.00	0.00	0.00	0.00	509.00	0
0.00	0.00	0.00	0.00	0.00	0.00	0.00	0.00	0.00	0.00	539.00	0
0.00	0.00	0.00	0.00	0.00	0.00	0.00	0.00	0.00	0.00	572.00	0
0.00	0.00	0.00	0.00	0.00	0.00	0.00	0.00	0.00	0.00	621.00	0
0.00	0.00	0.00	0.00	0.00	0.00	0.00	0.00	0.00	0.00	649.00	0

Pond 1 Resaturation Monitoring Chemical Data CHLORIDE CONCENTRATION, ppm VS. DEPTH, m uz-6

The AVERAGE represents average of non-zero concentrations.
Zero values represent no sample recovery at that depth.

pond	0.15	0.30	0.46	0.61	0.76	0.91	1.07	1.22	AVERAGE	DAY	NO. OF SAMPLES
0.00	0.00	0.00	6823.00	4637.00	5680.00	5275.00	5190.00	5297.00	5433.67	28.00	6
0.00	0.00	5573.00	4999.00	4524.00	5680.00	5332.00	5275.00	5346.00	5247.00	61.00	7
0.00	0.00	5672.00	4999.00	4687.00	5290.00	5382.00	5205.00	5282.00	5216.71	90.00	7
0.00	9480.00	13380.00	11409.00	0.00	5240.00	5205.00	5105.00	5155.00	7853.43	98.00	7
1230.00	14295.00	15940.00	10969.00	5027.00	5134.00	5410.00	5148.00	5130.00	8381.63	102.00	8
1393.00	13990.00	14961.00	9906.00	6048.00	5226.00	5215.00	5013.00	4948.00	8163.38	106.00	8
1482.00	14692.00	13713.00	9165.00	6548.00	5307.00	5350.00	5077.00	5208.00	8132.50	112.00	8
1340.00	14089.00	12139.00	7995.00	6633.00	5279.00	5265.00	4939.00	4917.00	7857.00	117.00	8
0.00	13777.00	11497.00	7700.00	6825.00	5414.00	5516.00	5052.00	5169.00	7618.75	120.00	8
1489.00	13578.00	10146.00	6862.00	7176.00	5146.00	5303.00	5084.00	5136.00	7303.88	132.00	8
2238.00	14206.00	9701.00	6860.00	7856.00	5428.00	5587.00	5438.00	5456.00	7566.50	144.00	8
1418.00	13692.00	9289.00	6786.00	7580.00	5435.00	5680.00	5399.00	5407.00	7408.50	174.00	8
1499.66	12135.56	8200.28	6619.00	7119.00	5375.00	5687.00	5311.00	0.00	7206.69	203.00	7
1379.70	10894.38	7928.90	6322.16	6374.55	5274.29	5770.28	5326.68	5354.63	6655.73	231.00	8
1900.14	0.00	7880.00	6213.88	5782.51	5337.16	5744.08	5284.77	5396.54	5948.42	286.00	7
5701.00	6883.00	6977.00	6538.00	5533.00	5439.00	5889.00	5377.00	5513.00	6018.63	337.00	8
5868.00	7992.00	7510.00	7699.00	5774.00	5481.00	5805.00	5408.00	5554.00	6402.88	398.00	8
0.00	0.00	0.00	0.00	0.00	0.00	0.00	0.00	0.00	0.00	468.00	0
0.00	0.00	0.00	0.00	0.00	0.00	0.00	0.00	0.00	0.00	472.00	0
0.00	0.00	0.00	0.00	0.00	0.00	0.00	0.00	0.00	0.00	476.00	0
0.00	0.00	0.00	0.00	0.00	0.00	0.00	0.00	0.00	0.00	483.47	0
0.00	0.00	0.00	0.00	0.00	0.00	0.00	0.00	0.00	0.00	484.46	0
0.00	0.00	0.00	0.00	0.00	0.00	0.00	0.00	0.00	0.00	487.00	0
0.00	0.00	0.00	0.00	0.00	0.00	0.00	0.00	0.00	0.00	488.00	0
0.00	0.00	0.00	0.00	0.00	0.00	0.00	0.00	0.00	0.00	495.00	0
0.00	0.00	0.00	0.00	0.00	0.00	0.00	0.00	0.00	0.00	509.00	0
0.00	0.00	0.00	0.00	0.00	0.00	0.00	0.00	0.00	0.00	539.00	0
0.00	0.00	0.00	0.00	0.00	0.00	0.00	0.00	0.00	0.00	572.00	0
0.00	0.00	0.00	0.00	0.00	0.00	0.00	0.00	0.00	0.00	821.00	0
0.00	0.00	0.00	0.00	0.00	0.00	0.00	0.00	0.00	0.00	849.00	0

Pond 1 Resaturation Monitoring Chemical Data CHLORIDE CONCENTRATION, ppm VS. DEPTH, m uz-8

The AVERAGE represents average of non-zero concentrations.
Zero values represent no sample recovery at that depth.

pond	0.15	0.30	0.46	0.61	0.76	0.91	1.07	1.22	AVERAGE	DAY	NO. OF SAMPLES
0.00	0.00	0.00	3022.44	3359.05	0.00	3555.40	2706.87	2868.16	3102.38	53.00	5
0.00	6487.25	4348.44	2804.53	0.00	3470.25	3569.41	2648.73	2875.36	3743.42	92.00	7
0.00	0.00	0.00	0.00	7048.06	0.00	0.00	0.00	3481.48	5264.77	95.38	2
0.00	2624.64	8008.60	5544.41	5472.78	2621.78	4977.74	3427.30	3916.90	4574.27	95.75	8
0.00	0.00	0.00	0.00	6069.55	0.00	0.00	0.00	3846.65	4958.10	99.00	2
898.98	0.00	7370.68	5750.48	6792.79	3314.86	5910.02	2502.98	3928.19	5081.43	104.00	7
801.24	6629.71	6739.62	5289.59	6984.24	2800.79	5782.38	2031.46	3903.38	5020.15	110.00	8
705.17	6870.00	7534.48	6310.34	7908.54	2512.44	5622.06	1810.00	0.00	5509.69	113.00	7
886.33	6250.36	5030.78	4311.08	7445.13	2736.97	5516.49	1900.00	3403.49	4574.29	117.00	8
0.00	6204.28	4467.08	3687.11	7420.00	2765.33	4715.25	2013.73	3658.75	4366.44	120.00	8
811.87	5481.03	3960.10	3644.57	6750.25	3524.03	5523.58	2194.86	4002.64	4385.13	124.00	8
779.97	4981.15	3670.12	3201.41	6342.54	3871.47	5427.85	2101.40	4201.18	4212.14	133.00	8
865.28	4493.38	2985.45	2418.72	5844.40	0.00	4680.58	0.00	2707.14	3854.94	145.00	6
992.68	3080.86	2404.36	1818.74	5183.23	4233.09	4289.81	2992.23	3651.66	3456.75	173.00	8
1091.95	2375.35	1840.01	1442.94	4052.28	4761.34	4988.24	3364.49	2325.72	3143.80	203.00	8
939.59	1715.02	1501.95	1292.38	3430.03	4575.71	3398.10	3108.69	1501.95	2565.48	232.00	8
1470.51	1584.03	1348.26	1208.55	2897.37	4104.17	2806.55	2574.27	1599.75	2265.37	286.00	8
1790.00	1820.00	1480.00	2030.00	2610.00	2880.00	2060.00	2860.00	1460.00	2150.00	336.00	8
1720.00	2740.00	2820.00	3310.00	3090.00	1430.00	1570.00	2580.00	2900.00	2555.00	350.00	8
1710.00	2290.00	2190.00	2170.00	2960.00	2080.00	1160.00	2350.00	2930.00	2266.25	398.00	8
0.00	0.00	0.00	0.00	0.00	0.00	0.00	0.00	0.00	0.00	448.00	0
0.00	0.00	0.00	0.00	0.00	0.00	0.00	0.00	0.00	0.00	468.00	0
0.00	0.00	0.00	0.00	0.00	0.00	0.00	0.00	0.00	0.00	472.00	0
0.00	0.00	0.00	0.00	0.00	0.00	0.00	0.00	0.00	0.00	475.00	0
0.00	0.00	0.00	0.00	0.00	0.00	0.00	0.00	0.00	0.00	476.75	0
0.00	0.00	0.00	0.00	0.00	0.00	0.00	0.00	0.00	0.00	477.38	0
0.00	0.00	0.00	0.00	0.00	0.00	0.00	0.00	0.00	0.00	477.52	0
0.00	0.00	0.00	0.00	0.00	0.00	0.00	0.00	0.00	0.00	477.73	0
0.00	0.00	0.00	0.00	0.00	0.00	0.00	0.00	0.00	0.00	478.38	0
0.00	0.00	0.00	0.00	0.00	0.00	0.00	0.00	0.00	0.00	478.60	0
0.00	0.00	0.00	0.00	0.00	0.00	0.00	0.00	0.00	0.00	479.46	0
0.00	0.00	0.00	0.00	0.00	0.00	0.00	0.00	0.00	0.00	481.67	0
0.00	0.00	0.00	0.00	0.00	0.00	0.00	0.00	0.00	0.00	482.63	0
0.00	0.00	0.00	0.00	0.00	0.00	0.00	0.00	0.00	0.00	483.67	0
0.00	0.00	0.00	0.00	0.00	0.00	0.00	0.00	0.00	0.00	484.50	0
0.00	0.00	0.00	0.00	0.00	0.00	0.00	0.00	0.00	0.00	487.00	0
0.00	0.00	0.00	0.00	0.00	0.00	0.00	0.00	0.00	0.00	495.00	0
0.00	0.00	0.00	0.00	0.00	0.00	0.00	0.00	0.00	0.00	509.00	0
0.00	0.00	0.00	0.00	0.00	0.00	0.00	0.00	0.00	0.00	539.00	0
0.00	0.00	0.00	0.00	0.00	0.00	0.00	0.00	0.00	0.00	572.00	0
0.00	0.00	0.00	0.00	0.00	0.00	0.00	0.00	0.00	0.00	621.00	0
0.00	0.00	0.00	0.00	0.00	0.00	0.00	0.00	0.00	0.00	648.00	0

Pond 1 Resaturation Monitoring Chemical Data Groundwater Monitoring Wells
TOTAL SELENIUM CONCENTRATION, ppb VS. DEPTH, m

monitoring well screened intervals, with reference to the ground surface

SITE	1.8-3.0	1.8-2.4	2.4-3.0	3.0-4.6	4.6-6.1	6.1-7.6	7.6-9.1	9.1-10.7	10.7-12.2	DAY
UZ-1				2.1	1.1	1.0	1.0	1.3	1.4	34
				4.6	1.6	2.7	1.1	1.8	1.7	119
				6.2	0.9	0.8	0.2	0.9	0.8	174
				19.7						286
				2.7	1.4	1.5	1.3	1.7	1.7	498
UZ-2		5.8	5.8							82
		6.3	5.6							118
		3.9	3.7							174
		4.4	3.9							286
UZ-3		2.7	2.3							119
		2.5	0.9							176
		1.9	2.0							286
		2.4	2.9							498
UZ-4	5.6			4.5	1.9	1.6	3.3	2.3	2.5	82
	5.6			4.3	2.6	2.2	3.7	2.7	2.7	118
	36.2			3.7	1.1	0.6	1.8	1.2	1.2	175
	26.8			5.4						286
UZ-5		4.9								82
		4.5								119
		2.9								176
		2.9								287
		3.4								496
UZ-6		6.0	3.3							120
		4.4	1.3							286
		3.9	2.2							337
		4.3	0.7							496
UZ-7				3.5	0.8	0.8	1.7	2.3		82
			2.8	3.7	1.5	1.4	2.1	2.4		120
				2.1	1.4	0.5	0.4	0.8		176
UZ-8		77.0	12.0							120
		186.6	74.4							176
		333.	322.4							232
		258.2	261.8							288
		45.8	88.9							336
		33.7	15.8							478
		16.5	33.4							496
UZ-9	24.6									82
	15.9									176
	12.9									286

Selenate to Selenite Ratios uz-1

Zero values represent no sample recovery at that depth.

pond	0.15	0.30	0.46	0.61	0.76	0.91	1.07	1.22	DAY
0.00	0.00	4.33	0.00	33.83	0.00	2.80	0.00	0.00	19.00
0.00	88.50	5.80	76.14	0.00	121.97	6.26	11.31	5.03	28.00
0.00	155.55	0.00	37.94	19.31	17.84	3.05	8.25	0.00	53.00
0.00	381.31	0.00	56.79	0.00	0.00	5.00	10.85	0.00	84.00
0.00	0.00	29.45	116.07	18.45	20.32	7.09	26.07	13.31	96.00
0.00	99.10	13.83	18.37	27.77	50.38	5.59	31.86	25.01	97.00
0.00	0.00	76.66	1.34	12.43	74.03	2.65	48.23	44.05	104.00
0.97	1.06	8.70	0.99	1.10	119.32	2.52	103.50	83.27	109.00
0.97	1.08	3.28	1.22	5.05	86.43	2.28	108.08	78.80	116.00
0.00	15.04	14.67	20.47	23.78	117.11	2.63	147.73	108.73	119.00
0.61	0.72	1.69	2.02	0.97	106.67	14.19	32.62	88.60	124.00
1.22	1.21	4.09	2.27	1.25	90.28	3.39	173.21	99.17	132.00
1.67	2.50	1.03	2.43	1.88	119.17	4.64	195.63	76.51	144.00
1.18	1.25	0.69	0.89	2.54	68.05	9.47	151.40	88.88	173.00
1.16	1.97	0.98	1.16	0.72	16.23	8.46	168.80	88.20	204.00
3.47	3.37	2.42	2.97	2.36	12.37	14.41	136.56	86.86	232.00
0.57	1.18	1.11	1.70	0.60	8.21	13.03	76.95	151.08	286.00
0.62	4.73	1.21	2.42	0.73	0.73	9.06	2.43	27.07	337.00
0.65	0.74	1.10	0.73	0.66	0.58	6.18	7.68	17.93	341.00
0.93	1.22	1.85	1.21	1.01	0.77	5.00	1.42	13.91	344.00
1.00	1.11	1.30	1.56	0.60	0.79	4.02	0.93	20.10	398.00
0.00	0.71	1.19	1.08	0.57	0.44	1.71	0.40	1.78	420.00
0.00	0.00	0.00	3.08	0.00	0.00	2.65	1.84	3.53	448.00
0.00	4.64	38.73	19.15	7.06	9.08	2.80	3.78	5.96	451.00
0.00	45.16	6.19	30.29	13.22	9.42	5.77	12.86	13.44	476.00
14.33	64.35	17.60	36.59	27.07	15.90	8.49	26.17	17.04	478.40
5.34	0.00	65.58	52.10	48.08	19.22	9.29	31.83	21.50	478.71
5.13	65.50	75.26	82.70	572.50	17.41	9.61	28.95	23.01	479.69
0.00	86.48	47.03	137.58	52.34	18.71	18.08	32.02	29.22	481.79
0.00	76.90	37.65	177.34	40.60	19.13	25.54	33.29	45.99	482.55
6.47	25.47	79.15	180.76	22.70	16.88	18.40	34.82	45.63	483.71
8.29	15.78	89.51	261.69	18.67	20.15	18.00	49.25	37.13	484.55
0.00	84.60	9.07	226.55	7.16	16.64	12.64	30.72	49.56	487.00
9.09	25.03	2.32	53.65	3.95	16.78	15.24	39.88	53.55	495.00
5.33	3.93	1.15	9.22	4.01	15.73	15.27	30.01	43.68	502.00
2.13	0.57	0.55	0.98	4.35	11.99	13.28	24.51	44.04	509.00
1.81	0.42	0.58	0.59	2.00	7.50	12.45	21.74	43.85	539.00
4.46	0.74	1.40	0.74	1.47	9.79	16.05	16.14	57.10	572.00
0.00	0.00	0.00	0.00	0.35	2.02	2.22	3.12	32.41	621.00
0.00	0.00	0.00	0.94	1.00	1.09	1.86	0.42	1.72	648.00

Selenate to Selenite Ratios uz-2

Zero values represent no sample recovery at that depth.

pond	0.15	0.30	0.46	0.56	0.71	DAY
0.00	2.57	1.39	4.07	1.83	1.06	72.00
0.00	3.09	1.60	1.96	2.85	2.18	94.00
0.00	2.80	0.82	0.22	0.06	2.57	113.00
0.00	2.55	0.90	5.54	3.22	1.97	120.00
0.00	2.45	0.48	0.00	0.00	0.29	133.00
0.00	3.48	5.88	1.38	1.28	1.68	145.00
0.00	0.00	0.00	0.00	0.00	0.00	148.00
0.00	12.14	3.86	3.68	3.51	6.75	155.00
1.23	19.23	7.62	1.80	2.24	2.14	173.00
3.36	6.79	0.00	1.10	0.46	0.82	204.00
3.43	1.70	2.18	3.86	1.21	1.55	231.00
0.00	0.00	1.51	2.27	2.20	1.98	286.00
0.00	1.84	0.65	0.63	0.54	0.74	336.00
0.00	0.00	0.59	1.34	1.12	1.26	397.00
0.00	7.81	0.86	0.97	0.21	0.00	478.00
0.00	9.70	0.86	1.43	1.05	1.12	649.00

Selenate to Selenite Ratios uz-3

Zero values represent no sample recovery at that depth.

pond	0.15	0.30	0.46	0.61	0.76	0.91	1.07	1.22	DAY
0.00	0.00	0.00	0.00	0.00	3.72	18.10	5.83	18.30	19.00
0.00	19.38	16.67	2.33	1.02	6.06	6.68	1.72	15.81	53.00
0.00	0.00	0.00	0.00	0.00	12.54	7.16	0.00	0.00	89.00
0.00	52.87	0.00	0.00	0.00	0.00	0.00	0.00	7.40	97.00
0.00	53.77	55.16	82.31	30.29	46.53	84.19	89.04	89.93	98.00
0.00	19.99	18.52	4.12	0.67	15.99	4.32	4.33	34.06	102.00
0.00	17.78	9.59	0.50	0.26	10.44	2.46	0.76	7.93	109.00
1.27	10.97	6.96	0.36	0.39	10.25	16.44	4.19	5.39	116.00
2.33	6.78	6.91	0.48	1.84	11.94	0.76	1.13	4.63	119.00
1.57	3.07	4.62	0.94	2.90	10.37	0.68	1.81	3.36	132.00
3.11	0.77	1.72	0.76	2.50	7.36	0.73	1.76	3.24	144.00
1.17	0.62	0.81	0.68	1.39	3.06	0.42	1.20	1.73	174.00
1.37	0.40	0.71	0.34	0.98	0.76	0.38	1.25	1.37	204.00
19.68	0.58	0.77	0.51	1.48	0.41	0.60	1.16	2.24	232.00
0.00	0.78	1.46	0.50	4.21	0.59	0.49	1.30	2.51	286.00
0.00	0.00	0.00	0.86	0.00	0.00	0.33	0.62	24.46	336.00
0.00	0.00	0.00	0.00	0.00	4.04	0.00	1.54	2.32	341.00
0.00	0.00	0.00	6.04	0.78	4.11	1.86	0.93	4.46	344.00
0.00	9.08	5.23	4.09	2.81	2.32	1.08	0.82	4.56	350.00
0.00	5.82	5.67	2.09	0.69	2.25	1.06	1.45	2.10	397.00
0.00	0.00	0.00	1.13	0.96	1.13	0.77	0.96	2.14	420.00
0.00	9.22	13.62	0.00	1.19	10.49	6.21	2.74	3.99	468.00
0.00	0.00	0.00	2.32	1.44	15.08	6.70	0.00	4.84	475.00
0.00	19.84	35.88	21.49	3.07	6.99	5.63	15.18	4.11	482.46
0.00	18.63	42.11	34.55	8.38	15.81	5.76	10.25	4.67	482.67
8.09	19.96	31.58	34.95	6.13	18.60	7.17	34.14	5.45	483.51
7.52	18.29	42.54	87.44	5.72	23.72	7.66	36.47	7.73	484.54
0.00	14.78	36.08	88.65	1.45	27.69	7.73	34.02	17.37	487.00
12.27	11.29	22.87	54.60	0.59	26.57	8.17	27.14	19.25	488.00
9.95	5.48	18.90	27.78	0.36	26.25	8.09	17.76	23.02	495.00
7.99	0.00	11.59	16.26	0.30	21.80	7.46	8.56	16.18	502.00
2.07	0.69	6.45	8.93	0.39	14.04	0.00	6.87	11.68	509.00
1.51	0.84	2.48	1.53	0.54	4.69	9.35	4.46	8.11	539.00
0.00	1.21	0.78	0.49	0.77	1.38	10.07	10.01	6.22	572.00
0.00	0.00	0.00	0.00	0.00	1.72	6.46	1.29	3.77	621.00
0.00	21.23	17.39	5.22	0.88	1.29	4.44	0.00	3.13	648.00

Selenate to Selenite Ratios uz-4

Zero values represent no sample recovery at that depth.

pond	0.15	0.30	0.46	0.61	0.76	0.91	1.07	1.22	DAY
0.00	0.00	0.00	110.90	0.00	69.36	88.76	14.18	7.44	19.00
0.00	0.00	126.68	15.28	131.91	51.15	85.64	2.73	2.22	44.00
0.00	0.00	95.27	70.25	75.19	0.00	0.00	4.06	3.61	61.00
0.00	0.00	89.78	45.77	43.64	261.55	24.80	12.84	3.37	112.00
0.00	0.00	16.62	44.96	34.06	160.58	13.37	2.40	2.20	133.00
0.00	0.00	23.79	61.98	58.52	206.44	97.27	27.61	133.34	145.00
0.53	62.30	1.72	1.95	8.38	112.94	15.17	17.00	22.48	148.00
1.48	13.44	1.34	1.05	3.13	74.45	1.98	3.78	3.56	155.00
1.24	2.40	1.69	1.46	1.47	9.45	1.54	1.45	1.38	174.00
1.59	6.55	0.00	4.80	3.83	3.14	3.09	4.20	4.13	203.00
1.87	4.04	3.18	5.49	4.27	1.45	2.92	5.26	3.48	231.00
0.00	4.48	2.40	5.70	2.54	3.82	3.38	2.91	2.60	286.00
0.00	0.00	0.00	0.00	0.00	0.00	0.00	0.00	1.46	336.00
0.00	0.00	0.00	0.00	0.00	0.00	0.00	2.97	1.59	341.00
0.00	0.00	0.00	0.00	21.30	0.00	4.88	4.50	1.20	344.00
0.00	0.00	0.00	0.00	13.97	0.00	6.47	3.48	1.87	350.00
0.00	0.00	0.00	0.00	0.00	6.82	0.98	1.07	0.86	397.00
0.00	0.00	0.00	0.00	4.84	11.68	1.07	0.84	0.74	420.00
0.00	0.00	0.00	0.00	20.93	13.65	1.58	0.00	1.67	451.00
0.00	0.00	30.61	24.03	16.58	7.83	1.61	1.19	1.88	472.00
0.00	0.00	26.53	28.61	23.04	6.11	3.99	0.95	1.92	478.00
2.13	118.40	22.35	23.27	14.10	9.62	8.21	13.11	11.21	502.00
1.82	24.43	21.09	2.87	1.45	1.28	1.86	2.68	6.16	509.00
2.91	10.42	4.10	2.52	1.98	1.35	2.31	1.98	2.24	539.00
0.00	0.00	0.00	0.00	0.00	0.00	0.00	0.00	1.32	621.00
0.00	0.00	36.56	61.40	18.52	10.89	0.00	1.08	0.54	649.00

Selenate to Selenite Ratios uz-5

Zero values represent no sample recovery at that depth.

pond	0.15	0.30	0.46	0.61	0.76	0.91	1.07	1.22	DAY
0.00	16.28	0.00	0.00	0.00	0.00	0.00	0.00	0.00	28.00
0.00	0.00	0.00	0.00	0.00	3.10	2.46	2.01	1.54	44.00
0.00	12.23	26.48	0.00	0.00	0.00	1.34	0.82	0.81	72.00
0.00	15.21	0.00	5.47	0.00	0.00	2.56	1.07	3.16	83.00
0.00	1.20	5.81	2.61	0.00	22.98	3.53	1.78	2.00	102.00
0.00	4.37	2.38	1.41	5.03	26.13	2.62	1.06	0.92	106.00
1.06	31.98	2.51	11.23	2.09	28.57	1.90	1.42	2.61	112.00
1.74	2.76	2.00	1.32	1.65	21.08	3.18	2.24	7.63	117.00
0.00	21.08	72.67	18.32	1.53	28.13	4.09	11.60	23.11	120.00
0.90	0.00	0.00	0.00	1.45	19.64	2.93	1.71	8.00	123.00
2.00	44.53	5.06	1.07	1.32	11.45	3.86	2.26	11.16	133.00
3.13	19.95	6.25	0.12	1.32	10.87	4.20	2.02	11.19	144.00
1.47	10.66	2.63	2.20	1.91	4.22	5.25	4.18	11.85	174.00
1.82	3.82	3.40	1.55	2.52	2.94	4.86	3.01	9.94	204.00
12.47	2.07	4.10	3.05	2.94	1.81	4.36	2.98	4.33	232.00
0.00	0.89	1.78	1.74	7.49	1.34	5.79	2.46	2.18	287.00
0.19	2.82	1.51	1.87	6.28	0.62	2.40	1.52	0.98	336.00
0.00	0.89	2.34	2.99	3.40	3.35	2.70	1.58	0.98	337.00
0.00	1.74	2.16	2.93	0.00	1.97	2.96	1.47	1.68	341.00
0.00	0.37	1.77	1.65	0.00	1.04	2.09	0.91	0.58	344.00
0.00	1.26	1.55	0.90	0.00	1.87	1.70	0.78	0.51	350.00
0.00	0.00	0.00	0.00	0.00	0.00	0.00	0.76	0.79	397.00
0.00	0.00	0.00	0.00	0.00	0.00	0.00	1.96	0.00	405.00
0.00	0.00	0.00	0.00	0.00	0.00	0.00	1.59	0.18	420.00
0.00	0.00	0.00	0.00	0.00	0.00	0.00	1.85	0.48	448.00
0.00	0.00	3.63	12.48	4.05	4.73	0.00	1.05	0.31	451.00
0.00	0.00	4.26	14.40	2.41	6.35	1.84	1.31	0.81	472.00
0.00	0.00	4.31	19.41	2.18	6.46	2.02	0.72	0.37	476.00
0.00	0.00	6.74	7.95	0.13	11.29	2.01	2.14	1.24	487.00
2.72	0.00	0.00	15.55	3.42	14.53	2.59	3.50	1.64	488.00
6.42	0.00	0.00	4.69	4.16	20.69	2.64	2.92	4.01	495.00
1.45	0.00	0.00	0.00	5.43	15.09	3.21	2.65	6.85	509.00
2.08	0.00	0.00	0.00	0.94	13.70	5.43	4.24	11.95	539.00
0.00	2.73	2.70	1.95	0.91	4.81	9.96	5.09	14.76	572.00
-0.97	1.59	0.87	1.81	1.12	0.50	10.08	5.97	7.92	621.00
-0.83	1.50	2.03	1.70	1.18	0.55	12.94	3.62	2.63	649.00

Selenate to Selenite Ratios uz-6

Zero values represent no sample recovery at that depth.

pond	0.15	0.30	0.46	0.61	0.76	0.91	1.07	1.22	DAY
0.00	0.00	0.00	12.34	6.23	2.21	1.66	0.72	0.35	28.00
0.00	0.00	6.56	4.10	1.80	0.38	0.67	0.52	0.04	61.00
0.00	0.00	12.78	5.88	3.26	0.59	0.73	0.27	0.02	90.00
0.00	8.54	28.87	26.23	0.00	4.28	1.56	1.10	1.37	98.00
0.00	1.84	11.14	12.65	3.93	1.80	1.80	1.15	0.86	102.00
0.00	3.80	5.01	7.75	1.37	0.79	0.86	0.05	0.00	106.00
0.60	3.35	2.61	4.04	1.04	1.09	1.83	0.45	0.46	112.00
2.52	12.73	16.86	12.04	2.23	2.35	4.79	3.23	3.36	117.00
0.00	1.72	4.34	5.04	4.43	1.10	3.70	1.02	0.30	120.00
1.77	1.54	0.97	4.80	1.25	0.00	2.91	0.12	0.00	132.00
3.13	2.03	3.74	4.54	2.40	1.81	4.09	0.98	0.97	144.00
4.05	1.09	3.04	4.81	2.18	2.14	6.28	1.43	0.92	174.00
2.72	1.13	2.80	5.25	2.38	1.43	5.90	1.10	0.26	203.00
7.43	0.92	1.87	4.03	1.89	1.01	4.33	0.59	0.22	231.00
0.00	0.00	1.14	2.81	1.40	0.40	3.78	0.24	0.00	286.00
0.77	1.00	0.89	0.26	0.49	0.22	1.67	0.26	0.06	337.00
0.80	1.15	0.96	0.41	0.67	0.00	0.18	0.00	0.00	398.00
0.00	0.00	0.00	0.00	0.00	0.37	0.64	0.43	0.07	468.00
0.00	7.41	6.85	0.00	14.12	0.00	0.07	0.00	0.00	472.00
0.00	6.26	5.75	4.47	5.25	0.00	0.13	0.00	0.00	476.00
5.71	14.76	20.32	28.38	10.45	0.49	0.53	0.14	0.35	483.47
11.18	3.80	12.24	19.53	10.81	0.44	0.63	0.00	0.00	484.46
0.00	1.78	3.19	8.73	2.04	0.20	0.40	0.03	0.00	487.00
4.69	1.70	1.61	8.67	0.94	0.04	0.51	0.13	0.10	488.00
5.70	1.42	1.07	6.92	1.47	0.17	0.41	0.15	0.14	495.00
1.07	1.56	1.47	2.41	2.49	0.08	0.34	0.00	0.00	509.00
7.98	1.65	1.69	15.37	1.58	0.85	1.02	0.08	0.03	539.00
0.00	1.73	1.35	0.65	1.04	0.40	0.67	0.00	0.00	572.00
0.80	2.02	2.58	1.19	1.99	0.43	1.00	0.42	0.10	621.00
-0.01	1.65	1.53	0.49	0.98	-0.15	0.05	-0.17	-0.26	649.00

Selenate to Selenite Ratios uz-7

Zero values represent no sample recovery at that depth.

pond	0.15	0.30	0.46	0.61	0.76	0.91	1.07	1.22	DAY
0.00	0.00	0.00	0.00	0.00	0.00	0.00	10.68	4.45	44.00
0.00	0.00	0.00	0.00	21.50	48.63	14.40	11.51	5.81	61.00
0.00	122.10	0.00	0.00	37.98	69.71	13.17	0.00	0.00	84.00
0.00	0.00	0.00	0.00	0.00	20.58	11.55	23.69	20.53	113.00
0.00	0.00	0.00	30.26	0.00	20.51	15.72	27.09	20.50	120.00
0.00	0.00	0.00	31.79	3.89	19.37	17.15	25.23	16.00	145.00
0.00	0.00	0.00	1.87	3.51	3.66	13.14	20.67	11.91	203.00
0.00	0.00	0.30	1.92	0.55	2.57	1.94	4.35	1.20	231.00
0.00	0.00	0.00	0.78	0.44	0.72	0.55	0.50	0.60	287.00
0.00	0.00	4.03	1.38	0.00	0.29	0.00	0.27	0.35	337.00
0.00	0.00	0.00	0.00	0.00	4.31	0.00	0.37	0.00	398.00
0.00	0.00	0.00	0.00	0.00	13.73	0.00	2.16	0.00	478.00
0.00	0.00	6.62	4.75	0.00	0.61	0.00	14.31	0.58	649.00

Selenate to Selenite Ratios uz-8

Zero values represent no sample recovery at that depth.

pond	0.15	0.30	0.46	0.61	0.76	0.91	1.07	1.22	DAY
0.00	0.00	0.00	7.67	12.15	0.00	15.23	12.10	2.12	53.00
0.00	28.63	11.51	12.65	0.00	30.86	15.79	22.71	3.44	92.00
0.00	9.81	28.37	35.36	34.87	15.05	62.43	27.84	0.00	95.38
3.60	8.17	27.76	19.45	21.33	8.30	68.37	11.61	60.03	95.75
0.00	7.49	17.09	11.46	13.50	5.61	65.97	6.77	47.29	99.00
0.00	5.43	10.21	6.14	12.91	2.05	60.59	2.86	69.41	104.00
0.00	3.32	4.72	4.64	12.80	0.77	69.60	2.38	78.06	110.00
0.70	2.29	2.75	5.16	17.04	1.11	92.78	1.41	0.00	113.00
0.88	0.29	0.86	2.87	11.20	1.72	38.08	0.13	11.07	117.00
0.00	0.68	2.43	2.01	15.65	4.36	45.45	1.74	82.76	120.00
0.67	1.67	3.09	1.27	19.13	4.34	47.41	1.86	99.35	124.00
1.00	1.15	3.23	1.34	16.81	4.25	33.36	1.50	103.13	133.00
1.33	1.89	4.14	0.19	11.75	4.69	37.84	1.80	89.55	145.00
1.00	0.97	2.14	1.34	8.70	4.01	31.62	1.57	81.70	173.00
2.13	1.08	1.48	1.05	1.25	3.70	32.43	1.56	31.39	203.00
5.96	1.41	1.89	0.78	1.00	2.12	18.09	0.61	9.71	232.00
0.00	1.00	1.39	0.75	0.49	1.11	7.11	0.52	10.27	286.00
0.52	0.97	1.00	1.19	0.58	0.35	3.34	0.81	3.58	336.00
0.40	1.30	1.74	1.61	0.91	0.50	0.82	1.31	7.50	350.00
1.39	0.86	0.70	0.39	0.64	1.21	0.50	0.80	1.02	398.00
0.00	0.00	0.00	0.00	0.34	1.10	0.68	0.71	1.06	448.00
0.00	8.66	0.00	0.00	0.46	0.68	1.06	0.98	0.80	468.00
0.00	11.11	3.67	1.20	0.53	0.70	0.83	1.19	0.77	472.00
0.00	11.94	2.05	0.46	0.55	0.52	0.65	1.04	0.68	475.00
0.00	20.11	2.78	0.36	0.80	0.61	0.73	0.00	0.38	476.75
2.58	11.55	7.58	7.44	10.13	0.39	0.48	22.66	0.33	477.38
2.77	5.81	9.79	18.03	18.04	0.43	0.60	57.69	0.50	477.52
0.00	0.00	10.75	20.50	26.10	0.61	0.75	62.45	0.65	477.73
2.58	7.32	12.80	24.58	23.92	0.67	0.83	43.18	0.90	478.38
1.98	0.00	13.20	20.51	14.62	0.54	0.47	0.00	0.70	478.60
4.70	5.91	6.51	14.89	5.25	0.59	0.60	6.33	0.87	479.46
0.00	3.80	1.66	8.75	2.43	0.36	0.40	0.80	0.58	481.67
0.00	0.00	0.75	3.60	1.11	0.51	0.71	0.81	1.31	482.63
1.47	2.23	0.52	1.29	0.30	0.21	0.36	0.58	0.69	483.67
1.54	1.15	0.30	0.51	0.25	0.29	0.36	0.68	0.45	484.50
0.00	0.94	0.24	0.21	0.36	0.27	0.61	0.80	0.62	487.00
0.99	0.52	0.37	0.36	0.99	0.55	0.75	1.08	0.61	495.00
1.05	0.52	1.17	0.14	1.73	0.90	1.07	1.35	0.76	509.00
11.36	0.79	1.19	0.86	2.12	1.29	1.98	1.07	1.10	539.00
0.00	0.62	0.50	0.59	1.35	2.16	2.26	1.95	1.01	572.00
0.65	0.65	0.83	0.75	1.68	2.37	1.63	1.00	1.06	621.00
0.34	0.48	0.72	0.39	1.04	1.60	0.94	0.94	1.07	648.00

Selenate to Selenite Ratios uz-9

Zero values represent no sample recovery at that depth.

pond	0.15	0.30	0.46	0.61	0.76	0.91	1.07	1.22	DAY
0.00	0.00	0.00	43.88	0.00	0.00	26.54	0.00	0.00	61.00
0.00	69.23	0.00	31.76	0.00	32.74	11.22	1.28	1.30	79.00
0.00	0.00	31.05	29.39	23.77	7.06	2.71	1.05	2.63	104.00
0.00	0.00	23.00	30.91	17.05	2.96	1.75	1.90	1.12	113.00
0.00	0.00	19.25	26.20	3.76	1.28	1.97	4.64	2.60	133.00
0.00	0.00	16.79	9.41	1.50	0.93	1.93	1.53	1.97	145.00
0.00	0.00	13.91	10.16	21.39	1.82	10.76	38.81	4.64	173.00
0.00	0.00	0.00	0.61	1.61	0.95	1.01	2.74	1.37	204.00
0.00	32.47	5.16	5.91	7.56	3.41	2.85	6.48	7.07	231.00
0.00	5.36	0.63	0.82	0.74	0.85	0.81	0.52	0.47	286.00
0.00	0.00	0.00	0.00	0.00	0.00	0.00	0.00	0.73	336.00
0.00	0.00	3.19	4.21	1.03	0.85	0.52	0.54	1.09	341.00
0.00	0.00	33.45	4.18	0.61	0.58	0.26	0.26	1.79	350.00
0.00	0.00	2.92	4.30	1.12	0.79	0.45	0.35	0.91	397.00
0.00	0.00	4.61	5.16	2.42	0.78	0.25	0.19	0.59	468.00
0.00	0.00	4.30	5.24	1.64	0.60	0.92	0.97	1.03	478.00
0.00	0.00	3.80	1.38	0.65	0.79	1.15	0.81	0.42	649.00

Pond 1 Resaturation Monitoring Fluid Potential Data Hydraulic Head, m water vs. depth, m uz-1

* - indicates a higher degree of confidence associated with the measurement

DATE	0.15		0.30		0.46		0.61		0.76		0.91		1.07		1.22
"7 -25-86"		*	-1.02			*	-1.27			*	-1.17				
"7 -31-86"		*	-1.43			*	-1.38			*	-1.27				
"8 -8-86"		*	-1.53			*	-1.27			*	-1.27				
"8 -21-86"	* -3.47			*	-1.73	*	-1.78	*	-1.63	*	-1.68	*	-1.63		
"9 -15-86"	* -2.96	*	-2.04	*	-2.04	*	-2.09	*	-1.84	*	-1.99	*	-1.94		
"9 -19-86"	* -4.59	*	-2.14	*	-1.84	*	-2.09	*	-2.04	*	-1.99	*	-2.04		
"9 -29-86"	* -3.47	*	-2.14	*	-1.94	*	-2.19	*	-2.04	*	-1.99	*	-2.04		
"10 -1-86"	* -2.88	*	-1.94	*	-1.73	*	-2.14	*	-2.35	*	-1.84	*	-2.14		
"10 -4-86"	.88		.39		.78		.74		-0.37		1.24		-1.07		-1.35
"10 -8-86"	1.33		.32		1.10		.89		-0.53		.93		-0.89		-1.30
"10 -9-86"	-1.74		.02		1.22		.53		-1.29		-0.61		-1.81		-1.60
"10-10-86"	-2.20		-1.69		-1.75		-1.83		-1.76		-1.68		-0.91		-1.90
"10-16-86"	-2.27		-1.64		-1.68		-1.67		-1.76		-1.67		-1.74		-1.83
"10-22-86"	* -2.36	*	-1.74		-1.49	*	-1.93	*	-1.71	*	-1.63		-1.78	*	-1.54
"10-26-86"	-1.71	*	-1.26		-1.16	*	-1.54	*	-1.52	*	-1.24		-0.47		-1.37
"10-28-86"	-1.32		-1.31		-1.17		-1.54		-1.35		-1.26		-1.23		-1.32
"10-29-86"	* .27	*	.21	*	.13	*	.17	*	.08	*	.20	*	-0.08	*	.17
"10-31-86"	* .67	*	.56	*	.67	*	.65	*	.63	*	.57	*	.53	*	.69
"11 -4-86"	* .55	*	.47	*	.46		.73	*	.39	*	.42	*	.40		.83
"11 -5-86"	.47		.40		.39		.42		.39		.42		.42		.43
"11 -7-86"	.63	*	.37	*	.38	*	.42		.39	*	.42	*	.35	*	.38
"11-10-86"	.95		.64		.68	*	.41	*	.38	*	.39	*	.36	*	.39
"11-11-86"	.61	*	.37	*	.37	*	.40	*	.35		.42	*	.33	*	.38
"11-14-86"	.36		.36		.50		.41		.40		.38		.39		.39
"11-17-86"	* .42	*	.60		.51	*	.44		.40	*	.42	*	.47	*	.41
"11-19-86"	* .47	*	.39		.56	*	.45		.38	*	.42	*	.36	*	.38
"11-21-86"	* .46	*	.50		.38	*	.42	*	.50	*	.44	*	.40	*	.40
"11-25-86"	* .46	*	.49	*	.43	*	.44	*	.38	*	.45	*	.43	*	.43
"12 -3-86"	* .67	*	.61	*	.61	*	.60	*	.66	*	.66	*	.64	*	.62
"1 -2-87"	* .65	*	.61	*	.77	*	.59	*	.52	*	.58	*	.54	*	.83
"1 -13-87"	* .61	*	.62	*	.63	*	.63	*	.62	*	.64	*	.62	*	.63
"2 -13-87"	* .67	*	.64	*	.66		.85	*	.63	*	.62	*	.61	*	.62
"3 -13-87"	* .60	*	.63	*	.67		.84	*	.62	*	.62	*	.60	*	.61
"5 -6-87"	* .60		.91	*	.60		.85	*	.61	*	.57	*	.59	*	.63
"6 -25-87"	.28	*	.08	*	.10	*	.13	*	.11	*	.12	*	.13		.29
"6 -30-87"	* .19	*	.19	*	.23	*	.17	*	.13	*	.21	*	.16	*	.15
"7 -3-87"	* .24	*	.20	*	.22	*	.22	*	.19	*	.22	*	.23	*	.29

Pond 1 Resaturation Monitoring Fluid Potential Data Hydraulic Head, m water vs. depth, m uz-2

* - indicates a higher degree of confidence associated with the measurement

DATE		0.30		0.61		0.91
"7 -25-86"	*	-0.36	*	-0.36	*	-0.20
"7 -31-86"	*	-0.51	*	-0.46	*	-0.51
"8 -8-86"	*	-0.31	*	-0.25	*	-0.31
"8 -21-86"	*	-0.41	*	-0.46	*	-0.51
"9 -19-86"	*	-0.51	*	-0.46	*	-0.61
"9 -23-86"	*	-0.41	*	-0.56	*	-0.51
"9 -29-86"	*	-0.41	*	-0.46	*	-0.41
"10 -4-86"						
"10-11-86"	*	-0.31	*	-0.25	*	-0.41
"10-17-86"	*	-0.31	*	-0.25	*	-0.32
"10-22-86"	*	-0.32	*	-0.23	*	-0.28
"10-26-86"						
"10-27-86"	*	-0.28	*	-0.27		-0.30
"10-29-86"		.66	*	-0.17	*	-0.21
"10-31-86"	*	-0.12	*	-0.10	*	-0.13
"11 -4-86"	*	-0.16	*	-0.14	*	-0.15
"11-11-86"		-0.09	*	-0.12	*	-0.14
"11-14-86"		-0.17		-0.11		-0.12
"11-18-86"	*	.06	*	-0.11	*	-0.09
"11-19-86"	*	.07	*	-0.08	*	-0.09
"11-21-86"	*	-0.14	*	-0.06	*	-0.11
"11-26-86"		.23		-0.12		.01
"12 -4-86"		.33		.71		.10
"12-26-86"		.84		.72		.79
"1 -2-87"	*	-0.01	*	.01	*	.02
"1 -13-87"	*	.05	*	.09	*	.09
"2 -13-87"					*	.14
"3 -12-87"	*	.03	*	.10		.53
"5 -6-87"	*	.00	*	.05	*	.0
"6 -25-87"	*	-.25	*	-.22		-.01

Pond 1 Resaturation Monitoring Fluid Potential Data Hydraulic Head, m water vs. depth, m uz-3

* - indicates a higher degree of confidence associated with the measurement

DATE		0.15		0.30		0.46		0.61		0.76		0.91		1.07		1.22
"8 -7-86"	*	-1.22	*	-2.03	*	-1.73	*	-3.06	*	-2.75	*	-3.16	*	-1.63		
"8 -8-86"	*	-1.22	*	-1.63	*	-1.73	*	-1.84	*	-1.63	*	-1.73	*	-1.53		
"8 -21-86"	*	-1.63	*	-1.43	*	-1.12	*	-1.43	*	-1.33	*	-1.63	*	-1.53		
"9 -11-86"	*	-2.14	*	-1.53	*	-1.43	*	-1.43	*	-1.43	*	-2.14	*	-1.73		
"9 -15-86"	*	-2.55	*	-2.03	*	-2.03	*	-1.84	*	-1.84	*	-1.73	*	-1.84		
"9 -19-86"	*	-2.65	*	-1.94	*	-2.03	*	-1.84	*	-1.84	*	-1.73	*	-1.84		
"9 -29-86"	*	-2.86	*	-2.35	*	-2.35	*	-2.03	*	-1.94	*	-1.94	*	-1.94		
"10-14-86"	*	-2.75	*	-2.03	*	-2.03	*	-1.84	*	-1.73	*	-1.84	*	-1.94		
"10-16-86"	*	-2.35	*	-1.55	*	-1.36	*	-1.37	*	-1.22	*	-1.35	*	-1.18		-0.19
"10-17-86"	*	-2.43	*	-1.92	*	-1.50	*	-1.49	*	-1.30	*	-1.30	*	-1.27	*	-1.04
"10-22-86"		-2.84		-0.96		-1.82	*	-1.92		-1.79	*	-1.69	*	-1.68		-0.54
"10-26-86"	*	-3.22	*	-2.44		-1.75	*	-1.94	*	-1.98	*	-1.87	*	-1.62	*	-1.68
"10-29-86"	*	-2.94		-1.32	*	- 1.54	*	-1.63	*	-1.51	*	-1.39	*	-1.52		-0.97
"10-30-86"		.27	*	.10	*	.24		0.00	*	.10	*	.08	*	.20	*	.35
"10-31-86"	*	.36	*	.34	*	.51	*	.25	*	.31	*	.17	*	.31	*	.31
"11 -3-86"		.17		.21		-0.06		.08		.11		.67		.54		.83
"11 -4-86"		.23	*	.15	*	.29	*	.05	*	.07		.05		.42		.53
"11-10-86"	*	.08		.38	*	.16	*	0.01	*	-0.01		.75		.46	*	.13
"11-11-86"	*	.08	*	.10	*	.34	*	0.00	*	.02	*	.01	*	-0.01	*	.38
"11-14-86"		.11		.07		.04		.50		0.00		.04		-0.01		.10
"11-17-86"	*	.11	*	.08	*	.08	*	.11		.32	*	.02	*	.02	*	.22
"11-19-86"	*	.09	*	.08		-0.17	*	.08	*	.18	*	.01	*	-0.03	*	0.00
"11-20-86"	*	.20	*	.14	*	-0.15	*	.12	*	.01	*	.05	*	.10	*	.02
"11-25-86"	*	.14	*	.15	*	.24	*	.20	*	.04	*	.05	*	.16	*	.38
"12 -3-86"	*	.41	*	.34	*	.53	*	.30	*	.32	*	.25	*	.36	*	.45
"1 -13-87"	*	.34	*	.34	*	.34	*	.25	*	.27	*	.28	*	.31	*	.34
"2 -13-87"	*	.41	*	.25	*	.31	*	.18	*	.23	*	.24	*	.24		1.02
"3 -13-87"		.28	*	.22		.47	*	.20	*	.23	*	.24	*	.30	*	.39
"5 -6-87"	*	.30	*	.25	*	.53	*	.43	*	.18	*	.17	*	.29	*	.47
"6 -25-87"		-.81	*	-.72	*	-.21		-.75	*	-.79	*	-.76	*	-.34	*	-.42
"6 -30-87"		-1.12	*	-.35		.59		-.39		-.52		-.17	*	-.17	*	.03
"7 -3-87"	*	-.05	*	-.05		.60	*	-.10		.05		.09	*	.05	*	.23

Pond 1 Resaturation Monitoring Fluid Potential Data Hydraulic Head, m water vs. depth, m uz-4

* - indicates a higher degree of confidence associated with the measurement

DATE		0.15		0.30		0.46		0.61		0.76		0.91		1.07
"8 -8-86"	*	-2.24	*	-2.45	*	-2.45	*	-1.53	*	-0.71	*	-0.92	*	-1.63
"8 -21-86"	*	-2.75	*	-2.65	*	-2.86	*	-1.53	*	-1.43	*	-1.43	*	-1.43
"9 -6-86"	*	-1.90	*	-2.65	*	-4.39	*	-1.53	*	-1.43	*	-1.53	*	-1.43
"9 -17-86"	*	-3.47	*	-5.30	*	-5.81	*	-1.53	*	-1.43	*	-1.43	*	-1.43
"9 -17-86"	*	-3.98	*	-5.61	*	-5.81	*	-1.53	*	-1.43	*	-1.43	*	-1.43
"9 -18-86"	*	-1.84	*	-2.35	*	-5.71	*	-1.53	*	-1.33	*	-1.43	*	-1.43
"9 -18-86"	*	-3.06	*	-3.67	*	-5.51	*	-1.53	*	-1.43	*	-1.33	*	-1.43
"9 -18-86"	*	-3.88	*	-4.69	*	-5.61	*	-1.53	*	-1.43	*	-1.33	*	-1.43
"9 -19-86"	*	-2.14	*	-1.22	*	-4.49	*	-1.53	*	-1.43	*	-1.43	*	-1.43
"9 -19-86"	*	-4.28	*	-4.79	*	-5.20	*	-1.53	*	-1.43	*	-1.33	*	-1.43
"9 -23-86"	*	-2.65	*	-4.18	*	-6.12	*	-1.53	*	-1.43	*	-1.33	*	-1.43
"10 -4-86"	*	-2.14	*	-5.20	*	-6.32	*	-1.53	*	-1.43	*	-1.33	*	-1.33
"10-10-86"	*	-2.14	*	-5.71	*	-6.12	*	-1.53	*	-1.43	*	-1.22	*	-1.22
"10-11-86"					*	-6.63					*	-1.33	*	-1.22
"10-15-86"		-1.84		-5.98		-0.56		-1.19		-1.28		-0.48		-0.11
"10-17-86"		-1.83		-0.18		-0.31	*	-0.92		-1.11		0.09		0.12
"10-20-86"	*	-2.66		-0.36	*	-3.84		-1.03		0.25	*	-0.98	*	-1.00
"10-22-86"	*	-4.53		-0.57	*	-4.77	*	-0.86		-0.42	*	-0.91	*	-0.93
"10-26-86"		-5.02		-3.56		-2.49	*	-0.99	*	-1.38	*	-1.10	*	-1.04
"10-29-86"		-1.27		-3.36		-1.10	*	-0.99		-0.63	*	-0.87	*	-0.68
"10-30-86"		-0.07	*	-0.63	*	-1.01	*	-0.57		0.56	*	-0.61	*	-0.46
"10-31-86"		0.67		-0.16	*	-0.57	*	-0.48		-0.42	*	-0.46	*	-0.33
"11 -3-86"	*	-3.34		-0.49		-0.34	*	-0.43	*	-0.50		0.41	*	-0.41
"11 -4-86"		-1.08	*	-1.07		-0.25	*	-0.41	*	-0.54		-0.04	*	-0.42
"11-10-86"	*	-3.13		-0.05		-0.04		-0.28	*	-0.65		0.33	*	-0.41
"11-11-86"	*	-4.69	*	-2.08	*	-1.00	*	-0.51	*	-0.57	*	-0.58	*	-0.36
"11-13-86"		-5.43		-2.89		-0.92		-0.51		-0.58		-0.52		-0.46
"11-18-86"	*	-3.92		-1.01	*	-0.88	*	-0.59	*	-0.52	*	-0.53	*	-0.46
"11-19-86"		-3.70		-0.84	*	-0.60	*	-0.39	*	-0.56	*	-0.59	*	-0.46
"11-25-86"	*	-8.18	*	-1.55	*	-0.60		0.70	*	-0.52	*	-0.53	*	-0.40
"12 -4-86"		-1.04	*	-0.29		0.49		0.66	*	0.07	*	-0.21		1.09
"12-26-86"	*	0.11	*	0.03	*	0.00		0.57	*	0.05		0.84		0.47
"1 -2-87"		0.06	*	0.00	*	0.01	*	-0.23	*	0.03	*	-0.12	*	-0.23
"1 -13-87"	*	0.15	*	0.11	*	0.13	*	-0.10	*	0.14	*	-0.07	*	-0.12
"3 -12-87"	*	.18	*	.12	*	.35	*	.06	*	.11		.23	*	.01
"5 -6-87"	*	.15		.42		.47	*	-0.20	*	-0.03	*	-0.04	*	-0.11
"6 -25-87"		-6.83		-7.24	*	-2.38	*	-.97		-1.57	*	-1.08	*	-.87
"6 -30-87"		-7.11		-8.08	*	-3.27	*	-.93	*	-1.53	*	-1.01	*	-.83
"7 -3-87"		-5.48		-7.63	*	-4.19		-.47	*	-.79	*	-.68		-.33

Pond 1 Resaturation Monitoring Fluid Potential Data Hydraulic Head, m water vs. depth, m uz-5

* - indicates a higher degree of confidence associated with the measurement

DATE		0.15		0.30		0.46		0.61		0.76		0.91		1.07
"8 -14-86"	*	-1.22	*	-1.02		1.22	*	-1.12	*	-1.02	*	-0.92	*	-0.92
"8 -21-86"	*	-1.48	*	-1.33	*	-1.12	*	-1.02	*	-1.02	*	-0.87	*	-0.92
"9 -6-86"	*	-2.14	*	-1.63	*	-1.02	*	-1.12	*	-1.07	*	-0.97	*	-0.97
"9 -19-86"	*	-2.24	*	-1.84	*	-1.02	*	-1.02	*	-1.02	*	-0.82	*	-0.92
"9 -29-86"	*	-1.33	*	-1.53	*	-1.22	*	-1.12	*	-1.12	*	-0.92	*	-1.12
"10 -3-86"	*	-1.63	*	-1.63	*	-1.12	*	-1.22	*	-1.22	*	-1.22	*	-1.12
"10 -4-86"		1.22		1.22		1.22		1.22		1.22		1.22		1.22
"10 -7-86"		-0.55	*	-1.63		1.22		1.22		0.30		0.14		0.67
"10 -8-86"		-1.01	*	-1.63		0.76		0.45		0.45		-0.06		0.10
"10 -9-86"		-1.03		0.48		-0.43		-0.84		-0.93		-0.58		-0.96
"10-10-86"		-1.09		-1.22		0.36		-1.02		-1.07		-0.05		-0.99
"10-15-86"		1.22		1.22		1.22		1.22		1.22		1.22		1.22
"10-17-86"		-0.30	*	-1.53		0.89		-0.50	*	-1.07		0.60		-0.39
"10-20-86"	*	-2.03		-1.15		0.61	*	-0.69		-1.04	*	-1.15		-1.03
"10-22-86"	*	-1.22		1.22		0.61		-0.25		-1.02	*	-1.02		-0.82
"10-27-86"	*	-1.12	*	-1.56		-0.62		0.98	*	-0.87		-0.41	*	-0.78
"10-31-86"	*	0.04	*	-1.56	*	-0.60	*	-0.60	*	-0.25	*	0.04		-0.29
"11 -3-86"	*	0.30	*	0.40		0.88		0.04	*	0.09		0.56	*	-0.06
"11 -4-86"	*	0.36	*	0.13	*	0.02	*	-0.07	*	0.12	*	0.11	*	-0.01
"11 -7-86"	*	0.42	*	0.30		0.73	*	-0.03		0.21		0.37	*	-0.02
"11-11-86"	*	0.40	*	0.40		0.53	*	-0.02	*	0.19	*	-0.02	*	0.01
"11-13-86"		0.41		0.42		0.04		0.03		0.19		0.01		0.09
"11-18-86"	*	0.40	*	0.38	*	0.12	*	0.04	*	0.17	*	0.02	*	0.08
"11-19-86"	*	0.42	*	0.30	*	0.05	*	0.06	*	0.20	*	0.05	*	0.07
"11-21-86"	*	0.44	*	0.40	*	0.07	*	0.04	*	0.16	*	0.02	*	0.02
"11-24-86"	*	0.49	*	0.18	*	0.01	*	0.03	*	0.21	*	0.08	*	0.07
"12 -4-86"	*	0.65		0.80		0.40	*	0.28		0.42	*	0.28		1.19
"1 -13-87"		1.27		0.93		0.83	*	0.40		0.51	*	0.41		1.18
"2 -13-87"	*	.65		.88			*	.54	*	.56	*	.49		.54
"3 -13-87"	*	.63	*	.69			*	.51	*	.51	*	.44	*	.45
"5 -7-87"	*	.60	*	.57		.48	*	.31	*	.35		.54	*	.25
"6 -25-87"	*	-.03	*	.14		1.23	*	-.31	*	-.24	*	-.50		-.31
"6 -30-87"	*	-.20	*	.10	*	-.46	*	-.46	*	-.58	*	-.64	*	-.49
"7 -3-87"	*	-.39	*	-.36	*	-.67	*	-.61	*	-.68	*	-.64	*	-.60

Pond 1 Resaturation Monitoring Fluid Potential Data Hydraulic Head, m water vs. depth, m uz-6

* - indicates a higher degree of confidence associated with the measurement

DATE		0.15		0.30		0.46		0.61		0.76		0.91		1.07
"8 -21-86"	*	-0.61	*	-0.61	*	-0.61	*	-0.46	*	-0.46	*	-0.46	*	-0.31
"9 -19-86"	*	-1.12	*	-0.92	*	-0.92	*	-0.71	*	-0.82	*	-0.71	*	-0.92
"9 -23-86"	*	-0.92	*	-0.92	*	-1.02	*	-0.92	*	-0.92	*	-0.92	*	-0.92
"9 -29-86"	*	-1.02	*	-1.02	*	-1.02	*	-0.92	*	-1.02	*	-0.83	*	-1.02
"10-16-86"	*	-1.02	*	-0.92	*	-0.92	*	-0.71	*	-0.82	*	-0.82	*	-0.82
"10-17-86"	*	-0.59	*	-0.70	*	-0.80	*	-0.74		-0.83	*	-0.91	*	-0.34
"10-20-86"	*	-0.86	*	-0.83	*	-0.82		-0.90		-0.31	*	-0.91	*	-0.31
"10-22-86"	*	-0.89	*	-0.91	*	-0.89	*	-0.82	*	-0.71	*	-0.90	*	-0.78
"10-27-86"	*	-0.99	*	-0.87	*	-0.81	*	-0.71	*	-0.75	*	-0.89	*	-0.58
"10-30-86"		0.21		0.18		0.14		0.18		0.15		0.16		0.10
"11 -3-86"	*	0.47	*	0.48	*	0.49	*	0.49	*	0.49	*	0.48	*	0.53
"11 -4-86"	*	0.40	*	0.45	*	0.49	*	0.49	*	0.45	*	0.49	*	0.35
"11 -7-86"	*	0.52	*	0.51	*	0.55	*	0.54		0.60	*	0.55	*	0.50
"11-13-86"		0.57		0.58		0.75		0.59		0.73		0.60		0.65
"11-18-86"	*	0.59	*	0.60		0.84	*	0.60	*	0.59	*	0.59	*	0.69
"11-19-86"	*	0.54	*	0.54		0.87	*	0.58	*	0.55	*	0.57	*	0.52
"11-21-86"	*	0.58	*	0.60	*	0.61	*	0.61	*	0.59	*	0.60	*	0.68
"11-25-86"		0.64		0.64		0.63		0.59	*	0.61	*	0.62	*	0.70
"12 -3-86"	*	0.57	*	0.72		0.85	*	0.75	*	0.80	*	0.78	*	0.79
"1 -1-87"	*	0.76	*	0.75		0.83		0.85	*	0.80	*	0.78	*	0.81
"3 -12-87"	*	.95	*	.78	*	.74	*	.80	*	.72	*	.79	*	.79
"5 -6-87"	*	.75	*	.74	*	.80	*	.79	*	.80	*	.75	*	.76
"6 -25-87"	*	.37	*	.36	*	.37	*	.41	*	.38	*	.53	*	.47

Pond 1 Resaturation Monitoring Fluid Potential Data Hydraulic Head, m water vs. depth, m uz-7

* - indicates a higher degree of confidence associated with the measurement

DATE		0.15		0.30		0.46		0.61		0.76		0.91		1.07		1.22
"9 -6-86"	*	-7.34	*	-6.12		-2.55	*	-2.35	*	-1.94	*	-1.27	*	-1.73		
"9 -19-86"	*	-7.34	*	-6.53		-4.59	*	-3.08	*	-2.45	*	-1.84	*	-1.94		
"9 -23-86"	*	-6.83	*	-5.61		-3.77	*	-2.88	*	-2.35	*	-2.14	*	-1.94		
"9 -29-86"	*	-6.02	*	-6.22		-3.67	*	-2.98	*	-2.24	*	-2.14	*	-2.04		
"10 -1-86"	*	-7.09	*	-6.32	*	-3.77	*	-3.37	*	-2.45	*	-2.14	*	-2.04	*	-2.14
"10 -3-86"		0.84		0.71		0.17		0.43		0.06		0.20		-0.34		-0.45
"10 -7-86"		1.62		1.18		-0.19		0.47		-0.51		-0.34		-0.35		-0.30
"10-10-86"		0.55		0.90		0.15		0.88		0.17		0.20		0.09		-0.07
"10-17-86"		-5.42		-3.17		0.08		-2.61		-1.44		0.03		0.04	*	-0.15
"10-20-86"	*	-4.70	*	-4.05		0.58		0.18	*	-2.04	*	-1.74	*	-1.81	*	-1.17
"10-22-86"		-4.61	*	-4.26		-2.85	*	-1.99		-1.71	*	-1.82	*	-1.84	*	-0.78
"10-27-86"	*	-4.42	*	-5.14		-4.34		-2.38	*	-1.38	*	-1.78	*	-1.77	*	-1.20
"10-31-86"	*	-5.04	*	-4.71	*	-4.94	*	-2.62	*	-1.70	*	-1.76	*	-1.89	*	-1.45
"11 -4-86"	*	-5.33	*	-5.37	*	-5.78	*	-2.78	*	-1.48	*	-1.27	*	-1.11	*	-1.11
"11-11-86"		-3.66	*	-4.97		-0.13	*	-0.78	*	-0.87	*	-0.83	*	-0.93		-0.29
"11-14-86"		-3.24		-0.73		-0.71		-0.66		-0.69		-0.71		-0.85		-0.45
"11-18-86"	*	-4.73	*	-2.31	*	-0.69	*	-0.63	*	-0.42	*	-0.63	*	-0.74	*	-0.31
"11-19-86"	*	-4.62	*	-4.16	*	-0.75	*	-0.70	*	-0.73	*	-0.70	*	-0.81	*	-0.33
"11-21-86"	*	-4.32	*	-4.15	*	-0.63	*	-0.68	*	-0.71	*	-0.62	*	-0.73	*	-0.42
"11-25-86"	*	-3.69	*	-1.91	*	-0.65	*	-0.57	*	-0.65	*	-0.62	*	-0.71	*	-0.32
"1 -13-87"	*	-0.25	*	-0.22	*	-0.18	*	-0.17	*	-0.22	*	-0.15	*	-0.13	*	-0.28
"2 -12-87"	*	-0.19	*	-0.18	*	-0.20	*	.01	*	-0.15	*	-0.08	*	-0.18		
"3 -12-87"	*	-0.25	*	-0.28	*	-0.28	*	-0.20	*	-0.24	*	-0.18	*	-0.18		
"5 -7-87"		.17	*	-0.18	*	-0.34	*	-0.10		.58	*	-0.23	*	-0.29	*	.08
"6 -25-87"	*	-1.71	*	-1.57	*	-1.15	*	-.97		-.46	*	-1.17		-.20	*	-.37

Pond 1 Resaturation Monitoring Fluid Potential Data Hydraulic Head, m water vs. depth, m uz-8

* - indicates a higher degree of confidence associated with the measurement

DATE		0.15		0.30		0.46		0.61		0.76		0.91		1.07		1.22
"9 -11-86"		-3.37		-1.73		-1.43		-1.53				-1.22		-1.22		-0.41
"9 -15-86"		-3.57		-1.94		-1.53		-1.53				-1.33		-1.33		-1.33
"9 -19-86"		-4.39		-2.24		-1.53		-1.43				-1.22		-1.33		-1.33
"10 -4-86"	*	-2.35	*	-1.84	*	-1.53	*	-1.84			*	-1.33	*	-1.43	*	-1.43
"10-17-86"	*	-2.98	*	-1.73	*	-1.63	*	-1.43			*	-1.33	*	-1.43	*	-1.43
"10-20-86"	*	-3.57	*	-2.14	*	-1.63	*	-1.43			*	-1.33	*	-1.33	*	-1.43
"10-21-86"	*	-3.16	*	-1.73	*	-1.63	*	-1.53			*	-1.33	*	-1.33	*	-1.33
"10-22-86"	*	-2.92	*	-0.11	*	-0.67	*	-1.43	*		*	-1.39	*	-1.35	*	-1.45
"10-24-86"		1.22		1.22		1.22		1.22				1.22		1.22		1.22
"10-27-86"	*	-3.23	*	-0.36	*	-1.22	*	-1.42	*		*	-1.36	*	-1.27	*	-1.39
"10-28-86"		0.61		0.27		-0.21		0.01				-0.37		-0.32		-0.22
"10-28-86"		0.28		0.41		-0.12		-0.09				-0.14		-0.16		-0.15
"10-30-86"		0.36		0.55		0.16		0.29				0.15		0.17		0.14
"10-31-86"	*	0.34		0.67	*	0.16	*	0.15			*	0.08		0.33		0.13
"11 -4-86"		0.38	*	0.49		0.61	*	0.33			*	0.22	*	0.22		0.39
"11 -5-86"		0.33		0.38		0.20		0.06				0.21		0.28		0.14
"11 -7-86"	*	0.31		1.22		0.13		0.21			*	0.15	*	0.13	*	0.06
"11-11-86"	*	0.35		1.05		0.29		0.88			*	0.16	*	0.15	*	0.13
"11-11-86"	*	0.24	*	-0.37	*	0.12	*	0.12			*	0.13	*	0.12	*	0.11
"11-14-86"		0.53		0.38		0.25		0.13				0.17		0.16		0.13
"11-18-86"	*	0.34	*	0.63	*	0.24	*	0.27			*	0.16	*	0.18	*	0.14
"11-19-86"	*	0.29	*	0.17	*	0.21	*	0.23			*	0.15	*	0.13	*	0.11
"11-21-86"	*	0.32	*	0.94	*	0.23	*	0.21			*	0.17	*	0.15	*	0.15
"11-25-86"	*	0.29			*	0.28	*	0.39			*	0.19	*	0.44	*	0.17
"12 -4-86"	*	0.61	*	0.73	*	0.51	*	0.48			*	0.44	*	0.40	*	0.46
"1 -2-87"	*	0.38		0.51	*	0.32	*	0.46			*	0.33	*	0.43	*	0.32
"1 -13-87"	*	0.44	*	0.60	*	0.42	*	0.42			*	0.41	*	0.42	*	0.40
"2 -13-87"	*	0.42	*	0.59	*	0.39	*	0.47			*	0.36	*	0.41	*	0.39
"3 -13-87"		0.66		0.88	*	0.47		0.66			*	0.40	*	0.44	*	0.40
"5 -6-87"	*	.42	*	.72	*	.50	*	.57			*	.43	*	.46	*	.40
"6 -25-87"	*	.22	*	.07	*	.15	*	.08			*	.21	*	.12	*	.14

Pond 1 Resaturation Monitoring Fluid Potential Data Hydraulic Head, m water vs. depth, m uz-9

* - indicates a higher degree of confidence associated with the measurement

DATE		0.15		0.30		0.46		0.61		0.76		0.91	1.07		1.22
"9 -19-86"	*	-1.63	*	-1.43	*	-2.45	*	-1.12			*	-0.92		*	-1.02
"9 -23-86"	*	-3.98	*	-6.63	*	-4.28	*	-1.33			*	-1.22		*	-1.33
"9 -29-86"	*	-2.86	*	-6.32	*	-3.77	*	-1.33			*	-1.22		*	-1.22
"10 -2-86"	*	-2.96	*	-7.14	*	-3.77	*	-1.33			*	-2.14		*	-2.14
"10 -4-86"		0.02		-1.34		0.95		-0.16				1.04			0.47
"10 -8-86"		2.19		-1.73		1.89		0.28				1.30			1.09
"10 -9-86"		-1.17		-2.94		1.90		-0.39				1.34			0.93
"10-10-86"		-1.54		-2.91		-1.05		-1.09				0.01			-1.03
"10-11-86"		-0.75		-2.92		-1.50		-1.09				0.47			-0.98
"10-14-86"		-0.14		-1.73		-2.01		-1.04		-0.92		0.92			-0.94
"10-17-86"	*	-1.28		-2.98	*	-2.10		-0.79		-0.05		0.17			-0.94
"10-21-86"	*	-1.84		-0.61	*	-1.36	*	-1.02	*	-0.98		0.29		*	-0.20
"10-22-86"	*	-1.61	*	-3.33	*	-1.31	*	-0.72	*	-1.01		0.28		*	-0.90
"10-26-86"	*	-1.79	*	-5.78	*	-1.32	*	-1.02	*	-0.97	*	-0.82		*	-0.87
"10-31-86"	*	-1.75	*	-6.54		0.45	*	-0.84	*	-0.71	*	-0.70		*	-0.62
"11 -4-86"		-0.70	*	-5.17		0.09	*	-0.66	*	-0.65	*	-0.60		*	-0.59
"11 -5-86"		-0.28		-4.69		-0.79		-0.63		-0.62		-0.54			-0.50
"11-11-86"		-0.36		-0.92		0.96	*	-0.58		-0.33	*	-0.53			0.46
"11-14-86"		-0.79		-1.08		1.22		-0.58		-0.58		-0.52			-0.56
"11-17-86"	*	-0.21	*	-0.92		1.12	*	-0.55		-0.07	*	-0.50		*	-0.42
"11-19-86"	*	-1.02	*	-0.82		1.36	*	-0.55		0.10	*	-0.49		*	-0.44
"11-24-86"	*	-0.68	*	-0.72	*	-0.52	*	-0.55	*	-0.54	*	-0.48		*	-0.32
"12 -4-86"	*	0.22		1.22		1.22		1.06	*	-0.25	*	-0.14			0.78
"1 -2-87"	*	-0.32	*	-0.46		-0.16		-0.44	*	-0.43	*	-0.40		*	-0.25
"1 -13-87"		-0.32	*	-0.35	*	-0.09		-0.28	*	-0.24	*	-0.25		*	-0.22
"2 -13-87"												.11			
"3 -12-87"	*	-0.20	*	-0.29	*	-0.14	*	-0.22	*	-0.20	*	-0.13		*	-0.07
"5 -6-87"	*	-0.67		-0.38	*	-0.59	*	-0.56	*	-0.56	*	-0.50		*	-0.37
"6 -25-87"	*	-2.78	*	-2.30	*	-1.42	*	-1.03	*	-1.01	*	-.98			-.82
"6 -30-87"	*	-2.17	*	-1.82	*	-1.39	*	-1.03	*	-.98	*	-.92			-.43

Appendix III SUGGESTED EXPERIMENTAL IMPROVEMENTS

This Appendix is included as a brief listing of suggested improvements that could be made in a future study of similar scope and purpose. In the interest of brevity, the items are presented without detailed discussion or justification. The list primarily includes changes in field procedures, i.e. in monitoring site design and sample collection, that were suggested either in the literature or in the course of performing the experiment.

(1) In the collection of soil water samples, recording the volume of water found within the soil water sampler at each sampling episode may be a useful measurement. It may be possible to determine soil matrix permeability in the area immediately surrounding the porous cup in an approximate fashion. Permeability estimation in this manner, however, may be obscured by the fact that the soil immediately adjacent to the cup may have been disturbed during sampler installation and by questions regarding what the sampler is actually sampling, as discussed in Section 3.7. In any event, this measurement should be made as one means of monitoring the general behavior and state of the system. It is one component of a thorough and complete sampling procedure.

(2) It is suggested that a tracer be used which is not already present in the system. The specification of boundary-initial conditions in a modeling effort is greatly simplified by constant initial conditions and step-inputs. It may be difficult, however, to identify a tracer which satisfies the necessary requirements, i.e. that it is absent from the system initially, non-reactive, inexpensive, and easily analysed. In addition, the quantity of artificial tracer required in this study could have been enormous due to the large volumes of water (100's of acre-ft) involved.

(3) A platform of some sort should be constructed so that the pond bottom surface is not disturbed during sampling. While the pond was submerged, personnel walking around the monitoring sites during sampling often caused the soft and often muddy pond bottoms to became rutted and uneven. This fact may have little effect on the flow of water to deeper soil water samplers, however, water flow to the shallow samplers, especially the 0.15 m (6 in) deep samplers, may be occurring along flow paths that vary significantly in length

from the assumed depth.

(4) The sampling intervals during the first flooding episode were probably not sufficiently small. Resolution of rapid variations in solute concentrations, especially with selenium, was often poor during the initial periods after flooding when samples were collected every few days. During the second flooding event, where initial post-flooding samples were collected at least as rapidly as one per day, rising and declining solute levels were observed with much greater resolution.

(5) The sampling intervals during later portions of the experiment as well should be shortened, or at least, attention should be directed to the timing of sample entry into the cup. In this study, a sample was designated to be representative of conditions in the soil solution for *the day in which it was collected.* It is possible that rather than being representative of solute concentrations for the instant of sample collection, the sample actually reflects conditions immediately after the previous sampling episode when a gradient existed for flow into the cup. Shorter sampling intervals would increase the likelihood that the collected sample was representative of solute concentrations in the soil water at the moment of sampling. Also, any chemical transformations that might occur in the sampler tube may be minimized by shorter intervals.

(6) If possible, soil water samplers should be installed months, possibly a year, prior to the time when they are actually required. This provides more time for the establishment of a good hydraulic connection between the cup and adjacent soil and a return to relatively undisturbed soil conditions.

(7) In the 1-dimensional modeling of solute transport that was performed in this study, initial solute distributions were constructed from observations made areally throughout a site. Construction of a soil water sampler that could accomodate more than one sampling point would allow for the monitoring of vertically continuous solute profiles rather than only solute variations at areally distributed points.

(8) Utilize methods that reduce the variability, between adjacent samplers, in the *timing* of sample collection. Such procedures involve controlling sampler intake rate and volume, and include: selecting samples with similar intake rates (permeabilities), using a uniform

sampler length (i.e. a constant volume), and when applying a vacuum - using the same initial vacuum for all the samplers. A device that shuts off automatically when the desired volume of sample is collected would address this issue.

(9) Due to the highly variable nature of soil structure and the resulting heterogeneous composition and concentration of soil solutions, it is suggested that replicate samplers be installed to particular depths.

REFERENCES

Adriano, D.C. 1986. Trace elements in the terrestrial environment. Springer-Verlag, N.Y.

Amoozegar-Fard, A.D., D.R. Nielsen and A.W. Warrick. 1982. Soil solute concentration distributions for spatially varying pore water velocities and apparent diffusion coefficients. Soil Sci. Soc. Am. J. 46:3-9.

Anderson, M.P. 1979. Using models to simulate the movement of contaminants through ground water flow systems. Chemical Rubber Company Critical Reviews in Environmental Control 9:97-156

Anderson, M.S., H.W. Lakin, K.C. Beeson, F.F. Smith and E. Thacker. 1961. Selenium in Agriculture. Agricultural Handbook 200, USDA, Washington, D.C.

Anderson, T.L. and J. Bouma. 1973. Relationships between saturated hydraulic conductivity and morphometric data of an argillic horizon. Soil Sci. Soc. Am. Proc. 37:408-413.

Anderson, T.L. and J. Bouma. 1977. Water movement through pedal soils: I. Saturated flow. J. Soil Sci. Soc. Am. 41:413-418.

Aubertin, G.M. 1971. Nature and extent of macropores in forest soils and their influence on subsurface water movement. USDA For. Serv. Res. Pap. NE-192.

Balistrieri, L.S. and T.T. Chao. 1987. Selenium adsorption by goethite. Soil Sci. Soc. Am. J. 51:1145-1151.

Beven, K. and P. Germann. 1982. Macropores and water flow in soils. Water Res. Res. 18:1311-1325.

Biggar, J.W. and D.R. Nielsen. 1962. Miscible displacement: II. Behavior of Tracers. Soil Sci. Soc. Am. Proc. 26:125-128.

Biggar, J.W. and D.R. Nielsen. 1967. Miscible displacement and leaching phenomenon. Agronomy 11:254-274.

Biggar, J.W. and D.R. Nielsen. 1976. Spatial Variability of the Leaching Characteristics of a Field Soil. Water Resources Res. 12:78-84.

Biggar, J.W. and D.R. Nielsen. 1980. Mechanisms of Chemical Movement in Soils. p. 213-227. *In* A. Banin and U. Kafkafi (*Ed.*) Agrochemicals in Soil. Pergamon Press, N.Y.

Blanchar, R.W. and C.E. Marshall. 1981. Eh and pH measurements in Menfro and Mexico soils. *In* Chemistry in the Soil Environment, American Society of Agronomy Special Publication No. 40, Madison, Wi.

Bohn, H.L., B.L. McNeal and G.A. O'Connor. 1985. Soil Chemistry. John Wiley and Sons, Inc. New York.

Bouma, J., L.W. Dekkar and H.L. Verlinden. 1976. Drainage and vertical hydraulic conductivity of some Dutch 'knik' clay soil. Agric. Water Manage. 1:67-78.

Bredehoeft, J.D., H.B. Counts, S.G. Robson and J.B. Robertson. 1976. Solute transport in groundwater systems. *In* Facets of Hydrology, John Wiley and Sons, N.Y.

Bresler, E. 1973. Anion exclusion and coupling effects in nonsteady transport through unsaturated soils: I. Theory. Soil Sci. Soc. Am. Proc. 37:663-669.

Bresler, E. and G. Dagan. 1979. Solute dispersion in unsaturated heterogeneous soil at field scale: II. Applications. Soil Sci. Soc. Am. J. 43:367-472.

Briggs, L.J. and A.G. McCall. 1904. An artificial root for inducing capillary movement of soil moisture. Science 20:566-569.

Byers, H.G., J.T. Miller, K.T. Williams and H.W. Lakin. 1938. Selenium occurrence in certain soils of the United States, with a discussion of related topics, Third Report. US Dept. Agr. Tech. Bull. 601.

CH2M Hill and Jones and Stokes Associates. 1985. Working Paper No. 1, Data Review Report for Kesterson Environmental Impact Statement.

Cherry, J.A., R.W. Gillham and J.F. Pickens. 1975. Contaminant hydrogeology: I. Physical processes. Geosci. Can. 2:76-83.

Coats, K.W. and B.D. Smith. 1964. Dead-end pore volume and dispersion in porous media. Soc Petr. Eng. J. 4:73-84.

Dagan, G. and E. Bresler. 1979. Solute dispersion in unsaturated heterogeneous soil at field scale: I. Theory. Soil Sci. Soc. Am. J. 43:461-467.

Danckwerts, P.V. 1953. Continuous Flow Systems: Distribution of Residence Times. Chem. Eng. Sci. 2:1-13.

Davidson, J.M., P.S.C. Rao and P. Nkedi-Kizza. 1983. Physical Processes Influencing Water and Solute Transport in Soils, *In* Chemical Mobility and Reactivity in Soil Systems.

Day, P.R. 1956. Dispersion of a moving salt water boundary advancing through a saturated sand. Trans. Am. Geophys. Union 37:595-601.

Eardley, A.J. 1951. Structural Geology of North America. Harper and Bros. New York.

Elrashidi, M.A., D.C. Adriano, S.M. Workman and W.L. Lindsay. 1987. Chemical equilibria of selenium in soils: a theoretical development. Soil Sci. 144:141-152.

Elrick, D.E. and L.K. French. 1966. Miscible displacement patterns on disturbed and undisturbed soil cores. Soil Sci. Soc. Am. Proc. 30:153-156.

Fleischer, M. 1953. Recent estimates of the abundances of the elements in the earths crust. US Geol. Surv. Cir. 285.

Freeze, R.A. and J.A. Cherry. 1979. Groundwater, Prentice-Hall, Inc. Englewood Cliffs, N.J.

Fried, J.J. and M.A. Combarnous. 1971. Dispersion in Porous Media. Adv. Hydrosci. 7:169-282.

Fried, J.J. 1975. Groundwater Pollution. Elsevier Science Publishing Co., Amsterdam, The Netherlands.

Frost, D.V. 1967. Significance of the Symposium. Symposium: Selenium in Biomedicine. Oregon State University, 7-26.

Gaudet, J.P., H. Jegat, G. Vachaud and P.J. Wierenga. 1977. Solute transfer, with exchange between mobile and stagnant water, through unsaturated sand. Soil Sci. Soc. Am J. 41:665-671.

Geering, H.R., E.E. Cary, L.H. Jones and W.H. Allaway. 1968. Solubility and redox criteria for the possible forms of selenium in soils. Soil Sci. Soc. Am. Proc. 32:35-40.

Gelhar, L.W., A. Montaglou, C. Welty and K.R. Rehfeldt. 1985. A review of field-scale transport processes in saturated and unsaturated porous media. Electric Power Research Institute, Palo Alto, Ca., Research Project 2485-5.

Godfrey, C.L. 1964. A summary of the soils of the blacklands praire of Texas. Texas Agr. Exp. Sta. Misc. Publ. 698.

Goldberg, S. and G. Sposito. 1984. A chemical model of phosphate adsorption by soils. I: Reference oxide minerals. Soil Sci. Soc. Am. J. 48:722-772

Goldschmidt, V.M. 1937. Geochemische verteilungs-gesetze der elemente. IX. Mengenverhaltnisse der elemente und der atomarten. Dybwab in Komm., Oslo, Norway.

Green, R.E., P.S.C. Rao and J.C. Corey. 1972. Solute transport in aggregated soils:Tracer zone shape in relation to pore velocity distribution and absorption. *In* Proc 2nd Symp. on Fundamentals of Transport Phenomena in Porous Media. IAHR-ISSS. Guelph, Canada. 2:732-752.

Gunnison, D., R.M. Engler and W.H. Patrick. 1985. Chemistry and microbiology of newly flooded soils: Relationship to reservoir water quality. In Gunnison,D., (ed.), Microbial Processes in Reservoirs, Dr. W. Junk Publishers, Boston, 39-56.

Gupta, R.K., R.J. Millington and A. Klute. 1973. Hydrodynamic dispersion in unsaturated porous media: II. The stagnant zone concept and the dispersion coefficient. J. Indian

Soc. Soil Sci. 21:121-128.

Gupta, S.K., K.K. Tanji and J.N. Luthin. 1973. A Three-Dimensional finite element ground water model. Report No. UCAL-WRC-C-152. NTIS Report No. PB 248925. California Water Resources Center, University of California, Davis, California.

Hamdy A.A. and G. Gissel-Nielsen. 1977. Fixation of selenium by clay minerals and iron oxides. Z. Pflanzenernaehr. Bodenkd. 140:63-70.

Hansen, E.A. and A.R. Harris. 1975. Validity of soil-water samples collected with porous ceramic cups. Soil Sci. Soc. Am. Proc. 39:528-536.

Harleman, D.R.F. and R.R. Rumer. 1962. The dynamics of salt-water intrusion in porous media. Civ. Eng. Dept. No. 55, M.I.T. Press, Cambridge, Mass.

Hingston, F.J. 1981. A review of anion adsorption. p. 51-90. *In* M.A. Anderson and A.J. Rubin (*Ed.*) Adsorption of inorganics at solid-liquid interfaces. Ann Arbor Science. Ann Arbor, Mi.

Hillel, D. 1980. Fundamentals of Soil Physics. Academic Press, New York.

Hotchkiss, W.R. and G.O. Balding. 1971. Geology, hydrology, and water quality of the Tracy-Dos Palos area, San Joaquin Valley, Ca. US Geol. Surv. Open File Report. August 6, 1971.

John, M.K., W.M.H. Saunders and J.H. Watkinson. 1976. Selenium adsorption by New Zealand soils. N.Z.J. Agric. Res. 19:143-151.

Jurinak, J.J., J.C. Whitmore and R.J. Wagenet. 1977. Kinetics of salt release from a saline soil. Soil Sci. Soc. Am. J. 41:721-724.

Jury, W.A. 1982. Simulation of solute transport using a transfer function model. Water Resour. Res. 18:363-368.

Kanchanasut, P., D.R. Scotter and R.W. Tillman. 1978. Preferential solute movement through larger soil voids. II. Experiments with saturated soil. Austr. J. Soil Res. 16:269-276.

Kies, B. 1981. Solute transport in unsaturated field soil and in groundwater. Ph.D Dissertation, Dept. of Agronomy, New Mexico State University, Las Cruces, NM.

Kissel, D.E., J.T. Ritchie and E. Burnett. 1973. Chloride movement in undisturbed swelling clay soil. Soil Sci. Soc. Am. Proc. 37:21-24.

Komroff, Jr. (*Ed.*) 1926. The Travels of Marco Polo, revised from Marsden's translation. Liveright, N.Y.

Krumbien, W.C. and F.A. Graybill. 1965. An Introduction to Statistical Models in Geology. McGraw-Hill Book Co., New York.

Lakin, W.H. 1961. Geochemistry of selenium in relation to agriculture. Agric. Handbook 200, USDA, Washington,D.C.

Lawrence Berkeley Laboratory. 1985. Hydrological, Geochemical and Ecological Characterization of Kesterson Reservoir. Progress Report 1. LBID-1101. Berkeley, CA.

Lawrence Berkeley Laboratory. 1986. Hydrological, Geochemical and Ecological Characterization of Kesterson Reservoir. Progress Report 2. LBID-1188. Berkeley, CA.

Lawrence Berkeley Laboratory. 1986. Hydrological, Geochemical and Ecological Characterization of Kesterson Reservoir. Progress Report 3. LBID-1213. Berkeley, CA.

Lawrence Berkeley Laboratory. 1986. Hydrological, Geochemical and Ecological Characterization of Kesterson Reservoir. Progress Report 4. LBID-1250. Berkeley, CA.

Lawrence Berkeley Laboratory. 1987. Hydrological, Geochemical and Ecological Characterization of Kesterson Reservoir. Progress Report 5. LBID-1291. Berkeley, CA.

Lawrence Berkeley Laboratory. 1987. Hydrological, Geochemical and Ecological Characterization of Kesterson Reservoir. Progress Report 6. LBID-1312. Berkeley, CA.

Lawrence Berkeley Laboratory. 1987. Hydrological, Geochemical and Ecological Characterization of Kesterson Reservoir. Annual Report. LBL-24520. Berkeley, CA.

Lawrence Berkeley Laboratory. 1988. Hydrological, Geochemical and Ecological Characterization of Kesterson Reservoir. Progress Report 8. LBID-1420. Berkeley, CA.

Litaor, M.I. 1988. Review of soil solution samplers. Water Res. Res. 24:727-733.

Luthin, J.N. 1966. Final report on seepage from reservoir sites in the Dos Palos and Kesterson areas, Western Merced Co.,Report on expected seepage into Salt Slough and the San Joaquin River from the Kesterson Enhancement Area W. Merced Co., Special consultants report to the California Dept. of Water Res.

Madison, T.C. 1860. Sanitary Report - Fort Randall. *In* Coolidge, R.H. Statistical Report on the Sickness and Mortality in the Army of the United States. 36th Cong., 1st Session. Senate Exec. Doc. (January 1855 to January 1860) 52:37-41.

Mandle, R.J. and A.L. Kontis. 1986. Directions and rates of ground-water movement in the vicinity of Kesterson Reservoir, San Joaquin Valley, California. US Geological Survey, Water Resources Investigations Report 86-4196.

Marthaler, H.P., W. Vogelsanger, F. Richard and P.J. Wierenga. 1983. A pressure transducer for field tensiometers. Soil Sci. Soc. Am. J. 47:624-627.

McMahon, M.A. and G.W. Thomas. 1974. Chloride and tritiated water flow in disturbed and undisturbed soil cores. Soil Sci. Soc. Am. Proc. 38:727-732.

Measures C.I. and J.D. Burton. 1980. The vertical distribution and oxidation states of dissolved selenium in the northeast Atlantic Ocean and their relationship to biological processes. Earth Planet. Sci. Lett. 46:385-396.

Miller, R.J., J.W. Biggar and D.R. Nielsen. 1965. Chloride displacement in Panoche clay loam in relation to water movement and distribution. Water Res. Res. 1:63-73.

Misra, C. and B.K. Mishra. 1977. Miscible displacement of nitrate and chloride under field conditions. Soil Sci. Soc. Am. J. 41:496-499.

Narasimhan, T.N. and P.W. Witherspoon. 1977. Numerical Model for Saturated-Unsaturated Flow in Deformable Porous Media. I. Theory. Water Resour. Res. 13:657-664.

Narasimhan, T.N., M. Alavi and C.W. Liu. 1985. CHAMP-A computer code for modeling transient fluid flow and chemical transport with hydrodynamic dispersion in variably saturated systems. *In* Proc. Symposium on groundwater flow and transport modeling for performance assessment of deep geological disposal of radioactive waste. Pacific Northwest Laboratory, NUREG/CP-0079.

Neal R.H., G. Sposito, K.M. Holtzclaw and S.J. Traina. 1987. Selenite adsorption on alluvial soils: I. Soil composition and pH effects. Soil Sci. Soc. Am. J. 51:1161-1165.

Neal R.H., G. Sposito, K.M. Holtzclaw and S.J. Traina. 1987. Selenite adsorption on alluvial soils: II. Solution composition effects. Soil Sci. Soc. Am. J. 51:1165-1169.

Nielsen, D.R. and J.W. Biggar. 1961. Miscible displacement in soils: I. Experimental information. Soil Sci. Soc. Am. Proc. 25:1-5.

Nielsen, D.R. and J.W. Biggar. 1962. Miscible displacement: III. Theoretical considerations. Soil Sci. Soc. Am. Proc. 26:216-221.

Nielsen, D.R., J.W. Biggar and K.T. Erh. 1973. Spatial variability of field-measured soil-water properties. Hilgardia 42:215-259.

Nkedi-Kizza, P., J.W. Biggar, M.Th. van Genuchten, P.J. Wierenga, H.M. Selim, J.M. Davidson and D.R. Nielsen. 1983. Modeling tritium and chloride-36 transport through a porous medium exhibiting physical non-equilibrium. Water Resour. Res. 19:691-700.

Ohlendorf, H.M., R.L. Hothem, C.M. Bunck, T.W. Aldrich and J.F. Moore. 1986. Relationships between selenium concentrations and avian reproduction. 51st Annual Wildlife and Natural Resources Conference, Wildlife Management Institute, Reno, Nevada.

Peck, A.J., R.J. Luxmoore and J.L. Stolzy. 1977. Effects of spatial variability on soil hydraulic properties in water budget modeling. Water Resour. Res., 13:348-354.

Passioura, J.B. 1971. Hydrodynamic dispersion in aggregated media: I. Theory. Soil Sci. 111:339-344.

Ponnamperuma, F.N. 1965. Dynamic aspects of flooded soils and the nutrition of the rice plant. Proc. Symposium Mineral Nutrition of the Rice Plant, 1964. p. 295-328. The Johns Hopkins Press, Baltimore, Md.

Ponnamperuma, F.N., E.M. Tianco and T. Loy. 1967. Redox equilibria in flooded soils: I. The iron hydroxide systems. Soil Science 103:374-382.

Prokopovich, N.P. 1967. Geology and hydrology progress report, San Luis Drain - South Dos Palos to Kettleman City. US Bureau of Reclamation, Sacramento, Ca.

Rao, P.S.C., R.E. Green, V. Balasubramanian and Y. Kanehiro. 1974. Field study of solute movement in a highly aggregated Oxisol with intermittent flooding: II. Picloram. J. Environ. Qual. 3:197-202.

Rao, P.S.C., R.E. Green, L.R. Ahuja and J.M. Davidson. 1976. Evaluation of a capillary bundle model for describing solute dispersion in aggregated soils. Soil Sci. Soc. Am. J. 40:815-820.

Rao, P.S.C., D.E. Rolston, R.E. Jessup and J.M. Davidson. 1980. Solute transport in aggregated porous media: Theoretical and experimental evaluation. Soil Sci. Soc. Am. J. 44:1139-1146.

Rosenfeld, I. and O.A. Beath. 1964. Selenium geobotany, biochemistry, toxicity, and nutrition. Academic Press, New York.

Rowell, J.H., H.L. Dillingham, L.D. Creasy and N.W. Cederquist. 1983. Kesterson Reservoir - first stage technical report in support of the report of waste discharge to the California Regional Water Quality Control Board. US Bureau of Reclamation.

Saffigna, P.G., D.R. Keeney and C.B. Tanner. 1977. Lysimeter and field measurements of chloride and bromide leaching in an uncultivated loamy sand. Soil Sci. Soc. Am. J. 41:478-482.

Scotter, D.R., 1978. Preferential solute movement through larger soil voids. I. Some computations using simple theory. Austr. J. Soil Res. 16:257-267.

Singh M., N. Singh and P.S. Relan. 1981. Adsorption and desorption of selenate and selenite on different soils. Soil Sci. 132:134-141.

Sharma S. and R. Singh. 1983. Selenium in soil, plant, and animal systems. CRC Critical Reviews in Environmental Control 13:23-50.

Skoog, D.A. and D.M. West. 1963. Fundamentals of Analytical Chemistry. Holt, Rinehart and Winston. New York.

Smith, K.A. 1977. Soil aeration. Soil Science 123:284-291.

Soil Conservation Service, US Department of Agriculture. 1952. Soil Survey of the Los Baños Area, California, Series 1939, (12).

State of California, Department of Water Resources, San Joaquin District. 1967. Monthly shallow ground water elevations - San Joaquin Master Drain Reservoir sites - Gustine-Kesterson and South Dos Palos Areas, Draft Office Report.

Stumm, W. and J.J. Morgan. 1981. Aquatic Chemistry. John Wiley, New York.

Takai, Y., T. Koyama and T. Kamura. 1956. Microbial metabolism in reduction processes of paddy soils: I. Soil Science and Plant Nutrition 2:63-66.

Thomas, G.W. and A.R. Swoboda. 1970. Anion exclusion effects on chloride movement in soil. Soil Sci. 110:163-166.

Tripathi, N. and S.G. Misra. 1975. Selenium retention in some Indian soils. J. Indian Soc. Soil Sci. 23:103-108.

UC Salinity/Drainage Task Force. 1987. Selenium transport in San Joaquin Valley soils: Influence of physical and chemical properties of soil and water. 1986-1987 Technical

Progress Report. pp. 46-53.

US Bureau of Reclamation. 1964. Kesterson Reservoir and Waterfowl. Inf. Bull. 1. Sacramento Ca.

US Bureau of Reclamation. 1965. Groundwater conditions and potential pumping resources above Corcoran Clay: Addendum to the groundwater geology and resources definite plan index 1963. Sacramento Ca.

US Bureau of Reclamation. 1967. Kesterson Reservoir site summary of geologic data. Sacramento Ca.

US Bureau of Reclamation. 1986. Final Environmental Impact Statement, Volume 2, Kesterson Program. Sacramento Ca.

US Bureau of Reclamation. 1987. Kesterson Program Report of Waste Discharge, Sacramento, Ca.

Van De Pol, R.M., P.J. Wierenga and D.R. Nielsen. 1977. Solute movement in a field soil. Soil Sci. Soc. Am. J. 41:10-13.

Van Genuchten, H. Th. and J.P. Wierenga. 1976. Mass transfer studies in sorbing porous media: I. Analytical Solutions. Soil Sci. Soc. Am. J. 40:473-480.

Verhoeven, W. 1956. Some remarks on nitrate and nitrite metabolism in micro-organisms. *In* W.D. McElroy and B. Glass (*Ed.*) A Symposium on Inorganic Nitrogen Metabolism, p. 61-86. The Johns Hopkins Press, Baltimore, Md.

Warrick, A.W. and A. Amoozegar-Fard. 1979. Infiltration and drainage calculations using spatially scaled hydraulic properties. Water Res. Res. 15:1116-1120.

Warrick, A.W. and D. R. Nielsen. 1980. Spatial variability of soil physical properties in the field. *In* D. Hillel, Applications of Soil Physics. Academic Press, New York, p.319-344.

Weres, O., A.F. White, H.A. Wollenberg and A. Yee. 1985. Geochemistry of selenium at Kesterson Reservoir: Possible Remedial Measures. Lawrence Berkeley Laboratory, Earth Sciences v8 no. 3.

White, A.F. 1985. Geochemical barriers to groundwater contamination. p. 69-77. *In* J. DeVries (*Ed.*) Proceedings, 15th Biennial Conference on Groundwater. San Diego, Ca. 23-25 September. California Water Resources Center, Davis.

Wierenga, P. J. 1982 Solute Transport through Soils:mobile-immobile water concepts. Review of Ground-Water Flow and Transport Models in The Unsaturated Zone. Report NUREG/CR-2917, PNL-4427, US Nuclear Regulatory Commission, Washington,D.C.

Yamane, I. and K. Sato. 1968. Initial rapid drop of oxidation-reduction potential in submerged air-dried soils. Soil Science and Plant Nutrition 14:68-72.

Yläranta, T. 1983. Sorption of selenite and selenate in soil. Ann. Agric. Fenn. 22:29-39.

LAWRENCE BERKELEY LABORATORY
TECHNICAL INFORMATION DEPARTMENT
UNIVERSITY OF CALIFORNIA
BERKELEY, CALIFORNIA 94720